

Hudson Bay Systems Study (BaySys)

Phase 1 Report: Campaign Reports and Data Collection

Project Managers:
Dr. David Barber and Mr. Kevin Sydor



**University
of Manitoba**



**NSERC
CRSNG**

This document should be cited as:

Barber, D.G., Sydor, K. 2020. Hudson Bay Systems Study (BaySys) Phase 1 Report: Campaign Reports and Data Collection. (Eds.) Landry, D.L., Candlish L. Unpublished Project Report. University of Manitoba, Winnipeg, MB. Canada.

This report can be downloaded through:

<http://umanitoba.ca/faculties/environment/departments/ceos/index.html>

<http://lwbins-datahub.ad.umanitoba.ca/>

Team Leads of the BaySys Project

Project Managers: David Barber and Kevin Sydor

Project Coordinators: David Landry, Lauren Candlish, and Karen Wong

Team 1: Jens Ehn, Kevin Sydor and Karen Wong

Team 2: Tricia Stadnyk and Kristina Koenig

Team 3: Jean-Éric Tremblay, Gary Swanson, and Marilyn Kullman

Team 4: Tim Papakyriakou and Bob Gill

Team 5: Feiyue Wang, Sarah Wakelin, and Allison Zacharias

Team 6: Jennifer Lukovich, Paul Myers, and Karen Wong

Editorial Team

Editors: David Landry, Lauren Candlish, Karen Wong

Final Review: Kevin Sydor, David Barber

Research Advisory Committee

Robert Young (Fisheries and Oceans Canada), Robert E Hecky (University of Minnesota), Norm Halden (University of Manitoba), Efreem Teklemariam (Manitoba Hydro), Shelley Matkowski (Manitoba Hydro)

Funding and Support

This project is part of the NSERC-Manitoba Hydro funded Collaborative Research and Development (CRD) program. Primary data collection for this research would not have been possible without the support and hospitality of the CCGS *Amundsen* crew during the 2018 field season, along with Amundsen Science. Much of the HQP and graduate student research has been supported by the University of Manitoba Graduate Fellowship (UMGF), the Northern Scientific Training Program (NSTP), and NSERC Masters and Doctoral Awards. This work is a contribution to the ArcticNet Networks of Centres of Excellence and the Arctic Science Partnership (ASP, asp-net.org).



ABSTRACT	VI
CHAPTER 1 - MOORING PROGRAM – CCGS DES GROSEILLIER	2
1.1 <i>Fieldwork Objectives</i>	3
1.2 <i>Mooring Operations</i>	4
1.6 <i>Water Sampling</i>	15
1.3 <i>Freshwater Dynamics</i>	21
1.4 <i>Nutrients and Biological Sampling</i>	22
1.5 <i>Distribution of Phytoplankton</i>	26
1.6 <i>Carbon Cycling</i>	26
1.7 <i>Sediment Sampling</i>	27
Appendix 1A: <i>Water Parameters</i>	29
Appendix 1B: <i>CCGS Des Groseilliers Science Logbook</i>	33
WINTER/SPRING 2017	38
CHAPTER 2 - CHURCHILL RIVER AND MOBILE ICE SURVEY	39
2.1 <i>Fieldwork Objectives</i>	40
2.2 <i>Study Area</i>	41
2.3 <i>Logistical Summary</i>	42
2.4 <i>Ice Conditions in the Study Area</i>	43
2.5 <i>Team 1 – Climate and Marine System</i>	46
2.6 <i>Team 3 – Marine Ecosystems</i>	51
2.7 <i>Team 4 – Carbon System</i>	56
2.8 <i>Team 5 – Contaminants</i>	59
Appendix 2A: <i>Work Schedule</i>	62
Appendix 2B: <i>Sampling Schedule</i>	63
CHAPTER 3 - NELSON ESTUARY LANDFAST ICE SURVEY	67
3.1 <i>Fieldwork Objectives</i>	68
3.2 <i>Logistical Summary</i>	68
3.3 <i>Team 1 – Sea and Oceanography</i>	69
3.4 <i>Team 3 – Marine Ecosystems</i>	83
3.5 <i>Team 4 – Carbon System</i>	85
3.6 <i>Team 5 – Contaminants</i>	87
Appendix 3A: <i>Sampling Schedule</i>	91
CHAPTER 4 - SEDIMENT CORING AND WATER QUALITY	94
4.1 <i>Fieldwork Objectives</i>	95
4.2 <i>Logistical Summary</i>	95
4.3 <i>Sediment Coring</i>	95
4.4 <i>Methods</i>	96
4.5 <i>Water Sampling</i>	97
SUMMER/FALL 2017	98
CHAPTER 5 - SEDIMENT, SOIL, AND WATER QUALITY	99
5.1 <i>Fieldwork Objectives</i>	100
5.2 <i>Logistical Summary</i>	100
5.3 <i>Sediment and Organic Matter Fingerprinting</i>	101

5.4	<i>Sediment Budgeting and Inorganic Fingerprinting</i>	104
5.5	<i>Methyl Mercury in Lakes and Rivers</i>	106
CHAPTER 6 - MOORING PROGRAM – CCGS HENRY LARSEN		109
6.1	<i>Fieldwork Objectives</i>	110
6.2	<i>Mooring Operations</i>	110
6.3	<i>Early Results</i>	117
6.4	<i>Preliminary Results of Thermohaline Stratification in the Mooring Positions from CTD Profiles</i>	120
6.5	<i>Water Sampling</i>	122
	<i>Appendix 6A</i>	124
SPRING/SUMMER 2018		126
CHAPTER 7 - BAY-WIDE SURVEY – CCGS AMUNDSEN (LEG-1 & 2)		127
7.1	<i>LEG 1a/b – Hudson Bay-Wide Survey</i>	128
7.2	<i>Community Visits and the Knowledge Exchange Workshop</i>	130
7.3	<i>Marine and Climate System - Sea Ice</i>	134
7.4	<i>Mooring Operations in Hudson Bay</i>	141
7.5	<i>BaySys Team 3 – Optical Properties of Open and Ice-covered Hudson Bay</i>	150
7.6	<i>Zooplankton and Fish Ecology/Acoustics</i>	162
7.7	<i>Marine Productivity: Carbon and Nutrients Fluxes</i>	166
7.8	<i>Macrofauna Diversity Across Hudson Bay Complex</i>	171
7.9	<i>Freshwater Influence on Microbial Communities of the Hudson Bay System</i>	173
7.10	<i>Carbon Exchange Dynamics, Air-Surface Fluxes and Surface Climate</i>	176
7.11	<i>Contaminants</i>	184
7.12	<i>Amundsen Science – Seabed Mapping, MVP & Sub-Bottom Profiling</i>	198
7.13	<i>LEG 2a – Eastern Hudson Bay Sampling and Rivers</i>	204
	<i>Appendix 7A – Station Type Definitions</i>	208
	<i>Appendix 7B – Complete Station List</i>	208
CHAPTER 8 - MOORING PROGRAM – WILLIAM KENNEDY		214
8.1	<i>Fieldwork Objectives</i>	215
8.2	<i>Mooring Operations</i>	217
8.3	<i>Early Results</i>	220
8.4	<i>CTD Sampling</i>	221
8.5	<i>Water Sampling</i>	222
HYPE AND NEMO MODELING		224
CHAPTER 9 FRESHWATER HYDROLOGIC MODELING		225
9.1	<i>Objectives and Background</i>	226
9.2	<i>Models and Methods</i>	231
9.3	<i>Operations and Progress to Date</i>	233
9.4	<i>Summary of Results to Date</i>	235
CHAPTER 10 NEMO MODELING		260
10.1	<i>Objectives and Background</i>	261
10.2	<i>Models</i>	262
10.3	<i>Methods</i>	266
10.4	<i>Inputs</i>	267
10.5	<i>Operations and Progress to Date</i>	268

10.6 Preliminary Results	269
BAYSYS CAMPAIGN STATIONS 2016-2018.....	272
BAYSYS STATION DETAILS FROM ALL 2016 CAMPAIGNS	276
BAYSYS STATION DETAILS FROM ALL 2017 CAMPAIGNS.	277
BAYSYS STATION DETAILS FROM ALL 2018 CAMPAIGNS.	288

ABSTRACT

BaySys is a comprehensive and interdisciplinary study that aimed to provide a scientific basis towards understanding the relative contributions of climate change and regulation on the Hudson Bay system. The role of freshwater in Hudson Bay was investigated through numerous field-based experimentation and sampling coupled with climatic-hydrological-oceanographic-biogeochemical modeling. BaySys was built on a partnership between the University of Manitoba, Manitoba Hydro, Hydro Québec, Ouranos, Environment and Climate Change Canada, as well as other academic institutions across Canada (University of Northern British Columbia, University of Alberta, University of Calgary, University of Guelph, Université de Sherbrooke, Université de Laval, and Université de Québec à Rimouski). Six teams led by an academic and industry co-lead were established to investigate a number of interconnected systems including: marine/climate systems, freshwater systems, marine ecosystems, carbon cycling, contaminants, and modeling. This multidisciplinary project will vastly expand knowledge of climate impacts on the Arctic system, in a region where there are substantial gaps and limitations in existing knowledge. The BaySys Phase 1 report documents the eight field campaigns conducted throughout a two-year period from 2016 to 2018. Each field report details the objectives of each campaign, the station sites and descriptions, field methods and data collection, and some preliminary field analysis, where applicable. In addition, the Phase 1 report provides an overview of the project modeling endeavours (HYPE and NEMO) that had been developed in conjunction with the observational data collection.

FALL 2016



The BaySys mooring team and crew onboard the CCGS Des Groseilliers. Five oceanographic moorings were deployed from September 26-October 3, 2016. The team attempted to retrieve the lost ArcticNet mooring, AN01, but were not successful. Opportunistic water and sediment sampling were executed at each possible station.

CHAPTER 1 - MOORING PROGRAM – CCGS DES GROSEILLIER

PROJECT PIs David Barber¹ (Project lead), Jens Ehn¹ (Team 1), Jean-Éric Tremblay³ (Team 3), Tim Papakyriakou¹ (Team 4), Céline Guéguen (Team 4), Zou Zou Kuyzk¹ (Team 4/5), Fei Wang¹ (Team 5), David Lobb² (Team 5)

FIELD/SHIP COORDINATION Jens Ehn (Chief Scientist), Claire Hornby¹ (Project Coordinator)

MOORING OPERATIONS Sergei Kirillov¹ (RA), Igor Dmitrenko¹ (Prof), Jens Ehn (Prof), Sylvain Blondeau³ (Tech)

ROSETTE OPERATOR Sylvain Blondeau

WATER SAMPLING TEAM Lisa Matthes¹ (Ph.D.), Atreya Basu¹ (Ph.D.), Michelle Kamula¹ (RA), Zakhar Kazmiruk¹ (MSc), Jake (Janghan) Lee³ (Ph.D.), Masoud Goharrokhi² (Ph.D.), Mary O'Brien (ISO, DFO)

¹Centre for Earth Observation Science, University of Manitoba, 535 Wallace Building, Winnipeg, MB

²Department of Soil Science, University of Manitoba, 535 Wallace Building, Winnipeg, MB

³Québec-Océan, Department of Biology, Pavillon Alexandre-Vachon, 1045, Avenue de la Médecine, Local 2078, Université Laval, Québec, QC

REPORT AUTHORS Hornby C, Ehn J, Matthes L, Kamula K, Lee J, Blondeau S, Basu A, Goharrokhi M, Kazmiruk Z, and Kirilov S

RESEARCH VESSEL Canadian Coast Guard Ship CCGS Des Groseilliers

CITE CHAPTER AS Hornby C, Ehn J, Matthes L, Kamula K, Lee J, Blondeau S, Basu A, Goharrokhi M, Kazmiruk Z, and Kirilov S, 2019. Mooring Program – CCGS Des Groseillier. Chapter 1 in, *Hudson Bay Systems Study (BaySys) Phase 1 Report: Campaign Reports and Data Collection*. (Eds.) Landry, DL & Candlish, LM. pp. 2-37.

1.1 Fieldwork Objectives

Background and Regional Setting

As the largest continental shelf sea in the world, Hudson Bay (low Arctic, Canada) receives an annual freshwater loading of about 760 km³ from more than 42 rivers within a drainage basin of over 3×10⁶ km² in area. An even larger seasonal freshwater flux, estimated at 1200 km³ or more, is withdrawn from or added to the water column due to the formation or decay of sea ice in the Bay. The timing, duration, volume, and location of freshwater loading to Hudson Bay thus have a major influence on the properties and processes of the marine waters and the dynamics of sea ice, which in turn strongly influence primary productivity, carbon and contaminant cycling in the Bay. Distinguishing between runoff and sea-ice melt is especially important in Hudson Bay because each contributes considerable annual fluxes of freshwater to Hudson Bay, and yet they may be affected differently by climate change and regulation. To address the overarching goal of providing a scientific basis to separate climate change and regulation impacts on the Hudson Bay system, BaySys (2015-2019) will integrate field-based experimentation with coupled climatic-hydrological-oceanographic-biogeochemical modeling.

The 2016 mooring field program took place in southern Hudson Bay from September 26 (Churchill) to October 4 (Kujjaurapik) (Figure 1.1). Opportunistic sampling continued from October 5 to October 12 in northern Hudson Bay (Figure 1.1), after which the ship returned to Iqaluit for crew change and all scientists disembarked. During the main eight-day cruise, members of all five multi-disciplinary teams collected CTD profiles, water, and sediment samples, and deployed oceanographic moorings along the full length of the southern coast of Hudson Bay. The focus of this field program was on the Nelson Estuary region and James Bay mouth, which are the major sources of riverine freshwater to the Hudson Bay system.

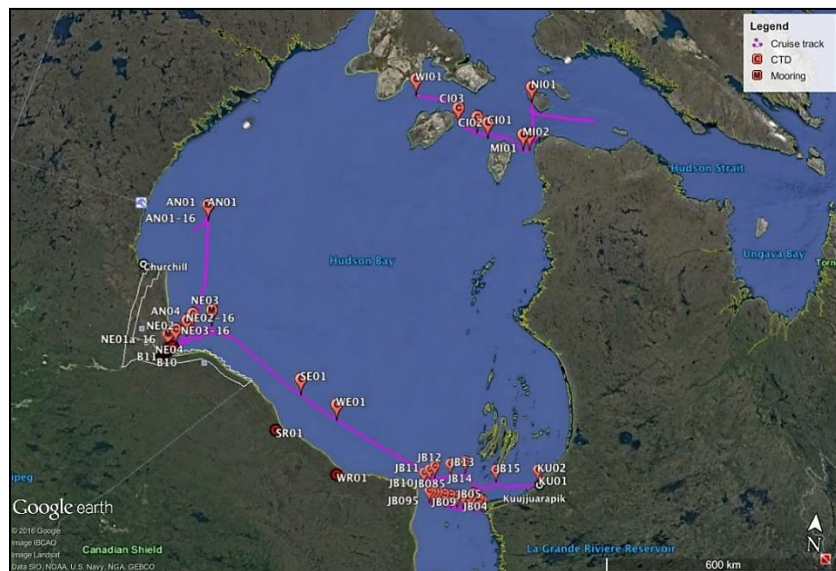


FIGURE 1.1 BaySys 2016 cruise track, mooring sites, and CTD stations

1.2 *Mooring Operations*

Five oceanographic moorings were deployed from September 26-October 1, 2016 (Table 1.1). All mooring components and their depths are shown in Figures 1.2-1.6. Three of the moorings located in deeper waters (i.e. AN01, NE03, and JB02) included custom-built buoyant mooring frames with upward-looking Nortek Signature 500 Acoustic Doppler Current Meters (ADCPs). These are capable of measuring high-resolution near-surface current profiles, ice draft, and surface wave characterization. The TRDI Workhorse ADCPs, located further below mounted inline or in trawl-resistant bottom mounts, provide an additional current profile of the water column and surface tracking. Only the JB02 lacked a TRDI Workhorse ADCP; however, instead, it included a downward-looking Nortek Aquadopp 600 kHz ADCP to provide observations of the currents below ~50 m depth (Figure 1.7). Trawl-resistant bottom mounts were deployed in the inner (NE01; Figure 1.5) and outer estuary (NE02; Figure 1.6) stations where higher water column dynamics are expected leading to high current speeds and ice ridging. Numerous RBR conductivity (C) and temperature (T) loggers, some with an additional Seapoint turbidity meter (Tu), were provided in-kind by Manitoba Hydro and attached to the mooring lines at select locations. In addition, 7 Wetlabs ECO triplet loggers were attached to near-surface locations and on the trawl-resistant bottom mount on NE01 (inner estuary, Figure 1.5) to record chlorophyll-a fluorescence, CDOM fluorescence, and turbidity.

A special addition to AN01, NE01 (however lost), NE02, and NE03, was the buoyant tubes moored at depths near the surface so that instrument embedded within the tubes can record the surface layer properties near the ice cover. Due to the length and smoothness of the tubes, they will resist being caught and carried off by drifting ice ridges. The drifting ice ridges, with sufficient draft to reach the tubes, will (hopefully) push down the tubes instead of catching them. However, in the event of tubes getting trapped and dragged by drifting, weak links were placed on the lines connecting the tubes to the moorings so that only the tube component of the moorings would be lost. Four sediment traps (see next section) were attached to AN01, NE02, NE03, and JB02 (Table 1.1), and are a contribution from Dr. Zou Zou Kuzyk of BaySys Team 4/5.

The mooring components are programmed for a one-year deployment with the planned recovery in fall 2017. However, if there was no suitable ship available for fall 2017, they would have been recovered in June/July 2017 during the originally planned CCGS Amundsen cruise in Hudson Bay.

TABLE 1.1 Summary of BaySys mooring locations, station IDs, sediment trap depths, and bottom depth at deployment.

Date	Mooring location	ID	Latitude	Longitude	Bottom Depth (m)	Sediment trap depth (m)	Trap serial number
2016-09-26	Churchill Estuary	AN01	59.9693	-91.9524	109	85	718630
2016-09-27	Nelson Estuary (outer)	NE02	57.5001	-91.8016	46	35	718631
2016-09-28	Nelson Estuary (shelf)	NE03	57.8294	-90.8815	54	28	718632*
2016-09-29	Nelson Estuary (inner)	NE01	57.1321	-92.4117	29.7	No trap	
2016-10-01	James Bay	JB02	54.6829	-80.1871	101	75	718633*

*Note: The rosette and motors for these two sediment traps were accidentally swapped.

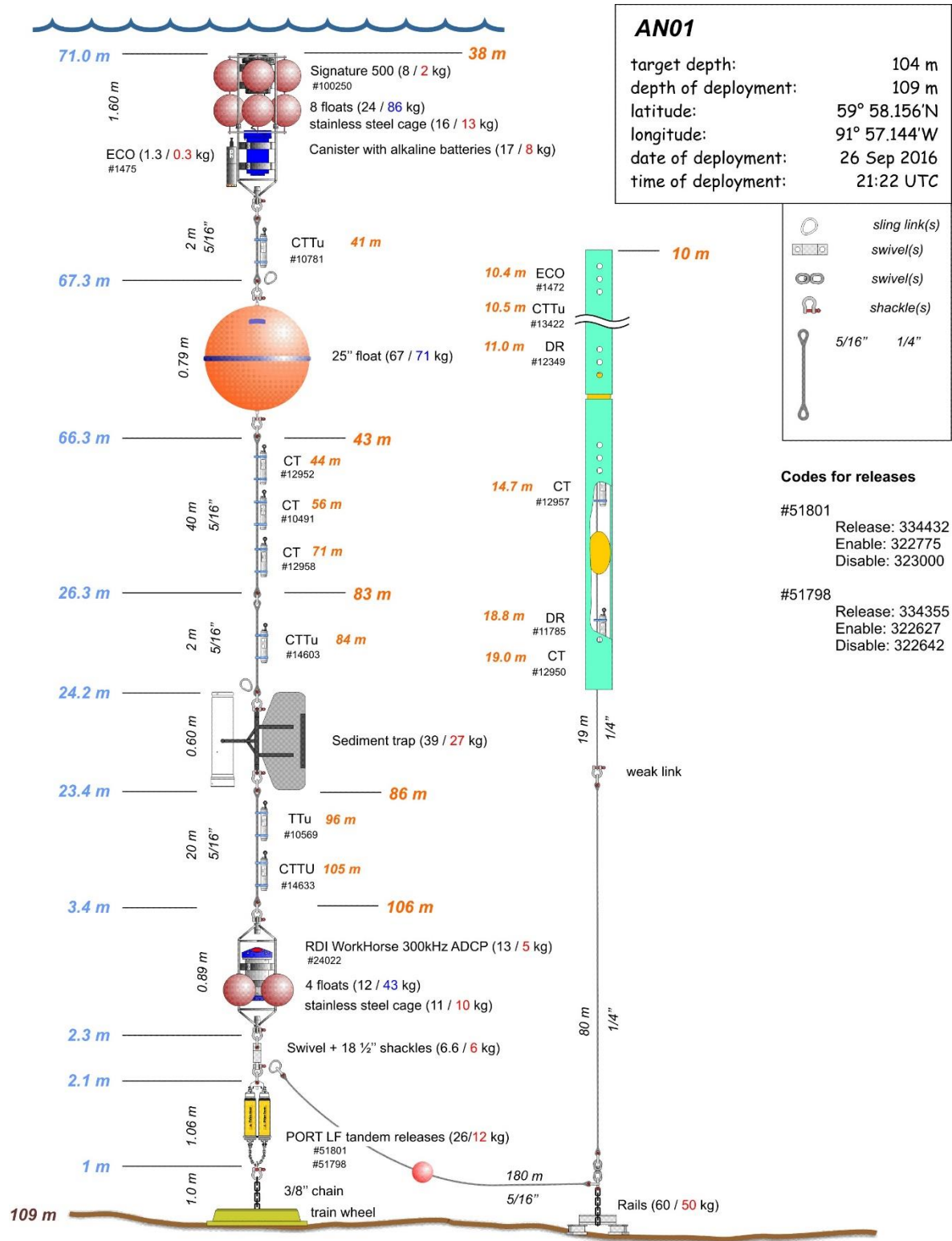


FIGURE 1.2 AN01 (Churchill shelf) mooring configuration, location, and depth.

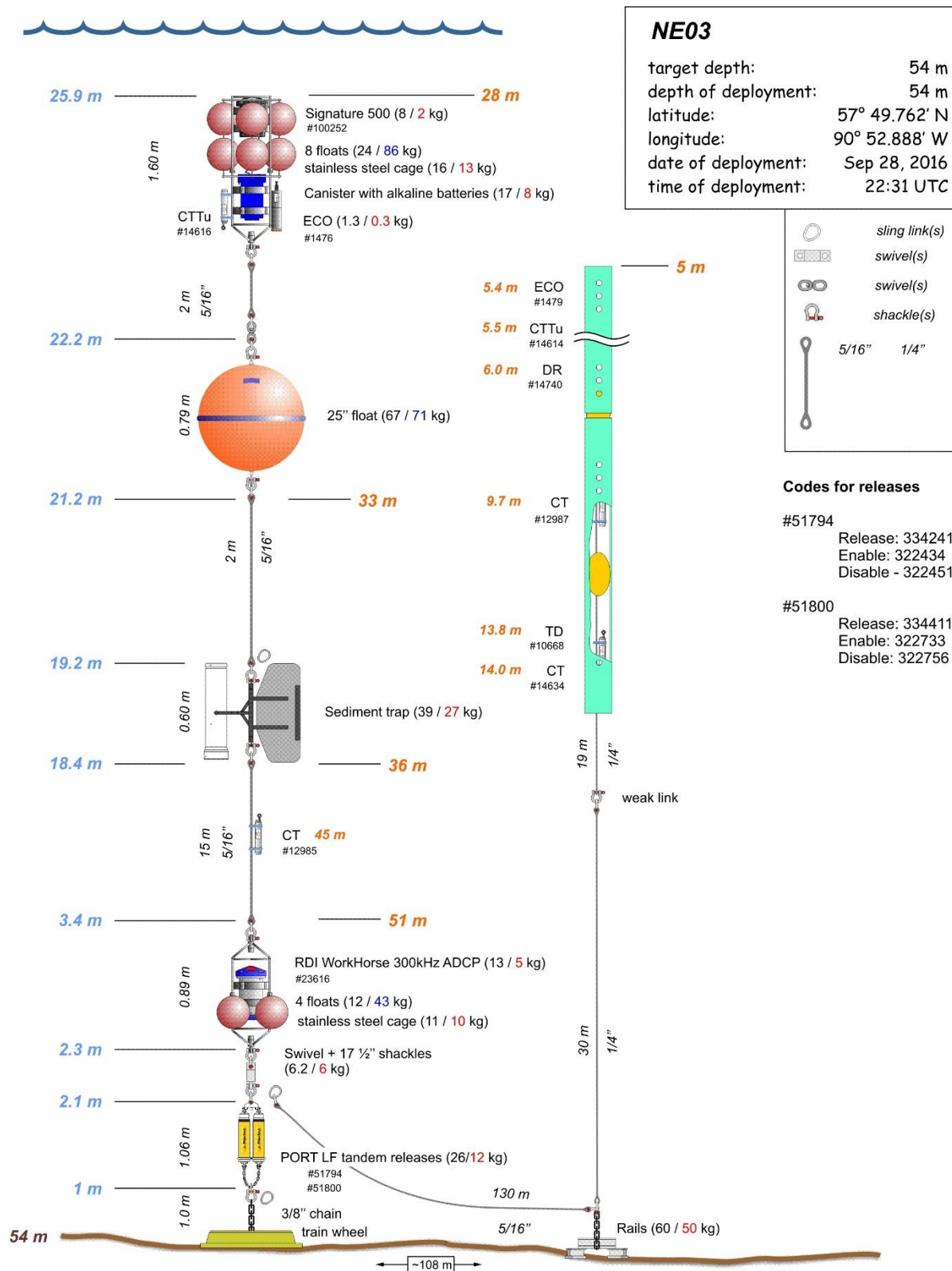


FIGURE 1.3 NE03 (Nelson River outer shelf) mooring configuration, location, and depth.

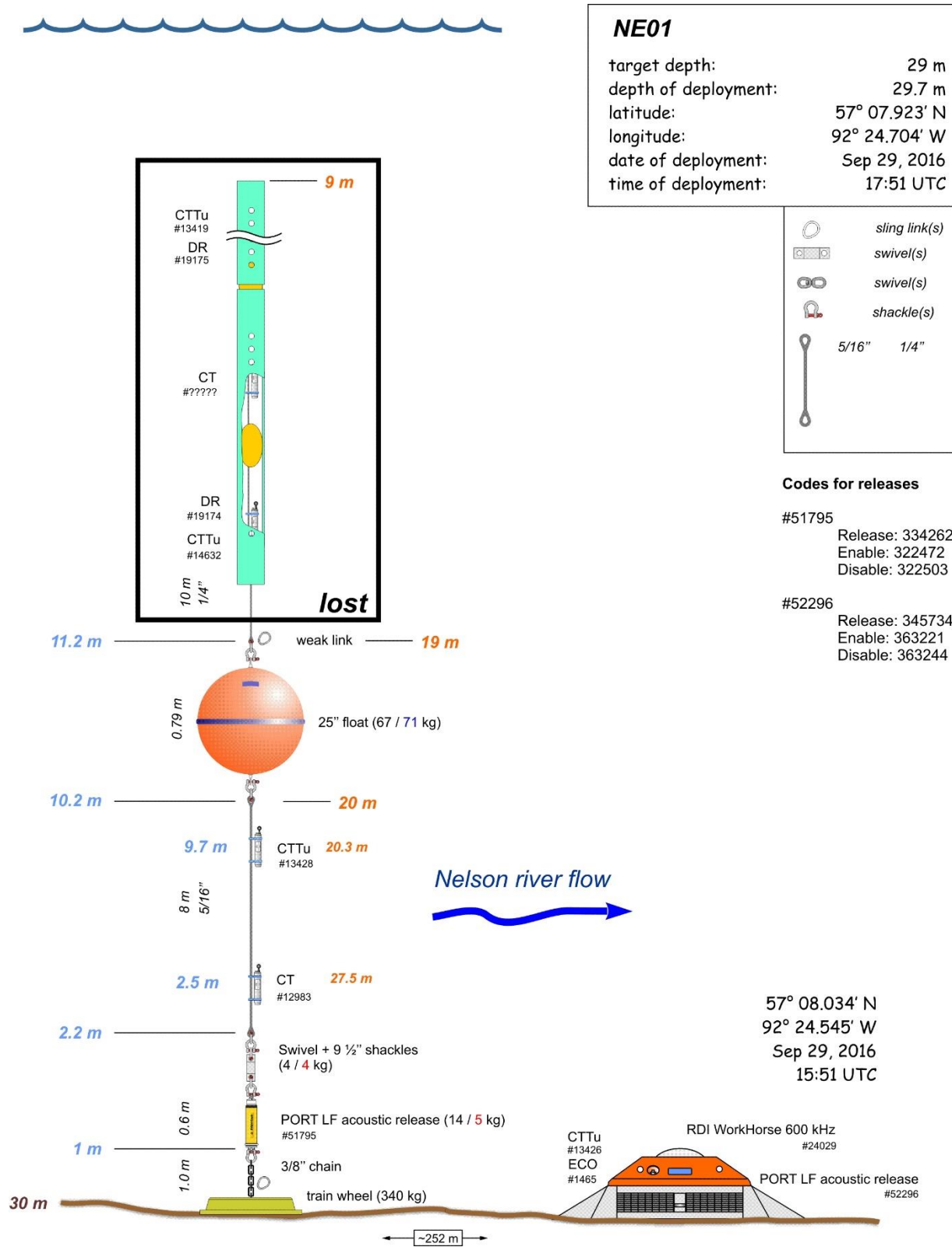


FIGURE 1.4 NE01 (Nelson Inner Estuary) mooring configuration, location, and depth.

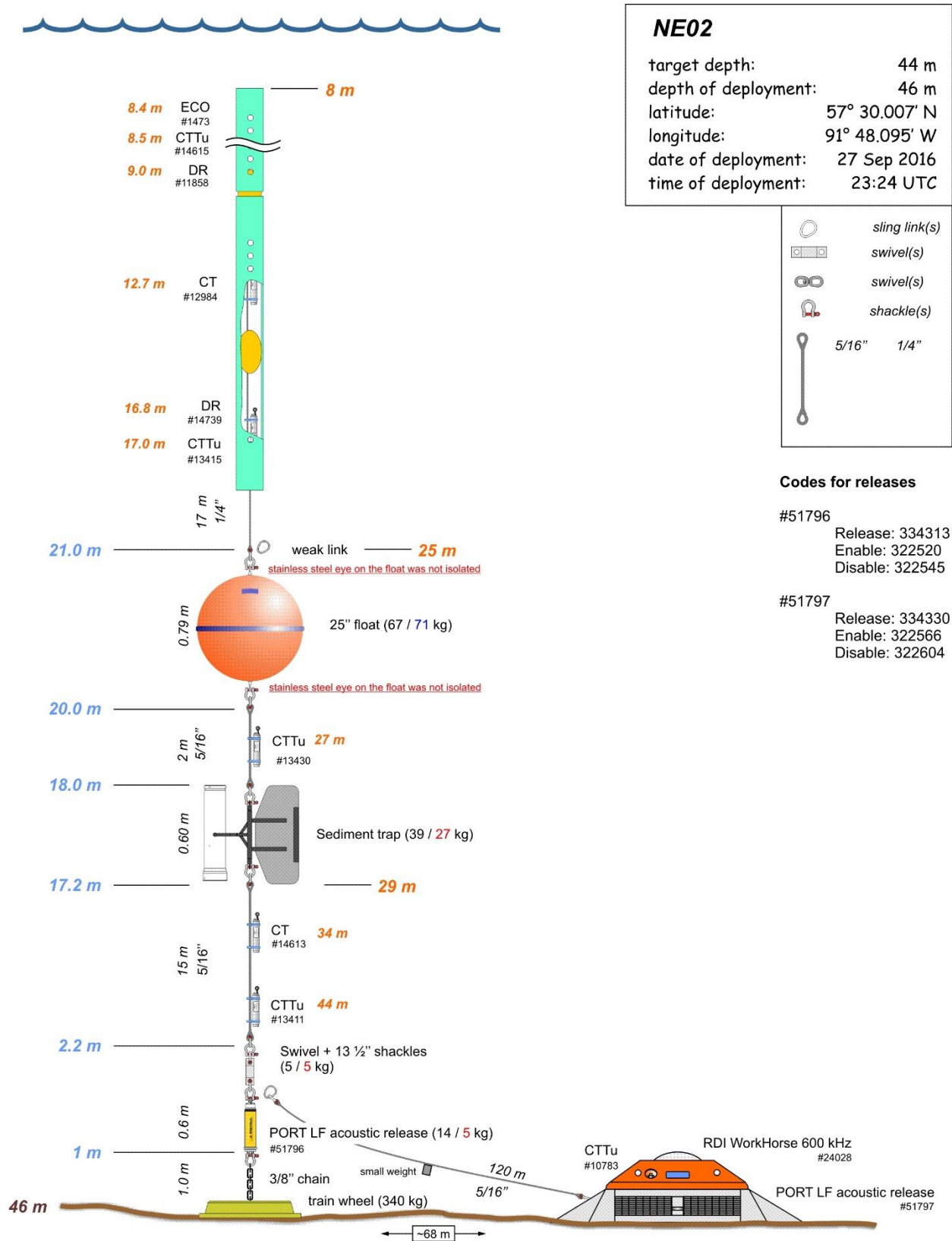


FIGURE 1.5 NE02 (Nelson Outer Estuary) mooring configuration, location, and depth.

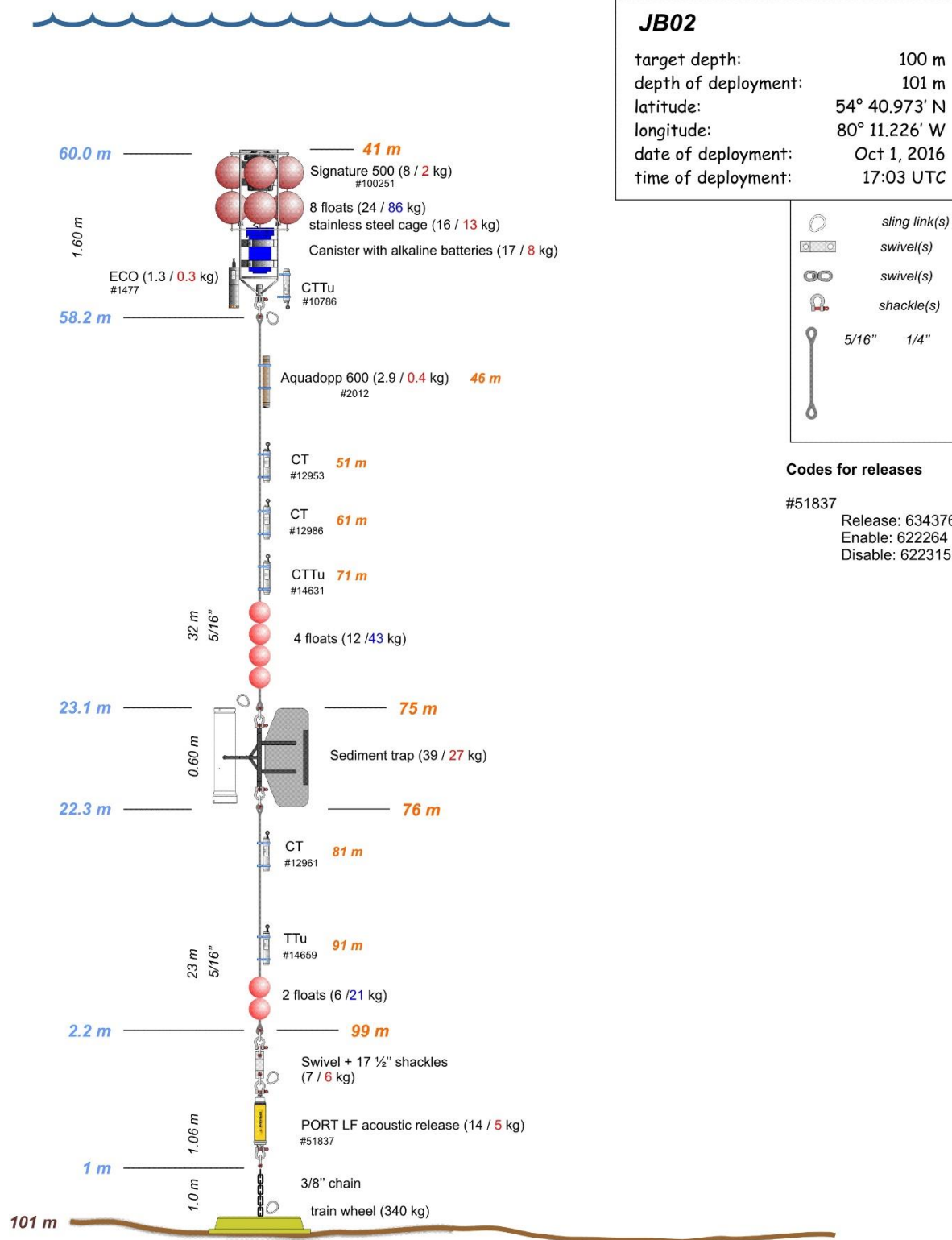


FIGURE 1.6 JB02 (James Bay) mooring configuration, location, and depth.

Mooring Deployment

All moorings (except NE01) were deployed from the foredeck by using the crane at the starboard side of the ship. The relatively short length of all moorings allowed deploying them “anchor last”. The design of mooring AN04, NE02, and NE03 included a second component (surface buoyant tubes or TRBM) connected to a major line with a long rope near the bottom. Since each mooring carry two acoustic releases only, such a connection aims to increase the mooring survivability in the case of one of the failures of the release. The connecting line also facilitates the recovery by dragging in the case that both releases fail to respond at the moment of recovery.

Two elements of mooring NE01 were deployed separately in the inner estuarine area from the helicopter. The deployment was supported by crew and scientist in the zodiac: the mooring elements were smoothly dropped into the water in the designated areas marked from the zodiac with the small, anchored surface floats.

Sediment Traps

The objective of the sediment trap program, as part of BaySys Team 4/5, is to determine the sinking fluxes of particulates (organic and lithogenic) through the water column. Four Gurney Instrument “Baker Type” sequential type sediment traps were deployed from the CCGS Des Groseilliers fixed to moorings AN01, NE02, NE03, and JB02 at depths ranging from 28 to 85 m below the water surface (Table 1.1).

Before embarking on the ship, sediment trap solution, or density gradient solution, was prepared at the Churchill Northern Studies Centre (CNSC). To prepare the solution, 10L of seawater was collected from the port wharf and filtered through a 0.7 μ m GF/F filter. The salinity of the filtered seawater was adjusted from 26.7 psu to 37 psu with 88.065g of ultra-clean sea salt. Borax (44.4 g) was slowly added to 37% formaldehyde (0.45L) and placed on a magnetic stir plate overnight to dissolve. The solution was removed from the stir plate and, after settling for approx. 4 hours, was decanted and poured into 8.55 L of filtered seawater. The solution was stored in a 10L polypropylene aqua pak water container until sediment traps were ready to be assembled, which took place before deployed.

Once on board the ship, all four sediment trap motor/timers were removed from their cases, checked over, including batteries and o-rings, and timer intervals were set simultaneously in Central Standard Time (See Table 1.2). All four sediment trap motors (see Figure 1.7A/B) were turned on at exactly 18:00 on 25-September-16 (interval 0) so that, simultaneously, they would begin collecting particulates at 0:00 CST 4-October-16 (interval 1).

TABLE 1.2 Sediment trap sample intervals.

Interval	Start Date	Start Time (CST)	End Date	End Time (CST)	Interval Days	Collection Area
delay	25-Sep-16	18:00	4-Oct-16	0:00	8.25	N/A
1	4-Oct-16	0:00	8-Nov-16	0:00	35	0.032 m ²
2	8-Nov-16	0:00	13-Dec-16	0:00	35	0.032 m ²
3	13-Dec-16	0:00	17-Jan-17	0:00	35	0.032 m ²
4	17-Jan-17	0:00	21-Feb-17	0:00	35	0.032 m ²
5	21-Feb-17	0:00	28-Mar-17	0:00	35	0.032 m ²
6	28-Mar-17	0:00	2-May-17	0:00	35	0.032 m ²
7	2-May-17	0:00	6-Jun-17	0:00	35	0.032 m ²
8	6-Jun-17	0:00	11-Jul-17	0:00	35	0.032 m ²
9	11-Jul-17	0:00	15-Aug-17	0:00	35	0.032 m ²
10	15-Aug-17	0:00	19-Sep-17	0:00	35	0.032 m ²

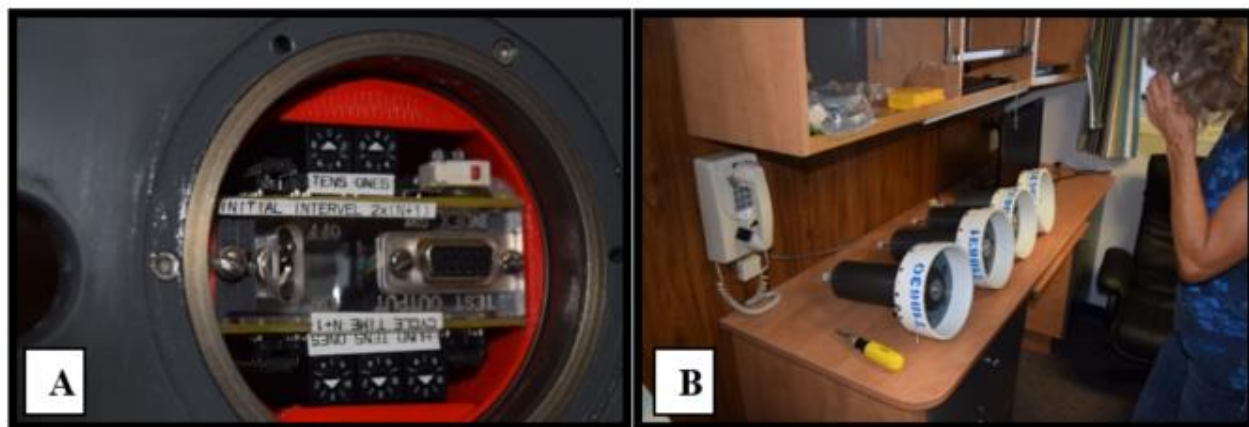


FIGURE 1.7 Photographs showing sediment trap with timers.

All timers were set simultaneously and turned on at the same time at 0:00 Hr on 4-October-2016.



FIGURE 1.8 (A) Mary O'Brien fills sediment trap tubes with density gradient solution that are housed in a rosette assembly that also contains the motor/timer, and (B) then places and secures the corresponding PVC tube that houses an asymmetrical funnel over the sediment trap tubes. (C) Michelle Kamula and Mary O'Brien ensure the sediment trap tubes are lined up with the asymmetrical funnel and that the rosette, motor/timer smoothly rotates inside the PVC tube. (D) Before deployment, a fin is securely fastened to the sediment trap and attached to the mooring line.

Prior to deployment, each sediment trap was assembled by placing 10 sample tubes in the corresponding sediment trap rosette and filled to the surface with a density gradient solution, leaving no headspace (see preparation above and Figure 1.8A). The rosette was set to position “0” or the start position, which held no tube. The corresponding PVC tube that houses an asymmetrical Teflon funnel was washed thoroughly using fresh water to remove any dust or particles and placed over the top of the motor/timer and sample tube rosette assembly (Figure 1.8B). Using a magnet, the rosette was turned slowly, and each sample tube was checked to ensure it lined up with the funnel and that the rosette rotated smoothly inside the PVC tube housing (Figure 1.8C). Fins containing a weight at the bottom were assembled and attached to the sediment trap directly before deployment (Figure 1.8D). The sediment trap assembly was attached to the mooring by shackles and lowered into the water by crew and crane operator.

Attempted Mooring Retrieval

On September 26, the BaySys and Des Groseilliers crew attempted to retrieve lost ArcticNet mooring AN01. Several efforts were made to communicate with the mooring with the use of an acoustic release. Unfortunately, no signal was located. The ship then attempted to dredge for the mooring (Figure 1.9) and was unsuccessful. We will attempt to retrieve this mooring again using a multibeam survey with the CCGS Amundsen in June 2017.

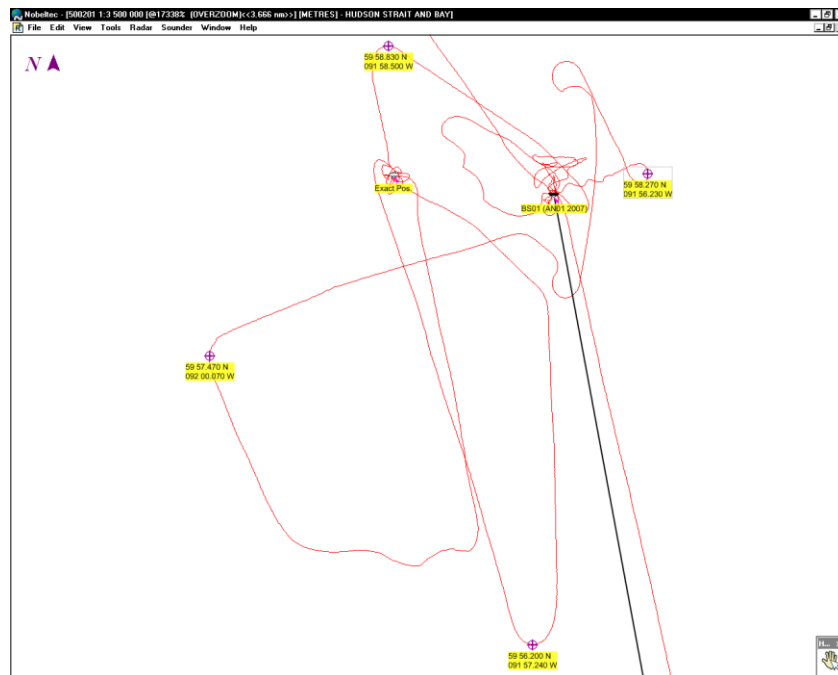


FIGURE 1.9 Map of dredging locations during attempt to locate lost AN01 mooring.

1.6 Water Sampling

The second objective of our shipboard fieldwork was to characterize the physical and chemical properties in the water column, such as temperature, salinity, fluorescence, dissolved oxygen concentration, light penetration, and turbidity. Water sampling was carried out using a CTD-Rosette (donated by Quebec Ocean), Niskin bottles, and buckets (in the river systems).

TABLE 1.3 Water sampling parameters collected by BaySys teams 1, 3, 4, 5 (see Appendix 1A for a full list of stations and parameters).

Instrument	Sample Parameters
CTD	Conductivity temperature-depth probe of two manufacturers (Seabird, Idronaut)
SPM	Suspended particular matter
CDOM	Colored dissolved organic matter
O18	Oxygen Isotopes
ap	Particle absorption
HPLC	High-performance liquid chromatography
POC	Particular organic carbon/ nitrogen
Lugol	Preserved phytoplankton samples
FlowCam	Dynamic imaging particle analyzer
NO ₃ , NO ₂ , Si, PO ₄	Nitrite, nitrate, orthophosphate, and orthosilicic acid
NH ₄	Ammonium
Chl a	Chlorophyll a

CTD-Rosette

We used a SBE 25CTD with various other sensors (see Table 1.4 - 1.5) mounted on a cylindrical frame known as a rosette. The rosette frame was originally equipped with 12 x 8-liter bottles but due to the maximum safe working load of the winch, it was limited to 10 bottles (Figure 1.10). The rosette supplied water samples, surface and at depth, for the teams on board.

Probes Calibration

Seabird CT Probes temperature, conductivity, and oxygen was calibrated at the Sea-Bird factory before the ship departure from Quebec City. Seabird Pressure sensor was calibrated at Laval University before the ship departure from Quebec City. The Biospherical light sensor was new and did not require calibration, while the SeaTech fluorometer and transmissometer could not be calibrated but verified for min and max measurement and worked properly.



FIGURE 1.10 Rosette (10 bottle) operations on board CCGS Des Groseilliers.

TABLE 1.4 Rosette Sensors.

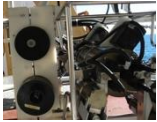


Photo	Instrument	Manufacturer	Type & Properties	Serial Number
	Data Logger	SeaBird	SBE-25 Sampling rate: 8 Hz	0039
	Temperature	SeaBird	SBE 3 Range: -5oC to + 35oC Accuracy: 0.001	031116
	Pressure	SeaBird	Accuracy: 0.015% of full range	290114
	Conductivity	SeaBird	SBE 4C Range: 0 to 7 S/m Accuracy: 0.0003	040819
	Oxygen	SeaBird	SBE-43 Range: 120% of saturation Accuracy: 2% of saturation	431007
	PAR	Biospherical	QSP2300	70422
	Fluorometer	Sea Tech	Minimum Detectable Level 0.02 µg/l Gain Sens, V/(µg/l) Range/(µg/l), 30x 1.0 5 10x 0.33 15 3x 0.1 50 1x 0.033 150	149
	Transmissometer	SeaTech	Path length: 25 cm Sensitivity: 1.25 mV	171

TABLE 1.5 Sensor specifications.

Parameter	Sensor	Instrument	Range	Accuracy	Resolution
Data Logger	SeaBird	SBE-25 1	600 m		
Temperature	SeaBird	SBE-03 2	-5°C +35°C	0.001°C	0.0002°C
Conductivity	SeaBird	SBE-4C 2	0-7 S/m (0-70mmho/cm)	0.0003 S/m (0.003mmho/cm)	0.00004 S/m (0.0004 mmho/cm)
Pressure			up to 600m (1 000psia)	0.015% of full scale	0.01% of full scale
Dissolved oxygen	SeaBird	SBE-43 2	120% of surface saturation ⁴	2% of saturation	unknown
Light intensity (PAR)	Biospherical	QSP-23003	400-700 nm		
Fluorescence	SeaTech	Chlorophyll-fluorometer	0-5 V	unknown	
Transmissometer	SeaTech		0-5 V	unknown	

Notes: 1 Maximum depth of 600m; 2 Maximum depth of 6800m; 3 Maximum depth of 2000m

Salinity samples

Salinity samples have been taken on most of the rosette cast for comparison with the conductivity sensor on the rosette.

Rosette water sampling

Water was sampled with the rosette according to each team's requests. To identify each water sample, we used the term "rosette cast" to describe one CTD-rosette operation. A different cast number is associated with each cast. The cast number is incremented every time the rosette is lowered in the water. The cast number is a seven-digit number: *xyyzzz*, with *xx*: The last two digits of the current year; *yy*: A sequential (Québec-Océan) cruise number; *zzz*: The sequential cast number. For this cruise, the first cast number is 1606001. To identify the nine rosette bottles on this cast we simply append the bottle number: 1606001nn, where "nn" is the bottle number (01 to 09).

The two types of casts are defined as either CTD or Rosette casts where CTD profiles are only used to collect data from the water column and Rosette samples are obtained for Chlorophyll, Nutriment, Dissolved Oxygen, CDOM, Salinity, Flow Cam, among other specified parameters.

Sampling stations (Leg 1)

All the information concerning the Rosette casts is summarized in the CTD Logbook (one line per cast) and an example is shown here in Figure 1.11. The information includes the cast number and station ID, date, and time of sampling in UTC, latitude, and longitude, bottom and cast depths, and comments concerning the casts.

Cast	Station	Date début	UTC	Heure UTC	Lat. (N)	Long. (W)	Fond (m)	Prof. cast (db)	Commentaires	Type	Init
001	pcbc2	30 / 09 /		19 : 43	71 ° 5.450	071 ° 50.920	696	697		Full	SB
002	pcbc3	01 / 10 /		13 : 11	70 ° 46.042	072 ° 15.617	444	437		basic	LB
003	Gibbs N	01 / 10 /		22 : 58	71 ° 7.378	070 ° 57.670	446	439		Nutrient	LB
004	176	02 / 10 /		13 : 13	69 ° 35.527	065 ° 26.024	195	187		Nutrient	LB
005	179a	03 / 10 /		08 : 34	67 ° 20.380	062 ° 36.947	110	96.4		Nutrient	LB
006	179	03 / 10 /		10 : 22	67 ° 24.974	062 ° 11.004	190	182		Nutrient	SB
007	180	03 / 10 /		13 : 55	67 ° 28.666	061 ° 45.314	210	200		basic-n	SB
008	181	03 / 10 /		16 : 41	67 ° 33.199	061 ° 22.589	1140	1130		Nutrient	LB
009	640	07 / 10 /		17 : 20	58 ° 55.486	062 ° 9.276	143	135.6		Nutrient	LB
010	645	08 / 10 /		04 : 16	56 ° 42.206	059 ° 42.230	119	109		Nutrient	SB
011	650	08 / 10 /		19 : 51	53 ° 48.293	055 ° 26.112	204	195		Nutrient	LB

FIGURE 1.11 CTD Logbook example, one line per cast.

An Excel® Rosette Sheet was created for every single cast. This file includes the same information as the CTD Logbook, plus a table of what was sampled and at what depth. Weather information at sampling time was also included in each Rosette Sheet and is summarized in a Meteorological Logbook (one line per cast). For every cast, data from three seconds after a bottle is closed, to seven seconds later, is averaged and recorded in the ASCII ‘bottle files’ (files with a btl extension). The information includes the bottle number, time and date, trip pressure, temperature, salinity, light transmission, fluorescence, dissolved oxygen. These files will be made available as soon as the data is processed and corrected, if necessary.

Problems encountered with CTD-Rosette

We encountered a transistor failure in the power supply of the transmissometer and fluorometer sensors at the beginning of the cruise. To fix the problem technician, Sylvain Blondeau had to short-cut the transistor circuit to bring power back to the sensors. However, when the pump was activated after some time in the saltwater, the current drawn to the batteries was too much causing it to lose memory and configuration of the ctd, ultimately stopping the connectivity with the computer on deck. After a few casts, the pump finally burst. After this, the oxygen and conductivity had to be disconnected from the pump and positioned vertically so that water could pass thru them during the cast. The ctd was then configured so that it would not activate the pump during the cast.

Preliminary results of thermohaline stratification in Hudson Bay (CTD profiles)

Temperature and salinity was recorded from the inner to the outer Nelson estuary as well as at James Bay mouth by the Idronaut CTD probe. Vertical CTD profiles show the distribution of riverine freshwater coming from Nelson River into Hudson Bay (Figure 1.12). Fresh and salty water start mixing in shallow water, whereby a strong outflow current of Nelson River might be the reason why salinity above 20 is measured in deeper water further away from the estuary. The warmer temperatures of the river water are following the same trend.

The high riverine freshwater input in James Bay is causing a strong thermohaline stratification at the entrance to Hudson Bay (Figure 1.13). A 20 m thick layer of less salty, warm water was found at the surface. According to the five CTD profiles in the centre of James Bay mouth, the halocline was slightly lower (30 m) than the thermocline (20 m).

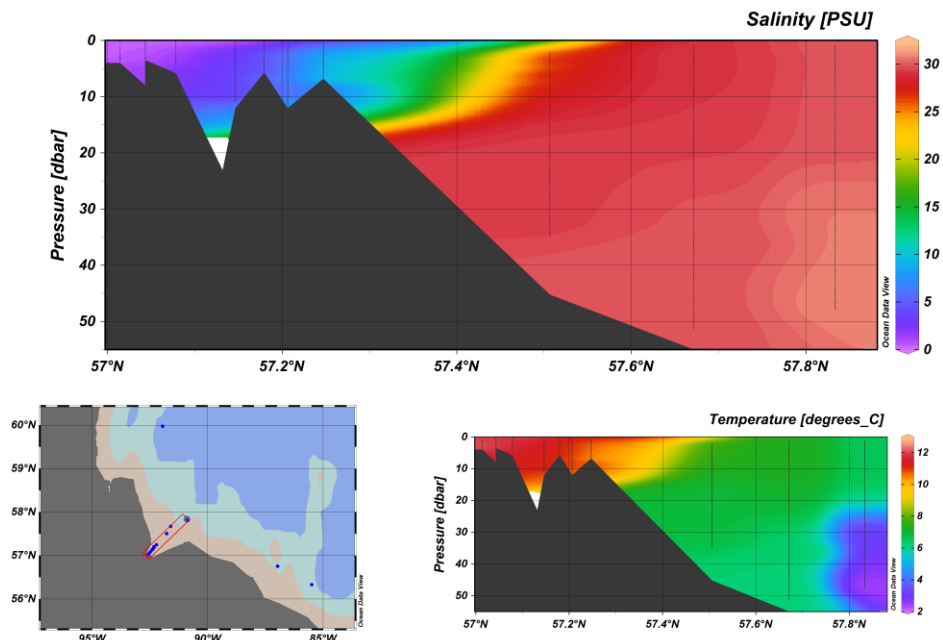


FIGURE 1.12 Temperature and salinity profile of Nelson Estuary CTD profiles (black lines) were taken in the inner and outer estuary.

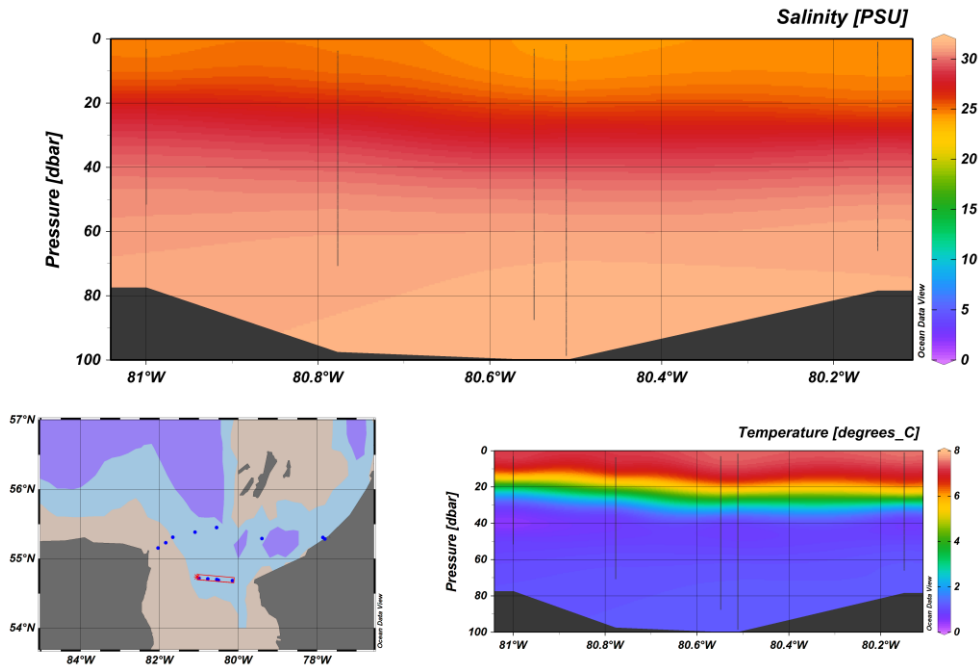


FIGURE 1.13 Temperature and salinity profile of James Bay mouth CTD profiles (black lines) were taken in the deep center of the opening to Hudson Bay.

1.3 Freshwater Dynamics

To understand the freshwater dynamics of the Hudson Bay before the onset of winter, water samplings were carried out by members of Team 1 all along the south and south-east coastal belt of Hudson Bay. The emphasis was on assessing the distribution of runoff from the Nelson and Churchill River and from the James Bay which normally accounts for 80% of the riverine input into the Hudson Bay. Few water samples were also collected in the northern Hudson Bay, near Coats and Mansel Island. Water samples collected, were intended for Total Suspended Solid (TSS) analysis along with CDOM and O18 measurement. Infield processing of the water samples was carried out for TSS retrieval, using vacuum filtration technique. Filters of pore size of $0.7 \mu\text{m}$ were used, and the filtered samples were stored in a -4°C freezer. CDOM samples were prepared by syringe filtration using a $0.2 \mu\text{m}$ filter in a 40ml amber coloured bottle. The filtered CDOM samples were stored in the $+4^\circ\text{C}$ refrigerator. Also, O18 and salinity samples were prepared. Salinity samples will serve as a calibration for the field measured salinity profile using the Idranaut/Rosette CTD. The filtered TSS and CDOM samples along with the O18 and salinity has been brought back to CEOS for laboratory analysis.

1.4 Nutrients and Biological Sampling

The composition and distribution of the phytoplankton community in Hudson Bay fluctuate throughout the year depending on the thermohaline stratification, nutrient supply, and the availability of solar radiation. The main goals for BaySys Team 3 were to assess the nutrient loading, phytoplankton biomass, and size distribution of the micro- and nano fraction concerning inshore/offshore gradients in oceanographic parameters (main focus on underwater downwelling irradiance) and the influence of regulated or unregulated rivers. The participation in the fall cruise aimed to gain a baseline in biological productivity when there is sufficient light but a likely low nutrient concentration found in the upper water column.

Optical and Biological Characterization of pre-freezing Conditions

The spectral light climate of the euphotic zone was investigated by in situ measurements of downwelling and upwelling irradiance as well as hyperspectral attenuation and transmission along the coast of southern Hudson Bay from Churchill, crossing James Bay, to Kuujjuarapik and at the entrance of the Bay between Coats Island, Mansel Island and Ivujivik. In Hudson Bay, a massive freshwater input by river runoff causes a strong stratification restricting upward nutrient flux into the surface layer and limiting phytoplankton production, particularly in summer. The resulting low chlorophyll-a concentration is expected to cause a high light transmission in the upper water column. However, coastal waters are strongly influenced by the sediment load from the numerous rivers which has a direct effect on the light attenuation coefficient. The aim of this investigation (under Team 1) was to describe the light conditions and inherent optical properties of the upper euphotic zone of Hudson Bay in fall before sea ice starts to form. To do so, a metal frame equipped with two UV-visible spectral radiometers (spherical RAMSES-ASC, TriOS GmbH, and Germany) and one hyperspectral VIS photometer (VIPER G2, TriOS) was lowered from the front of the vessel in the direction of the sun.

Measurements were taken from the surface to a depth of 30 m every 0.5 m, roughly. Incident solar radiation was recorded with one UV-visible spectral radiometer (Cosine RAMSES-ACC, TriOS GmbH, and Germany) at the same time (Figure 1.14). Inherent optical properties of the water column were investigated in terms of particle absorption, chlorophyll-a concentration, and the content of particulate organic carbon and nitrogen. Water for filtration was sampled by a rosette at three different depth levels: surface water between 1 m and 5 m, the depth of the chlorophyll maximum, and 10 m above the bottom. For laboratory analysis of particle absorption (a_p) by spectrophotometry as well as the analysis of chlorophyll-a concentration by high-performance liquid chromatography (HPLC) at the University of Manitoba, water samples of 1L were filtered through 25 mm Whatman GF/F filters and stored in a -80 °C freezer. Particulate organic carbon and nitrogen (POC/N) samples (0.5L) were filtered through 21 mm Whatman GF/F filters and stored at -80 °C.



FIGURE 1.14 Measurements of incident solar radiation (left, radiometer attached to a stick pointing upward), total underwater irradiance and hyperspectral absorption and transmission within the water column (right, radiometers mounted to a metal frame and lowered with a weight a straight alignment).

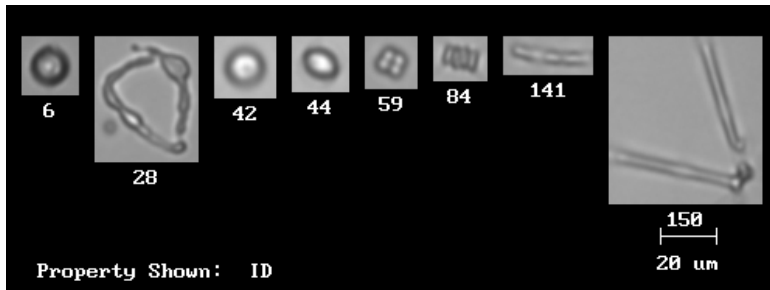
Characterizing the size distribution of the present micro-and nanophytoplankton

Water samples (100 mL) from the three depths were preserved with Lugol's solution in Amber bottles for later microscopic analysis. Furthermore, particles in the water from the same depth levels were directly analyzed by automated imaging technology (FlowCam, Fluid Imaging Technologies, INC., USA). The FlowCam is a dynamic imaging particle analyzer that examines a fluid under a microscope which is pumped through a flow cell. An integrated camera takes images of particles within the fluid and characterizes them in terms of particle size and shape. For this project, water samples of 10mL were pre-filtered through a 100 mm mesh to analyze the particle size fraction between 10 – 100 mm.

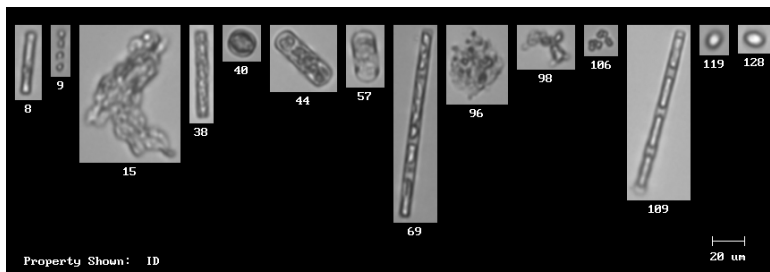
Preliminary FlowCam results support the assumption of a low number of phytoplankton in the water column. Many particles of the investigated size fraction were identified as zooplankton (protozoa), detrital organic matter, and inorganic sediment. Additionally, plankton appeared to differ in size and composition between Southern and Northern Hudson Bay. One reason might be the massive river runoff in the South flushing freshwater species into the Bay while in the northern part marine species are mainly found due to the strong inflow of seawater from the Atlantic Ocean. Differences in size might be linked with the low nutrient supply in the stratified southern Hudson Bay and the high nutrient concentration of the salty Atlantic water in the North. Particle composition also varied with depth. Small sediments as well as plankton with extensions (spikes, flagella) were mainly found in the upper water column. Penetrate phytoplankton of high abundance was often found in the bottom water. The following images represent a selection of imaged particles from different stations and depth levels.

Station M06 – Nelson estuary

Surface water (1 m)

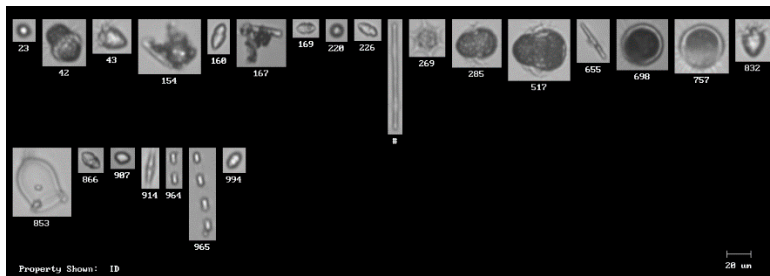


Bottom water (20 m)

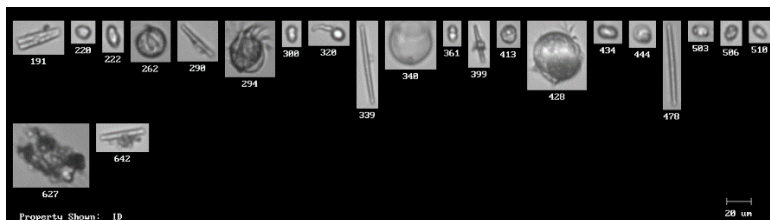


Station NE03 – Outer Nelson estuary

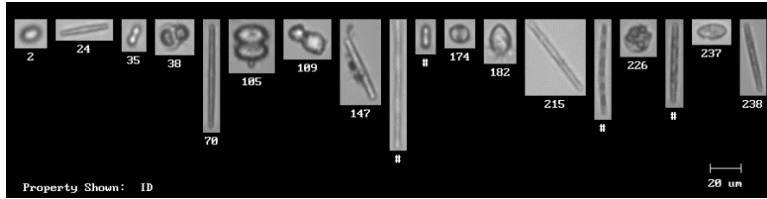
Surface water (1 m)



Chlorophyll maximum depth (20 m)



Bottom water (50 m)

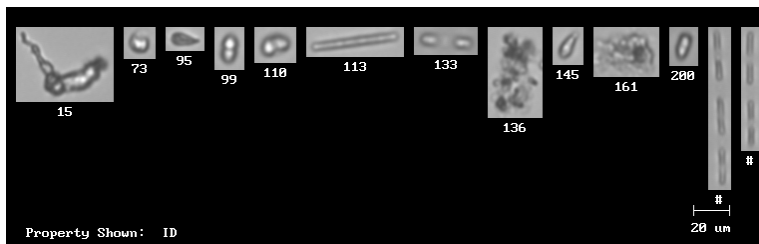


JB05 – James Bay

Surface water (1 m)

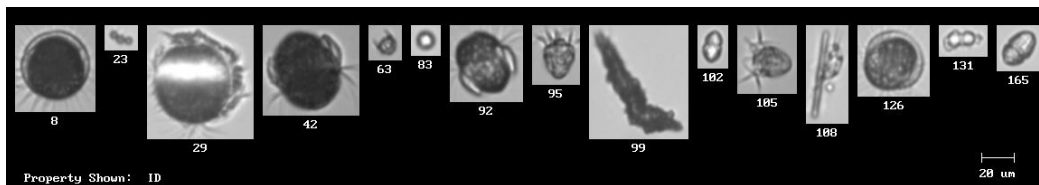


Bottom water (20 m)

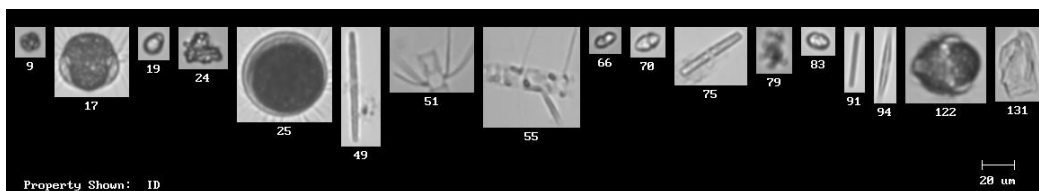


CI01 – Coats Island, Northern Hudson Bay

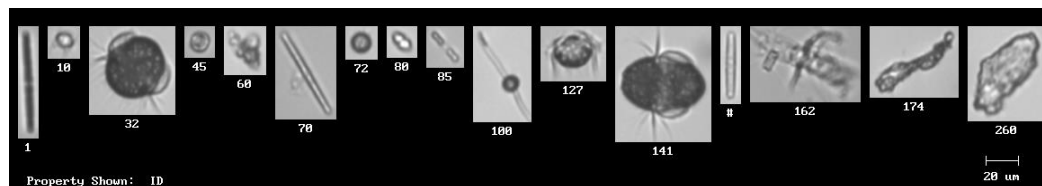
Surface water (1 m)



Chlorophyll maximum depth (40 m)



Bottom water (184 m)



1.5 Distribution of Phytoplankton

Samples for inorganic nutrients (ammonium, nitrite, nitrate, orthophosphate, and orthosilicic acid) were taken at the stations (see Appendix 1A) to establish detailed vertical profiles. Nitrite, nitrate, orthophosphate, and orthosilicic acid samples were stored at -20 °C in a freezer and sent for analysis using a Bran+Luebbe AutoAnalyzer 3 based on standard colorimetric methods adapted for the analyzer (Grasshoff et al. 1999) at the home laboratory. Ammonium samples were processed immediately after collection using the fluorometric method of Holmes et al. (1999). Water samples for chlorophyll-a in the water column (maximum 100 m depth) were filtered through 25mm GF/F filters and the filters were incubated in 90% acetone in a fridge (4 °C) for 24 h. Chlorophyll-a concentrations were measured using the fluorometric method of Parsons et al. 1984.

1.6 Carbon Cycling

The objective of Team 4 was to collect dissolved inorganic carbon (DIC) and dissolved organic carbon (DOC) to understand the carbon cycle in the coastal Arctic ocean environment.

Methods

We collected almost 100 DIC and DOC samples along the coast of Hudson Bay, from the Churchill River to James Bay. A novel experimental incubation approach, involving Pyro Science technology, was used to measure dissolved oxygen (DO) (see Figure 1.15 A/B/C). The objective of this experimental approach is to evaluate the rates of terrestrial OC remineralization in the Hudson Bay coastal waters during the June 2017 cruise.



FIGURE 1.15 Incubation setup, method, and equipment.

1.7 Sediment Sampling

One of Team 5's main sampling objectives was to collect a significant quantity of suspended sediment in the Hudson Bay by applying two techniques.

Methods

One approach was to use an industrial centrifuge device (3'W * 4'L * 2'H; weighs 315 kg; 2 hp motor; 115/230 V; 22.6/11.3 amp AC power), which was fixed to the deck of the ship with straps (Figure 1.16A). Fortunately, no electrical modifications were needed to accommodate the centrifuge. The other form of sediment collection was the filtration system.

To run the whole suspended sediment collection while the ship was moving, an inline water system (fire hydrant on the forward deck) was used to draw seawater from the ship's plumbing. During the entire period of the trip, suspended sediments were frequently collected and stored, approximately every 12 hours (Figure 1.16 B). Later, by matching the ship track to the time of sample collections (Figure 1.1), the physical and chemical properties of the suspended sediments will be linked back to the locations and the origin (source) of the materials in the suspended sediment can be determined by using a fingerprinting technique.

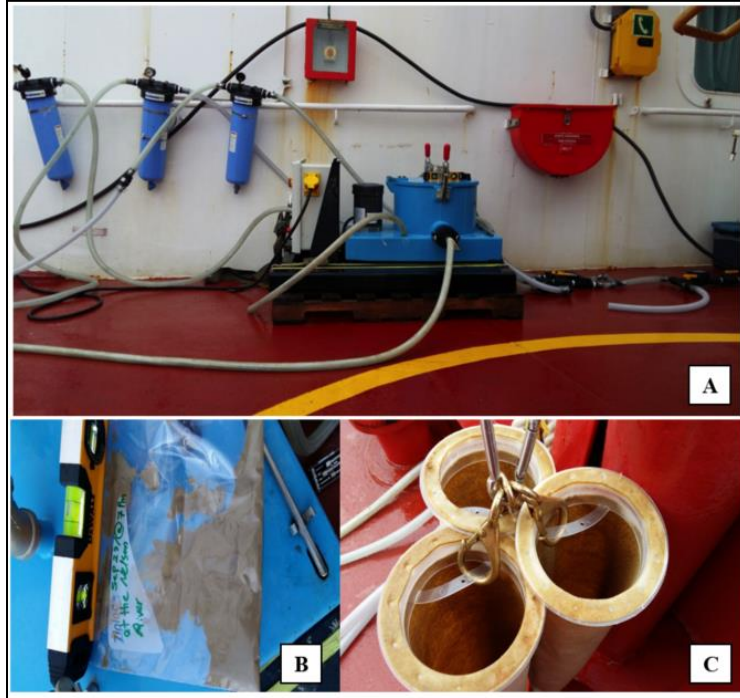


FIGURE 1.16 Industrial centrifuge set up, suspended-sediment samples, and collection tubes.

Appendix 1A: Water Parameters

Parameters collected at each station of the BaySys Des Groseilliers fieldwork between September 26 and October 8, 2016

Date	Station	Bottom depth [m]	CTD (Sea)	CTD (Iridronaut)	SPM	CDOM	O18	Salinity	Vertical light trap	HPLC	POC/N	Lugol	Flow cam	NO3, NO2, Si, PO4	NH4	Chl a
09/26/16	AN01	107	x	x	5, 30	5, 30, 100	5, 30, 100	5, 30, 100	0 - 30	5, 30, 100	5, 30, 100	-	-	5, 30, 100	5, 30, 100	5, 30, 100
09/27/16	AN04	60	x	x	1, 20, 50	1, 20, 50	1, 20, 50	1, 20, 50	0 - 30	1, 20, 50	1, 20, 50	1, 20, 50	1, 20, 50	1, 20, 50	1, 20, 50	1, 20, 50
	NE02	45	x	x	1, 20	1, 20, 35	1, 20, 35	1, 20, 35	0 - 30	1, 20, 35	1, 20, 35	1, 20, 35	1, 20, 35	1, 20, 35	1, 20, 35	1, 20, 35
09/28/16	NE03	55	x	-	1, 20, 50	1, 20, 50	1, 20, 50	1, 10, 20, 30, 40, 50	0 - 30	1, 20, 50	1, 20, 50	1, 20, 50	1, 20, 50	1, 10, 20, 30, 40, 50	1, 10, 20, 30, 40, 50	1, 10, 20, 30, 40, 50
09/29/16	NE04	11	-	x	-	-	-	-	0 - 30	-	-	-	-	-	-	-
	B3	3.5	-	x	1	1	1	1	-	1	1	1	1	1	1	1
	B5	5.8	-	x	1	1	1	1	-	1	1	1	1	1	1	1
	M6	23	-	x	1, 20	1, 20	1, 20	1, 20	-	1, 20	1, 20	1, 20	1, 20	1, 10, 20	1, 10, 20	1, 10, 20
	B7	12	-	x	-	-	-	-	-	-	-	-	-	-	-	-
	B8	5.7	-	x	-	-	-	-	-	-	-	-	-	-	-	-

	B11	12	-	x	-	-	-	-	-	-	-	-	-	-	-	-	-
	B12	6.8	-	-	-	-	-	-	-	-	-	-	-	-	-	-	-
09/30/16	SE01	63	x	x	1, 15, 56	1, 15, 56	1, 15, 56	1, 15, 56	0 - 30	1, 15, 56	1, 15, 56	1, 15, 56	1, 15, 56	1, 15, 56	1, 15, 56	1, 15, 56	1, 15, 56
	SR01	-	-	-	1	1	1	1	-	-	-	1	-	-	1	1	1
	WE01	110	x	x	2, 40, 100	2, 40, 100	2, 40, 100	2, 40, 100	0 - 30	2, 40, 100	2, 40, 100	2, 40, 100	2, 40, 100	2, 40, 100	2, 40, 100	2, 40, 100	2, 40, 100
	WR01	-	-	-	1	1	1	1	-	-	-	1	-	-	1	1	1
10/01/16	JB02	78	x	x	1, 25, 65	1, 25, 65	1, 25, 65	1, 25, 65	0 - 30	1, 25, 65	1, 25, 65	1, 25, 65	1, 25, 65	1, 25, 65	1, 15, 35, 45, 65	1, 15, 35, 45, 65	1, 15, 35, 45, 65
	JB01	50	x	-	1	1	1	1	-	-	-	1	-	-	1	-	-
	JB00	46	x	-	2, 10, 37	2, 10, 37	2, 10, 37	2, 10, 37	0 - 30	2, 10, 37	2, 10, 37	2, 10, 37	2, 10, 37	2, 10, 37	1, 10, 20, 30, 37	1, 10, 20, 30, 37	1, 10, 20, 30, 37
10/02/16	JB03	111	x	x	1	1	1	-	-	-	-	1	-	-	1	-	-
	JB04	107	x	x	1	1	1	-	-	-	-	1	-	-	1	-	-

	JB05	97	x	x	7, 20, 50, 87	7, 20, 50, 87	7, 20, 50, 87	-	-	7, 20, 87	7, 20, 87	7, 20, 87	7, 20, 87	7, 20, 87	7, 20, 30, 50, 60, 87	7, 20, 30, 50, 60, 87	7, 20, 30, 50, 60, 87
	JB06	77	x	x	1	1	1	-	-	-	-	1	-	-	1	-	-
	JB07	63	x	-	1	1	1	-	-	-	-	1	-	-	1	-	-
	JB08	45	x	-	1	1	1	-	-	-	-	1	-	-	1	-	-
	JB09	33	x	-	2, 10, 26	2, 10, 26	2, 10, 26	-	-	2, 10, 26	2, 10, 26	2, 10, 26	2, 10, 26	2, 10, 26	5, 10, 15, 20, 26	5, 10, 15, 20, 26	5, 10, 15, 20, 26
	JB09.5	27	x	-	5, 21	5, 21	5, 21	-	-	-	-	5	-	-	5, 21	5, 21	-
	JB08.5	37	x	-	5, 27	5, 27	5, 27	-	-	-	-	5	-	-	5, 27	5, 27	-
10/03/16	JB10	24	x	x	5	5	5	-	-	-	-	5	-	-	5	-	-
	JB11	47	x	x	5, 37	5, 37	5, 37	-	-	5, 37	5, 37	5, 37	5, 37	5, 37	5, 37	5, 37	5, 37
	JB12	64	x	x	5, 50	5, 50	5, 50	-	-	-	-	5, 50	-	-	5, 50	5, 50	5, 50
	JB13	95	x	x	5, 86	5, 86	5, 86	-	-	5, 86	5, 86	5, 86	5, 86	5, 86	5,2 0,4 5,8 6	5,2 0,4 5,8 6	5,2 0,4 5,8 6
	JB14	105	x	x	5, 45, 97	5, 45, 97	5, 45, 97	-	0 - 30	5, 45, 97	5, 45, 97	5, 45, 97	5, 45, 97	5, 45, 97	5, 45, 97	5, 45, 97	5, 45, 97

					5,70,160	5,30,70,100,160	5,30,70,100,160	5,30,70,100,160	0 - 30	5,30,160	5,30,160	5,30,70,160	5,30,160	5,30,160	5,40,50,70,100,160	5,40,50,70,100,160	5,40,50,70,100
	10/04/16	JB15	170	x	x												
		KU02	97	x	x	4,45,87	4,45,87	4,45,87	-	-	4,45,87	4,45,87	4,45,87	4,45,87	4,45,87	4,45,87	4,45,87
		KU01	43	x	x	-	-	-	-	-	-	5	-	-	5	5	
	10/06/16	C101	194	x	x	1,40,160,184	1,40,160,184	1,40,160,184	0 - 30	2,40,184	2,40,184	2,40,184	2,40,184	2,40,184	2,15,40,60,100,160,184	2,15,40,60,100,160,184	2,15,40,60,100
	10/07/16	W101	108	-	x	-	-	-	-	-	-	-	-	-	-	-	-
	10/08/16	C103	106	x	-	5,40	5,40	5,40	5,40	-	5,40	5,40	5,40	5,40	5,20,30,40	5,20,30,40	5,20,30,40
		C102	208	x	-	5,20,100,199	5,20,100,199	5,20,100,199	-	5,20,199	5,20,199	5,20,199	5,20,199	5,20,199	5,20,40,60,100,150,199	5,20,40,60,100,150,199	5,20,40,60

	MI02	125	x	x	2, 10, 60, 117	2, 10, 60, 117	2, 10, 60, 117	2, 10, 60, 117	0 - 30	2, 10, 117	2, 10, 117	2, 10, 117	2, 10, 117	2, 10, 117	2, 10, 20, 40, 60, 100, 117	2, 10, 20, 40, 60, 100, 117	2, 10, 20, 40, 60
	MI01	68	x	x	5, 15, 60	5, 15, 60	5, 15, 60	5, 15, 60	0 - 30	5, 15, 60	5, 15, 60	5, 15, 60	5, 15, 60	5, 15, 60	5, 15, 25, 35, 45, 60	5, 15, 25, 35, 45, 60	5, 15, 25, 35, 45, 60
	NO1	50	x	x	-	-	-	-	-	-	-	-	-	-	-	-	-

Appendix 1B: CCGS Des Groseilliers Science Logbook

Date	Station Name	Latitude (N)	Longitude (W)	Device deployed	Time submerging (UTC)	Water depth (m)	Time surfaced (UTC)	Air Temp (deg. C)	True wind (direction-deg)	True wind (speed, kn)	Sea state (m)	Comments
26-Sep	AN01	60.0525	92.10417	Acoustic release	14:45	98	14:54	5.4	160	11	2.5	Attempted AN retrieval
26-Sep	AN01	60.03444	92.10722	Acoustic release	14:57	96	15:03	5.5	160	11	2.5	
26-Sep	AN01	60.04278	92.07639	Acoustic release	15:06	96	15:15	5.5	160	11	2.5	
26-Sep	AN01	60.08611	92.055	Light profiler	18:15	105	18:19	5.4	180	5	3	
26-Sep	AN01	60.09778	92.11528	Light profiler	18:20	100	18:24	5.4	180	5	3	
26-Sep	AN01	60.01	91.99	Mooring	21:22	112	na	5.2	270	3	2.5	
26-Sep	AN01	60.05917	92.17611	Rosette	23:43	107	23:46	5.3	350	14	2	Attempt 1

26-Sep	AN01	60.06139	92.16472	Rosette	23:50	107	0:01	5.3	350	14	2	Attempt 2
26-Sep	AN01	60.055	91.96611	Rosette (not completed)	0:25	100	0:32	5.2	0	13	1.5	Attempt 3
26-Sep	AN01	60.05111	91.96917	Idronaut	0:37	100	0:48	5.4	0	15	1.5	
26-Sep	AN01	60.04139	91.97472	Niskin sampling	0:51	100	0:58	5.3	0	15	1.5	
27-Sep	AN04	57.7575	91.68139	Light profiler	15:07	54	15:21	6.5	40	14	1.5	
27-Sep	AN04	57.76444	91.69611	Light profiler	15:27	53	15:37	6.5	45	14	1.5	
27-Sep	AN04	57.73833	91.64389	Rosette	16:30	60	16:47	6.7	350	15	2	
27-Sep	BS03	Canceled	Canceled					7.2	40	15	2.5	Transiting over night
27-Sep	BS04	57.55333	91.92306	Rosette	19:45	44	19:49	6.8	50	15	2.5	
27-Sep	BS04	57.60861	92.03917	Rosette	20:08	45	20:19	6.7	45	12	2	
27-Sep	BS04	57.55444	91.84806	Light profiler	20:36	45	20:42	6.7	75	13	2	
27-Sep	BS04	57.53972	91.89722	Light profiler	20:48	45	20:59	6.7	80	13	2	
27-Sep	BS04	57.50194	91.82639	Mooring (wheel)	23:24	46	na	7.4	90	8	1.5	
27-Sep	BS04	57.50833	91.91167	Mooring (ADCP)	23:23	46	na					Same unit
27-Sep	BS04	57.55722	91.8425	Niskin sampling	23:43	47	23:44	7.3	90	10	1.5	Failed- too much current
27-Sep	BS04	57.53389	91.87472	Niskin sampling	23:49	47	23:53	7.3	90	10	1.5	Failed- too much current
28-Sep	BS06	58.02917	91.00583	Rosette	20:30	57	20:43	8.6	230	20	1.5	

28-Sep	BS06	57.83528	91.02306	Rosette	20:51	55	20:53	8.6	230	20	1	
28-Sep	BS06	58.03361	91.0825	Mooring (tube)	22:31	54	na	9.4	250	15	1	Position of tube
28-Sep	BS06	58.02833	91.11333	Mooring (train wheel)		54	na	9.4	250	15	1	Train wheel
28-Sep	BS06	58.03194	91.02167	Light profiler	22:55	56	23:06	9.2	270	13	1	
28-Sep	BS06	58.02444	90.97361	Rosette	23:10	59	23:24	9.2	270	12	1	
29-Sep	BS07	57.51333	92.38361	Light profiler	15:29	11	15:37	8.2	215	12	0.5	
29-Sep	M6 (drop 1)	57.14278	92.55139	Mooring (ADCP)	15:51	29.7	na		225	15		Helicopter
29-Sep	M6 (drop 2)	57.37306	92.59556	Mooring (train wheel)	17:51	29	na		225	20		Helicopter
30-Sep	BS08	56.88917	87.06	Light profiler	13:50	62	14:04	8.3	230	12	1	
30-Sep	S01	56.13056	87.82222	River sample								Severn River-helicopter
30-Sep	BS08	56.84944	87.08028	Rosette	15:17	63	15:36	8.5	250	10	1	
30-Sep	W01	55.44722	85.36111	River sample								Winisk-helicopter
30-Sep	BS09	56.34056	85.75417	Rosette	19:46	110	20:04	8.4	240	15	1	
30-Sep	BS09	56.37583	85.69556	Light profiler	20:12	109	20:14	9.8	250	14	1	
30-Sep	BS09	56.38278	85.67472	Light profiler	20:18	108	20:38	9.8	250	14	1	
01-Oct	JB02	54.72944	80.39306	Rosette	14:27	78	14:45	8.6	180	10	1	
01-Oct	JB02	54.71944	80.35417	Light profiler	14:56	73	15:15	8.1	170	5	1	

01-Oct	JB02	54.93694	80.24611	Mooring	17:03	101	na	9	220	10	1	
01-Oct	JB01	54.85611	80.08611	Rosette	18:14	50	18:26	8.6	180	10	0.5	
01-Oct	JB01	54.84306	80.07889	Rosette	18:39	51	18:42	8.5	180	10	0.5	
01-Oct	JB00	54.75833	80.04167	Rosette	19:16	46	19:29	8.9	190	15	1	
01-Oct	JB00	54.75417	80.03833	Light profiler	19:39	46	19:47	8.8	190	15	0.5	
01-Oct	JB03	Canceled	Canceled	Rosette								
02-Oct	JB03	54.85444	80.68333	Rosette	10:21	111	10:31	6	45	20	2	
02-Oct	JB04	54.74806	80.78889	Rosette	11:11	107	11:21	6	30	24	2	
02-Oct	JB05	54.86917	80.93972	Rosette	12:20	97	12:39	6.1	35	25	2	
02-Oct	JB06	54.80389	81.25639	Rosette	13:29	77	13:41	6.1	15	22	2	
02-Oct	JB07	54.75556	81.42611	Rosette	14:26	63	14:34	5.9	20	22	2	
02-Oct	JB08	54.85861	81.54194	Rosette	16:59	45	17:08	4.9	0	25	3	
02-Oct	JB09	54.92778	81.91472	Rosette	17:55	33	18:09	5.8	35	23	3	
02-Oct	JB95	55.04167	82.00889	Rosette	18:45	27	18:54	6.8	35	22	2	
02-Oct	JB85	54.81806	81.84028	Rosette	19:48	37	19:57	5.2	30	20	2.5	
03-Oct	JB10	55.24472	82.15278	Rosette	10:20	24	10:25	5	160	13	1	
03-Oct	JB11	55.46111	82.03111	Rosette	11:18	47	11:27	5.5	170	18	1	
03-Oct	JB12	55.51611	81.86833	Rosette	12:22	64	12:32	5	170	20	1.5	

03-Oct	JB13	55.64417	81.34361	Rosette	14:16	95	14:32	5.7	175	18	1.5	
03-Oct	JB14	55.45139	80.61389	Rosette	16:23	105	16:36	6.4	170	25	1.5	
03-Oct	JB14	55.51361	80.58806	Light profiler	16:42	102	16:51	6.5	180	23	1.5-2	
03-Oct	JB15	55.41833	79.43167	Rosette	21:46	170	22:07	8.4	200	27	2.5	
03-Oct	JB15	55.39778	79.63861	Light profiler	22:13	166	22:21	8.4	200	27	2.5	
04-Oct	KU02	55.45361	77.92444	Rosette	10:20	97	10:37	10.7	210	19	1	
04-Oct	KU01	55.35194	77.89028	Rosette	11:18	43	11:24	1.2	225		1	
06-Oct	CI01	62.66583	80.36361	Rosette	19:00	194	20:12	-0.6	25	15	2	
06-Oct	CI01	62.63056	80.37111	Light Profiler	20:17	191	-	-0.6	10	18	1	Cancelled
06-Oct	WI01	62.59222	80.41167	Light profiler	20:24	191	20:30	-0.6	10	18	1	
07-Oct	CI03	63.30361	83.89944	Idronaut (CTD)	14:10	108	14:15	-1.6	320	6	0.5	
08-Oct	CI02	62.9775	81.75056	Rosette	11:00	106	11:19	-0.5	20	16	1	
08-Oct	MI02	62.82056	81.04361	Rosette	13:34	208	13:56	-0.8	25	20	1	
08-Oct	MI02	62.46472	78.83722	Rosette	18:51	125	19:10	-0.5	15	20	1	
08-Oct	MI01	62.28306	78.85444	Light Profiler	19:16	131	19:24	-0.5	20	18	1	
08-Oct	MI01	62.44139	78.44222	Rosette	20:10	68	20:24	-0.2	20	18	2	
08-Oct	MI01	62.375	78.52222	Light Profiler	20:31	70	20:38	-0.5	20	18	1	
09-Oct	NI01	63.4175	78.41667	Rosette CTD only	18:17	50	18:24	0	310	15	1	

WINTER/SPRING 2017



Helicopter lifting off from ice after dropping research teams off during a mobile ice survey. This sea ice survey was conducted from February 1 to February 15, 2017, off the coast of Churchill, Manitoba.

CHAPTER 2 - CHURCHILL RIVER AND MOBILE ICE SURVEY

FIELDWORK PARTICIPANTS

Team 1: David Babb¹, Dr. Jack Landy¹, and Nic Zilinski¹

Team 3: Gabrièle Deslongchamps², Lisa Matthes¹ and Laura Dalman¹

Team 4: Dr. David Capelle¹ and Dr. Nicolaus Xavier Geilfus¹

Team 5: Dr. Kathleen Munson¹

¹Centre for Earth Observation Science, University of Manitoba, 535 Wallace Building, Winnipeg, MB

²Québec-Océan, Department of Biology, Pavillon Alexandre-Vachon, 1045, Avenue de la Médecine, Local 2078, Université Laval, Québec, QC

CITE CHAPTER AS Babb, D., Deslongchamps, G., Capelle, D., and Munson, K. 2019. Churchill River and Mobile Ice Survey. Chapter 2 in, *Hudson Bay Systems Study (BaySys) Phase 1 Report: Campaign Reports and Data Collection*. (Eds.) Landry, DL & Candlish, LM. pp. 39-66.

2.1 *Fieldwork Objectives*

A series of focused field programs took place within Hudson Bay during 2017 to provide a time series of winter and summer observations from the Bay. The first of these field programs was a winter survey of the Churchill River estuary and mobile ice pack offshore from Cape Churchill in Southwestern Hudson Bay. Nine participants from four of the five teams that comprise BaySys spent two weeks in Churchill to conduct in situ sampling of the ice and underlying water column, while also deploying an array of autonomous equipment to collect a longer temporal dataset of key variables both in the estuary and in the mobile ice pack. Scientists stayed at the Churchill Northern Studies Centre (CNSC) who provided snowmobiles for the estuary sampling (Figure 2.1), while two A-Star helicopters from Great Slave Helicopters were used to access the offshore ice pack (Figure 2.2).



FIGURE 2.1 Ice and water sampling in the Churchill River estuary and Button Bay. CTD casts were taken at the same sites. The river site includes water sampling only.

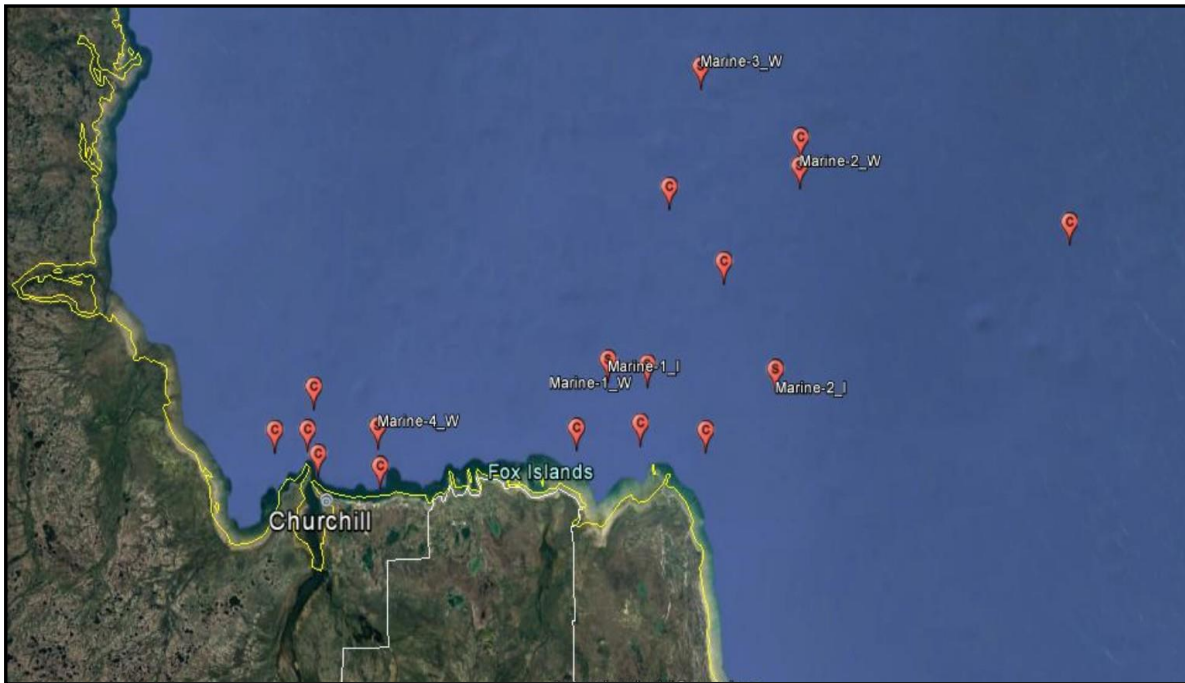


FIGURE 2.2 Ice and water sampling (S) on the mobile ice in Hudson Bay. CTD casts were taken at the same sites and at separate CTD stations (C).

2.2 Study Area

This study took place on the mobile ice pack offshore from Cape Churchill in southwestern Hudson Bay. The study area was confined by a maximum flight radius of 150 km from the Churchill Northern Studies Center that is located 28km east of Churchill (white circle Figure 2.1). The study area is comprised of a mix of landfast and mobile ice with a large lead located along the landfast ice edge, furthermore, there are large shallow tidal flats and a large input of freshwater from the Churchill River that influence the area. This freshwater typically flows out of the Churchill River Estuary to the west-northwest along Cape Churchill.

Within this project, we are specifically interested in sampling the ice and water column, and deploying an array of autonomous equipment on the mobile ice pack, while collecting water samples along the landfast ice to track the fate of the under-ice freshwater layer. The mobile ice is located offshore from the landfast ice that forms along Cape Churchill and varies in width from 1-2 km up to 5-6 km.

Between the landfast and mobile ice is a large lead that opens and closes according to the surface winds, and can thus change quickly. The mobile ice pack is in near-constant motion as a result of surface winds, ocean currents, sea slope, the Coriolis force, and internal stresses that arise due to ice floes interacting with each other. Ultimately the combination of these forces creates a dynamic ice pack that is comprised of large pans of ice that have thermodynamically thickened, large rubble fields that are completely ridged with no discernable pans, areas of open water, and areas of new ice that were recently areas of open water where new ice has formed and is thickening. Like any mobile ice cover, the ice pack can either thicken

dynamically, through ridging and rafting events or thermodynamically, through the accretion of sea ice along the underside of the ice due to the vertical temperature gradient (cold atmosphere, warm ocean). Dynamic thickening is especially strong along the edge of the landfast ice where the Stamukhi builds as the mobile ice pack is continuously pushed against the landfast ice. From personal accounts we know the Stamukhi along Cape Churchill is quite large, meaning that it also extends quite far below the water level as well and may trap buoyant freshwater under the landfast ice.

2.3 *Logistical Summary*

The research team was comprised of 9 persons. David Babb (Team 1) acted as Chief Scientist during this campaign. He is currently a research associate with Dr. David Barber at CEOS studying sea ice dynamics and thermodynamics. Dr. Jack Landy (Team 1) is a Postdoctoral Research fellow with Dr. David Barber at CEOS studying sea ice thermodynamics and remote sensing of sea ice. Nicholas Zilinski (Team 1) is an undergraduate student in the faculty of Engineering at the University of Manitoba, NSERC summer student with Dr. Ryan Galley at CEOS developing an inexpensive Ice Mass Balance buoy. Gabrièle Deslongchamps (Team 3) is a research associate with Dr. J.E. Tremblay at U. Laval studying the biological availability of nutrients in the water column. Lisa Matthes (Team 3) is a Ph.D. candidate with Dr. C.J. Mundy and Dr. Jens Ehn at CEOS studying the optical properties of the sea ice-covered water column and their relation to biological productivity. Laura Dalman (Team 3) is a M.Sc student with Dr. C.J. Mundy and Dr. David Barber at CEOS studying under-ice algae. Dr. David Capelle (Team 4) is a Postdoctoral Research fellow with Dr. Tim Papakyriakou at CEOS studying the Carbon system in Hudson Bay. Dr. Kathleen Munson (Team 5) is a Postdoctoral Research fellow with Dr. Fei Wang at CEOS studying contaminant chemistry in Hudson Bay. Lastely, Dr. Nicolas Xavier Geilfus (Team 4/5) is a research associate with Dr. Fei Wang and Dr. Soren Rysgaard at CEOS studying the Carbon system in Hudson Bay.

Two A-Star 350 B2 helicopters were hired from Great Slave Helicopters in Yellowknife to support the research program. Two Pilots, Jon Talon and Patrick Robert, and one mechanic, Peter Murdoch, ferried two machines to Churchill from Yellowknife on February 6th, 2017. We subsequently had 8 consecutive days of good weather and worked on the ice each day from February 7th to 14th, 2017.

The helicopters require 18.5” (47 cm) of sea ice to safely shut down the engines on the ice surface. At each landing site, one scientist would exit with a manually operated 2” auger and drill until they reached 18.5” depth (pre-marked on each auger). If the ice thickness was thinner than 18.5” they would return to the helicopter and look for a new floe, but if the ice were thicker than 18.5” they would drill two more holes to re-ensure the floe was suitable. Helicopters would also start up every hour to keep the engines warm out on the ice.

All 12 members of the team stayed at the Churchill Northern Studies Center (CNSC), located 28 km east of Churchill. Lodging, food, lab space, and logistical support were provided by CNSC, specifically the scientific Director LeeAnn Fishback. The helicopters parked in the CNSC parking lot overnight and

would typically make a fuel run to the airport first thing in the morning or right after returning from the ice depending on daylight.

2.4 *Ice Conditions in the Study Area*

The ice cover in Hudson Bay is seasonal, meaning that it melts out every summer. Fall freeze-up typically begins around mid-November in northwestern Hudson Bay and progresses to the southeast, eventually covering the entire Bay by early to mid-December. During Fall 2016, freeze-up within Hudson Bay was delayed. Using weekly ice charts from the Canadian Ice Service we can see that the landfast ice around the Bay began forming in mid to late November (Figure 2.4). Freeze-up proceeded through Northwestern Hudson Bay until the entire Bay became ice-covered around December 19. Note that once the Bay froze over in mid-December we have switched from presenting ice charts displaying sea ice concentration to those displaying a stage of development. Concentration can still be gleaned from the ice egg code for each polygon, but stage of development is more descriptive of the seasonal growth of the ice cover. On December 19 the entire Bay was covered with sea ice, however, it was predominantly new ice (light purple), Grey ice (dark purple), and Grey white ice (purple). Through January and into February we see the seasonal transition towards thicker ice types as the existing ice cover within Hudson Bay thickens through both thermodynamic and dynamic processes. By the start of our helicopter survey, the Bay was predominantly covered by thin, first-year sea ice which the CIS characterizes as being 30-70cm thick.

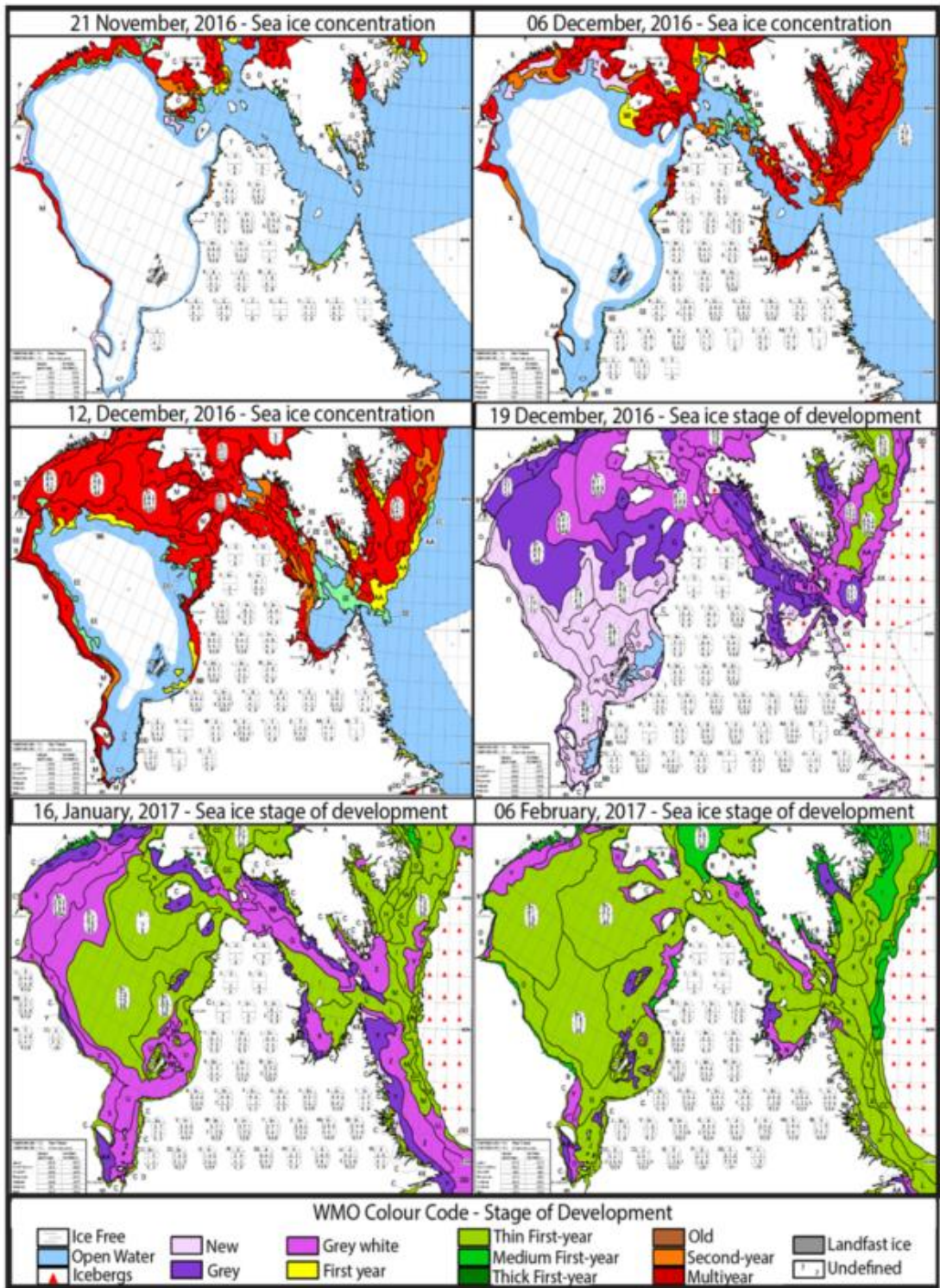


FIGURE 2.3 CIS ice charts during winter 2016-2017 over the study area.

Northwesterly winds are most common over our study area and contribute to the semi-permanent formation of a lead along the fast ice edge in Northwestern Hudson Bay. This lead or polynya, depending on the size, is obvious in

the ice chart from February 6, 2017, as the band of Grey-white ice that separates the narrow band of landfast ice from the Thin First-year ice pack. This lead varies according to the winds, but under strong northwesterly winds, the lead can extend 100s of km's and essentially push the older thicker ice types out of the study area (Figure 2.3). Looking at ice charts from our study period during recent years we can see that generally, the lead remains within 10s of km's of the northwestern coast of Hudson Bay (e.g. 2012, 2014, 2015, 2016), however, in 2011 and again in 2013 strong northwesterly winds caused the lead to open quite wide and form a large polynya across all of Northwestern Hudson Bay. In 2011 we likely would have found suitable ice near Cape Churchill, however, in 2013 we likely would not have found suitable ice to land on within range of the helicopters.

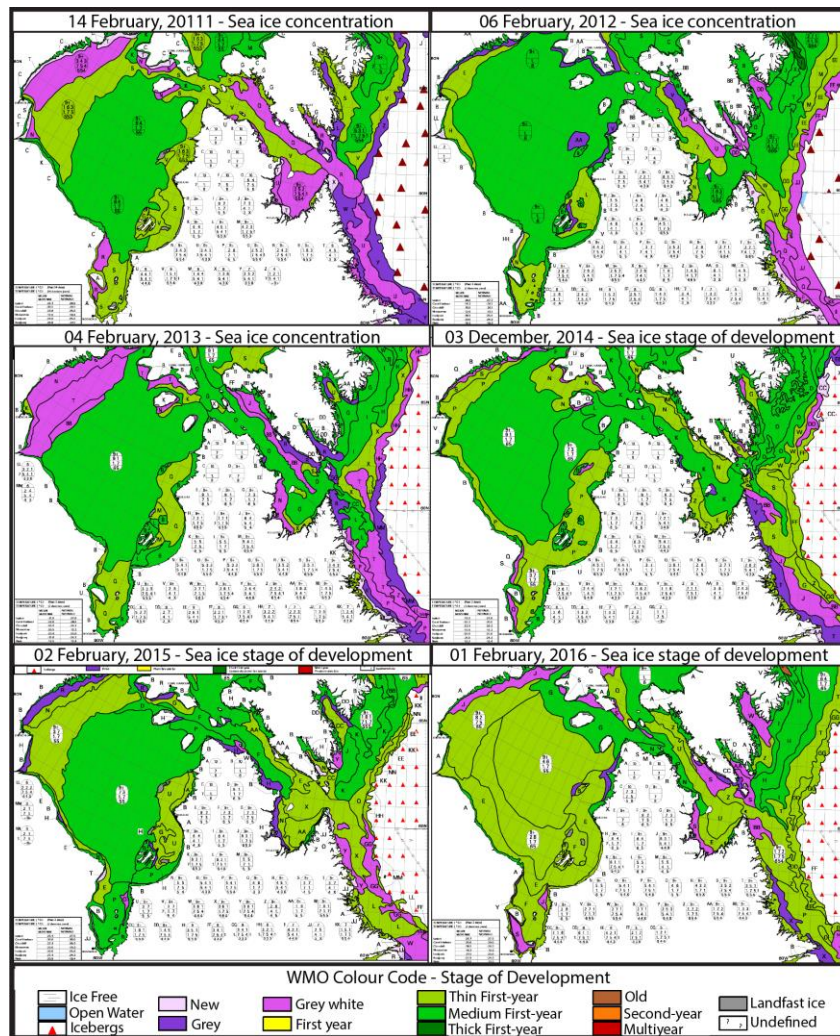


FIGURE 2.4 CIS ice charts over the study area during the 6 previous years.

2.5 Team 1 – Climate and Marine System

The campaign objectives for Team 1 were to conduct CTD's in the offshore marine environment and under the landfast sea ice to identify the under-ice freshwater layer and to deploy an array of autonomous equipment to track the seasonal evolution of the dynamic and thermodynamic nature of the ice pack. Beyond these tasks, David and Jack collected several Radarsat and Sentinel scenes over the study area that were used to target potential study sites and will subsequently be used to provide a broader context to our observations. Radarsat imagery will continue to be collected over the drifting array every week in collaboration with the Canadian Ice Service, and opportunistic Sentinel imagery over the study area will also be collected.

A CTD survey was conducted via helicopter from the mouth of the Churchill River Estuary to the northeast corner of the landfast ice off of Cape Churchill with two additional CTD's done near the mouth of the estuary on the mobile ice pack. Starting from the Estuary to Cape Churchill 7 CTD's (West to east: EST4, Fast4, Fast5, Fast6, Fast3, Fast2, and Fast1) were collected at variable intervals depending on flying conditions. Overall, we saw a large freshwater river plume at Est4 that gradually diminishes as you move west through Fast4 and Fast5 before ultimately disappearing by Fast 6. A freshwater signal was also detected at MB10 in the offshore mobile ice pack, but the other offshore site (STM3) that was located to the northwest of the Churchill River Estuary shows a completely marine signal. The final 3 stations (Fast 1, 2 & 3) also show a completely marine signal with salinities of 32.5 (Figure 2.5). Overall, it appeared that the freshwater from the Churchill River is partially retained behind the stamukhi and funneled westward under the landfast ice, but that within 30 km's the fresh water is lost to the Bay. A portion of this signal is present in the area just beyond the stamukhi. Furthermore, the water column at each site was at or very near the freezing point.

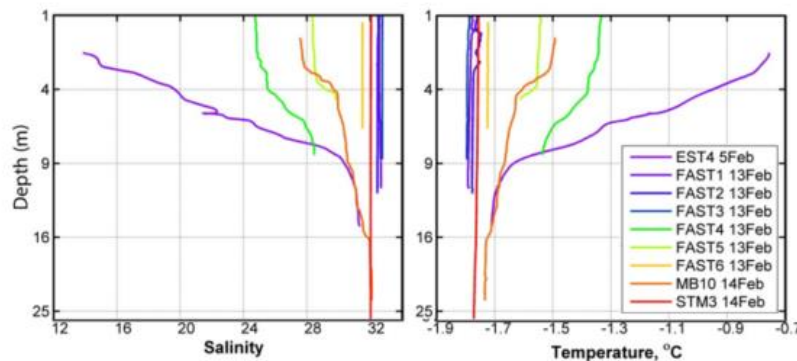


FIGURE 2.5 CTD profiles from the landfast ice and offshore near the Churchill River Estuary.

Moving onto the offshore area, we present 7 additional CTD's from the mobile ice pack and the three furthest west CTD's from the landfast ice. In the offshore area, we find a clear marine signal through the unstratified water column. Again, all profiles showed the water column at the freezing point. All profiles show no vertical stratification indicating a well-mixed water column. Interestingly there is substantial horizontal variability in the salinity of each profile, with the highest salinity being present in the 3 profiles

collected under the western end of the landfast ice (Figure 2.6). A first guess at this is that these sites are influenced by brine rejection from the nearby lead where brine enriched waters may be tidally pumped under the landfast ice. Future work with physical oceanographers should help to elucidate these mechanisms.

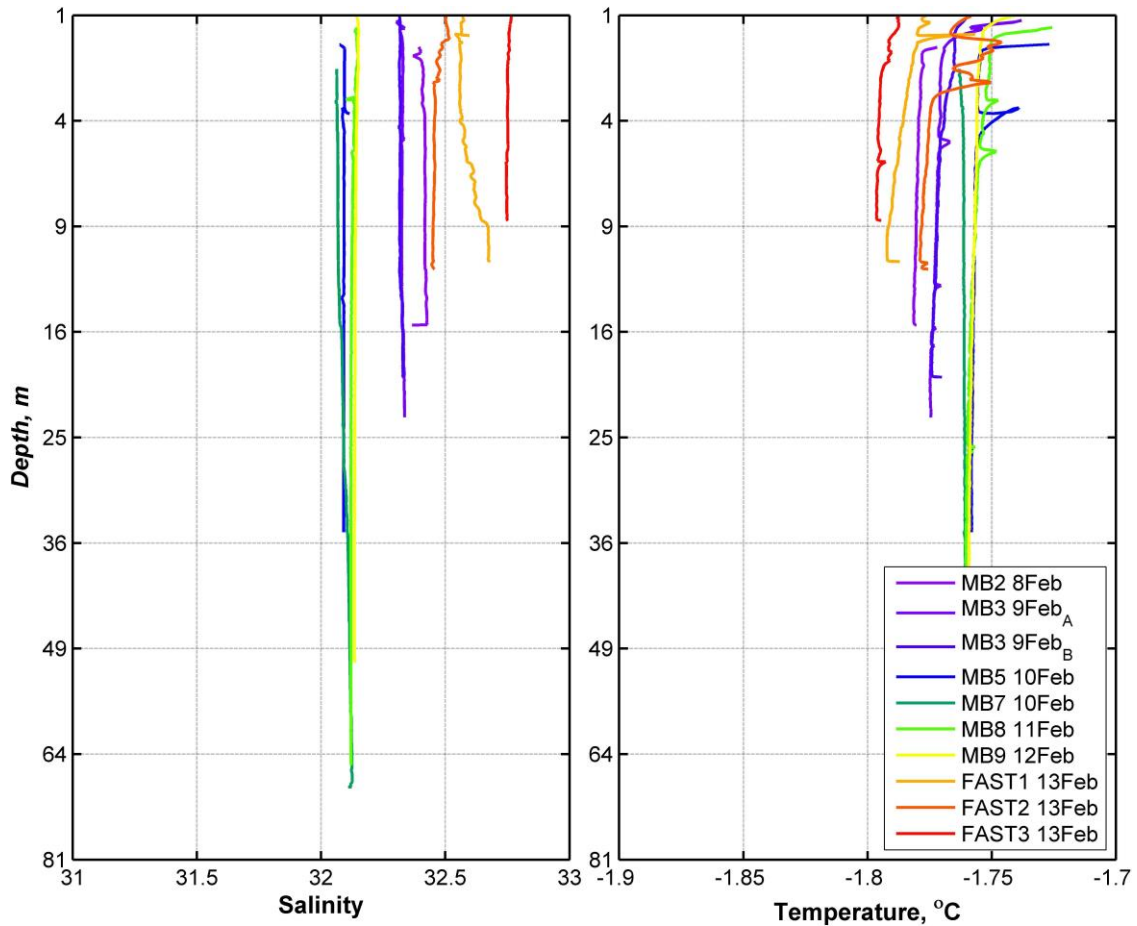


FIGURE 2.6 CTD profiles from the offshore marine area.

Four different autonomous systems that all use the Iridium communications network were deployed on the mobile ice. Ice drift beacons (x14): built by Solara Communications and David Babb from CEOS. The ice beacons simply transmit their GPS location every hour to an online data portal, allowing us to track the drift of individual ice floes and the relative drift of ice beacons deployed in pairs or arrays. The beacons are enclosed within a 20" long tube comprised of 6" internal diameter Drain Water Ventilation PVC (DWV-PVC) with a sealed cap at the bottom end and a waterproof screw-on cap at the upper end. An internal frame comprised of acrylic rods and PVC sheets houses the batteries and iridium/GPS unit. The beacon is deployed into a 10-12" deep 8" auger hole that anchors the beacon in the ice and keeps the batteries partially insulated from extreme air temperatures (Figure 2.7). Live data can be accessed through the Solara online data portal where the transmission frequency can also be adjusted.



FIGURE 2.7 Ice beacon deployed on a mobile ice floe. Approximately 12" is visible above the snow.

Note that one ice beacon unit (IMEI 300134010906880) was built into a larger surface float with a line suspended below that had 4 Alec CT sensors and 2 HOBO pressure transducers attached. CT sensors were set at 2m (#1583), 4m (#1592), 8m (#1574), and 16m (#1300), depths while the pressure transducers were at 1.68 m (#11013571) and 18m (#11013570) depth. None of the data from the CT or pressure transducers will be telemetered, but the plan is to recover this buoy with the Amundsen this June and download 5 months of continuous data from the 6 sensors. There is a chance that this buoy will remain in the ice until we recover it, but there is also a chance the ice floe it is on will melt out. As a result, the buoy was deployed with 4 large floats attached around the PVC tubing to provide flotation but also ensure that it stays upright and continues to transmit its position. CEOS Ice Mass Balance buoy (x1): A prototype of the new CEOS IMB built in house by Nic Zilinski, Ryan Galley, and David Babb. The system measures air temperature, air pressure, snow depth, ice thickness, and a vertical temperature profile through the ice into the surface water, and transmits hourly data via Iridium. The system historically was based on Campbell Scientific's CR1000 data logger and associated Loggernet software, however, this new version runs off of an Arduino and uses various components to communicate with the various sensors. The entire system was mounted on a steel tripod and anchored to the ice with ice screws and a central mast for the underwater sounder.



FIGURE 2.8 CEOS IMB deployed on the mobile ice. Note the yellow logger case that houses the batteries and hardware, acoustic snow sounder deployed to the left of the tower, air temperature and pressure shields at the top of the tripod and the iridium antenna at the very top.

SAMS Ice Mass Balance buoy (x3): Purchased from the Scottish Association of Marine Sciences, the SIMBA unit doesn't use sounders to detect the top and bottom ice interfaces. Instead, it relies on a high resolution 4.5 m long temperature string with sensors at 2 cm intervals to provide a vertical temperature gradient through the air, snow, ice, and water profile. The system is comprised of a pelican case that houses the batteries, hardware, and iridium/GPS antenna, and a thin temperature string that is simply deployed through a 2" auger hole through the ice with a small weight at the bottom to keep the line taut (Figure 2.8). A surface stand comprised of 4 PVC (1 1/2" inner diameter) legs and 1 temperature string arm was constructed to hold the pelican case above the snow and anchor the temperature string. The pelican case was secured to the stand with two ratchet straps, with attention paid to make sure the metal ratchets were underneath the case as to not interfere with Iridium communications, and to avoid pressure on the Temperature string. Temperatures are recorded every hour ($t = 0$), then a voltage is applied to each sensor and subsequent temperature readings are taken at $t = 15, 30,$ and 60 s delays. This provides data on the thermal conductivity of the surrounding medium and can further differentiate between air, snow, ice, and water.

TABLE 2.1 SIMBA deployment details.

	Deployment Date	Ice thickness (snow depth)	Coordinates	Notes
SIMBA 01	February 9, 2017	74 cm (5 cm)	59.32972 93.38028	
SIMBA 02	February 12, 2017	68 cm (5 cm)	59.37889 93.34417	Deployed with met tower
SIMBA 03	February 10, 2017	61 cm (3 cm)	59.39944 93.18833	Deployed with CT line



FIGURE 2.9 SIMBA deployed on the mobile ice. Note the temperature string runs down through the ice on the furthest right PVC tube.

On-ice weather station (x1): The on-ice weather station transmits hourly observations of surface winds, air temperature, and air pressure to provide information on the atmospheric forcing of the mobile ice pack. The system does not have a GPS, so it was deployed next to an ice beacon (#14) and SIMBA #2 (Figure 2.9). The system uses an electronic compass to correct wind direction for floe rotation, though a second ice beacon (#8) was deployed on the floe to provide direct observations of floe rotation that can then be compared against the compass rotation and ensure observations of wind direction are correct (Figure 2.10).

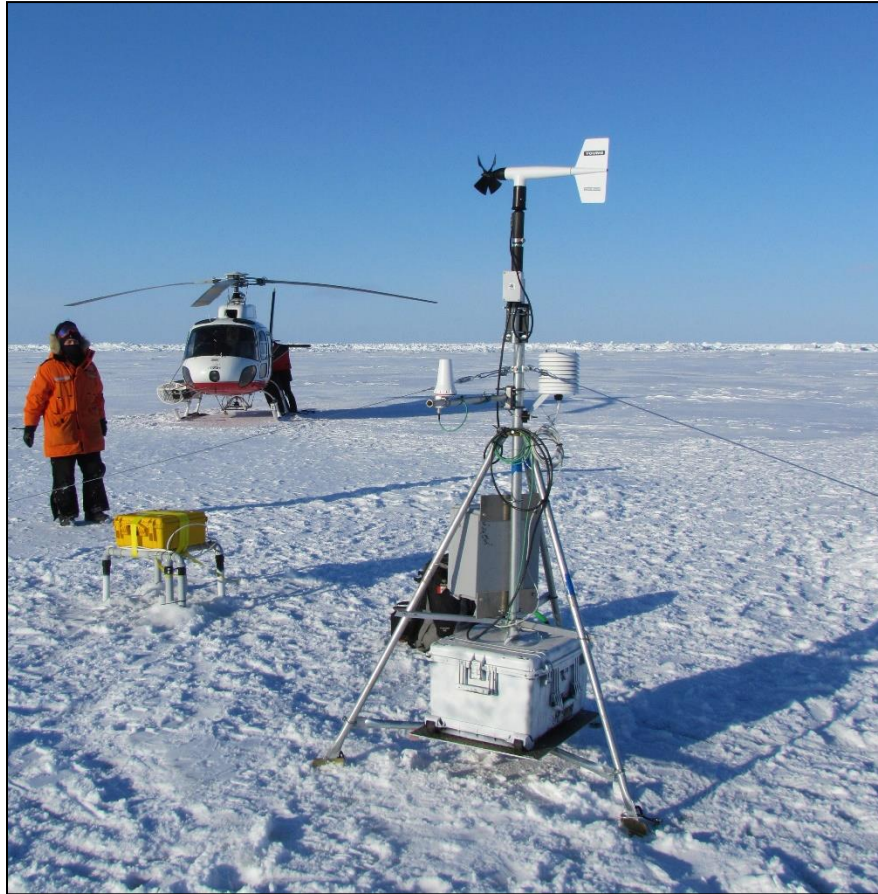


FIGURE 2.10 On ice weather station deployed next to SIMBA 02.

2.6 Team 3 – Marine Ecosystems

The availability of light and nutrients controlled by physical oceanic processes and river runoff determine the timing and magnitude of biological productivity. In winter, light transmission through snow-covered sea ice is very low while nutrient loading is influenced by different freshwater discharges of unregulated vs. regulated rivers. The aim of team 3 sampling was to collect a winter nutrient baseline of the unregulated Churchill River estuary and offshore marine waters. Simultaneously, light propagation through the ice cover and primary production at the ice bottom and in the water column was measured.

Ice core sampling

Ice samples were collected using a 9 cm Mark II Kovacs core barrel (Figure 2.11). The bottom 5 cm of 3-5 cores were pooled together for each site and the bottom skeletal layer (1-2 cm) of 3-5 cores were scraped into 500 mL of filtered seawater. A separate core was taken for analysis of bulk nutrients on the bottom 5 cm. A full core was also taken to measure temperature and salinity for 0-5 cm sections for a full ice profile. These values will be used to calculate the percent brine volume.



FIGURE 2.11 Left – Temperature measurements of a full ice core, Right – Sampling of bottom ice core after drilling through 70% of the ice layer by an ice auger.

The bottom 5 cm pooled cores were melted in the dark and 0.2 m filtered seawater (FSW) was added at a ratio of three parts FSW to one-part ice. The melted pooled cores were then subsampled for the following variables that were filtered on Whatmann GF/F filters, frozen at -80°C , and brought south for analyses: chlorophyll a, particulate organic carbon and nitrogen, high-performance liquid chromatography, particulate spectral absorption, and flow cytometry. The scraped cores were then subsampled for the following variables that were either fixed and/or frozen at -80°C for analyses: intracellular nutrients, chlorophyll a, particulate organic carbon and nitrogen, algal taxonomy (via visible microscopy) and used for oxygen incubations that are discussed further in a section below.

Under-ice light measurements

For ice algae available photosynthetic active radiation (PAR, 400 – 700 nm) was measured 10 cm below the ice bottom (Figure 2.12). A UV-visible hyperspectral radiometer (Cosine RAMSES-ACC, TriOS GmbH, Germany) was mounted to a metal arm and faced upward 1.50 m away from a drilled hole. To calculate light transmission incident radiation and albedo were measured with the same sensor at the ice surface. Ice thickness and snow depth were also recorded.



FIGURE 2.12 Preparation of under-ice light measurement through a metal arm with an attached radiometer.

Water sampling

Interface water at the ice bottom close to the river estuary and marine water of several depth levels at the offshore sampling sites was collected to characterize the physical, biological and chemical properties of the water column (Table 2.1).

TABLE 2.2 Water sampling parameters were collected by BaySys team 3 (see Appendix 2A for a full list of collection depths).

Acronym	Sampling Parameter
CDOM	Colored dissolved organic matter
ap	Particle absorption
HPLC	High-performance liquid chromatography for photosynthetic pigments
Chl a	Chlorophyll a concentration
Flow Cytometry	Preserved plankton samples (Analysis of pico- and nanoplankton)
Lugol	Preserved phytoplankton samples (Taxonomy)
FlowCam	Dynamic imaging particle analyzer (Plankton size distribution)

POC/N	Particular organic carbon/ nitrogen
NO ₃ , NO ₂ , Si, PO ₄	Nitrate, nitrite, silicate, and phosphate
NH ₄	Ammonium
DOC/TDN	Dissolved inorganic carbon and total dissolved nitrogen
Nat. Ab. NO ₃	Natural abundance of nitrate isotopes (18O and 15N)
15N and 13C uptake	Incubation with 15N and 13C tracers to determine nitrogen uptake rates and primary production estimates

Optical characterization of sea ice-covered water column

Sea ice and the snow cover on top reflect and scatter a high amount of incident solar radiation. The small portion reaching the water column underneath is also scattered and absorbed by particular (algae, detritus) and dissolved organic matter, however, their concentration is expected to be low in winter. To characterize the light conditions and inherent optical properties of the upper euphotic zone of Hudson Bay, two UV-visible spectral radiometers (spherical RAMSES-ASC, TriOS GmbH, Germany) were lowered through a hole at four mobile ice floes offshore. Measurements were taken from the surface to a depth of 30 m every 0.5 m, roughly, while one sensor was facing upwards, the other one downwards to record total irradiance. Surface radiation was measured with another UV-visible spectral radiometer (Cosine RAMSES-ACC, TriOS GmbH, Germany) and albedo and light transmission were calculated afterward.

Inherent optical properties of the water column were investigated in terms of particle absorption, pigment concentration, and the content of particulate organic carbon and nitrogen. Water for filtration was sampled by a Niskin bottle at six different depth levels (if possible): Ice interface water, 5 m, 10 m, 20 m, 30 m, and above the bottom. For laboratory analysis of particle absorption (*a_p*) by spectrophotometry, of photosynthetic pigment concentration by high-performance liquid chromatography (HPLC), and particular organic carbon and nitrogen (POC/N) concentration, water samples of 1 or 2 L were filtered and stored at -80 °C. Colored dissolved organic matter (CDOM) will be analyzed through spectrophotometry from 40 mL prefiltered water samples of each depth.

Characterizing the size distribution of the present micro-and nanophytoplankton

Water samples (200 mL) from three depths (interface, 10 m, bottom) were preserved with Lugol's solution for later microscopic analysis. Furthermore, particles in the water from the same depth levels were directly analyzed by automated imaging technology (FlowCam, Fluid Imaging Technologies, INC., USA). The FlowCam is a dynamic imaging particle analyzer that examines a fluid under a microscope which is pumped through a flow cell. An integrated camera takes images of particles within the fluid and characterizes them in terms of particle size and shape. For this project, water samples of 10 mL were pre-filtered through a 100 µm mesh to analyze the particle size fraction of phytoplankton between 10 – 100 µm. To get information about the size distribution of plankton smaller than 20 µm, water samples of 4 mL were preserved with Glutaraldehyde for later Flow Cytometry analysis.

Nutrient

Samples for inorganic nutrients (nitrite, nitrate, orthophosphate, and orthosilicic acid) were taken at nine different locations (estuaries and marine sites) to establish detailed vertical profiles. Triplicate samples were pre-filtered through a combusted GF/F filter and stored in acid-washed and sample rinsed 15 ml polyethylene tubes. Two samples were immediately frozen at -20°C and one sample was poisoned with mercury chloride (final concentration of $20\ \mu\text{g}/\text{mL}$). Nutrient concentrations will be determined using standard colorimetric methods adapted from Hansen and Koroleff (2007) with a Bran and Luebbe Autoanalyzer III at Laval University (analytical detection limit of $0.02\ \mu\text{mol l}^{-1}$ for NO_2 , $0.03\ \mu\text{mol l}^{-1}$ for NO_3 , $0.05\ \mu\text{mol l}^{-1}$ for PO_4 and $0.1\ \mu\text{mol l}^{-1}$ for $\text{Si}(\text{OH})_4$).

Subsamples for ammonium (NH_4) were taken at all sampling depths. Concentrations were determined upon collection by derivatization with OPA and fluorimetric detection according to Holmes et al. 1999 using a Turner Designs fluorometer (analytical detection limit of $0.02\ \mu\text{mol l}^{-1}$).

Chlorophyll a

Chlorophyll-a (Chl a) was determined with the fluorometrically (Parsons et al. 1984) by filtering 1 liter onto Whatman 25 mm GF/F filters using a low vacuum pressure (10 psi). Each filter was placed in a 20 ml scintillation vial, and pigments were immediately extracted in 10 ml of 90% acetone. Extraction continued for 24 h at 4°C in the dark.

After 24 h, the samples were allowed to warm to room temperature and fluorometric readings were taken before and after acidification using a Turner Designs fluorometer. Chlorophyll concentrations will be calculated according to Parsons et al. (1984).

Natural abundance of $^{18}\text{O}/^{15}\text{N}$ in nitrate

Water samples for natural abundances of nitrogen and carbon isotopes were also collected. Water was pre-filtered through a combusted GF/F filter and stored in 60 mL Nalgene bottles. Samples were immediately frozen and stored at -80°C . Isotopic analyses will be conducted at Julie Granger's laboratory (University of Connecticut) using the denitrifier method (Sigman et al. 2001; Casciotti et al. 2002).

Incubations

Incubations using oxygen optodes were performed to determine primary production. The chambers containing seven bottles (six clear bottles and one dark) were arranged consecutively in a dark chamber with one white-diffuse plexiglass end positioned towards the light source so that each sample bottle received varying light intensities. Each bottle was filled with the scrape sample using a peristaltic pump to avoid bubbles and overfilled to avoid any headspace upon closure with the glass stopper. The glass stopper contained a drilled hole that was approximately equivalent to the diameter of the optode sensors used. Average light intensity of PAR was measured with a scalar PAR probe (Walz model US-SQS/L) in each bottle before and after incubation. Three thermocouples were placed at the front, middle, and back of the chambers to monitor temperature continuously over the incubation period. Samples were incubated

for 72 hr with robust Firesting optodes in each bottle continuously measuring dissolved oxygen under constant illumination and mixing via magnetic stir bars.

To determine NH₄ and NO₃ uptake rates and primary production, surface water samples were incubated under two light intensities (low = 5 μE m²/s and high = 60 μE m²/s) using 15N and 13C tracers. All bottles were incubated for 24 h at 0°C. After 24 h, water samples were filtered through pre-combusted GF/F filters and the filters were dried for 24 h at 60°C for further analyses. Isotopic ratios of nitrogen and carbon from all GF/F filters will be analyzed using mass spectrometry at Laval University.

References

Casciotti KL, Sigman DM, Hastings MG, Bohlke JK, Hilkert A (2002) Measurement of the oxygen isotopic composition of nitrate in seawater and freshwater using the denitrifier method. *Analytical Chemistry* 74:4905–4912

Hansen HP, Koroleff F (2007) Determination of nutrients. In: Grasshoff K, Kremling K, Ehrhardt M, Weinheim W (eds) *Methods of Seawater Analysis*, New York

Holmes RM, Aminot A, Kerouel R, Hooker BA, Peterson BJ (1999) A simple and precise method for measuring ammonium in marine and freshwater ecosystems. *Canadian Journal of Fisheries and Aquatic Sciences* 56:1801–1808

Parsons TR, Maita Y, Lalli CM (1984) *A manual of chemical and biological methods for seawater analysis*. Pergamon Press, Toronto

Sigman DM, Casciotti KL, Andreani M, Barford C, Galanter M, Bohlke JK (2001) A bacterial method for the nitrogen isotopic analysis of nitrate in seawater and freshwater. *Analytical Chemistry* 73:4145–4153

2.7 Team 4 – Carbon System

Background

The objectives for Team 4 were to provide baseline measurements of wintertime carbon system parameters in the Churchill River and marine end-members, as well as the estuary, where river and marine water mix. This information can be used to estimate the supply of Carbon system parameters to the estuary and Hudson Bay system during winter.

Little is known about the Carbon system during winter in Hudson Bay. Riverine supply of nutrients and carbon may lead to accumulation of DIC in estuaries, which could cause sea-air CO₂ flux and acidic conditions, but may also help stimulate spring phytoplankton blooms which draw down atmospheric CO₂. Ice formation/melt can also affect the cycling and exchange of CO₂ between the atmosphere and underlying seawater. The melting of Carbon-rich permafrost may release both CO₂ and CH₄ to the water

that drains into the Churchill River. We, therefore, measured the ^{13}C -DIC and CH_4 concentrations in the river, estuary, and marine water. We also use ^{18}O to estimate the contributions of meteoric vs. seawater in each water and ice sample.

This information will be used to improve the accuracy of current carbon budgets in Hudson Bay, and to inform future projections of these parameters under various future scenarios related to hydroelectric demand, freshwater inputs, and sea-ice concentration.

Water sampling

Water samples were collected from the Churchill River (near the pumphouse), estuary (EST#1), and 2 marine sites (Marine#1 and Marine#2) between February 2 and 14. The following water depths were sampled where possible: under-ice, 5m, 10m, 20m, 30m, 50m, Bottom. Water was collected using a cyclone pump or Niskin bottle from under the ice and using a Niskin bottle for deeper depths. Water was transferred using flexible tubing into one 300mL and one 500mL BOD bottle, overfilling each bottle and taking care not to introduce air bubbles. The BOD bottles were stoppered and transported in coolers to the lab for processing.

One BOD bottle was poisoned with 200 μL saturated HgCl_2 and re-sealed at the lab, for DIC/TA analysis. The second (500mL) BOD bottle was subsampled at the laboratory into smaller bottles within 1-3 hours for DIC/TA, ^{18}O , ^{13}C -DIC, salinity, CH_4 , N_2O , and O_2/Ar . Subsampling was performed with a 50mL glass syringe with a short piece of plastic tubing on the end. The syringe was rinsed with sample water before subsampling, and care was taken to keep the syringe and tubing free of bubbles during subsampling.

Ice Core sampling

Ice cores were collected from the Churchill River estuary and two marine sites using a Kovacs 9" diameter Mark II core barrel. Ice cores were transported to the lab in plastic bags (in the dark), and segmented into 5cm sections in upper and lower 15cm, 10cm sections above/below. Ice core sections were individually vacuum sealed and melted overnight at room temperature in the dark, then sampled for all DIC/TA, ^{18}O , salinity, parameters, using a 50mL glass syringe with tubing on the end to transfer water from vacuum bags to sample containers. The salinity and temperature of melted sections were measured using a salinity probe, which was calibrated using Milli-Q water and 35 psu salinity standard. All water samples were stored at room temperature in the dark during transport back to the University of Manitoba.

DIC/TA

One 300mL and one 500mL glass BOD bottle were filled using flexible tubing from either a Niskin bottle or cyclone pump, taking care to avoid introducing bubbles and overfilling. These were stoppered without headspace in the field and transported in sealed coolers with hot water bottles to the lab for processing.

At the lab, 3mL of water (1%) was removed from the 300mL BOD bottle, which was then poisoned with 200 μL of saturated HgCl_2 solution, and sealed using a pre-greased glass stopper. DIC/TA samples with

being measured at both the Institute of Ocean Sciences in Sidney, BC, by Dr. L. Miller's group. The second set of DIC/TA samples were collected in 5 x 12mL exetainers, to be measured at the University of Manitoba for inter-calibration.

A glass syringe with a ~10cm length of plastic tubing was pre-rinsed with sample water from the 500mL BID bottle and used to transfer water from the BOD to the exetainers. Each exetainer was filled to the top and poisoned with 20µL of saturated HgCl₂ before being sealed with no headspace. Samples were stored in the dark at room temperature.

18O

Sample water for 18O was collected from the 500mL BOD bottle using a pre-rinsed glass syringe. One 13mL plastic vial and one 2mL glass exetainer were each filled and sealed with screw caps and parafilm, with no headspace. 13mL samples will be measured at McGill University in Montreal, QC by Dr. A. Mucci's group. 2mL samples will be measured at the University of Manitoba.

Salinity

Water for salinity was poured from the 500mL BOD bottle into a 125 glass bottle with a conical screw cap. The bottle was filled to the bottom of the neck, capped, and parafilm. Salinity from water column samples will be measured using a salinometer at Fisheries and Oceans Canada in Winnipeg, MB. For ice core samples, salinity was measured with a salinity probe only.

CH₄/N₂O/O₂/Ar

Water was transferred using a pre-rinsed glass syringe to 2 x 60mL glass serum bottles. Each bottle was filled to the top, poisoned with 40µL of saturated HgCl₂, and crimp-sealed with no headspace. CH₄, N₂O, O₂, and Ar will be measured at the University of Manitoba. CH₄ will be measured using GC-FID, N₂O using GC-ECD, and O₂/Ar by mass spectrometry.

13C-DIC

Water was transferred from the 500mL BOD bottle to one 50mL amber glass serum bottles with screw caps. The bottle was filled to the top, poisoned with 20µL saturated HgCl₂, capped with no headspace, and parafilm. 13C-DIC will be measured at McGill University in Montreal, QC by Dr. A. Mucci's group.

Comments/Issues

The cyclone pump flow rate was very high, causing bubble entrainment inside BOD bottles. This was only an issue in the Churchill River, and marine site#1. At all other sites, the Niskin bottle was used for 1m depth water sampling. A thin layer of ice formed inside BOD and serum vials collected at the Churchill River site during sampling. This was not a problem at subsequent sites due to the use of a tent with a heater during water sampling.

A heater was needed to warm up the Niskin (spigot and especially the release- trigger). The Niskin leaked slightly at the estuary site. A hairdryer or electric car-cabin heater (Lil' Buddy - Canadian Tire), with a generator, was required to heat the Niskin between casts. One of the auger motors leaked fuel from the carburetor and was often difficult to start. The second auger head suffered a broken recoil starter, and could not be repaired. It was important to have spare auger motors and extra blades for the core barrels and augers. It was recommended that we keep the augers outside instead of bringing them inside at the end of each day, to prevent water condensation in the fuel tanks.

The accommodations and laboratory facilities at the CNSC were excellent. Dr. Fishback, the staff and volunteers of the CNSC were extremely helpful in assisting us with our day to day needs, including providing us with supplies and transportation. We are particularly grateful for the help of a local guide, Len, for his assistance in navigating the landfast ice on snowmobiles and for loaning us a 10" auger. The helicopter pilots, Jon and Pat, and their mechanic, Pete, were extremely cooperative and transported us safely to and from our study regions and without any delays. They also assisted with site selection and sampling operations, for which we are extremely grateful. A great deal of help with sample preparation and collection was provided by Kathleen Munson, Gabrielle Deslongchamps, Nix Geilfus, Marcos Lemes, Emmelia Wiley, and Odile Crabeck.

2.8 Team 5 – Contaminants

The objective for Team 5 was to determine total mercury (THg) and methylated mercury (MeHg) concentrations in ice and water across the gradient between the Churchill River and marine waters of Hudson Bay during the winter period of minimal river flow.

The diversion of the Churchill River to augment the Burntwood-Nelson River System for hydroelectricity production reduced Churchill River flow to approximately a quarter of its pre-diversion volume. However, despite this lower water volume, concentrations of THg and MeHg are higher in Churchill River water than in Nelson River water (Kirk et al, 2008). In addition, THg in the Churchill River is primarily found in its dissolved form (Kirk et al, 2008), which may impact the persistence of THg from riverine sources and its potential for transformation to the bioaccumulating chemical form MeHg in estuarine and marine waters of Hudson Bay.

The goal of constraining the wintertime riverine source of THg and MeHg is to determine its importance relative to other potential sources into Hudson Bay, including marine waters, atmospheric, snowmelt, and how these are tempered by the seasonal sea ice boundary between the atmosphere and the marine water column.

Water Sampling

Surface water from the Churchill River was collected by dipping bottles through the 8" auger hole in the ice wearing clean vinyl gloves.

Water sampling from estuary and marine sites was accomplished by deploying a

2.5 L Niskin bottle from a metered line with a Teflon-coated messenger. All water sampling was accompanied by CTD deployment immediately prior to the deployment of the Niskin bottle. The Niskin bottle deployment required a 10" auger hole through which the Niskin bottle in the cocked position and trigger mechanism were lowered down by hand. At the desired sampling depth, the Teflon coated messenger was released gently to minimize splashing of water. The line was then raised and the Niskin bottle was observed to determine whether the messenger successfully triggered the closure of the bottle. At times, we observed the freezing of water on the spring in the trigger mechanism. The freezing of the spring would result in a bottle misfire as the depressed trigger would block the top of the Niskin bottle from closing.

To prevent both the freezing of the spring as well as the spigot and valve, water was most often sampled within the Eskimo brand ice-fishing tent using either a hairdryer or a Little Buddy brand car heater to thaw Niskin bottle components prior to deployment.

Samples were collected in 250 mL amber glass bottles. Bottles were rinsed with sample water prior to filling, filled to the shoulder, capped, and double bagged. Bagged samples were transferred to the lab at CNSC in coolers with hot water bottles to prevent freezing. Care was taken to avoid cross-contamination with sampling equipment and personnel involved in DIC/TA sampling and preservation, which requires the use of high concentrations of HgCl₂ as a preservative agent.

Ice Sampling

Ice cores were collected using the 9 cm Mark II Kovacs core barrel in conjunction with teams 1, 3, and 4 from 2 mobile ice floes. Cores were bagged in core bags, labeled in the field, and transferred to CNSC. Cores were cut with a metal Japanese saw into 5 cm portions outside of the CNSC main building (ambient temperature < -20 °C) to prevent thawing. All edges of each core section were then trimmed with ceramic knives to remove ice that came into contact with the core barrel or the metal saw. Trimmed sections were double bagged in new Ziploc bags and kept at room temperature to melt.

After melting indoors in Ziploc bags, the ice core sections were processed identically to water samples.

Sample Processing

Ideally, the processing of trace metal samples is carried out in cleanroom environments under HEPA-filtered, or equivalent, air supply. Because no certified cleanroom was available at CNSC, all sample processing for THg and MeHg, storage of sampling gear, and storage of samples were performed in a separate lab room from the main portion of the laboratory, where HgCl₂ was used as a preservative for DIC/TA samples. The last lab bench in the CNSC "clean room" was selected to minimize both proximity to areas where HgCl₂ was used and foot traffic that might increase the movement of air and particulates.

A small tent was constructed out of plastic sheeting on the lab bench to minimize falling dust or particles into open bottles during filtration and preservation. All sample filtration and preservation equipment was kept within this small tent throughout the field program.

Double-bagged samples were removed from coolers. Outer bags were removed and samples in inner bags were transferred to the lab bench tent and opened to remove sample bottles. Either a separate 250 mL bottle or ~125 mL of a sample were filtered through Thermo Scientific Nalgene disposable analytical filtration (0.45 μ m, 47 mm) units using a Nalgene hand pump under 5 – 10 psi pressure. Filtration unit and filtrate collection bottles were rinsed 3x prior to filtrate collection. Filter cups were kept covered as much as possible during filtration.

Filters were removed, stored in PetriSlides (EMD Millipore) marked with filtered volume, and stored at -20 °C. Unfiltered and filtered water and ice samples were preserved to 0.5% HCl (concentrated HCl, JT Baker) and stored in coolers in the dark until transfer to the University of Manitoba for future analysis.

References

Kirk JL, St. Louis VL, Hintelmann H, Lehnher I, Else B, Poissant L (2008) Methylated mercury species in marine waters of the Candian High and Sub Arctic. *Environ. Sci. Technol.* 42:8367-8373.

Appendix 2A: Work Schedule

Sunday	Monday	Tuesday	Wednesday	Thursday	Friday	Saturday
			1	2	3	4
			KM, NG, LD, LM, DC arrive	Sampling from the pump house	Weather day	Estuary sampling and CTD's LM, LD, NG, DC DB, JL, NZ, GD arrive
5	6	7	8	9	10	11
	Helicopters arrive at CNSC	Helo day 1 Ice recon flights w/ DB, JL, KM, NG CTD1, Beacon15	Helo day 2 AM: Ice recon flights w/ DB, JL, KM, NG PM: returned to PS1 1 for CEOS IMB deployment, ice sampling	Helo day 3 AM: Returned to PS1 for water sampling w/ DC, KM, LM, PM: Extended the ice survey NE w/ JL, DB, NG, LD, SIMBA01 Beacon array	Helo day 4 AM Ice team SIMBA03 CT Line CTD Beacons PM: Water team Water sampling PS 2	Helo day 5 AM: Water team PM: CTD Transect along the Landfast ice from Cape Churchill to Churchill Estuary NZ departs for WPG
12	13	14	15	16	17	18
Helo day 6 AM Ice team DB, JL, LM, NG, Met Tower SIMBA02 Beacons PM: n/a	Helo day 7 Landfast ice sampling and CTD profile w/ GD, DB, NG * Blue Helo maintenance	Helo day 8 AM: Water team CTD Light profile Water sampling PM: CTD transect just beyond Landfast ice near the Estuary	JL, NG, LD, LM depart for WPG	DB, DC, KM, GD depart for Thompson		

Appendix 2B: Sampling Schedule

Date	Station	Long (N)	Lat (W)	Bottom depth [m]	CTD (Seabird)	Light	Deployment (Beacons, Buoys)	Ice sampling	Water sampling
03-Feb-17	Churchill River								Dissolved and particulate THg, MeHg, DaveC sampling
04-Feb-17	Button Bay	58.93889	94.33889				CT		Surface water
04-Feb-17	Est-1	58.90611	94.37361				CT		Surface water
04-Feb-17	Est-2	58.95222	94.45444					T, S, Chl a, POC/N	
05-Feb-17	Est-1	58.90472	94.39889		x			T, S, Chl a, POC/N, Ap, Nutrients, Taxonomy, Flow Cytometry	Interface water
05-Feb-17	Est-2	58.95361	94.44861		x				
05-Feb-17	Est-3	58.99389	94.27944		x				
05-Feb-17	Est-4	59.00917	94.40056		x				
06-Feb-17	Button Bay	58.84472	94.52222		x	Under-ice arm		T, S, Chl a, POC/N, Ap, Nutrients, Taxonomy, Flow Cytometry	Interface water
06-Feb-17	Est-1	94.37361	94.37361			Under-ice arm			
06-Feb-17	Est-3	58.99389	94.27944					T, S, Chl a, POC/N	
06-Feb-17	Est-4	59.00917	94.40056					T, S, Chl a, POC/N	
07-Feb-17	Pan 1	59.26139	92.27972		x				Surface water
08-Feb-17	Pan 2	58.81139	93.84222		x		Beacon		
08-Feb-17	Pan 3, Marine 1	58.92778	93.49778		x		Beacon, IMB	T, S, Chl a, POC/N, Ap, Nutrients, Taxonomy, Flow Cytometry, dissolved and particulate THg	Hg, Interface water

								and MeHg (DaveC)	
08-Feb-17	Pan 4	59.12278	93.53333				Beacon		Hg
08-Feb-17	Pan 5	59.17	93.37				Beacon, IMB		
09-Feb-17	Pan 3, Marine 1	59.06	93.53694		x	Under- ice arm, Full profile	Beacon recovery		Depths: Interface, 5, 10, 15m Chl a, POC/N, Ap, Nutrients, HPLC, Taxonomy, Flow Cytometry, dissolved and particulate THg and MeHg DaveC
09-Feb-17	Pan 6	59.32972	93.38028		x		SIMBA 01		
09-Feb-17	Pan 7						Beacon		
09-Feb-17	Pan 8						Beacon		
09-Feb-17	Pan 9						Beacon		
10-Feb-17	Pan 10	59.205	93.31944		x				
10-Feb-17	Pan 11, Marine 2	59.39944	93.18833		x		CT, SIMBA 03	Chl a, POC/N, Ap, Nutrients, Taxonomy, Flow Cytometry, dissolved and particulate THg and MeHg (DaveC)	Interface water
10-Feb-17	Pan 12						Beacon		
10-Feb-17	Pan 13						Beacon		
10-Feb-17	Pan 14						Beacon		
10-Feb-17	Pan 15	59.29083	93.02417		x		Beacon		Surface water
11-Feb-17	Pan 11, Marine 2	59.18056	93.02556		x	Under- ice arm,	T, S		Depths: Interface, 5, 10, 20, 30, 50, 70m Chl a,

						Full profile			POC/N, Ap, HPLC, Nutrients, Taxonomy, Flow Cytometry, dissolved and particulate THg and MeHg DaveC,
11-Feb-17	Pan 16	59.01222	93.50528		x (Bad data)				
11-Feb-17	Pan 17	58.82111	93.21861		x (Bad data)				
11-Feb-17	Pan 18	59.04194	93.50417		x (Bad data)				
11-Feb-17	Pan 19	59.07917	93.64167		x (Bad data)				
11-Feb-17	Pan 20	58.92944	93.95944		x (Bad data)				
11-Feb-17	Pan 21	58.80472	93.95278		x (Bad data)				
12-Feb-17	Pan 22	59.29694	93.25278				Beacon		
12-Feb-17	Pan 23, Marine 3	59.37889	93.34417		x	Full profile	2 Beacons, SIMBA 02, Met tower		Depths: Interface, 5, 10, 20, 30, 50m Chl a, POC/N, Ap, HPLC, Nutrients, Taxonomy, Flow Cytometry
13-Feb-17	Pan 24 (Stn 1 Transect)	58.86778	93.31667		x				Depths: Interface, 5m, bottom
13-Feb-17	Pan 25 (Stn 2 Transect)	59.065	93.405		x				
13-Feb-17	Pan 26 (Stn 3 Transect)	58.99694	93.70083		x				
13-Feb-17	Pan 27 (Stn 4 Transect)	59.05	94.26417		x				
13-Feb-17	Pan 28 (Stn 5 Transect)	59.01722	94.05361		x				
13-Feb-17	Pan 29 (Stn 6 Transect)	59.02167	93.89972		x				

14-Feb-17	Pan 30, Marine 4	58.86556	94.12778		x	Full profile			Depths: Interface, 5, 10, 20, 23 Chl a POC/N, Ap, HPLC, Nutrients, Taxonomy, Flow Cytometry, dissolved and particulate THg, and MeHg
14-Feb-17	Pan 31 (Stn 7 Transect)	59.07222	94.47111		x				Surface water
14-Feb-17	Pan 32 (Stn 8 Transect)	59.08583	94.40167		x				Surface water
14-Feb-17	Pan 33 (Stn 9 Transect)	58.97639	94.42389		x				Surface water

Chapter 3 - Nelson Estuary Landfast Ice Survey



FIELDWORK PARTICIPANTS David Babb¹, Dr. Sergei Kirillov¹, Dr. Igor Dmitrenko¹, Dr. David Barber¹, Nathalie Theriault¹, Vlad Petrushevich¹, Dr. Greg McCullough¹, Atreya Basu¹, Laura Dalman¹, Dr. David Capelle¹, Gabrièle Deslongchamps², Janghan Lee², Kathleen Munson¹, Nicolas-Xavier Geilfus¹, Jiang Liu¹

¹Centre for Earth Observation Science, University of Manitoba, 535 Wallace Building, Winnipeg, MB

²Québec-Océan, Department of Biology, Pavillon Alexandre-Vachon, 1045, Avenue de la Médecine, Local 2078, Université Laval, Québec, QC

CITE CHAPTER AS Babb, D., Capelle, D, Deslongchamps, G., Munson K. 2019. Nelson Estuary Landfast Ice Survey. Chapter 3 in, *Hudson Bay Systems Study (BaySys) Phase 1 Report: Campaign Reports and Data Collection*. (Eds.) Landry, DL & Candlish, LM. pp. 67-93.

3.1 *Fieldwork Objectives*

This field program was designed to collect data for 4 BaySys research teams over 3 legs.

Leg 1: Feb 19 – Mar 11, 2017

Leg 2: Mar 18 - Apr 5, 2017

Leg 3: Apr 5 – Apr 15, 2017

This project campaign took place on the landfast sea ice in southwestern Hudson Bay, near the mouth of the Nelson Estuary. The program was based out of the Nanuk Polar Bear Lodge, which is located near the shore of Hudson Bay between the mouth of the Nelson River and Cape Tatnam (Figure 3.1). The seasonal ice cover that forms annually within Hudson Bay is composed of both mobile pack ice and landfast ice that forms a narrow band of stationary ice in the nearshore areas of Hudson Bay. In southwestern Hudson Bay, the landfast ice provided an excellent opportunity to study the freshwater-marine coupling near the mouth of the Nelson River. The area is typically ice-covered from November to June, though the landfast ice cover typically becomes unstable is forced offshore from May to early June.

Hudson Bay experiences large tides, for the Nelson Estuary the tidal range is ~4.5m. Hence, while the landfast ice is stationary it does move vertically and continue to behave dynamically. The large tidal range leads to grounding of some of the landfast ice, a concern for both collecting ice and water samples, but also deploying any sort of under-ice autonomous equipment.

3.2 *Logistical Summary*

In total, there were 8 members of BaySys Team 1 who took part in the Nanuk project:

David Babb – Leg 1 & 3 - Research associate with Dr. David Barber at CEOS. Studying

Dr. Igor Dmitrenko – Leg 1- Research scientist at CEOS, studying physical oceanography.

Dr. Sergei Kirillov – Leg 1 – Research associate with Dr. David Barber and Soren Rysgaard at CEOS, studying physical oceanography.

Dr. David Barber – Leg 2 – Canada Research Chair in Arctic-System Science, overall lead of BaySys.

Nathalie Theriault – Leg 2 & 3 - BaySys coordinator and research associate with Dr. David Barber at CEOS.

Vlad Petrusovich – Leg 2 & 3- Ph.D. student with Dr. Igor Dmitrenko and Dr. Jens Ehn at CEOS, studying physical oceanography.

Atreya Basu – Leg 2 – Ph.D. Student with Dr. Jens Ehn at CEOS, studying CDOM (Colored Dissolved Organic Matter) tracing in Hudson Bay.

Dr. Greg McCullough – Leg 2 – Research associate with Dr. David Barber at CEOS, studying freshwater in Hudson Bay and the Hudson Bay watershed.

3.3 Team 1 – Sea and Oceanography

Broadly, Team 1 had the objective of characterizing the physical properties of the landfast sea ice near the Nelson estuary and the underlying water column. Specifically, we were interested in observing the freshwater-marine coupling processes that occur beneath the landfast ice cover. The Nelson River is the largest source of freshwater to Hudson Bay and while a majority of the ice cover in the Nelson estuary is mobile pack ice that is transported through the region, there is landfast ice that forms to the north, Nelson River to Cape Churchill, and to the east, Nelson River to Cape Tatnam.

The sampling plan for the team consisted of 3 transects across the landfast ice (shore to ice edge) and sporadic sampling along (Nelson to Cape Tatnam) the landfast ice cover, with both ice cores and water samples collected at each site. At the ice edge end of each transect, there was an ice tethered mooring deployed for continuous monitoring of the water column, while an autonomous ice mass balance buoy was additionally deployed at one of the moorings to monitor the thermodynamic forcing of the ice cover. Below is a summary of the samples collected by Team 1.

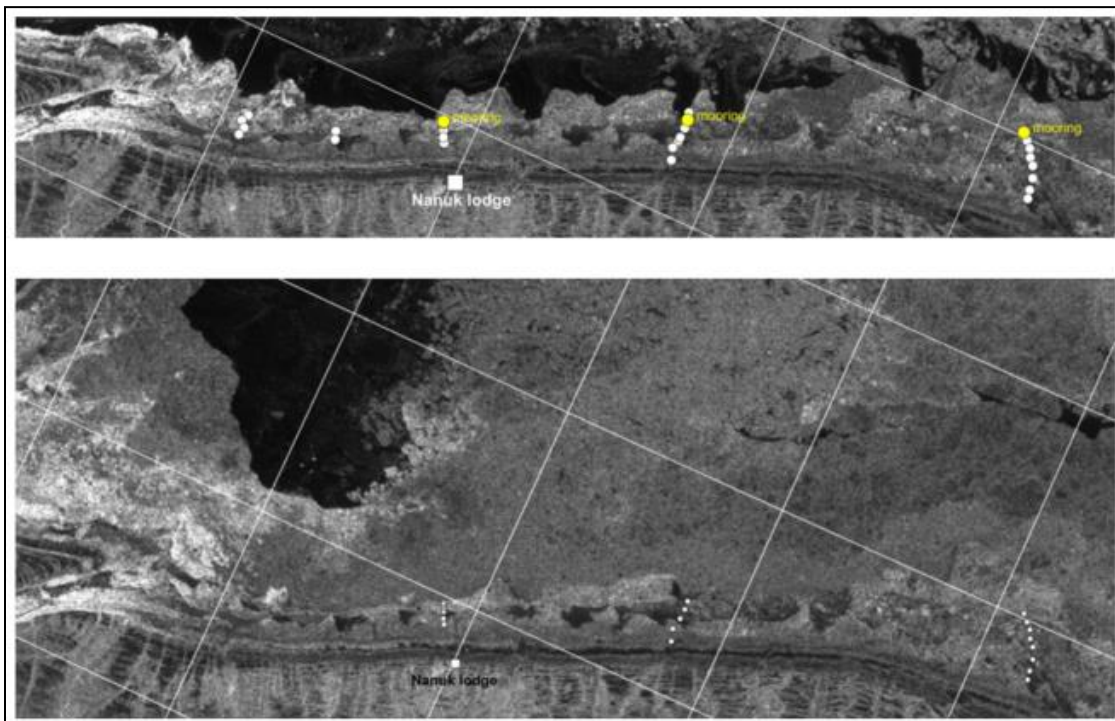


FIGURE 3.1 Sentinel SAR imagery along the coast in the area of research. The upper image shows the landfast ice configuration on February 12. The lower image represents the post-storm configuration of landfast ice as recorded on March 14. The white circles correspond to CTD stations carried out during leg 1.

Sea ice

Sea ice physical properties: To assess the physical properties of the landfast sea ice cover, a series of ice cores were collected. Ice cores were collected with a Kovacs Mark II Core Barrel (9.25 cm in diameter). For each ice core, the vertical temperature profile was sampled at 10cm intervals directly after the ice core was extracted from the core barrel. Subsequently, the cores were sectioned at 10cm intervals, bagged, melted, and sampled for salinity. An example of the salinity profiles from 4 locations along the landfast ice cover is presented below (Figure 3.2).

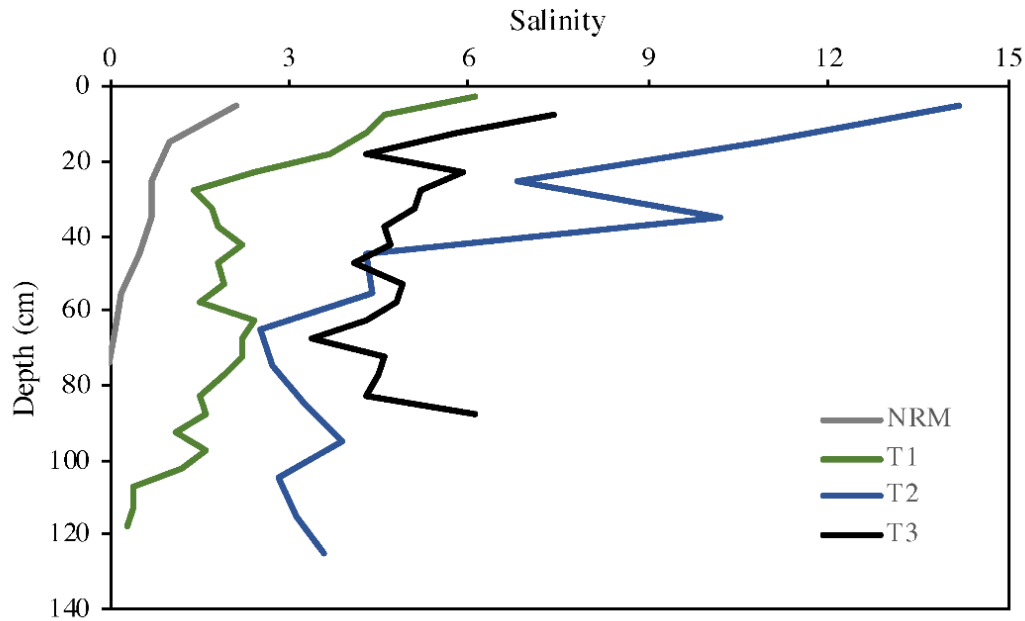


FIGURE 3.2 Sea ice salinity profiles from 4 locations on the landfast ice cover collected during Leg 3. NRM is the Nelson River Mouth. Samples were sectioned at 10 cm intervals.

Sea ice thermodynamic growth: To monitor the thermodynamic growth of sea ice during our field study, an autonomous ice mass balance buoy (IMB) was deployed at one of the mooring sites (Table 3.1). The IMB used a Campbell Scientific data logger to run an air temperature probe, barometer, snow depth sounder (189cm above ice surface), and a temperature string with sensors at 20 cm intervals from 40cm above the ice to 60cm depth, and then 10 cm intervals to the 320 cm depth. Data were collected at 30-minute intervals from February 23rd to April 12th. The snow sounder was deployed 189 cm above the ice surface. The air temperature probe and barometer were 155 and 157 cm above the ice surface, respectively (Figure 3.3).

TABLE 3.1 IMB details.

IMB Deployment		IMB Recovery	
Snow	10 cm	Snow	14 cm (SR50 – 175 cm)
Ice thickness	1.01 m	Ice thickness	
Notes:	<p>T String depths (cm): 40, 20, 0(ice:snow interface), -20, -40, -60, -70, -80 and on at 10 cm intervals to the end of the T string.</p> <p>Deployed in a level area of ice surrounded by large ridges and within ~100m of the landfast ice edge</p>	Notes:	<p>Bottom of the T string was damaged due to grounding.</p> <p>T sensors at 0, -20, and -40 cm depth did not work during the experiment.</p>

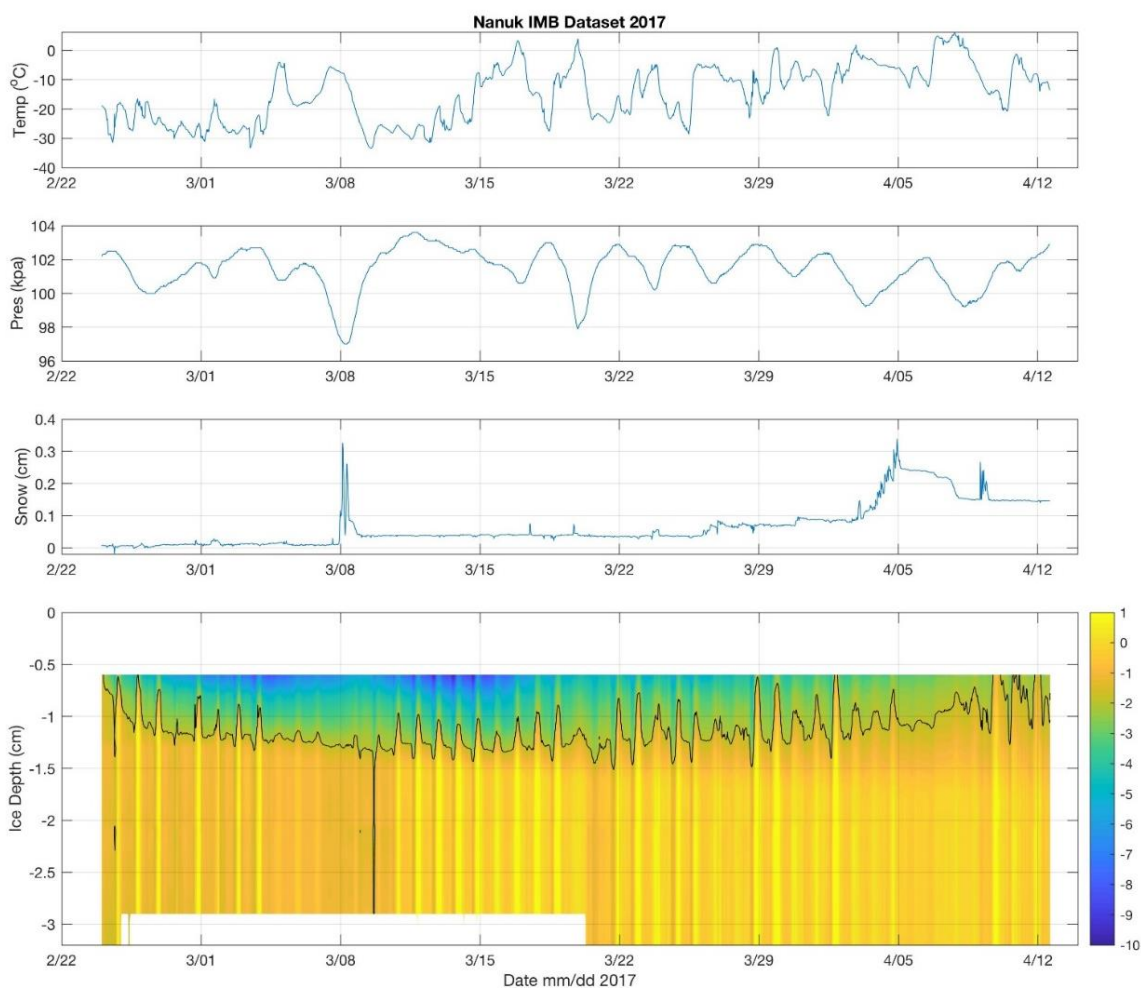


FIGURE 3.3 A sample of the data collected from the IMB at Mooring site 1 (near Nanuk Lodge). Air temperature (top panel), Air Pressure (second panel), Snow depth (third panel), vertical temperature profile (bottom panel).

Thickness: To characterize the ice thickness in the study area an electromagnetic induction system was brought to Nanuk to tow it behind a snowmobile and collect a continuous record of ice thickness.

However, there were technical issues with the instrument and due to very rough ice conditions, the instrument was not used.

Surface Roughness – Drone Surveys: To characterize the roughness of the landfast ice cover a DJI-Phantom-4 Drone was used to conduct aerial surveys of subsections of the study area. The drone collected visible imagery and subsequently used the Pix4D software that uses photogrammetric overlap to derive digital elevation models of the ice cover. The accuracy of the DEM is estimated to be 3x the pixel size (~2 cm). In total there were 27 surveys flown over the landfast ice near Nanuk (Table 3.2). A table of the flight details is provided below, along with a map of the survey locations and an example of the DEM over an ice ridge (Figures 3.4 and 3.5).

TABLE 3.2 List of drone surveys conducted near Nanuk.

Survey #	Date	X Coord	Y Coord	Notes
Survey 1	18-Mar	-91.66955943	57.12445518	
Survey 2	18-Mar	-91.67320923	57.12984728	
Survey 3	19-Mar	-91.67023956	57.12288419	
Survey 4	22-Mar	-92.48860972	57.05510674	
Survey 5	22-Mar	-92.48655937	57.05489372	
Survey 6	24-Mar	-91.71239372	57.16071564	
Survey 7	25-Mar	-91.71264315	57.16020565	
Survey 8	24-Mar	-91.71263653	57.16006889	Choppy DEM elevations, poor correction
Survey 9	25-Mar	-91.40073386	57.23999661	
Survey 10	25-Mar	-91.4021265	57.24039237	
Survey 11	25-Mar	-91.40522652	57.24903915	
Survey 12	25-Mar	-91.40483594	57.24662574	Many linear artefacts from correction
Survey 13	28-Mar	-90.9623231	57.33813783	
Survey 14	28-Mar	-90.95979698	57.33891903	
Survey 15	28-Mar	-90.96020263	57.33747226	
Survey 16	28-Mar	-90.97288718	57.33389766	
Survey 17	28-Mar	-90.97355595	57.33348371	
Survey 18	28-Mar	-90.97319522	57.33340299	
Survey 19	28-Mar	-91.67024242	57.1207665	
Survey 20	07-Apr	-91.96606171	57.10263883	
Survey 21	07-Apr	-91.9658484	57.10263337	
Survey 22	07-Apr	-91.8459039	57.12051569	
Survey 23	07-Apr	-91.83785999	57.10764032	
Survey 24	13-Apr	-91.71293308	57.16037872	
Survey 25	13-Apr	-91.7122521	57.16035942	
Survey 26	13-Apr	-91.70198954	57.14708244	
Survey 27	13-Apr	-91.70069303	57.14709552	

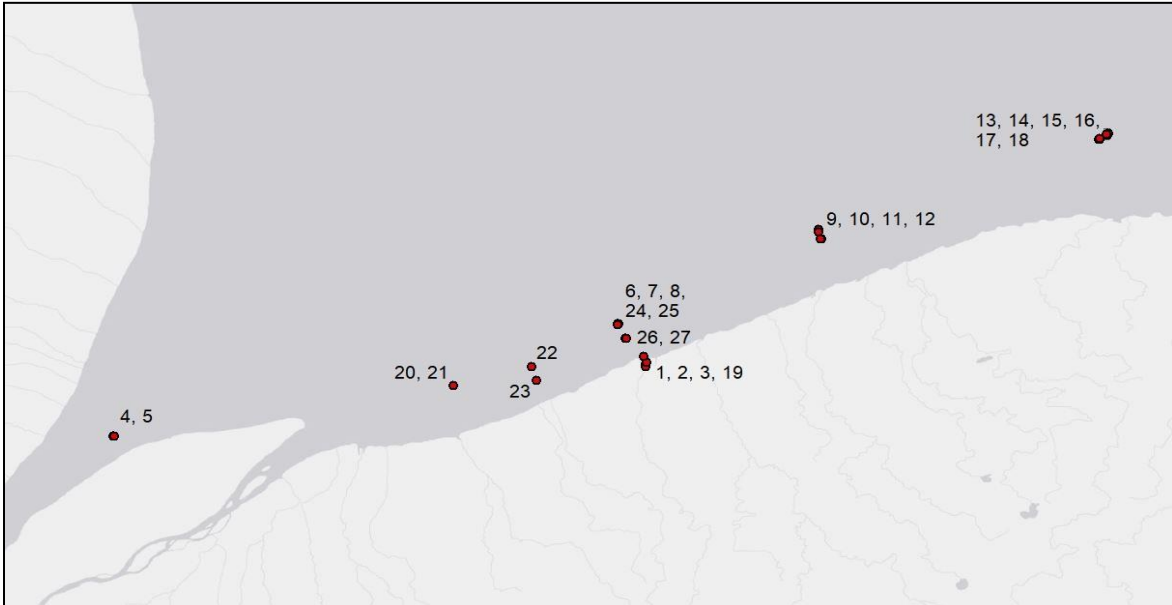


FIGURE 3.4 Map of the Drone survey locations.

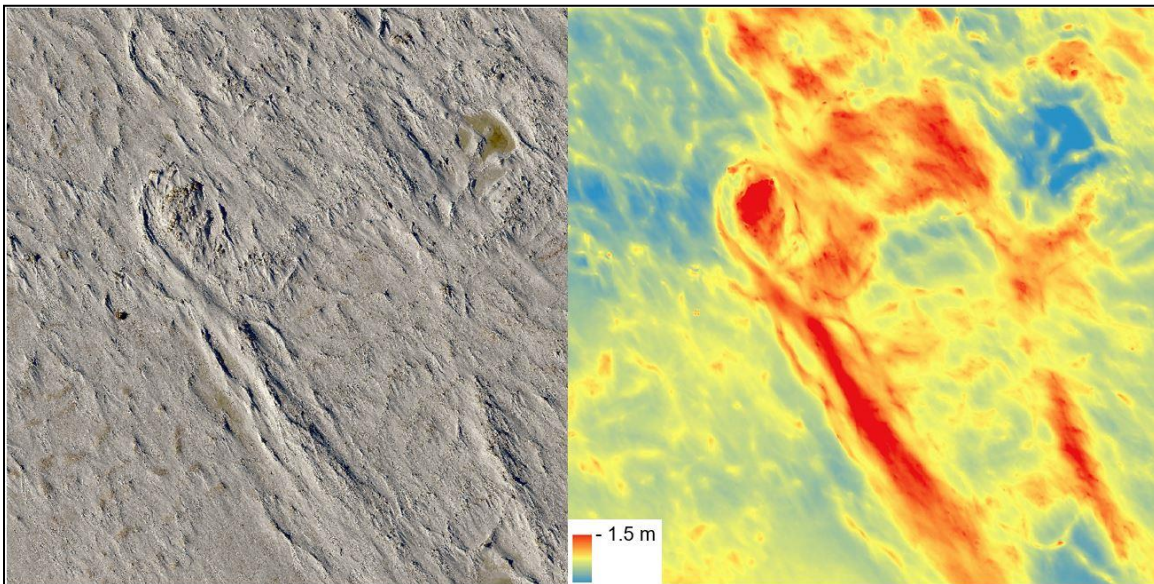


FIGURE 3.5 A sample photo mosaic and DEM derived from survey #27 over a ridge in the landfast ice cover near Nanuk.

Oceanography

To monitor the thermohaline changes and water dynamics under the landfast sea ice along the Nanum coast three moorings were deployed at the landfast edge, which corresponded to the marine termination of 3 basic CTD transects (Figure 3.4). All moorings were equipped with 3-4 CT (Tu) sensors deployed at different depths, bottom-mounted pressure sensors, and downward-looking 600 kHz Nortek ADCP. All

instruments were programmed to record data every 10 minutes but, due to unknown reasons, several CT sensors did not record any reliable data. The current velocities were also recorded every 10 min with a 50 cm vertical resolution. The overall length of records changed from 48 days at the mooring m01 to 40 days at m02, and it was 32 days only at m03 (Figure 3.6). It should be noted also that relatively high tidal amplitude and shallow water led to a situation when some instruments had periodically been touching seafloor.

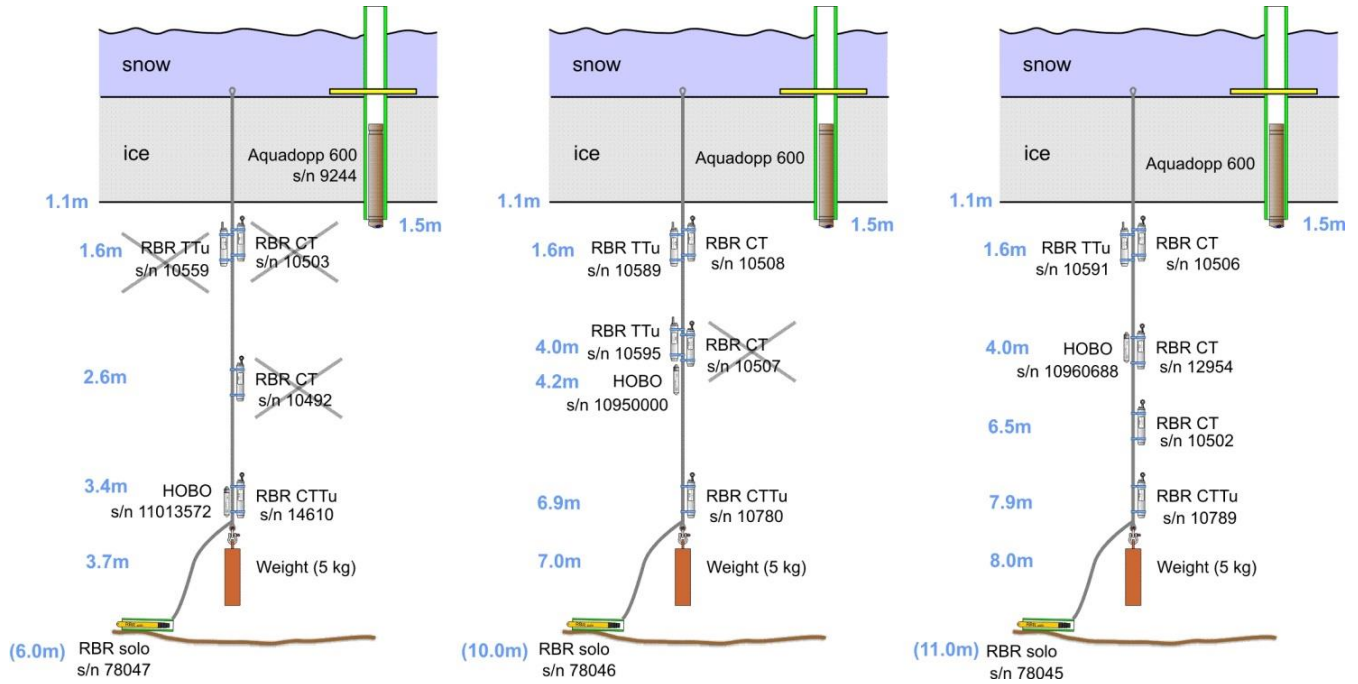


FIGURE 3.6 The schemes of m01, m02, and m03 moorings. Instruments with unreliable records are shown crossed.

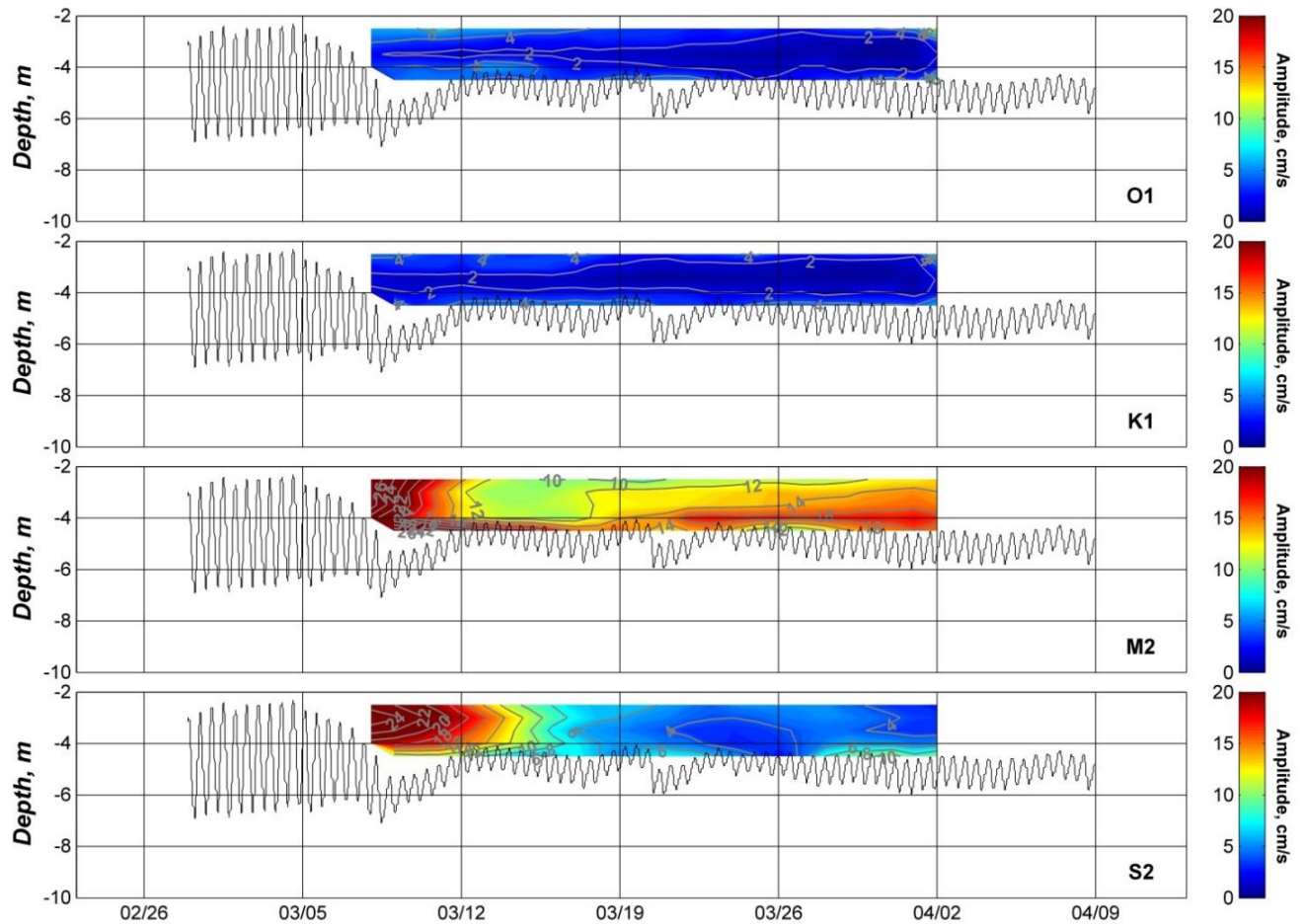


FIGURE 3.7 Temporal evolution of the most energetic constituents of tidal currents as measured in the m02 position.

Mooring records allowed us to determine the impact of landfast ice on water dynamics under the ice cover. Specifically, it was found that the storm-induced increase of landfast ice extent from 4-6 km to 15-20 m led to considerable damping of tidal energy penetrating under the ice. The lunar semidiurnal amplitudes at moorings m01 and m02 decreased from 1.5-2.0 to 0.5-0.6 m with a corresponding reduction of current velocities by a factor near 2 (Figure 3.7).

CTD Surveys

More than 120 oceanographic stations were made to specify the local thermohaline structure at different temporal and spatial scales. Temperature and salinity were measured with SeaBird 19plus profiler equipped with Chl-a fluorescence, turbidity, and dissolved oxygen external sensors. Additionally, an Idronaut CTD was used to supplement the spatial sampling. Strong dynamics associated with tides over the shallow water, which depth does not exceed 8 m, and highly ridged landfast cover and edge make the

area of research very difficult in terms of data interpretation. Some pronounced patterns can be distinguished though. First, all mentioned factors resulted in absence of any vertical stratification: the water column is well-mixed down to the bottom. Secondly, freshwater content decreased from west to east matching the distance increase from the Nelson and Hayes River mouths. Another interesting aspect of freshwater distribution involved off-shore decreasing of salinity at the first two transects, whereas salinity increased off-coast at the easternmost transect near cape Tatnam. This implies that fresher river waters were drawn toward the coast at some point between the second and third basic transects.

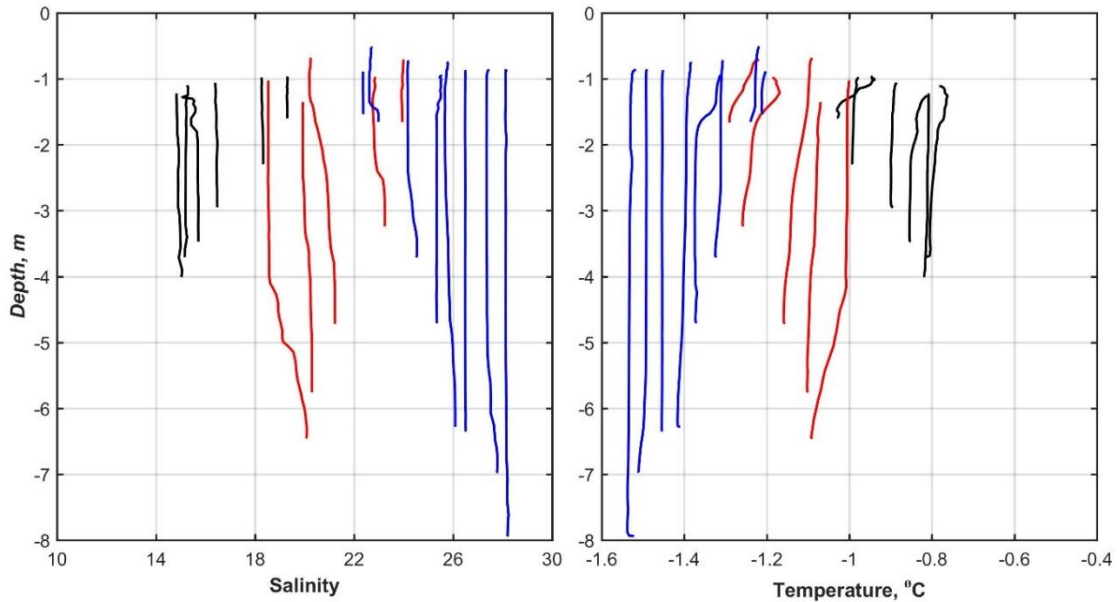


FIGURE 3.8 Salinity and temperature profiles recorded at 3 CTD transects across landfast ice. Black lines are associated with stations 1-6; red lines – stations 15-19; and blue lines – stations 7-14 (see Table 3.3)

TABLE 3.3 Coordinates of SeaBird CTD stations.

Station NN	Latitude, N	Longitude, W	Depth, m	Date
1_2017	57.1615	-91.7139	4.05	2017 Feb 23 11:07:51
2_2017	57.1601	-91.7129	3.72	2017 Feb 23 11:31:47
3_2017	57.1579	-91.7106	3.48	2017 Feb 23 11:51:10
4_2017	57.1556	-91.7088	2.95	2017 Feb 23 12:07:08
5_2017	57.1506	-91.7049	2.31	2017 Feb 23 12:25:13
6_2017	57.1467	-91.7007	1.62	2017 Feb 23 12:59:13
7_2017	57.3369	-90.9617	7.94	2017 Feb 25 12:28:26
8_2017	57.3320	-90.9530	7.00	2017 Feb 25 12:52:31

9_2017	57.3275	-90.9448	6.35	2017 Feb 25 13:08:04
10_2017	57.3213	-90.9391	6.30	2017 Feb 25 13:23:06
11_2017	57.3163	-90.9312	4.73	2017 Feb 25 13:44:09
12_2017	57.3076	-90.9241	3.72	2017 Feb 25 13:59:15
13_2017	57.2986	-90.9214	1.70	2017 Feb 25 14:16:09
14_2017	57.2919	-90.9190	1.56	2017 Feb 25 14:33:50
15_2017	57.2402	-91.4022	6.53	2017 Feb 27 11:17:23
16_2017	57.2336	-91.4010	5.79	2017 Feb 27 12:07:08
17_2017	57.2256	-91.4017	4.73	2017 Feb 27 12:26:17
18_2017	57.2163	-91.4053	3.24	2017 Feb 27 13:11:14
19_2017	57.2072	-91.3998	1.67	2017 Feb 27 13:39:33
20	57.1601	91.7129	2.46	2017 Feb 28 16:44:58
21	57.1506	91.7049	1.44	2017 Feb 28 18:22:20
63	57.1496	91.7038	2.54	2017 Mar 21 10:39:15
64	57.1601	91.7129	3.87	2017 Mar 21 11:46:26
65	57.1506	91.7049	2.33	2017 Mar 21 13:49:50
67	57.1615	91.7139	4.19	2017 Mar 24 08:57:13
68	57.1506	91.7049	1.97	2017 Mar 24 15:18:28
69	57.1561	91.7093	2.71	2017 Mar 24 15:43:19
70	57.1579	91.7106	3.05	2017 Mar 24 16:11:29
71	57.1615	91.7139	3.33	2017 Mar 24 16:37:32
72	57.1601	91.7129	3.14	2017 Mar 24 16:59:35
73	57.2456	91.4049	5.86	2017 Mar 25 11:20:13
74	57.2402	91.4022	5.18	2017 Mar 25 11:46:22
75	57.2402	91.4022	5.16	2017 Mar 25 11:52:32
76	57.2336	91.4010	4.25	2017 Mar 25 12:32:04
77	57.2226	91.4017	3.25	2017 Mar 25 13:15:20
78	57.2163	91.4053	1.96	2017 Mar 25 14:06:46
79	57.3369	90.9617	5.29	2017 Mar 30 13:06:39
80	57.3163	90.9312	8.05	2017 Mar 30 14:53:00

81	57.1506	91.7049	3.17	2017 Mar 31 12:41:09
82	57.1561	91.7093	4.11	2017 Mar 31 13:17:55
83	57.1579	91.7106	4.63	2017 Mar 31 13:49:51
84	57.1601	91.7129	5.02	2017 Mar 31 14:23:12
85	57.1615	91.7139	4.96	2017 Mar 31 14:56:39
86	57.1467	91.7007	2.79	2017 Mar 31 16:11:42
87	57.1506	91.7049	3.36	2017 Mar 31 16:29:02
88	57.1561	91.7093	3.91	2017 Mar 31 16:43:23
89	57.1579	91.7106	4.21	2017 Mar 31 16:54:49
90	57.1601	91.7129	4.53	2017 Mar 31 17:06:31
91	57.1615	91.7139	4.54	2017 Mar 31 17:16:01
92	57.1467	91.7007	1.79	2017 Apr 02 08:51:36
93	57.1506	91.7049	2.31	2017 Apr 02 09:15:25
94	57.1561	91.7093	2.90	2017 Apr 02 09:37:57
96	57.1579	91.7106	3.19	2017 Apr 02 09:59:27
97	57.1601	91.7129	3.38	2017 Apr 02 10:17:41
98	57.1615	91.7139	3.43	2017 Apr 02 10:28:49
99	57.1601	91.7129	3.26	2017 Apr 02 11:03:36
100	57.2402	91.4022	4.85	2017 Apr 05 10:58:07
101	57.2456	91.4049	5.28	2017 Apr 05 12:40:35
102	57.2256	91.4017	2.68	2017 Apr 05 14:02:34
103	57.2163	91.4053	1.72	2017 Apr 05 15:06:24
105	57.1615	91.7139	3.23	2017 Apr 06 14:20:22
106	57.1602	91.7129	3.21	2017 Apr 06 14:31:10
107	57.1580	91.7109	2.98	2017 Apr 06 14:39:30
108	57.1556	91.7088	2.69	2017 Apr 06 14:50:05
109	57.1556	91.7088	2.03	2017 Apr 06 14:59:01
110	57.1506	91.7049	1.36	2017 Apr 06 15:07:46
111	57.1615	91.7139	3.17	2017 Apr 06 15:26:43
112	57.1602	91.7129	3.13	2017 Apr 06 15:38:12

113	57.1580	91.7109	2.88	2017 Apr 06 15:46:18
116	57.1556	91.7088	2.61	2017 Apr 06 15:55:55
117	57.1556	91.7088	1.97	2017 Apr 06 16:04:59
118	57.1506	91.7049	1.34	2017 Apr 06 16:14:55
119	57.1615	91.7139	3.32	2017 Apr 06 16:39:26
120	57.1602	91.7129	3.28	2017 Apr 06 16:48:27
121	57.1580	91.7109	3.02	2017 Apr 06 16:58:43
122	57.1556	91.7088	2.77	2017 Apr 06 17:08:23
123	57.1556	91.7088	2.14	2017 Apr 06 17:18:27
125	57.1506	91.7049	1.52	2017 Apr 06 17:29:32
126	57.1615	91.7139	3.53	2017 Apr 06 18:01:23
127	57.1602	91.7129	3.56	2017 Apr 06 18:11:33
130	57.1580	91.7109	3.29	2017 Apr 06 18:23:17
131	57.1556	91.7088	3.07	2017 Apr 06 18:32:09
132	57.1556	91.7088	2.45	2017 Apr 06 18:40:20
133	57.1506	91.7049	1.79	2017 Apr 06 18:47:56
134	57.1615	91.7139	3.83	2017 Apr 06 19:01:36
135	57.1602	91.7129	3.81	2017 Apr 06 19:08:55
136	57.1580	91.7109	3.55	2017 Apr 06 19:17:00
137	57.1556	91.7088	3.28	2017 Apr 06 19:23:37
138	57.1556	91.7088	2.68	2017 Apr 06 19:32:39
139	57.1506	91.7049	2.02	2017 Apr 06 19:40:28
140	57.1615	91.7139	4.04	2017 Apr 06 19:53:09
141	57.0977	91.9720	3.16	2017 Apr 07 09:49:59
143	57.1032	91.9666	3.60	2017 Apr 07 10:45:38
144	57.1032	91.9666	3.58	2017 Apr 07 12:03:42
145	57.0977	91.9720	3.14	2017 Apr 07 12:13:55
146	57.0932	91.9647	3.17	2017 Apr 07 12:32:28
147	57.0870	91.9673	2.42	2017 Apr 07 12:53:41
148	57.1204	91.8459	2.89	2017 Apr 07 14:44:16

149	57.1143	91.8418	2.05	2017 Apr 07 15:30:55
151	57.1615	91.7139	4.14	2017 Apr 11 11:01:52
152	57.1601	91.7129	4.25	2017 Apr 11 11:31:33
153	57.1601	91.7129	4.49	2017 Apr 11 11:57:42
154	57.1615	91.7139	4.40	2017 Apr 11 12:05:25
155	57.1601	91.7129	4.48	2017 Apr 11 13:01:56
156	57.1615	91.7139	4.39	2017 Apr 11 13:07:29
157	57.1601	91.7129	4.32	2017 Apr 11 14:03:21
158	57.1615	91.7139	4.26	2017 Apr 11 14:08:18
159	57.1601	91.7129	4.17	2017 Apr 11 15:01:51
160	57.1615	91.7139	4.06	2017 Apr 11 15:06:14
161	57.1601	91.7129	3.99	2017 Apr 11 15:59:25
162	57.1615	91.7139	3.87	2017 Apr 11 16:05:09
163	57.1601	91.7129	3.79	2017 Apr 11 17:00:18
165	57.1601	91.7129	3.71	2017 Apr 11 17:07:21
166	57.1615	91.7139	3.63	2017 Apr 11 18:00:31
167	57.1601	91.7129	3.53	2017 Apr 11 18:05:52
168	57.1615	91.7139	3.46	2017 Apr 11 19:01:31
169	57.1601	91.7129	3.45	2017 Apr 11 19:03:44
170	57.1615	91.7139	3.36	2017 Apr 11 19:08:17

Under Ice CDOM and Suspended Sediments

Colored Dissolved Organic Matter (CDOM) was used as a proxy to trace the under-ice freshwater plume. Along with CDOM, suspended sediments in the water column were measured to assess the sediment load capacity of the Nelson-Hayes River plume during the winter months. Both parameters were collected for the under-ice water at the mooring locations. A tidal period-based sampling approach for CDOM and suspended sediment was adopted for the Mooring: M01. This sampling approach involved a transect sampling where the first sampling point was close to the Nanuk Polar Bear Lodge and the last point was the mooring: M01. Aquascat, an acoustic device to monitor the sediment suspension process in the water column was moored near the mooring M01. It was deployed for a period of Leg 2 and 3. Discrete samples collected for suspended sediment analysis were also analyzed in the temporary laboratory of Nanuk Polar Bear Lodge for particle size distribution analysis using Microtrek particle size analyzer. Collected CDOM samples were brought back to CEOS for its absorption measurement using Perkin

Elmer Lambda 650S UV-VIS spectrophotometer for a wavelength range of 250-800nm. Standard vacuum filtration technique was adopted for Total Suspended Solid (TSS) measurement. The filtered samples were brought to CEOS for oven drying at 104° and 500° followed by precision weighing after each drying step. The oven drying and weighing process were repeated for each sample until the error margin was below 0.0002 g/l.

Meteorological conditions: A meteorological station was deployed on land near the Nanuk lodge to collect a continuous record of surface meteorological conditions throughout the field program. Air temperature, winds, pressure, and humidity were collected at 10-minute intervals at a height of ~ 5m above ground. The system collected a complete record during leg 1, but failed in between legs and collected data intermittently during legs 2 and 3. The issue was the power supply to the station. A sample of the data is provided below.

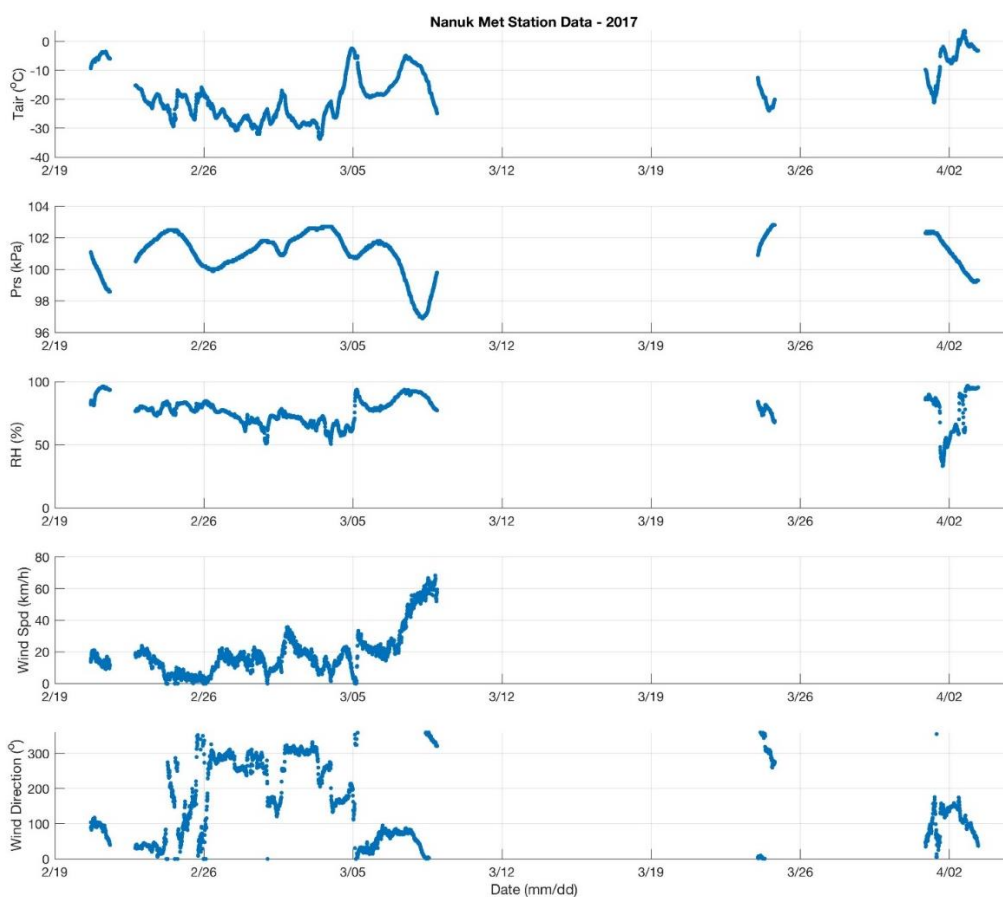


FIGURE 3.9 A sample of the MET data collected at Nanuk during the field program.

Additional observations

The landfast ice cover was much rougher than anticipated. While the landfast is stationary it was very dynamic during its initial formation and had continued to be dynamically deformed under tidal

fluctuations. At several places, there were very large ridges that formed parallel to the shore. It's likely that these ridges were grounded and were more pronounced during low tide when the free-floating ice surrounding them dropped with the tide.

The stamukhi at the landfast ice edge was very pronounced and was predominantly comprised of layers of thin ice that had been dynamically deformed into much larger pieces of ice. Due to the high tidal range, the landfast ice edge was a very dynamic area, with the formation of large areas of open water on a diurnal cycle as a result of the tidal cycle. With cold atmospheric temperatures, the exposure of open water along the landfast ice edge led to considerable new ice formation. However, this ice was subsequently deformed as rising tides pushed the mobile ice cover back towards the landfast ice.

The extent of the landfast ice cover increased episodically during winter 2017 as mobile ice adhered to the landfast ice and extended its coverage. Below are 4 images from Sentinel that show the growth of the landfast ice from mid-January to mid-February (Figure 3.10).

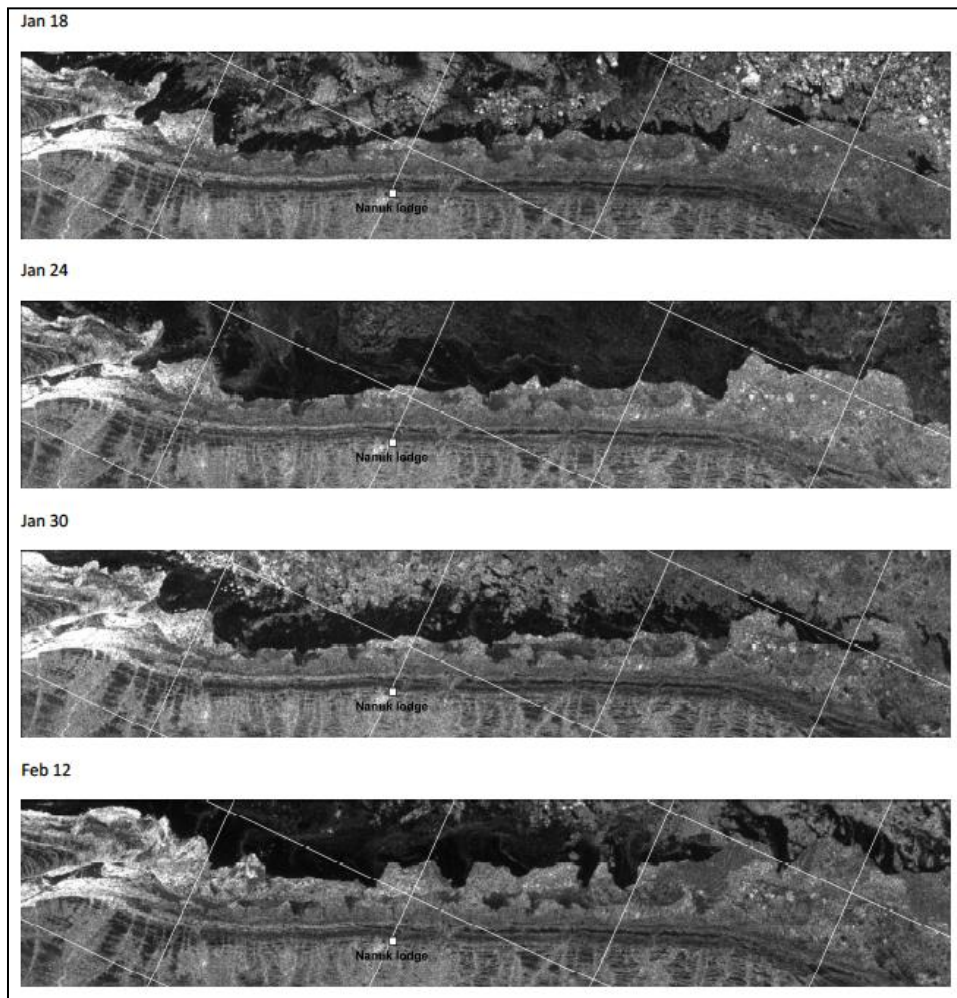


FIGURE 3.10 Sentinel-1 images over the landfast sea ice near Nanuk during 2017. The Nelson estuary is to the left and Cape Tatnam to the right. Black areas indicate open water, while the lower portion (south) of each image is land.

3.4 Team 3 – Marine Ecosystems

The availability of light and nutrients controlled by physical oceanic processes and river runoff determine the timing and magnitude of biological productivity. In winter, light transmission through snow-covered sea ice is very low while nutrient loading is influenced by different freshwater discharges of unregulated vs. regulated rivers. The aim of team 3 sampling was to examine the influence of the hydro-regulated Nelson River on the biological productivity under landfast sea ice during the winter-spring transition. Simultaneously, light propagation through the ice cover and primary productivity at the ice bottom and in the water column was measured.

Sea Ice sampling

Ice samples were collected using a 9 cm Mark II Kovacs core barrel. The bottom 5 cm and 5-10 cm of 3-5 cores were pooled together in their respective sections for each site and the bottom skeletal layer (1-2 cm) of 3-5 cores were scraped into 500 mL of filtered seawater. A separate core was taken for analysis of bulk nutrients on the bottom 5 cm and a section from 5-10 cm. A full core was also taken to measure temperature and salinity for 0-5 cm sections for a full ice profile. These values will be used to calculate percent brine volume.

The bottom 0-5 cm and 5-10 cm sectioned pooled cores were melted in the dark and 0.2 µm filtered seawater (FSW) was added at a ratio of three parts FSW to one-part ice. The melted pooled cores were then subsampled for the following variables that were filtered on Whatmann GF/F filters, frozen at -20°C and brought south for analyses: chlorophyll a, particulate organic carbon and nitrogen, high-performance liquid chromatography, particulate spectral absorption, algal taxonomy (via visible microscopy) and flow cytometry. The scraped cores were then subsampled for the following variables that were either fixed and/or frozen at -20°C for analyses: intracellular nutrients, chlorophyll a, and particulate organic carbon and nitrogen. Sample analysis is currently ongoing.

Under-ice light measurements

For ice algae available photosynthetic active radiation (PAR, 400 – 700 nm) was measured 10 cm below the ice bottom. A UV-visible hyperspectral radiometer (Cosine RAMSES-ACC, TriOS GmbH, Germany) was mounted to a metal arm and faced upward 1.50 m away from a drilled hole. To calculate light transmission incident radiation and albedo were measured with the same sensor at the ice surface. Ice thickness and snow depth were also recorded.

Water sampling

Interface water at the ice bottom close to the river estuary and marine water of several depth levels at the landfast sea ice sampling sites was collected to characterize the biological and chemical properties of the water column.

Samples for inorganic nutrients (ammonium, nitrite, nitrate, orthophosphate, and orthosilicic acid) were taken from the water column after filtration through pre-combusted GF/F filters inserted in a filter holder

at all stations. Samples for inorganic nutrients were collected into acid-washed 15ml polyethylene tubes and immediately frozen until further analysis at Laval University (Hansen and Koroleff 2007). Subsamples for ammonium (NH₄) were taken at all sampling depths. Concentrations were determined upon collection by derivatization with OPA and fluorimetric detection according to Holmes et al. 1999 using a Turner Designs fluorometer (analytical detection limit of 0.02 μmol l). Urea samples were analyzed using the method of Mulveena and Savidge [1992] and Goeyens et al. [1998]. Water samples for dissolved organic carbon (DOC) and total dissolved nitrogen (TDN) were pre-filtered through pre-combusted GF/F filters to remove large particles and acidified with hydrochloric acid. Samples for total dissolved nitrogen (TDN) will be analyzed by high-temperature catalytic combustion. DON will be calculated by the difference between TDN and inorganic N. The samples were stored at 4 °C in the fridge until further analysis. Samples for chlorophyll-a (chl-a) measurements were collected from the water column and filtered through GF/F filters. The pigments in filters were extracted in 90% acetone at 4 °C in the dark for 24h. The chl-a concentrations were measured using Turner Designs 700 fluorometer (before and after acidification).

To determine nitrate, ammonium uptake rates, and primary production, 500 ml or 1000 ml of water samples from the surface were incubated for 24h at high (about 60 μE m²/s) and low (about 5 μE m²/s) light intensities to compare different light regime with ¹³C- ¹⁵N stable isotopic labeling technique. After incubation, water samples from incubations were filtered through pre-combusted GF/F filters, and filters were immediately frozen. Isotopic ratios of nitrogen and carbon from GF/F filters and water samples will further be analyzed using mass spectrometry. Filtrate samples from ammonium uptake were also kept and frozen to determine nitrification rates. Water samples for natural abundances of nitrogen and carbon isotopes were also collected. Water was pre-filtered through a combusted GF/F filter and stored in 60 mL Nalgene bottles. Samples were immediately frozen and stored at -80 °C. Isotopic analyses will be conducted at Julie Granger's laboratory (University of Connecticut) using the denitrifier method (Sigman et al. 2001; Casciotti et al. 2002).

TABLE 3.3 Water sampling parameters collected by BaySys team 3.

Acronym	Sampling Parameters
Chl a	Chlorophyll a concentration
NO ₃ , NO ₂ , Si, PO ₄	Nitrate, nitrite, silicate, and phosphate
NH ₄	Ammonium
Nat. Ab. NO ₃	Natural abundance of nitrate isotopes (¹⁸ O and ¹⁵ N)
¹⁵ N and ¹³ C uptake	Incubation with ¹⁵ N and ¹³ C tracers to determine nitrogen uptake rates and primary production estimates

Reference

Holmes, R.M., Aminot, A., K erouel, R., Hooker, B.A., and Peterson, B.J., 1999. A simple and precise method for measuring ammonium in marine and freshwater ecosystems. *Canadian Journal of Fisheries and Aquatic Sciences*, 56(10), pp.1801-1808.

Hansen HP, Koroleff F (2007) Determination of nutrients. In: Grasshoff K, Kremling K, Ehrhardt M, Weinheim W (eds) *Methods of Seawater Analysis*, New York.

3.5 Team 4 – Carbon System

Participants:

David Capelle Leg 01 – Feb 19 – Mar 11

Nicolas-Xavier Geilfus Mar 18 – Apr 05

Zakhar Kazmiruk Apr 5 – Apr 15

Team 4 Objectives and Activities

The main objective of Team 4 was to characterize the carbon system in major rivers, estuaries, landfast ice, and under-ice water over the late winter-early spring period when carbon-system measurements are limited. Of particular interest was the influence of physical mixing of river water and marine water, as well as in-situ biogeochemical processes on the distributions of dissolved carbon, greenhouse gas (GHG) concentrations (including CO₂ and CH₄), and aragonite-saturation (Ω_{ar}), which is a proxy for ocean acidification.

Sample Collection

Water and ice samples were collected for dissolved inorganic carbon (DIC), total alkalinity (TA), dissolved organic carbon (DOC), methane (CH₄), carbon-13-DIC (13C-DIC), salinity, and oxygen-18 (18O). Additionally, meteorological measurements were collected continuously to characterize air temperature, relative humidity, and wind velocity. In addition to the above measurements, we relied on data collected by other teams to interpret our results, including conductivity, temperature, and depth (CTD) data, ice temperature, and ice salinity, chromophoric dissolved organic matter (CDOM), and total suspended sediment (TSS). Samples were collected at the same locations as team 3 and team 5, including the Nelson and Hayes Rivers, an estuary site downstream from the Nelson River mouth, and 3 cross-shelf transects spaced evenly along a ~50 km stretch of shoreline between the Hayes River and Cape Tatnum. Each transect was ~2 km long, and included between 2 and 3 stations, with a surface and bottom sample being collected at each site (only a surface sample was collected if water depth was less than 3 m beneath the ice).

i) Water Samples

Water samples were collected either by submerging a Niskin bottle through a hole in the ice or using a submersible pump. Samples for DIC and TA were collected in 250 mL or 500 mL glass bottles with a scintered glass stopper. The bottle was overfilled 3x without introducing bubbles via a silicone tube and sealed without a headspace in the field. In the lab, a headspace was added (1% of vial volume) to allow for thermal expansion, a 200 uL of saturated solution of HgCl₂ was added to preserve the sample, typically within 4 hours of sample collection. For all other water samples, a single 500mL glass bottle was overfilled 3 x without introducing air bubbles and sealed without a headspace in the field and brought back to the lab for processing. Water was transferred from this bottle using a 50 mL glass syringe with a 10 cm long piece of 1/8" O.D. silicone tubing attached to the end. The syringe was rinsed 3x with sample water, then filled without introducing air bubbles, then dispensed into 2x 60mL glass serum bottles (CH₄), one 30 mL amber borosilicate glass bottle (13C-DIC), and 13 mL plastic centrifuge tubes (18O). Each bottle was carefully overfilled without introducing air bubbles and sealed without a headspace after preserving with 40 uL saturated HgCl₂ (CH₄), 20 uL saturated HgCl₂ (13C-DIC). No preservative was added to the 18O or salinity samples. For DOC samples, an acid-washed 60 mL plastic syringe was triple-rinsed with sample water, then an acro-disc filter was rinsed with 10mL sample water, before rinsing (3x) and filling a 20 mL glass scintillation vial, and adding 10uL pure Hydrochloric Acid (HCl). Vials were capped, wrapped with parafilm, and stored at 4degC until analysis.

ii) Ice Samples

Ice cores were collected using 9 cm diameter Kovacs core barrels and sectioned into 5 cm or 10 cm sections, and vacuum-sealed in plastic freezer bags, then melted overnight in the dark. Once melted, the bags were unsealed, and the glass syringe was again used to subsample for DIC, TA, CH₄, 13C-DIC, and 18O from each section. Due to smaller sample volumes, DIC and TA samples were collected in 5 x 12 mL glass vials, preserved with 10 uL saturated HgCl₂, and sealed with no headspace. 18O samples were collected in 2 mL glass vials with no preservative and no headspace. Salinity was measured in the remaining water using a hand-held probe, which was calibrated regularly.

iii) Meteorological Data

A meteorological station was installed near the Nanuk lodge at the start of Leg 1 to measure temperature, relative humidity, and wind velocity. This included a 2-dimensional anemometer installed on a 4 m high tower, an air pressure sensor at x m height, and a radiation-shielding enclosure containing a thermometer and relative humidity sensor. Data was logged using a Campbell Scientific CR-1000 datalogger at 10-minute intervals, logging 10-minute averages, as well as min and max values, and standard deviations. The instruments and loggers were powered by a 12-volt lead-acid battery. The met tower operated properly between Feb 20 – Mar 04 but failed thereafter and was not able to be repaired despite repeated attempts.

Data and Preliminary Results

Preliminary results show the rivers display elevated CH₄ concentrations relative to marine waters, suggesting rivers supply CH₄ to Hudson Bay. The river was significantly super-saturated in CH₄, while

marine waters were only slightly supersaturated, suggesting the area would be a source of CH₄ to the atmosphere once the ice cover melts away. Data from the campaign are available online (CanWIN).

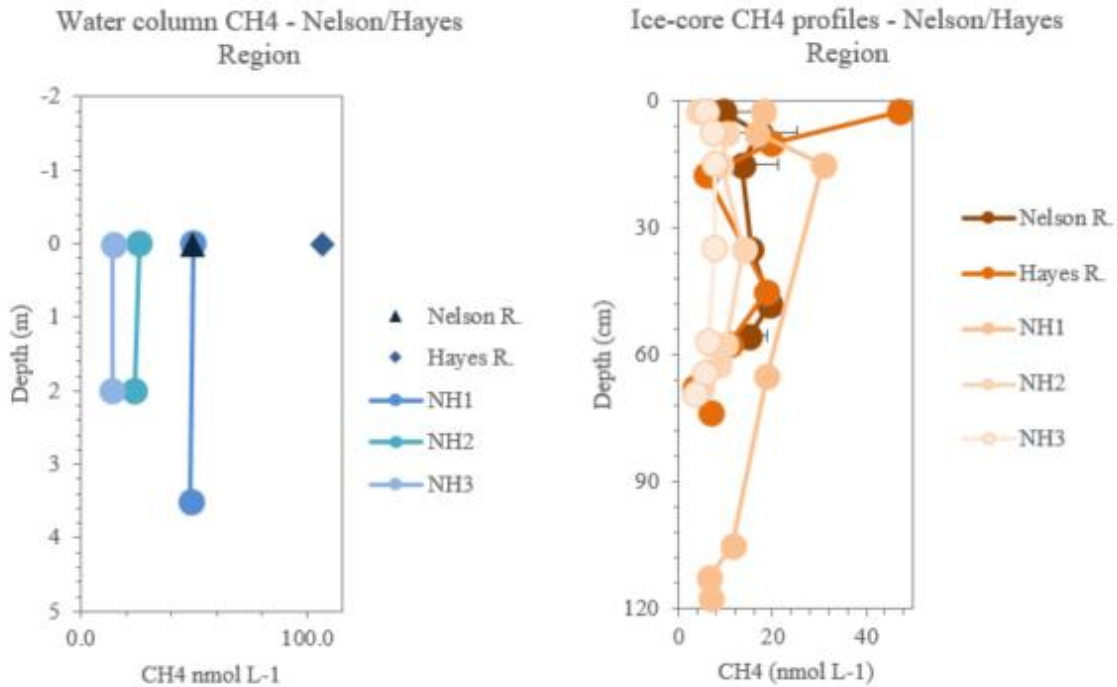


FIGURE 3.13 Example CH₄ concentration from water and ice samples collected during the Nanuk campaign.

3.6 Team 5 – Contaminants

The objective for Team 5 was to determine total mercury (THg) and methylated mercury (MeHg) concentrations in water and ice across the gradient between the Nelson and Hayes Rivers and more saline waters of Hudson Bay. We also aimed to characterize the winter transport of THg and MeHg across the coastal shelf corridor.

The diversion of the Churchill River to augment the Burntwood-Nelson River System for hydroelectricity production increased the winter flow of Nelson River. Despite the higher volume, concentrations of THg and MeHg are lower in the Nelson River than in the Churchill River (Kirk et al, 2008). In addition, THg in the Churchill River is primarily found in its dissolved form (Kirk et al, 2008), which may impact the persistence of THg from riverine sources and its potential for transformation to the bioaccumulating chemical form MeHg in estuarine and marine waters of Hudson Bay.

The goal of constraining the wintertime estuarine sources and transport of THg and MeHg is to determine its importance relative to other potential sources into Hudson Bay, including marine waters, atmospheric,

snowmelt, and how these are tempered by the seasonal sea ice boundary between the atmosphere and the marine water column.

Air Sampling

The Tekran 2537 atmospheric measurement system was set up in the rear portion of a staff cabin with the outside sampling components (1130 and 1131) installed outside the cabin facing northwest. The large power draw needed to run the particulate units prevented the collection of particulate mercury (Hg(II)) and reactive gaseous mercury species. As a result, only gaseous elemental mercury concentrations were measured for the majority of the field campaign.

Water Sampling

Surface water from stations was collected by dipping bottles through the 8" auger hole in the ice wearing clean vinyl gloves.

Water column sampling was also accomplished by deploying a 2.5 L Niskin bottle from a metered line with a Teflon-coated messenger. All water sampling was accompanied by CTD deployment immediately before the deployment of the Niskin bottle. The Niskin bottle deployment required a 10" auger hole through which the Niskin bottle in the cocked position and trigger mechanism were lowered down by hand. At the desired sampling depth, the Teflon coated messenger was released gently to minimize splashing of water. The line was then raised and the Niskin bottle was observed to determine whether the messenger successfully triggered the closure of the bottle. At times, we observed the freezing of water on the spring in the trigger mechanism. The freezing of the spring would result in a bottle misfire as the depressed trigger would block the top of the Niskin bottle from closing.

To prevent both the freezing of the spring as well as the spigot and valve, water was often sampled within the Eskimo brand ice-fishing tent using either a hairdryer or a Little Buddy brand car heater to thaw Niskin bottle components before deployment.

Samples were collected in 250 mL amber glass bottles. Bottles were rinsed with sample water before filling, filled to the shoulder, capped, and double bagged. Bagged samples were transferred to a filtered-air bubble constructed in a staff cabin at the Nanuk lodge in coolers with hot water bottles to prevent freezing. Care was taken to avoid cross-contamination with sampling equipment and personnel involved in DIC/TA sampling and preservation, which requires the use of high concentrations of HgCl₂ as a preservative agent.

Ice Sampling

Ice cores were collected using the 9 cm Mark II Kovacs core barrel in conjunction with teams 1, 3, and 4 from 2 landfast ice. Cores were bagged in core bags, labeled in the field, and transferred to the lodge. Cores were cut with a metal Japanese saw into 5 cm portions outside of the main building (ambient temperature < -20 °C) to prevent thawing. All edges of each core section were then trimmed with ceramic knives to remove ice that came into contact with the core barrel or the metal saw. Trimmed sections were double bagged in new Ziploc bags and kept at room temperature in order to melt. After melting indoors in Ziploc bags, the ice core sections were processed identically to water samples.

Sample Processing

Ideally, the processing of trace metal samples is carried out in cleanroom environments under HEPA-filtered, or equivalent, air supply. Because no certified cleanroom was available at the lodge, a small filtered air bubble was created using plastic sheeting around a Mac10 HEPA filter unit.

A bubble was constructed to minimize falling dust or particles into open bottles during filtration and preservation. All sample filtration and preservation equipment was kept within the bubble throughout the field program.

Double-bagged samples were removed from coolers. Outer bags were removed and samples in inner bags were transferred to the lab bench tent and opened to remove sample bottles. Either a separate 250 mL bottle or ~125 mL of a sample were filtered through Thermo Scientific Nalgene disposable analytical filtration (0.45 μm , 47 mm) units using a Nalgene hand pump under 5 – 10 psi pressure. Filtration unit and filtrate collection bottles were rinsed 3x before filtrate collection. Filter cups were kept covered as much as possible during filtration.

Filters were removed, stored in PetriSlides (EMD Millipore) marked with filtered volume, and stored at -20 °C.

Unfiltered and filtered water and ice samples were preserved to 0.5% HCl (concentrated HCl, JT Baker) and stored in coolers in the dark until transfer to the University of Manitoba for future analysis.

Incubation Experiments

Known amounts of isotope enriched mercury species (MM198Hg and ^{202}Hg (II)) were added to water and ice samples for known incubation times to measure potential rates of in situ mercury methylation and demethylation. Following incubation periods, and melting of ice core sections, samples were preserved as for water samples and transported for analysis.

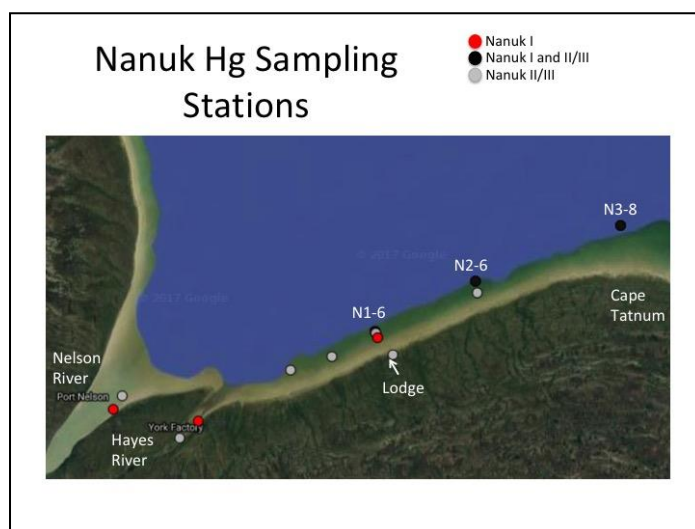


FIGURE 3.11 Sampling Station Locations during the Nanuk field campaign.

References

Kirk JL, St. Louis VL, Hintelmann H, Lehnher I, Else B, Poissant L (2008) Methylated mercury species in marine waters of the Candian High and Sub Arctic. *Enivron. Sci. Technol.* 42:8367-8373.

Appendix 3A: Sampling Schedule

Date	CTD Transect	Station	Hg-Water Sampling	Hg-Ice Sampling	Hg-Air Sampling	Notes
23-Feb-17	Lodge transect					IMB and Mooring #1 deployed
24-Feb-17						Gear arrived, set up clean lab
25-Feb-17	Cape Tatnum transect	N3-8	1m, 3m, 5m, 7m			
26-Feb-17	Middle transect					
27-Feb-17	Hayes and Nelson Rivers	Hayes River	Surface water			
28-Feb-17	Lodge transect	N1-5	1m, 2.5m			
		N1-2	Surface water			
01-Mar-17	Hayes River					No water sampled, auger hit ground
02-Mar-17					Air system maintenance	
03-Mar-17	Nelson River	Nelson River	Surface water			
04-Mar-17	Packing					
05-Mar-17	Blizzard delay					
06-Mar-17	Blizzard delay					
07-Mar-17	Blizzard delay					
08-Mar-17	Blizzard delay				Air system covered in snow	
09-Mar-17	Blizzard delay					
10-Mar-17	Blizzard delay				Air system restarted	
11-Mar-17	Departure					
18-Mar-17	Arrival				Air system maintenance	
19-Mar-17	Lodge transect				Air system restarted	
20-Mar-17	Snow				Air system tripped, restarted	
21-Mar-17	Lodge transect	N1-6	1m, 3m			Set up microplastic experiment with Nix
22-Mar-17	Nelson River	Nelson River	Surface water	Core collection		

23-Mar-17	Hayes River	Hayes River	Surface water	Core collection		
24-Mar-17	Lodge transect					
25-Mar-17	Middle transect	N2-6	1m, 2.5m, 5m			
	Opoyastin River	Opoyastin River	Surface water			
26-Mar-17	Cape Tatnum					Turned back from Cape Tatnum due to snow
27-Mar-17	Cape Tatnum					Escorted others to Cape Tatnum, no light for sampling
28-Mar-17	Lodge transect					Microplastic sampling
29-Mar-17	Crew change/lodge transect					
30-Mar-17	Cape Tatnum transect	N3-8	1m, 3.5m, 7m			
31-Mar-17						
01-Apr-17	Cape Tatnum	N3-8		Core collection for incubation		
02-Apr-17	Snow					
03-Apr-17	Snow					
04-Apr-17	Snow					
05-Apr-17	Middle transect	N2-6	1m, 2m water	Core collection		
06-Apr-17	Lodge transect	N1-6	1m, 2m water, 1m incubation water			
07-Apr-17	Lodge transect	N1-4	1m water, incubation water			
	Menahook River	Menahook River	1m, 3m			
	Fourteens River	Fourteens River	55cm, 2m			
08-Apr-17	Middle transect	N2-6	55cm, 6m, 55cm incubation water			
	Middle transect	N2-3	1m, 3m, 1m incubation water			
09-Apr-17						

10-Apr-17					Air system taken down, packed	
11-Apr-17	Lodge transect	N1-6	1m, 3m water, 1m incubation water			
		N1-4	1m, 2m water, 1m incubation water			
12-Apr-17	Lodge transect					Microplastic sampling; IMB and Mooring #1 Retrieved
13-Apr-17	Packing					
14-Apr-17	Packing					
15-Apr-17	Departure					

Chapter 4 - Sediment Coring and Water Quality



FIELDWORK PARTICIPANTS Dr. Zou Zou Kuzyk¹; Tassia Stainton¹; James Singer¹; Samantha Huyghe¹ (March 1-6); Skye Kushner¹ (April 2-5)

ORIGINAL REPORT DRAFTED BY T.M. Stainton and J. Singer

¹Centre for Earth Observation Science, University of Manitoba, 535 Wallace Building, Winnipeg, MB

CITE CHAPTER AS Kuzyk, Z.Z., Stainton, T., Singer, J., Huyghe, S., Kushner, S. 2019. Sediment Coring and Water Quality Fieldwork Summary. Chapter 4 in, *Hudson Bay Systems Study (BaySys) Phase 1 Report: Campaign Reports and Data Collection*. (Eds.) Landry, DL & Candlish, LM. pp. 94-97.

4.1 *Fieldwork Objectives*

The objective of this fieldwork was to investigate the nature of sediment, organic matter, and mercury contributions over time to lakes in the Nelson River system through the collection of sediment cores and water samples from 2 sites within the pre-and post-impoundment waterbody extents at 5 lakes in the Nelson River watershed:

On-system
 Stephens Lake
 Threepoint Lake

Split Lake Off-system
 Leftrook Lake
 Assean Lake

4.2 *Logistical Summary*

Lakes in this study were accessed by Otter on wheel-skis provided by Wings Over Kississing, flown from the airport in Thompson, Manitoba. A detailed flight summary is provided in the table below (Table 4.1). Flight duty days began at 7:30 am, therefore any delay in departure time was a result of unsuitable weather conditions. Flight days were canceled from March 4-8th due to a province-wide winter storm, and on April 3rd due to freezing rain conditions in Thompson. Transport by ski-doo to the coring site on April 3rd was provided by a local guide from Split Lake, Manitoba.

TABLE 4.1 Detailed flight summary including departures and arrivals to station sites.

Date	Lake	Depart	YTH	Arrive	Lake	Depart	Lake	Arrive	YTH	Miles	Flight Time
Mar 2	Threepoint Lake	12:50	13:10		18:15		18:35		82		40 min
Mar 3	Leftrook Lake	11:00	11:20		15:30		15:50		70		40 min
Apr 4	Stephens Lake	9:40	10:40		14:00		-		190		90 min
Apr 4	Split Lake	-	14:30		15:45		16:15		69		30 min

4.3 *Sediment Coring*

At on-system lakes, deep sites within the pre-flooding extent and shallow sites within the post-flooding extent were selected using waterbody boundary, bathymetry, and bottom substrate ArcGIS shapefiles generated as part of the Regional Cumulative Effects Assessment undertaken by Manitoba Hydro. At off-system lakes, deep and shallow sites were selected in areas likely to yield successful core recovery by reviewing bathymetry and bottom substrate maps provided by Manitoba Hydro.

4.4 Methods

At each lake, sediment coring was executed using two, water depth-specific coring systems deployed through a 10-inch hole drilled through the ice using a motorized ice auger.

At deep sites, sediment cores were collected using a KB-style gravity corer supported by a line strung through a block pulley mounted to a quadra-pod. Once settled in bottom sediment, the core was secured by tripping a closure lid on the gravity corer by the release of a messenger. Cores were retrieved by hand-hauling the gravity corer up through a 10-inch hole in the ice. Water atop each core was siphoned off to preserve the sediment surface during transport. Core samples were split at 1 cm intervals, stored in whirlpack bags, and refrigerated.

At shallow sites, pairs of sediment cores were collected using a manually operated, wetland push-style corer. Due to the nature of this coring equipment, it could only be deployed in less than 2 m water depth. Two cores were collected through separate holes to secure enough material, which was subsequently combined and homogenized during the core splitting process. Water atop each core was siphoned off to preserve the sediment surface during transport. Core samples were split at 1 cm intervals, stored in whirlpack bags, and refrigerated.

Sectioned core samples will be processed and prepared for various analytical methods at the Centre for Earth Observation Science at the University of Manitoba.

Sampling Summary

Sediment cores were successfully retrieved from both sites at all lakes but Stephens Lake, where the bottom substrate at the deep site would not allow for penetration of the gravity corer. The shallow site at Stephens Lake also proved difficult for core recovery due to the gravel-nature of the sediment, but a core was collected after several attempts.

At Threepoint Lake, the substrate at both deep and shallow sites was difficult to penetrate; cores at these sites were shorter than anticipated (8 cm and 7 cm respectively) and comprised sandier sediment than cores collected from off-system lakes.

At Split Lake (SpL-17-01-C), a 12 cm core was collected following several failed attempts; this site exhibited a faster water current than other sites on Split Lake, which inhibited the gravity corer's ability to effectively penetrate bottom sediments.

Sample Inventory

Sediment cores collected during March and April 2017 fieldwork are listed in the table below (Table 4.2). Sample IDs ending in "01" indicate a core collected using the KB-style gravity corer, whereas those ending in "02" indicate a core collected using the wetland corer.

TABLE 4.2 Sediment core details from fieldwork (March – April 2017).

Date	Lake	Sample ID	Water	Depth	Core Length	UTM	Zone	Easting	Northing
Mar 2	Threepoint Lake	TL-17-01	6.7 m	8 cm		14U	508097		6169531
Mar 2	Threepoint Lake	TL-17-02	1.4 m	7 cm		14U	507759		6170806
Mar 3	Leftrook Lake	LL-17-01	10.0 m	53 cm		14V	517586		6213052
Mar 3	Leftrook Lake	LL-17-02	1.0 m	24 cm		14V	516690		6213538
Mar 4	Assean Lake	AL-17-01	8.3 m	54 cm		14V	662680		6236546
Mar 5	Assean Lake	AL-17-02	1.0 m	20 cm		14V	663010		6236226
Apr 3	Split Lake	SpL-17-01-A	5.7 m	40 cm		14V	678487		6236828
Apr 3	Split Lake	SpL-17-01-B	5.7 m	42 cm		14V	678488		6236825
Apr 4	Split Lake	SpL-17-01-C	9.0 m	12 cm		14V	673290		6225306
Apr 4	Stephens Lake	StL-17-02	1.8 m	20 cm		15V	392760		6251882

4.5 Water Sampling

Methods

At all stations, water samples were collected for dissolved organic carbon (DOC), sulphide, and mercury. Water for all samples was collected through a 10 inch augured hole in the ice using a GO-FLO bottle on a weighted rope. Sulphide samples were collected into glass vials (containing 6M HCl, FeCl₃, N, N-dimethyl- p-phenylenediamine, and purged with nitrogen) using syringes. When the water is added to the vile, any sulphide in the water should form a blue complex with the reagents. This complex is stable when stored in an oxygen-free environment and can be analyzed by a UV-visible spectrometer in Winnipeg. DOC samples were filtered through a 0.45 µm filter and collected in a 2 mL vial. They were then preserved with 100 µL of 1M HCl. Mercury samples were collected using the clean hands-dirty hands technique. Both filtered and unfiltered samples were collected for total mercury and methyl mercury in glass amber pre-washed and spot-tested bottles. Filtering was done through 0.45 µm filters in the hotel bathroom and samples were preserved with 0.5% HCl. Blanks were taken for mercury, sulphide, and DOC at all sites. In addition, mercury blanks were taken in the hotel bathroom. Water samples were stored in coolers with ice until we returned to Winnipeg. Sample analysis is ongoing.

Sampling Summary

Water samples were successfully retrieved from two sites on all lakes except for Split Lake in which water was only collected from one site in the interest of time. Water samples were collected at deep sites from 2-3 depths. At shallow sites, water was collected at one depth in duplicate.

SUMMER/FALL 2017



Nelson River survey and water sampling fieldwork site. This work both supplemented previously collected samples that yielded insufficient material and provided new samples for the project.

CHAPTER 5 - SEDIMENT, SOIL, AND WATER QUALITY

FIELDWORK PARTICIPANTS Tassia Stainton: M.Sc. student with Dr. Zou Zou Kuzyk; Brendan Brooks: Technician and M.Sc. student with Dr. David Lobb; Jiang Liu: Ph.D. student with Dr. Feiyue Wang; Julie DePauw: Summer student with Dr. David Lobb

ORIGINAL REPORT DRAFTED BY Tassia Stainton

DATE OF FIELDWORK July 26 to August 1, 2017

CITE CHAPTER AS Stainton, T. 2019. Sediment, Soil, and Water Quality. Chapter 5 in, *Hudson Bay Systems Study (BaySys) Phase 1 Report: Campaign Reports and Data Collection*. (Eds.) Landry, DL & Candlish, LM. pp. 99-108.

5.1 Fieldwork Objectives

The goal of this fieldwork campaign was to collect water, sediment, and soil samples from the Nelson River system to be used by one Ph.D. and two M.Sc. students to fulfill the goals established by Team 5 of the Hudson Bay Systems (BaySys) study. Although site locations remain consistent, a range of sample types and quantities were collected for the individual analytical needs of each student at each site. Some material, such as bulk suspended-sediment samples, will be shared between students so that different analytical methods can be applied to the same sample. Other samples were collected independently for each project. The majority of sites were chosen before the summer 2016 field season, but two new sites in the upper Nelson River system were added this year to increase site density in that portion of the river system. This work will supplement previously collected samples that yielded insufficient material and provide new samples for each project. Sampling methods, summaries, and inventories for each Team 5 project goal will be outlined separately in Sections 4 through 6.

5.2 Logistical Summary

River, lake, and tributary sites were accessed between July 26th and August 1st, 2017 by truck using public and private roads, based out of Thompson and Gillam, Manitoba. A day-by-day plan of field operations is outlined in Table 5.1. Site locations are shown on the map in Figure 5.1.

TABLE 5.1 Day-by-day field plan for BaySys Team 5 July 2017 soil and sediment sampling. (GS: generating station).

Date	Site	Waterbody Description	MB Hydro Access
27-Jul-2017	NR7	Nelson River at Kichi Sipi bridge	
27-Jul-2017	NR8	Nelson River at Norway House ferry	
28-Jul-2017	NR1	Nelson River at Conwapa	Conwapa boat launch
29-Jul-2017	NR2	Nelson River downstream of Limestone GS	
29-Jul-2017	NR3	Nelson River downstream of Longspruce GS	
29-Jul-2017	NR4	Stephens Lake upstream of Kettle GS	
29-Jul-2017	NR6	Nelson River at Keeyask GS south	Keeyask South Access Rd.
29-Jul-2017	LR1	Limestone River	
29-Jul-2017	KR1	Kettle River	
30-Jul-2017	NR5	Stephens Lake northwest arm	
30-Jul-2017	AR1	Assean River	
30-Jul-2017	BR1	Burntwood River upstream of Split Lake	
30-Jul-2017	BR2	Burntwood River downstream of Odei River	
31-Jul-2017	OR1	Odei River	
31-Jul-2017	BR3	Burntwood River at Thompson	
31-Jul-2017	BR4	Burntwood River downstream of Wuskwatim GS	Wuskwatim GS gate
31-Jul-2017	BR5	Burntwood River downstream of Wuskwatim GS	Wuskwatim GS gate
31-Jul-2017	BR6	Notigi Lake upstream of control structure	

5.3 *Sediment and Organic Matter Fingerprinting*

To characterize the sources of sediment and terrestrial organic matter in the Nelson River system, the following sample suite was collected: surface water, suspended sediment, soils, bank material, and bottom sediment. Sites were selected on the main stem Nelson and Rat/Burntwood Rivers and their associated tributaries prior to preliminary fieldwork completed in August 2016 and are based on proximity to established Water Survey of Canada hydrometric stations and pre-existing monitoring stations associated with the Coordinated Aquatic Monitoring Program. All sites are accessible by truck; many are public bridges and boat launches, but three sites required special access from Manitoba Hydro (Table 5.1). This fieldwork provides supplementary samples to those acquired during the 2016 summer field season and includes 2 additional sites in the upper Nelson River region (NR7 and NR8) not visited in 2016. During the 2016 field season, 7 sites yielded an insufficient volume of suspended sediment, therefore new bulk suspended sediment samples from 2016 sites were only collected from sites that lacked material. Analytical methods applied to the sample suite include a panel of water quality parameters (total suspended solids (TSS), particulate organic carbon (POC), and particulate organic nitrogen (PON)), compound-specific stable isotope (CSSI) fingerprinting, elemental carbon analysis, and stable carbon isotope analysis. Sampling methods will be outlined in the following section.

Methods

Surface water samples were hand-dipped using 1 L amber Nalgene bottles that were pre-washed with 10 % HCl. At two sites (NR7 and BR3), a transect of surface water was sampled by collecting 1 L of water from 5 locations along each bridge using a weighted sample bottle holder. Transect samples will allow for comparison of TSS, POC, and PON in surface waters across the Nelson and Burntwood Rivers, since, due to the nature of sampling equipment used in this study, water and suspended sediment samples were collected near the shoreline.

Bulk suspended sediment samples were collected from <1.0 m depth using a gas generator-powered submersible pump connected by plastic hosing to Pentek bag filter housings lined with 1.0 µm nominal pore size Pentair BP-420-1 filter bags. Two filter housings were used at each site and filter bags were replaced after 1.5 hours of pump time to ensure maximum sediment collection and inhibit clogging. Pump time at each site was approximately 3 hours.

Soil, bank material, and bottom sediment were collected by shovel or trowel into Whirl-Pak QR bags.

Sampling Summary

Sampling was executed as planned at all sites except NR8, which did not yield any suspended sediment samples due to submersible pump failure. Equipment installation at site NR4 proved difficult since high winds produced large waves near the shoreline, so suspended sediment samples were anomalously filled with an excess of suspended terrestrial material. Sample collection for sediment and organic matter fingerprinting from each site are listed in Table 5.2.

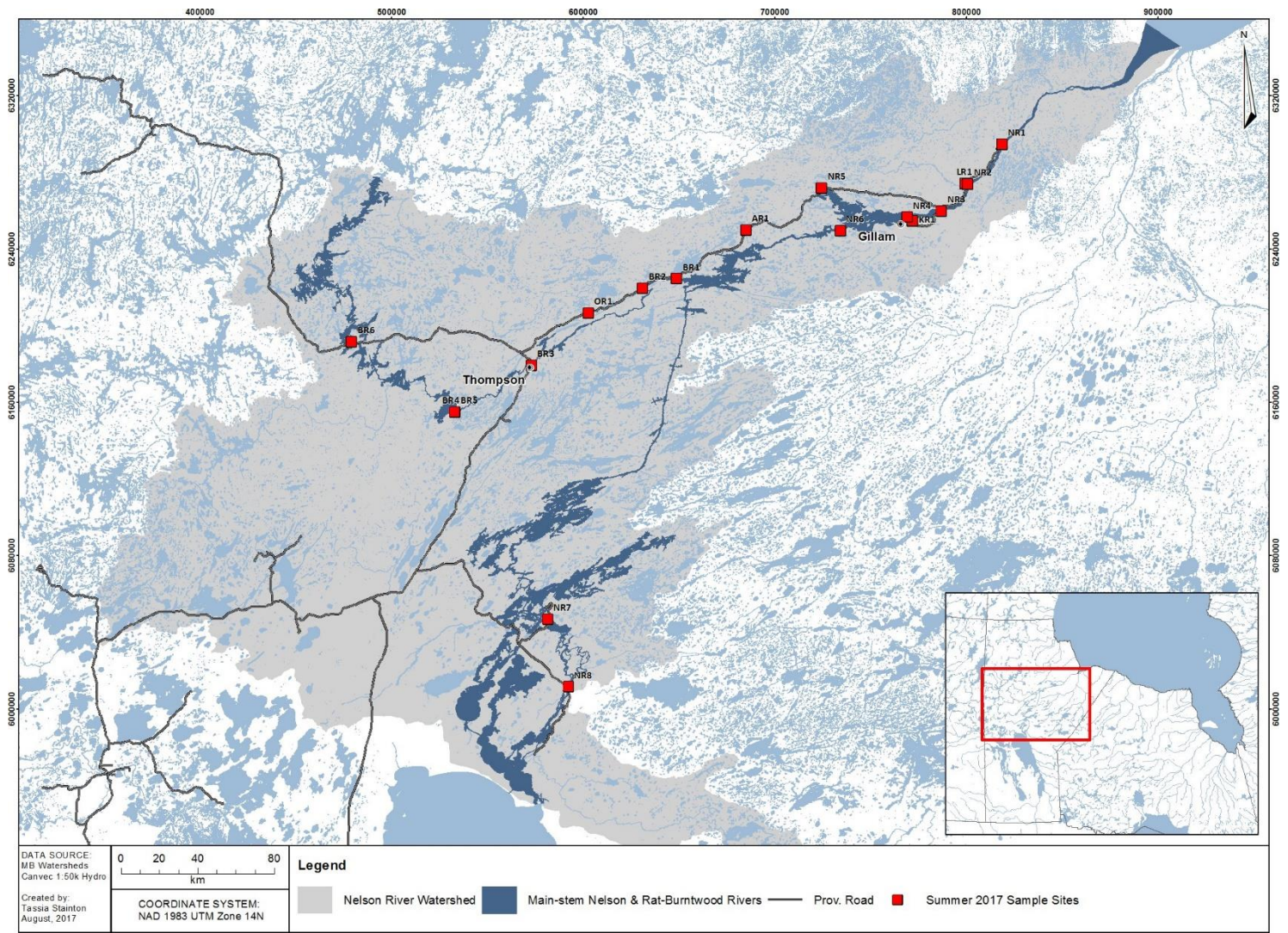


FIGURE 5.1 Map showing sampling locations visited during the July 2017 Team 5 soil and sediment sampling field program.

TABLE 5.2 Samples collected for sediment and organic matter fingerprinting during July 2017 fieldwork. Note that the "Filter Bag" sample type is indicative of a bulk suspended sediment sample.

Site ID	Waterbody	UTM	Zone	Latitude	Longitude	Sample ID	Sample Type
NR1	Nelson River	15 15	V V	56.687	-93.7983	NR1-17-01 NR1-17-06	Surface Water Filter Bag
NR2	Nelson River	15 15	V V	56.5152	-94.1139	NR2-17-01 NR2-17-06	Surface Water Filter Bag
NR3	Nelson River	15 15	V V	56.3957	-94.3521	NR3-17-01 NR3-17-06	Surface Water Filter Bag
NR4	Stephens Lake	15 15	V V	56.3772	-94.6448	NR4-17-01 NR4-17-06	Surface Water Filter Bag
NR5	Stephens Lake	15	V	56.5373	-95.3535	NR5-17-01	Surface Water
NR6	Nelson River	15	V	56.3319	-95.2131	NR6-17-01	Surface Water
NR7	Nelson River	14	U	54.5618	-97.7444	NR7-17-01	Surface Water
NR7	Nelson River	14	U	54.5618	-97.7444	NR7-17-01-a	Surface Water
NR7	Nelson River	14	U	54.5618	-97.7444	NR7-17-01-b	Surface Water
NR7	Nelson River	14	U	54.5618	-97.7444	NR7-17-01-c	Surface Water
NR7	Nelson River	14	U	54.5618	-97.7444	NR7-17-01-d	Surface Water
NR7	Nelson River	14	U	54.5618	-97.7444	NR7-17-01-e	Surface Water
NR7	Nelson River	14	U	54.5618	-97.7444	NR7-17-02-01	Soil Pit - O Horizon
NR7	Nelson River	14	U	54.5618	-97.7444	NR7-17-02-02	Soil Pit - A Horizon
NR7	Nelson River	14	U	54.5618	-97.7444	NR7-17-02-03	Soil Pit - C Horizon
NR7	Nelson River	14	U	54.5618	-97.7444	NR7-17-06	Filter Bag
NR8	Nelson River	14	U	54.2503	-98.3557	NR8-17-01	Surface Water
NR8	Nelson River	14	U	54.2503	-98.3557	NR8-17-02-01	Soil Pit - O Horizon
NR8	Nelson River	14	U	54.2503	-98.3557	NR8-17-02-02	Soil Pit - A Horizon
NR8	Nelson River	14	U	54.2503	-98.3557	NR8-17-02-03	Soil Pit - B Horizon
NR8	Nelson River	14	U	54.2503	-98.3557	NR8-17-02-04	Soil Pit - C Horizon
LR1	Limestone River	15	V	56.5167	-94.1353	LR1-17-01	Surface Water
KR1	Kettle River	15	V	56.3583	-94.5999	KR1-17-01	Surface Water
AR1	Assean River	14	V	56.3566	-96.0092	AR1-17-01	Surface Water
OR1	Odei River	14 14	U U	55.9948	-97.3574	OR1-17-01 OR1-17-06	Surface Water Filter Bag
BR1	Burntwood River	14 14	V V	56.1423	-96.6075	BR1-17-01 BR1-17-06	Surface Water Filter Bag

BR2	Burntwood River	14 14 14	V V V	56.1028	-96.8962	BR2-17-01 BR2-17-06 BR2-17-08	Surface Water Filter Bag Bank Sample Water
BR3	Burntwood River	14 14	U U	55.7538	-97.8413	BR3-17-01 BR3-17-01-a	Surface Water Surface Water
BR3	Burntwood River	14	U	55.7538	-97.8413	BR3-17-01-b	Surface Water
BR3	Burntwood River	14	U	55.7538	-97.8413	BR3-17-01-c	Surface Water
BR3	Burntwood River	14	U	55.7538	-97.8413	BR3-17-01-d	Surface Water
BR3	Burntwood River	14	U	55.7538	-97.8413	BR3-17-01-e	Surface Water
BR4	Burntwood River	14	U	55.5405	-98.4787	BR4-17-01	Surface Water
BR5	Burntwood River	14	U	55.5385	-98.4834	BR5-17-01	Surface Water
BR6	Burntwood River	14	U	55.8685	-99.3362	BR6-17-01	Surface Water

5.4 Sediment Budgeting and Inorganic Fingerprinting

To construct a sediment budget and employ inorganic fingerprinting techniques in the Nelson River system, the main objectives of this fieldwork were to collect samples (suspended sediment, surface water, soils, bank material, and bottom sediment) that could provide a better understanding of sediment transport, and evaluate the continuous-flow filtration system technique used to collect suspended sediment. Inorganic sediment source fingerprinting techniques, when applied to samples collected alongside the Nelson River system, aim to provide information on both the source of sediment transported by the river and the potential effects of hydroelectric dams on sediment transport dynamics. Thus, fieldwork for this project involved collecting suspended sediment samples at several points along the river system (Figure 5.1). Following sample analysis, information on the source of suspended sediment and the relative importance of the dis-connectivity of sediment transport can be obtained by comparing their physical or chemical properties with potential sources in the catchment area. Reliable interpretation of any sampler-derived data, with regard to sediment transport dynamics, is significantly linked to the accuracy of the sampling devices themselves. Therefore, the evaluation of suspended sediment collection techniques is a vital component of this research.

Methods

To address the first objective, it was important to access sites located both upstream and downstream of hydroelectric dams and reservoirs on the Nelson River system. Sampling around these features provides information on the effects of any dis-connectivity structure on sediment transport, therefore the following sample suite was collected from all sites using methods described in Section 5.3: surface water, suspended sediment, soils, bank material, and bottom sediment.

To meet the second objective, submersible pumps were used at selected sampling sites to collect water from the water bodies. Influent and effluent water was simultaneously sampled by collecting 1 L and 7.5 L water samples at different time intervals after pumping began to permit a direct comparison of the

efficiency of these devices. Pentek bag filter housings lined with 1.0 µm nominal pore size Pentair BP-420-1 filter bags were evaluated across different components collected from each site. The Pentek bag filter housings collect instantaneous suspended sediment samples which present discrete suspended sediment flux and properties of the river system. They are an ideal filtration instrument to collect bulk suspended sediment samples due to their capacity for use with a wide range of flow rates (up to 50 gallons per minute), and variance in length (up to 20 inches), and pore size (1 µm to 800 µm). Mass separation and particle size distribution efficiency of this device will be assessed by analyzing inlet and outlet waters.

Sampling Summary

As described in Section 5.3, sampling was executed as planned at all sites except NR8 and NR4.

Sample Inventory

Samples collected for inorganic fingerprinting and evaluating the continuous-flow filtration system technique are listed in Table 5.2 and Table 5.3, respectively.

TABLE 5.3 Samples collected to evaluate the continuous-flow filtration system technique.

Site	Waterbody	Sample ID	Sample Type
NR1	Nelson River	NR1-17-10 NR1-17-11 NR1-17-12 NR1-17-13 NR1-17-14 NR1-17-15	1 L effluent water 5 minutes after starting 1 L effluent water 15 minutes after starting 1 L effluent water 55 minutes after starting 1 L influent water 7.5 L influent water 7.5 L effluent water 5 minutes after starting
NR2	Nelson River	NR2-17-10 NR2-17-11 NR2-17-12	1 L effluent water 5 minutes after starting 1 L influent water 7.5 L influent water
NR3	Nelson River	NR3-17-10 NR3-17-11 NR3-17-12	1 L effluent water 5 minutes after starting 1 L influent water 7.5 L influent water
NR4	Nelson River	NR4-17-10 NR4-17-11 NR4-17-12	1 L effluent water 5 minutes after starting 1 L influent water 7.5 L influent water

NR7	Nelson River	NR7-17-10 NR7-17-11 NR7-17-12 NR7-17-13 NR7-17-14	1 L effluent water 5 minutes after starting 1 L effluent water 15 minutes after starting 1 L effluent water 55 minutes after starting 1 L influent water 7.5 L influent water
OR1	Odei River	OR1-17-10 OR1-17-11 OR1-17-12	1 L effluent water 5 minutes after starting 1 L influent water 7.5 L influent water
BR1	Burntwood River	BR1-17-10 BR1-17-11 BR1-17-12 BR1-17-11 BR1-17-12	1 L effluent water 5 minutes after starting 1 L effluent water 15 minutes after starting 1 L effluent water 55 minutes after starting 1 L influent water 7.5 L influent water
BR2	Burntwood River	BR2-17-10 BR2-17-11 BR2-17-12	1 L effluent water 5 minutes after starting 1 L influent water 7.5 L influent water

5.5 *Methyl Mercury in Lakes and Rivers*

To measure the source or sink of methyl mercury (MeHg) upon flooding soil, samples from both regulated and unregulated reservoirs were collected. Both near-shore and inland soil was sampled for flooding experiments in an attempt to measure the differences in occasionally flooded soil and un-flooded soil in these environments. The near-shore soil in the regulated lakes was collected within the water fluctuation zone to observe differences with the near-shore occasionally flooded soil of reference lakes. Water samples were collected on an opportunistic basis to assess differences in mercury that may be related to differences in the organic matter of the watershed. In addition, water leftover from water sampling was saved for flooding experiments.

Methods

At select stations, surface soil and sediment samples were collected for incubation experiments to determine the potential flux of MeHg from the soil upon flooding. Surface soil and sediment samples were collected using a trowel to remove the top 10 cm of a small area. Near-shore and inland soil samples were collected from each site sampled to distinguish differences between occasionally flooded and unflooded soils. Water samples were collected for total mercury (THg) and MeHg analysis to help understand spatial differences in mercury with varying organic matter in the watershed. Water was sampled for THg and MeHg using the clean hands-dirty hands method into pre-cleaned 2 L Teflon jars. The water was filtered to 0.45 μm through disposable filter cups using vacuum filtration for filtered samples and poured o^{e} directly into pre-cleaned amber bottles for unfiltered samples. All water samples were acidified to 0.5 % HCl.

Sampling Summary

Sampling was carried out as planned at selected sites. Additional opportunistic sampling was carried out during pump operations.

Sample Inventory

All soil, sediment, and water samples collected are listed in Table 5.4.

TABLE 5.4 Samples collected for methyl mercury in lakes and rivers during July 2017 fieldwork. (GS: Generating Station)

Site ID	Waterbody	UTM Zone	Latitude	Longitude	Sample Type
NR1	Nelson River	15 V	56.3993	-94.7375	Filtered water Unfiltered water 1 Unfiltered water 2
NR4	Stephens Lake east	15 V	56.3772	-94.6448	Sediment
					Nearshore soil
					Offshore soil
		15 V	56.3772	-94.6448	Filtered water
					Unfiltered water
NR5	Stephens Lake north	15 V	56.5373	-95.3535	Sediment Nearshore soil Offshore soil
NR6	Nelson River	15 V	56.3319	-95.2131	Filtered water Unfiltered water
Limestone GS	Upstream of Limestone GS	15 V	56.5029	-94.1221	Sediment
		15 V	56.5029	-94.1221	Nearshore soil
		15 V	56.5029	-94.1221	Offshore soil
AL	Assean Lake	14 V	56.2493	-96.3536	Sediment Nearshore soil Offshore soil
BR1	Burntwood River	14 V	56.1423	-96.6075	Sediment Nearshore soil Offshore soil
BR3	Burntwood River	14 U	55.7538	-97.8413	Sediment Nearshore soil Offshore soil Filtered water Unfiltered water 1 Unfiltered water 2 Unfiltered water 3

Acknowledgments

The author would like to acknowledge Masoud Goharrokhi and James Singer for providing content to Sections 5 and 6 respectively. Thanks go to Sarah Wakelin, Allison Zacharias, and Micheal Morris at Manitoba Hydro for their ongoing help with logistical planning and funding support for Team 5 fieldwork. The author would also like to acknowledge the support provided by Team 5 members Dr. Zou Zou Kuzyk, Dr. David Lobb, Dr. Feiyue Wang, and Dr. Kathleen Munson.

CHAPTER 6 - MOORING PROGRAM – CCGS HENRY LARSEN

FIELDWORK PARTICIPANTS PIs: David Barber¹, Jens Ehn¹, Jean-Éric Tremblay², Tim Papakyriakou¹, Celine Gueguen³, Zou Zou Kuyzk¹, Fei Wang¹, David Lobb¹; Field/Ship Coordination: Sergei Kirillov¹, Nathalie Thériault¹; Mooring Operations: Sergei Kirillov, Vladislav Petrushevich¹, Sylvain Blondeau²; Water Sampling Team: Christopher Peck¹

RESEARCH VESSEL Canadian Coast Guard Ship (CCGS) Henry Larsen

DATE OF FIELDWORK October 21 to November 1, 2017

¹Centre for Earth Observation Science, University of Manitoba, 535 Wallace Building, Winnipeg, MB

²Québec-Océan, Department of Biology, Pavillon Alexandre-Vachon, 1045, Avenue de la Médecine, Local 2078, Université Laval, Québec, QC

³Department of Chemistry, University of Sherbrooke (Formerly held position at Trent University)

CITE CHAPTER AS Kirillov, S., Peck, C., and Petrushevich, V. 2019. Mooring Program – CCGS Henry Larsen. Chapter 6 in, *Hudson Bay Systems Study (BaySys) Phase 1 Report: Campaign Reports and Data Collection*. (Eds.) Landry, DL & Candlish, LM. pp. 109-125.

6.1 *Fieldwork Objectives*

In late September 2016, five oceanographic moorings were deployed in the eastern Hudson Bay and at the entrance to James Bay (see chapter 1). These moorings were supposed to be recovered in summer 2017 during the BaySys cruise onboard CCGS Amundsen or White Diamond - a vessel refurbished in 2017 for the Churchill Marine Observatory. Later, a decision on turning the moorings from White Diamond instead of recovery was made. Unfortunately, the slow progress of the ship's inspection from Transport Canada caused multiple delays in the ship's departure from Prince Edward Island and the 2017 cruise was canceled. Because of the critical role of these moorings for the scientific objectives of the upcoming Amundsen cruise in spring 2018, the opportunistic cruise onboard CCGS Henry Larsen was conducted on October 26 – November 1, 2017, to maintain the uninterrupted measurements. The goals for this short cruise were to retrieve and re-deploy as many BaySys moorings as possible accompanied by the concurrent CTD and water sampling.

6.2 *Mooring Operations*

Mooring recovery

Although the late autumn is usually very windy in the Hudson Bay region, the last days of October 2017 were relatively calm with a relatively light wind speed. Such good weather allowed us to use the ship's barge for NE02 and NE03 mooring recoveries (Figure 6.1). The barge was equipped with two small winches that were used to pull the mooring line and instruments onboard. Taking into account the relatively short length of all moorings, the recovery of NE03 and NE02 took approximately 30-40 minutes after the mooring's release. The heavy Trawl Resistant Bottom Mount (TRBM) at NE02 was the only element that could not be lifted on the barge's deck and it was drawn to the ship for lifting with a crane (Figure 6.2). For AN01 mooring, the zodiac boat was used to assist the recovery that was made with a crane from the ship's foredeck.



FIGURE 6.1 Onboard the barge with a recovered mooring



FIGURE 6.2 Lifting the TRBM (NE02) onboard Henry Larsen

The configuration of recovered moorings

The information from all instruments was examined after recoveries to determine if all equipment worked properly and recorded reliable data. We also examined the pressure records from all available sensors to adjust the depths of moored instruments and prepare the final schemes of moorings' configurations (Figure 6.3). In general, all recovered instruments worked well and provided the year-long records of temperature, salinity, current velocities, ice thickness/waves, etc. However, due to the loss of the buoyant tubes the surface ~27 m layer was unresolved at NE02 and NE03 positions in terms of thermohaline properties. It is difficult to say what the reasons for the loss were but the wearing of weak links is mainly suspected for both moorings. Although the surface tubes at AN01 mooring persisted until recovery, the rope connecting the tubes with an anchor tangled around the major mooring line in 5 days after deployment, and the tubes became clung at the depth 30-40 m for the rest of the measuring period. As a result, no surface layer records are available from all three locations and a new strategy needs to be developed for the surface layer measurements throughout the seasonal cycle under the sea ice.

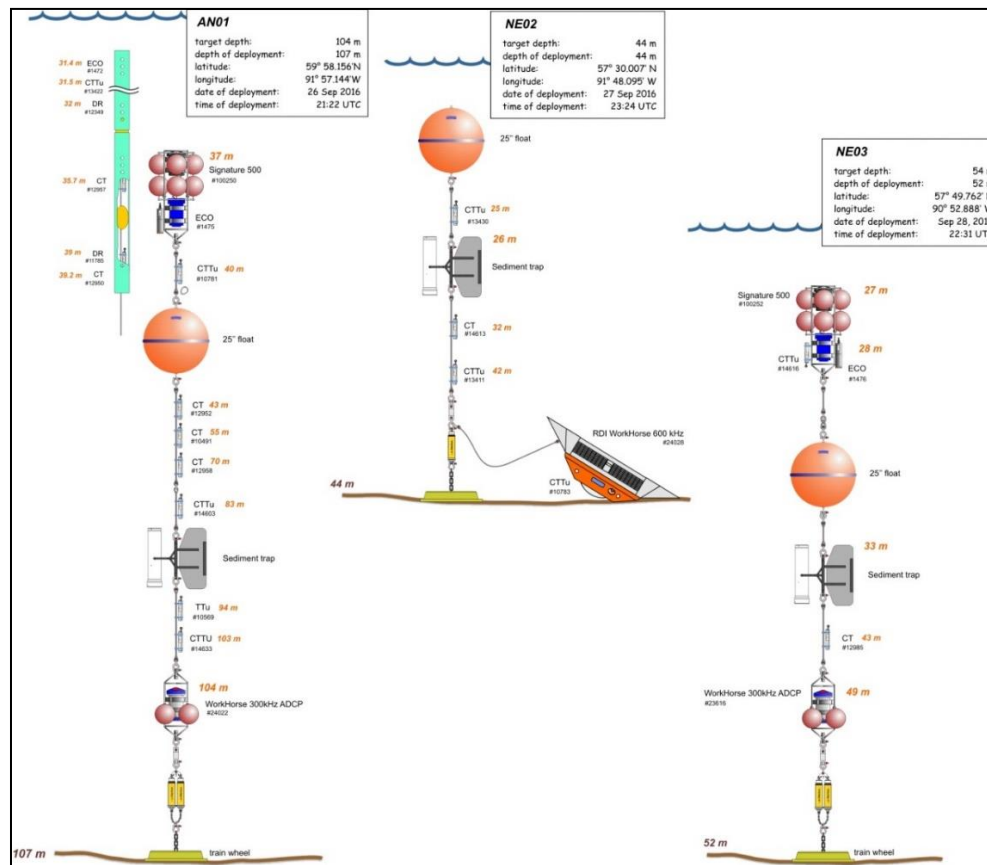


FIGURE 6.3 AN01 (Churchill shelf), NE02 (Nelson Outer Estuary) and NE03 (Nelson River outer shelf) mooring configurations as recovered

It was also found that the TRBM at NE02 flipped upside-down during deployment (Figure 6.3). The large cross-sectional area makes TRBM very unstable during free-fall deployment and its positioning on the sea-floor has to be done with precautions. Although the recommended method of deployment was used (Figure 6.4, left) and the bottom mount was released approximately 10m above the seafloor, the platform seems to have been initially tilted as the ship was drifting during deploying. This could further initialize the flipping as soon as the slip-lines had been released. An alternative approach (Figure 6.4, right) was used to deploy the TRBM at NE01 mooring with the helicopter. The floats were rigged above the platform acting to raise the height of the center of buoyancy and keep any external force from flipping the unit, although the success of that operation will remain unknown until recovery next year.

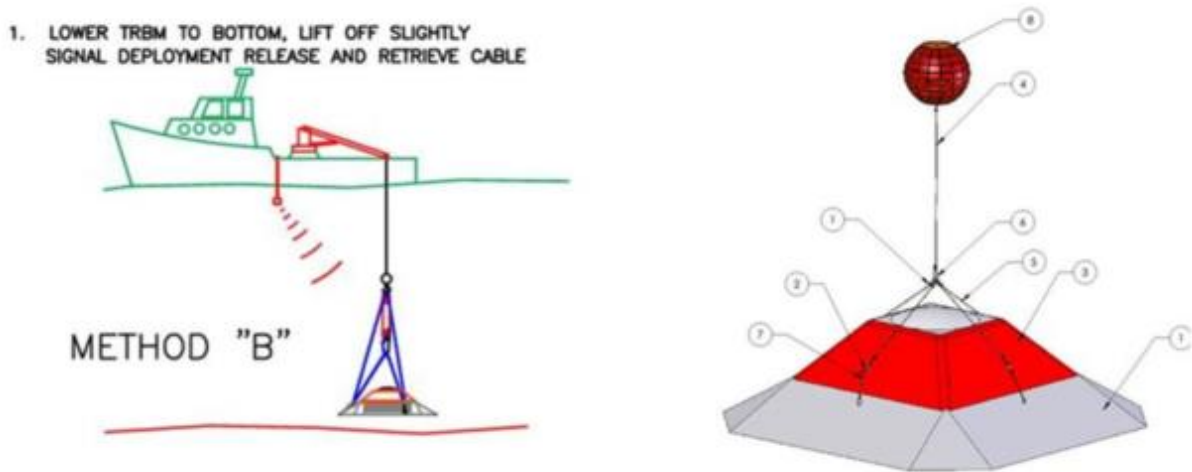


FIGURE 6.4 The deployment of TRBM with an acoustic release (left) and with a float (right)

Mooring re-deployment

The recovered moorings were re-deployed from the helicopter deck by using the crane at the starboard side of the ship (Figure 6.5). The relatively short length of all moorings allowed deploying them “anchor last” (Figure 6.6). Although acoustic releases were found functioning well, we kept using two acoustic releases at each mooring to increase the mooring survivability in case one of the releases failed. The moorings were deployed in the same positions (or in close vicinity) as in 2016.



FIGURE 6.5 Mooring deployment from the helicopter deck



FIGURE 6.6 Approaching the release of the anchor

We kept the same configurations of moored instruments at all three moorings with the minor changes related to the removal of sediment traps and buoyant tubes near the surface. The TRBM at NE02 was also replaced with an in-line not-magnetic frame for carrying the upward-looking ADCP near the bottom. All mooring components were programmed for a one-year deployment with the suggested recovery in early summer 2018 from CCGS Amundsen. The mooring configurations, time of deployments, coordinates, and the codes for acoustic releases are presented in Figure 6.7.

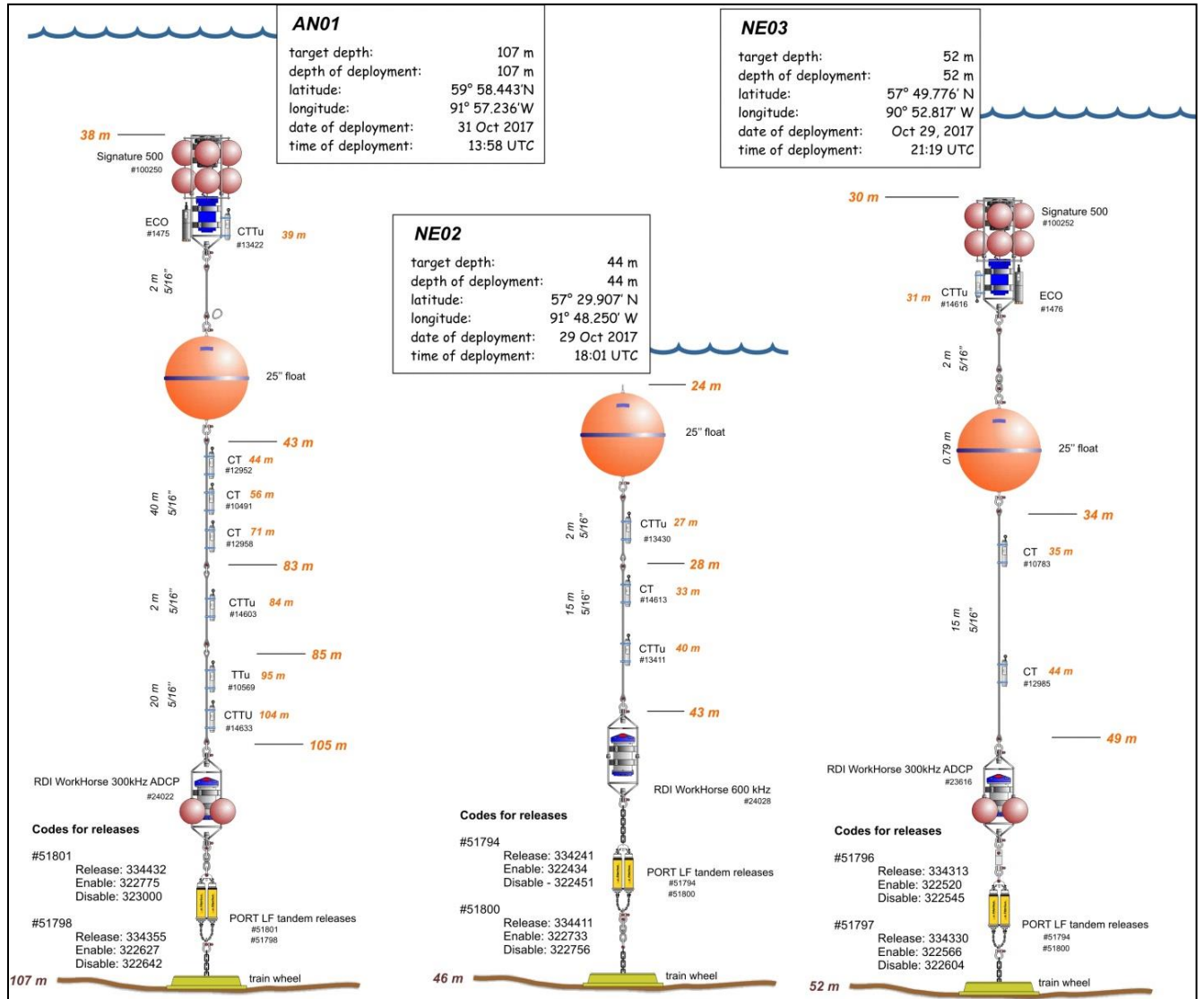


FIGURE 6.7 The new configuration of AN01, NE02, and NE03 moorings

Sediment Traps

The Sediment traps on moorings AN01, NE02, and NE03 were successfully recovered and were not redeployed. Mooring JB02 was not recovered during this operation. Once onboard the traps were dismantled, first removing the PVC tube that houses an asymmetrical funnel, the stabilizing fins, and then the sample vials from the rosette (Figure 6.8). The samples were placed into a vial rack numbered from 1 to 10 (Figure 6.9). The vials were then emptied into labeled amber jars which were then packed and stored in a cooler on the deck. The sediment traps were then reassembled, cleaned with fresh water, and then packed in their respective boxes for transport. The samples collected have been placed in cold storage (-4°C) and are yet to be analyzed.



FIGURE 6.8 The rosette of the sediment traps being filed with a density gradient solution before deployment



FIGURE 6.9 The vials from the sediment traps in the vial rack

6.3 Early Results

The CT sensors deployed at different depths captured the seasonal changes in vertical thermohaline structure at all three positions. These changes correspond to the impact of different processes such as the vertical mixing and redistribution of heat from the surface to the deeper layers in autumn; cooling of the water column and the following salinity increase due to the sea ice growth in winter; the freshening and warming associated with sea ice melting/river runoff and solar heating in summer (Figure 6.10).

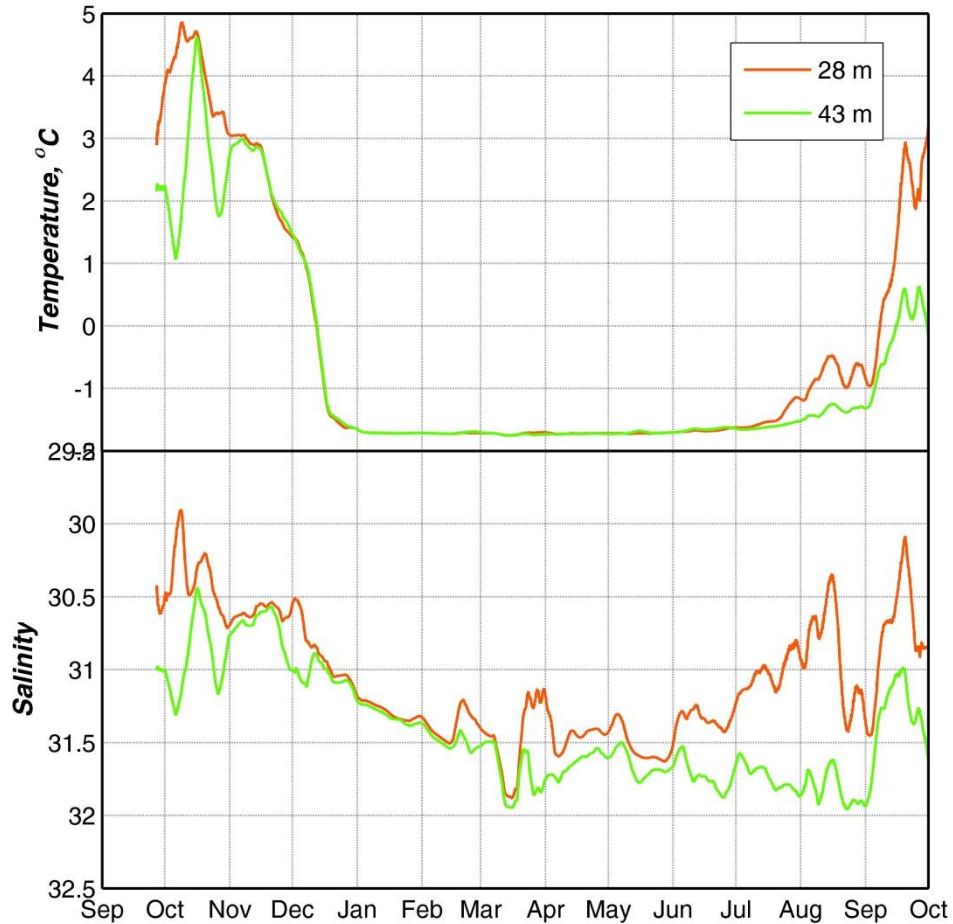


FIGURE 6.10 The one-year evolution of vertical thermohaline structure at NE03 mooring

The effect of atmospheric circulation on the vertical thermohaline structure and freshwater content is seen in CT data at NE02. The altering wind forcing led to the shift of the frontal zone formed by fresher coastal water (diluted by rivers' discharge) and saltier basin water. For instance, the considerable freshening observed at NE02 mooring on March 8 and September 3 was associated with low atmospheric pressure systems passing over the Hudson Bay. The storm winds resulted in on-shore water transport that blocked riverine waters near the shore and caused an abrupt salinity decrease by 1.5-2.0 (Figure 6.11).

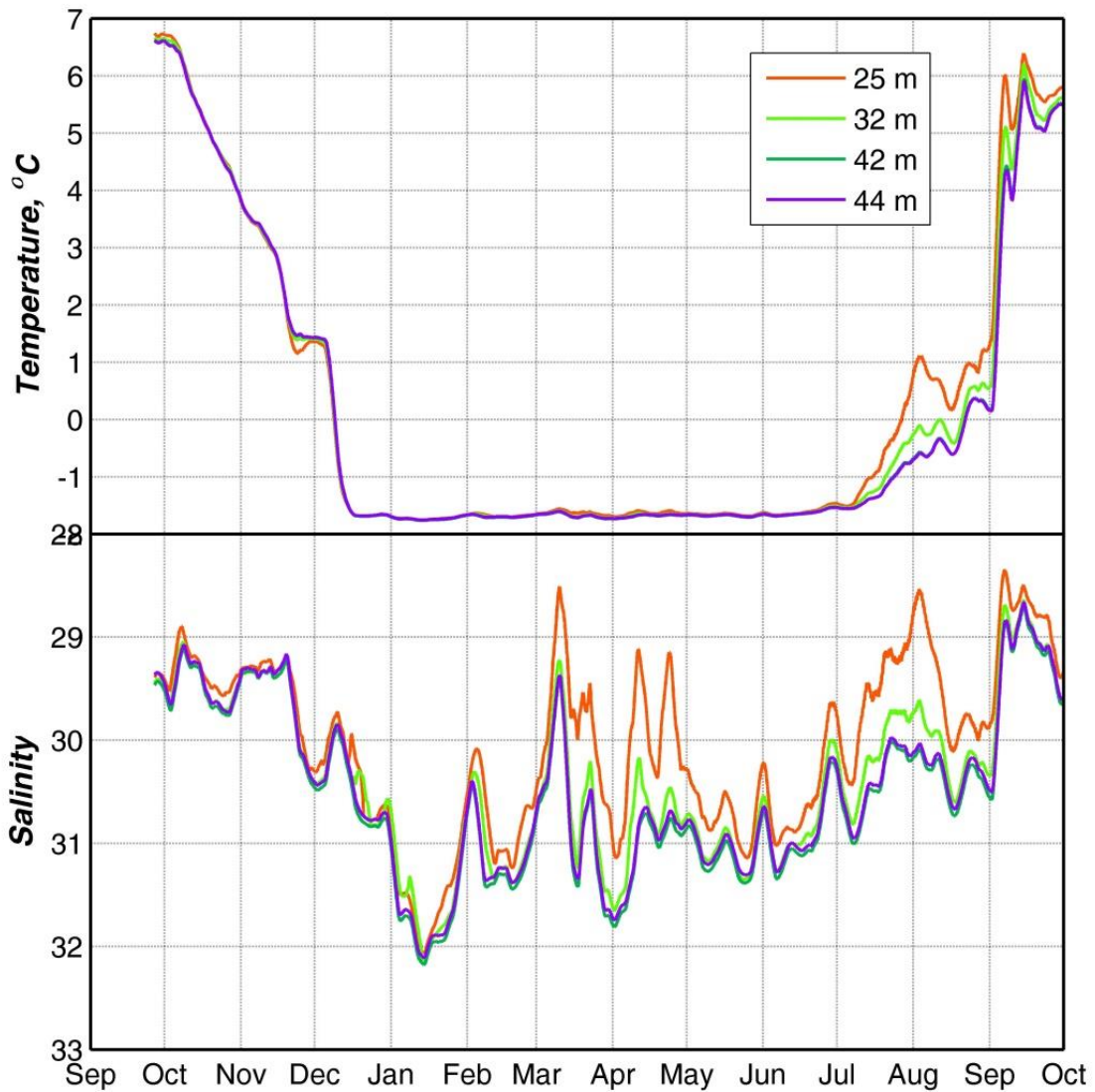


FIGURE 6.11 The one-year evolution of vertical thermohaline structure at NE02 mooring

Another piece of important information has been received from the combination of two upward-looking ADCPs: WorkHorse 300 kHz by RDI deployed near the seafloor and Signature 500 kHz by Nortek at AN01 and NE03. Both instruments provided continual records of water dynamic in the entire water column with 15 min recording interval. Moreover, Signature 500 was equipped with a fifth vertical beam that allowed measuring the wave heights and directions as well as the draft of ice throughout the full seasonal cycle (Figure 6.12).

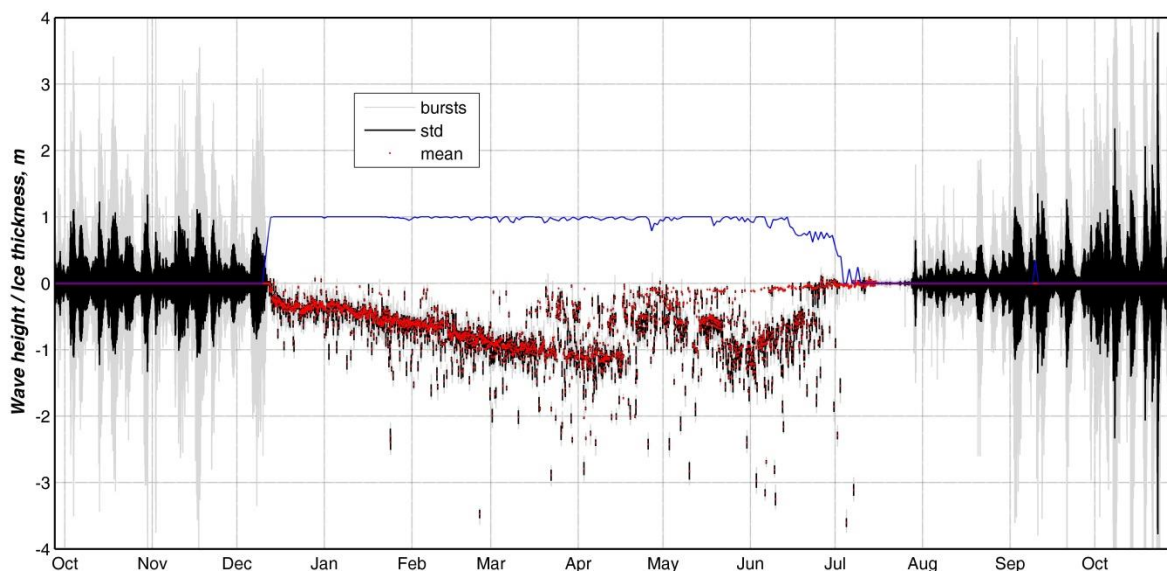


FIGURE 6.12 The sea-level heights and ice thicknesses recorded by upward-looking Nortek ADCP at AN01 mooring. Blue lines show AMSR2 sea ice concentration in the mooring position.

CTD

For the hydrological measurements, we used SBE 19plusV2 CTD profiler with a set of various sensors (see Table 6.1) mounted on a frame. CTD casts were made from the starboard side of the foredeck with the assistance of the ship’s crane and winch (Figure 6.13). The depth of each cast was limited by ~10 m above the seafloor from the safety considerations, although the maximum distance to the bottom at each station could be higher taking into account the tilt of the rope because of current and ship’s drift. 4 CTD casts were made at the mooring positions and one cast was made in between NE02 and NE01 positions (Table 6.2).

TABLE 6.1 CTD Sensors

Instrument	Manufacturer	Type & Properties	Serial Number	Date of calibration
Data Logger	SeaBird	SBE-19plus V2 Sampling rate: 4 Hz	6989	
Temperature	SeaBird	Range: -5oC to + 35oC Accuracy: 0.005	6989	6 July 2016
Pressure	SeaBird	Accuracy: 0.1% of full range Range 1000 m	3525364	1 July 2016
Conductivity	SeaBird	Range: 0 to 9 S/m Accuracy: 0.0005	6989	6 July 2016
Oxygen	SeaBird	SBE-43 Range: 120% of saturation Accuracy: 2% of saturation	2244	7 July 2016

Instrument	Manufacturer	Type & Properties	Serial Number	Date of calibration
PAR	Biospherical/Licor		70392	3 October 2011
Fluorometer	Seapoint		3491	3 April 2014
Turbidity	Seapoint		13052	3 April 2014



FIGURE 6.13 CTD cast from the foredeck

6.4 Preliminary Results of Thermohaline Stratification in the Mooring Positions from CTD Profiles

Temperature and salinity profiles were recorded at the mooring locations either before the mooring recovery (AN01, NE03, and NE02), or after re-deployment (AN01). The vertical CTD profiles collected at the AN01 position show the freshened (~2 psu) surface layer with a pycnocline located at 30-35 m (Figure 6.14). The fresher surface waters there seem to be mostly associated with a local melt of sea ice in summer. The melt of 1.5 m ice with a salinity of 4 would result in diluting of surface 30 m layer by 1.4 which is reasonably close to the observed salinity anomalies. In the Nelson area, the only station showing the presence of vertical stratification is HL17-04, where the salinity at surface ~3 psu lower compared to the bottom layer. The vertical stratification at the stations located further off-shore is absent. This fact is likely attributed to the intensive wind-driven vertical mixing initiated by several sequential strong storms in mid-October with an average wind speed exceeding 20 m/s. The thermal stratification matches, in general, the salinity profiles. The surface waters were well above freezing point and ranged from 1° C in AN01 position to 3-4° C north-east of the mouth of the Nelson River (Figure 6.14).

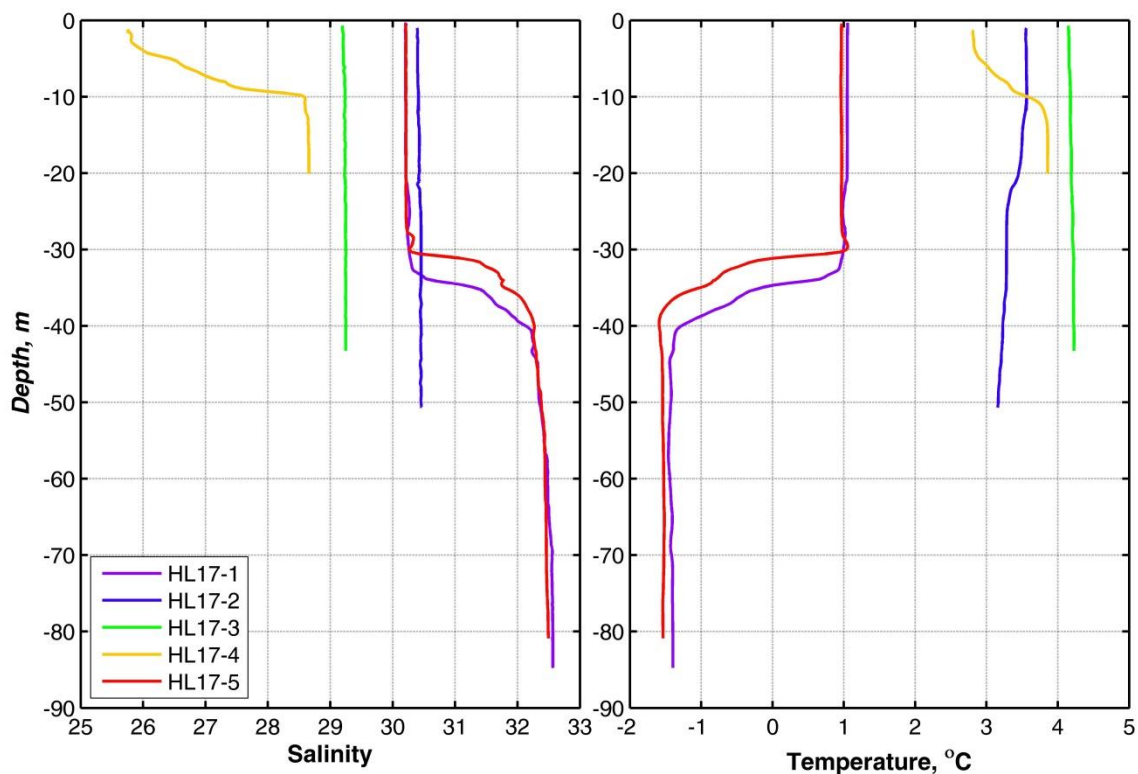


FIGURE 6.14 Temperature and salinity profiles collected during the cruise

TABLE 6.2 The positions of CTD stations, water sampling and moorings

Date	CTD cast	Mooring position	LAT (N) DD MM.SS	LON (W) DD MM.SS	Operation	Time (UTC)	Water depth (m)	Comments
27-Oct	HL17-01	AN01	59 57.7	091 56.9	CTD	08:17	107	
27-Oct		AN01	59 57.7	091 56.9	Water sampling		107	Surface, 20m, 40m, 100m
28-Oct	HL17-02	NE03	57 49.6	090 52.6	CTD	08:59	54	
28-Oct		NE03	57 49.6	090 52.6	Water sampling		54	Surface, 20m, 30m, 50m
28-Oct		NE03	57 49.8	090 52.9	Mooring recovery		54	
28-Oct	HL17-03	NE02	57 30.1	091 47.9	CTD	13:51	44	
28-Oct		NE02	57 30.1	091 47.9	Water sampling		44	Surface, 5m, 15m, 40m
28-Oct		NE02	57 30.0	091 48.1	Mooring recovery		44	

Date	CTD cast	Mooring position	LAT (N) DD MM.SS	LON (W) DD MM.SS	Operation	Time (UTC)	Water depth (m)	Comments
29-Oct	HL17-04		57 23.5	092 00.1	CTD	08:44	?	CTD cast to 20 m
29-Oct			57 23.5	092 00.1	Water sampling		?	Surface, 5m, 15m, 20m
29-Oct		NE02	57 29.907	091 48.250	Mooring deployment	18:01	44	
29-Oct		NE03	57 49.776	090 52.817	Mooring deployment	21:19	54	
30-Oct		AN01	59 58.2	091 57.1	Mooring recovery		107	
31-Oct		AN01	59 58.443	091 57.236	Mooring deployment	13:58	107	
31-Oct	HL17-04	AN01	59 57.7	091 56.9	CTD	14:24	107	

6.5 Water Sampling

The second objective of our shipboard fieldwork was to characterize the physical and chemical properties in the water column such as oxygen isotopes and nutrients. The water was sampled in the same location as the CTD casts using a Niskin bottle. At all stations, 4 depths were sampled, at the surface, above the pycnocline, below the pycnocline, and the bottom. The depths of the pycnocline samples were determined by looking at the CTD casts. The Niskin bottle was lowered over the side of the ship using a marked rope by hand to the approximate depths. The Niskin bottle was triggered using a messenger and then retrieved. The samples were then subsampled for the properties shown in Table 6.3.

TABLE 6.3 Water sampling parameters collected during the cruise

Instrument	Sampling Parameter
CTD	Conductivity temperature-depth probe of two manufacturers (Seabird, Idronaut)
CDOM	Colored dissolved organic matter
O18	Oxygen Isotopes
NO ₃ , NO ₂ , Si, PO ₄	Nitrite, nitrate, orthophosphate, and orthosilicic acid
Salinity	

All subsamples were stored in a cooler on the deck to remain cool, apart from the nutrient samples which were frozen. All information on Niskin bottle and CTD casts can be found in Table 6.2.

Acknowledgments

The BaySys teams would like to thank the CCG for their extraordinary collaboration to make this happen and the Captain and crew of the CCGS Henry Larsen for their commitment to this field project and ensuring safe deployment and recovery of the moorings. We would like to acknowledge Manitoba Hydro for their extensive logistical and in-kind support of this field program. Lastly, we are grateful to the Natural Sciences and Engineering Research Council of Canada (NSERC).

Appendix 6A

Mooring	Instrument	Depth m	Start time	End time	Frequency	Data status	Notes
AN01	Signature 500	37	27 Sep, 2016	30 Oct, 2017	15 min	OK	
	WorkHorse 300	104	27 Sep, 2016	30 Oct, 2017	15 min	OK	
	ECO	38	26 Sep, 2016	30 Oct, 2017	30 min	OK	
	RBR CTTu	40	27 Sep, 2016	01 Oct, 2017	15 min	OK	
	RBR CT	43	27 Sep, 2016	01 Oct, 2017	15 min	OK	
	RBR CT	55	27 Sep, 2016	01 Oct, 2017	15 min	OK	
	RBR CT	70	27 Sep, 2016	01 Oct, 2017	15 min	OK	
	RBR CTTu	83	27 Sep, 2016	01 Oct, 2017	15 min	OK	
	RBR TTu	94	27 Sep, 2016	01 Oct, 2017	15 min	OK	
	RBR CTTu	103	27 Sep, 2016	01 Oct, 2017	15 min	OK	
	Sediment trap	84	04-Oct-16 08-Nov-16 13-Dec-16 17-Jan-17 21-Feb-17 28-Mar-17 2-May-17 02-May-17 06-Jun-17 11-Jul-17 15-Aug-17	08-Nov-16 13-Dec-16 17-Jan-17 21-Feb-17 28-Mar-17 2-May-17 06-Jun-17 11-Jul-17 15-Aug-17 19-Sep-17	35 days 35 days 35 days 35 days 35 days 35 days 35 days 35 days 35 days 35 days	OK	
AN01 surface tubes	ECO	31.4	26 Sep, 2016	30 Oct, 2017	30 min	OK	
	RBR CTTu	31.5	20 Jun 2016	20 Jun 2016			No data recorded. Wrong timing
	RBR TD	32	27 Sep, 2016	01 Oct, 2017	15 min	OK	
	RBR CT	35.7	27 Sep, 2016	01 Oct, 2017	15 min	OK	
	RBR TD	39	27 Sep, 2016	01 Oct, 2017	15 min	OK	
	RBR CTTu	39.2	27 Sep, 2016	01 Oct, 2017	15 min	OK	
NE03	Signature 500	27	28 Sep, 2016	28 Oct, 2017	15 min	OK	
	WorkHorse 300	49	28 Sep, 2016	28 Oct, 2017	15 min	OK	
	ECO	28	28 Sep, 2016	28 Oct, 2017	30 min	OK	
	RBR CTTu	28	27 Sep, 2016	01 Oct, 2017	15 min	OK	
	RBR CT	43	27 Sep, 2016	01 Oct, 2017	15 min	OK	
	Sediment trap	33	04-Oct-16 08-Nov-16 13-Dec-16 17-Jan-17 21-Feb-17 28-Mar-17 2-May-17 02-May-17 06-Jun-17 11-Jul-17 15-Aug-17	08-Nov-16 13-Dec-16 17-Jan-17 21-Feb-17 28-Mar-17 2-May-17 06-Jun-17 11-Jul-17 15-Aug-17 19-Sep-17	35 days 35 days 35 days 35 days 35 days 35 days 35 days 35 days 35 days 35 days	OK	

NE03 surface tubes	Lost						
NE02	WorkHorse 600	44					The platform was flipped over during deployment. No data recorded.
	RBR CTTu	25	27 Sep, 2016	01 Oct, 2017	15 min	OK	
	RBR CT	32	27 Sep, 2016	01 Oct, 2017	15 min	OK	
	RBR CTTu	42	27 Sep, 2016	01 Oct, 2017	15 min	OK	
	RBR CTTu	44	27 Sep, 2016	01 Oct, 2017	15 min	OK	
	Sediment trap	26	01-Oct-17 26-Oct-17 21-Nov-17 16-Dec-17 11-Jan-18 05-Feb-18 03-Mar-18 28-Mar-18 23-Apr-18 18-May-18 13-Jun-18	26-Oct-17 21-Nov-17 16-Dec-17 11-Jan-18 05-Feb-18 03-Mar-18 28-Mar-18 23-Apr-18 18-May-18 13-Jun-18	25.5 days 25.5 days 25.5 days 25.5 days 25.5 days 25.5 days 25.5 days 25.5 days 25.5 days 25.5 days	OK	
NE02 surface tubes	Lost						

SPRING/SUMMER 2018



On-ice operations from the CCGS Amundsen. A six week bay-wide survey of Hudson Bay from May 25th to July 5th, 2018. The 40 scientists on board successfully sampled and surveyed 123 stations, both planned and opportunistic, across parts of the northern, western, central, and southern parts of the Bay. These stations included open water and on-ice sampling, as well as operations conducted via Amundsen helicopter, zodiac and barge vessels.

CHAPTER 7 - BAY-WIDE SURVEY – CCGS AMUNDSEN (LEG-1 & 2)

PROJECT PIs David Barber¹, Jens Ehn¹, Jean-Eric Tremblay², Tim Papakyriakou¹, Fei Wang¹

FIELD/SHIP COORDINATION David Landry¹, Lauren Candlish¹

MOORING OPERATIONS Sergei Kirillov¹, Keesha Peterson¹

ROSETTE OPERATORS Pascal Guillot³, Camille Wilhelmy³

¹Centre for Earth Observation Science, University of Manitoba, 535 Wallace Building, Winnipeg, MB

²Québec-Océan, Department of Biology, Pavillon Alexandre-Vachon, 1045, Avenue de la Médecine, Local 2078, Université Laval, Québec, QC

³Amundsen Science, Université Laval, Québec, QC.

RESEARCH VESSEL Canadian Coast Guard Ship CCGS Amundsen

CAMPAIGN DATES May 25 to July 05

CITE CHAPTER AS Barber, D. Landry, D. Babb, D., Kirillov, S., Aubry, C., Schembri, S., Gagnon, J., PierreJean, M., Jacquemot, L., Capelle, D., Munson, K., Huyghe, S., Loria, A., Karimi, P., Saltymakova, D., Stone, M., Adebayo, O., Downton, M. 2019. Bay-Wide Survey – CCGS Amundsen (LEG-1). Chapter 7 in, *Hudson Bay Systems Study (BaySys) Phase 1 Report: Campaign Reports and Data Collection*. (Eds.) Landry, DL & Candlish, LM. pp. 127-213.

7.1 LEG 1a/b – Hudson Bay-Wide Survey

Chief Scientist Report – Dr. David Barber

Leg 1 of the 2018 Amundsen cruise was successful. Many of our objectives for the cruise and BaySys project were achieved, barring a few locations in the bay in which were not able to access due to ice and weather conditions. Overall, data collection and sampling went exceptionally well, including all onboard and remote-based (i.e., helicopter; zodiac; barge; and on-ice) operations (see Table 7.1). The following is a summary of the completed cruise from May 25th to July 5th, 2018.

Week 1 of the cruise was predominately dedicated to transiting from Quebec City to the Hudson Strait via the Labrador coast. The transit took roughly 6 days and included a 7-hour Search and Rescue (SAR) call on May 30th, 2018. During the first 2 days of this transit, we completed Amundsen familiarization and safety tours onboard, and emergency alarm and procedures were tested. In addition, safe operations meetings for scientists and Amundsen crew were organized and held during the first week of the cruise. This included safety meetings for sea-ice work, river work, helicopter safety and operations, optical instrument operations, rosette operations, mooring operations, and general water sampling operations. Individual toolbox meetings were held before the start of each operation beginning on day 6, and the skippy boat – used for on-ice operations – was also briefly tested during this time. During the first week of Leg 1, general science meetings were scheduled each evening, and time allowed for a research presentation from six scientists/students.

The Amundsen crew and scientists shifted to a 24-hour schedule starting on May 31st and continued until the final week of operations. Our first stations were conducted on May 31st, 2018, along the entrance into the Hudson Strait. With the need to make up as much time as possible to enter Hudson Bay, the number of stations conducted along the strait was reduced to four. Thereafter, we began extensive station operations across the Bay entrances and used helicopter operations extensively for remote ice stations in areas of heavy ice concentration. This allowed for a much broader area coverage of operations. On June 5th, we deployed our first mooring (CMO03) just north of Coates Island, and by June 6th, we had entered into Hudson Bay for our first stations on Bay ice (Stn. 16). At station 16, three remote short-term ice instruments were deployed with the intent to be recovered later in the campaign. Before our June 7th community visit off the shore of Chesterfield Inlet (see below for more details), we conducted the first of three MVP transects along the west coast of Hudson Bay, providing a continuous profile of sea temperature, salinity, and depth, among other measurements.

We spent Week 3 sampling between the coast and the western-most ice-edge of Hudson Bay, at that time spaced about 110 nautical miles apart. Two additional MVP transect lines were completed from the coast into the open water, and five river systems were successfully sampled for water via helicopter (i.e., Chesterfield; Wilson; Ferguson; Tha-anne; Thlewiaza). Where possible, land-fast ice was also sampled. During this time-intensive drone surveys of the coastlines were conducted along with photo surveys of the sea ice edge via the helicopter. The zodiac also proved useful along this coast as two multi-station transects were conducted beginning at the edge of the land-fast ice of the Wilson and Thlewiaza Rivers, respectively, and continued out into the open water toward the Amundsen's position. From each of these major river regions, we positioned stations strategically out from the coast and into the ice edge of the

Hudson Bay with intermediate stations in between to provide information across the entire water continuum from the coast to the sea-ice. Before the crew change in Rankin Inlet, we located and recovered the short-term ice station instruments near station 16. On June 14th, we arrived in Rankin Inlet for a partial scientist crew change, and due to unfortunate circumstances, needed to change to Captain Alain Gariépy, as Captain Claude LaFrance had to unexpectedly depart for a family emergency.

Week 4 of Leg 1 saw many changes to the overall cruise plan. Originally planning a direct route across the bay in 4 days, we instead found that the ice was still heavily concentrated in this region and that we were unlikely to cross the bay in the proposed amount of time. After 2 days of transit (by June 16th) we made it to our second mooring station (Stn.29/CMO02) in the north-central region of the bay. After the successful deployment of the mooring and a few operations conducted on board, we were called to respond to a second SAR near Whale Cove, back on the west coast of the bay. This SAR call was completed in 1 day. After completing the call, the decision was made to head south on a direct route towards the Nelson Estuary, and from there to follow the southern coast of the bay to get to the eastern side. During this transit, we stopped at the mooring AN01 but determined that the ice cover remained too high to recover it at the moment. Once arriving at the Nelson Estuary by June 18th, the mooring NE02 was recovered and a short nearby station was completed and the Nelson and Hayes Rivers were sampled via helicopter. Navigating the southern coast proved to be more difficult than anticipated, as large, thick, and sediment-laden freshwater ice floes slowed progress. Along with two ice sampling stations in the ice edge, we managed to sample both the Severn and Winisk Rivers via helicopter. While in this region, the decision to deploy 10 ice beacons was made to track the movement of the ice pack and gain insight into the double gyre current movement in this area of the bay. By the end of week 4, we had completed 34 stations but needed to come up with a new plan to make it back to the Nelson as we were nearing the end of our allotted time for Leg 1.

As week 5 began, we decided to head north into the ice pack and towards deeper water in central Hudson Bay. We transited about 150 nm north and conducted stations along a direct route from the southern coast. Once the ice became too thick and concentrated, we began our transect line back south towards the Nelson Estuary. Following our arrival in the Nelson Estuary, we deployed a wave buoy along with an ADCP mooring (June 25th). Shortly after the start of our next station operation, we were called for our third SAR at the northern-most part of the bay, just outside Cape Dorset. This SAR response lasted 2.6 days. Following the completion of the call, and our new position north of Coates Island, it was decided that we resample station 15 for an extended time series with and without ice cover. During our transit back towards the Nelson, we recovered the AN01 mooring just north of Churchill and deployed the CMO01 mooring nearby. In addition to this deployment, we were able to sample the Seal, Knife, and Churchill Rivers all via helicopter.

Once back at the Nelson Estuary, we spent three days (June 29th – July 1st) doing intensive sampling by zodiac, barge, and a helicopter. The winds were high in this region making it difficult to manage all the operations on board smaller vessels, however, we sampled seven stations along the Nelson River transect, three stations along the south transect from the coast to the position of the Amundsen, and three stations along a modified western coast transect using Rosette casts and bucket sampling. In addition, onboard operations were conducted at two locations within the estuary. On June 29th, the helicopter was used to conduct a large scale gridded photo survey of the estuary to locate beluga pods and visual changes to the

water in the estuary, and the following day, it was sent out onto the coastal mudflats to collect sediment samples. The wave buoy and ADCP mooring deployed a few days earlier were recovered before leaving the area on July 1st and heading north towards Churchill to finish the campaign by July 2nd. Once back in Churchill we hosted a successful community visit onboard (~ 150 people) and held the Knowledge Exchange Workshop.

TABLE 7.1 List of all station types and number of times each were completed during Leg 1

Amundsen Station Type	Number Completed
Nutrient	20
Basic	09
Full	14
Other*	02
Total	45
Remote Station Type**	
Helicopter	54
Zodiac & Barge	24
Total	78
Total Stations Conducted	123

*opportunistic ice grab and single mooring turnovers with no other operations associated with the station ID

**all remote sea ice & landfast ice sampling, and open water and river sampling. Does NOT include ice sampling as part of Full Station Amundsen ice cage operations

7.2 *Community Visits and the Knowledge Exchange Workshop*

Chesterfield Inlet Community Visit

On June 7th, the Amundsen anchored offshore and hosted a community visit with Chesterfield Inlet. We brought 17 members of the community over to the ship via helicopter, including Mayor Simionie Sammurtoke, HTO council members, and younger high school graduates interested in ocean sciences. Overall, the visit went very well. After arriving, they were brought on a tour of the ship, which included seven science stations highlighting some of the many different operations and labs on board. These stations included a visit to the Rosette deployment area and data rooms to learn about oceanography and water sampling. The sea-ice team discusses their operations along with the radiometer, and the benthos and sediment labs were used to showcase and discuss some of the many diverse organisms that have been collected throughout the Bay. The aft labs were used to discuss oil contaminants and optical instruments, and on the foredeck, water chemistry was discussed. Lastly, the community guests were taken to the 600 deck labs to learn about food web sciences, including phytoplankton, nutrient, fish larvae, and adult fish. Following the tour, the members of Chester were invited inside for lunch in the Officer's mess, followed by a brief presentation detailing the BaySys project and what it is that we hope to accomplish in Hudson

Bay going forward. This presentation was followed by a discussion with the community on their experiences and the changes they see on the bay each year, including the reduction in the local goose and large beluga populations. Some of the fishermen also noted catching certain species of fish that are rarely seen in this part of the bay.

Churchill Community Visit and Knowledge Exchange Workshop

The Churchill community visit took place during the morning of Tuesday, July 3rd. For a 2 hour timeslot, the Amundsen hosted over 100 community members who were excited to visit the ship and given a tour of the exterior work stations and instruments, along with the wheelhouse. The community visitors we sent on a self-guided walking tour of the ship, while specific areas were designated for certain instruments and operation showcasing. Participants from our science teams answered any questions from the visitors and gave brief presentations of their research when the groups came on board.

The Knowledge Exchange Workshop event took place over two days, which included a zodiac-based beluga tour, and community-hosted wine and cheese reception on July 2nd, followed by a full-day tour, workshop, and discussion panel onboard the Amundsen on July 3rd. This workshop event was well attended (~40) by dignitaries and guests from all over Canada, and was organized as a way to bring discussions of the Arctic, and in particular Hudson Bay, from the scientists, and community leaders, to the policy-makers, stakeholders, and general public in the south. Overall, the Knowledge Exchange Workshop was a success.

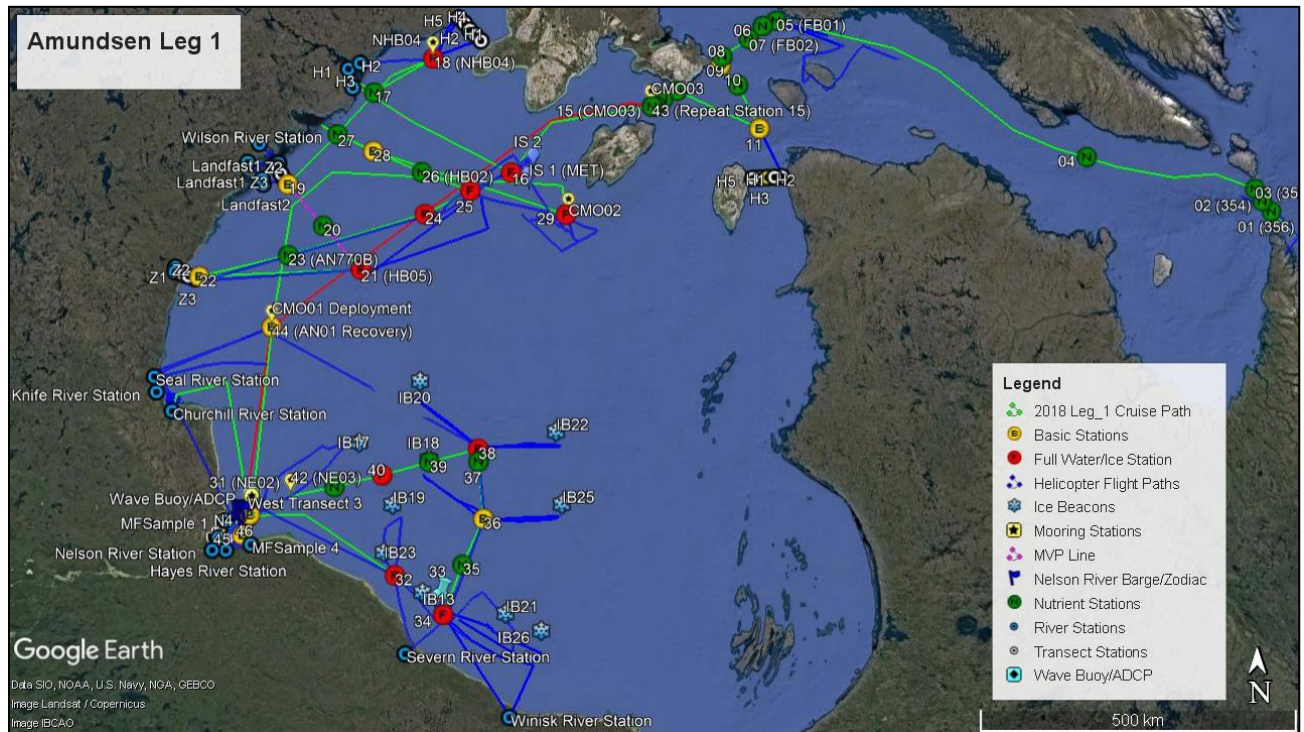


FIGURE 7.1 Complete Leg 1 cruise track with all stations and remote tracks included

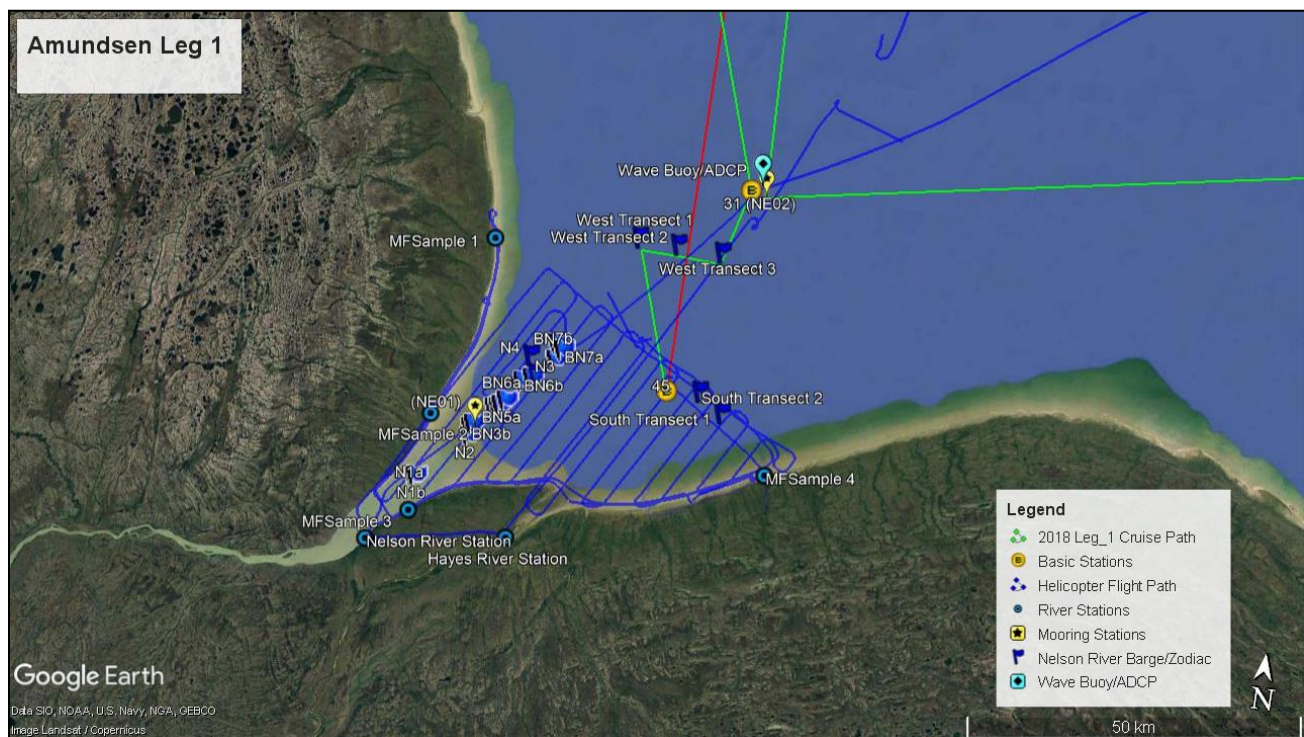


FIGURE 7.2 Nelson Estuary cruise track with all stations and remote tracks included

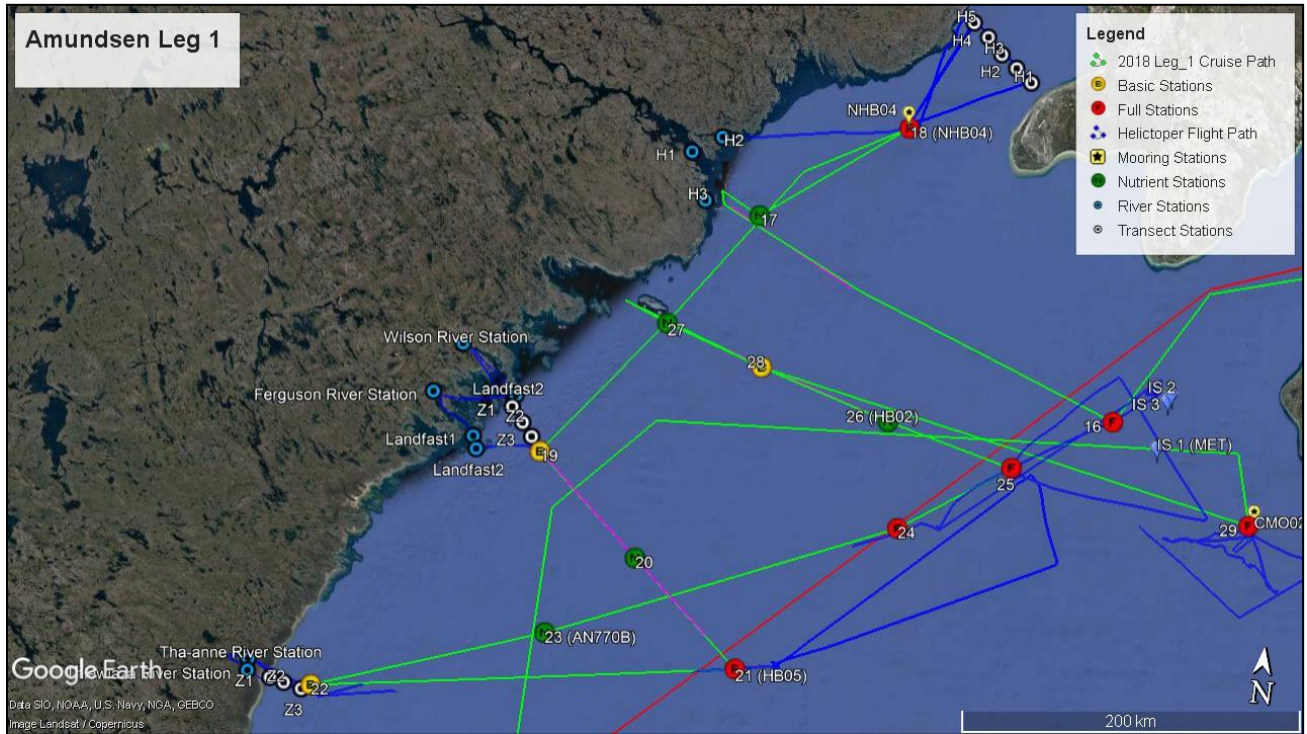


FIGURE 7.3 Western Hudson Bay cruise track with all stations and remote tracks included

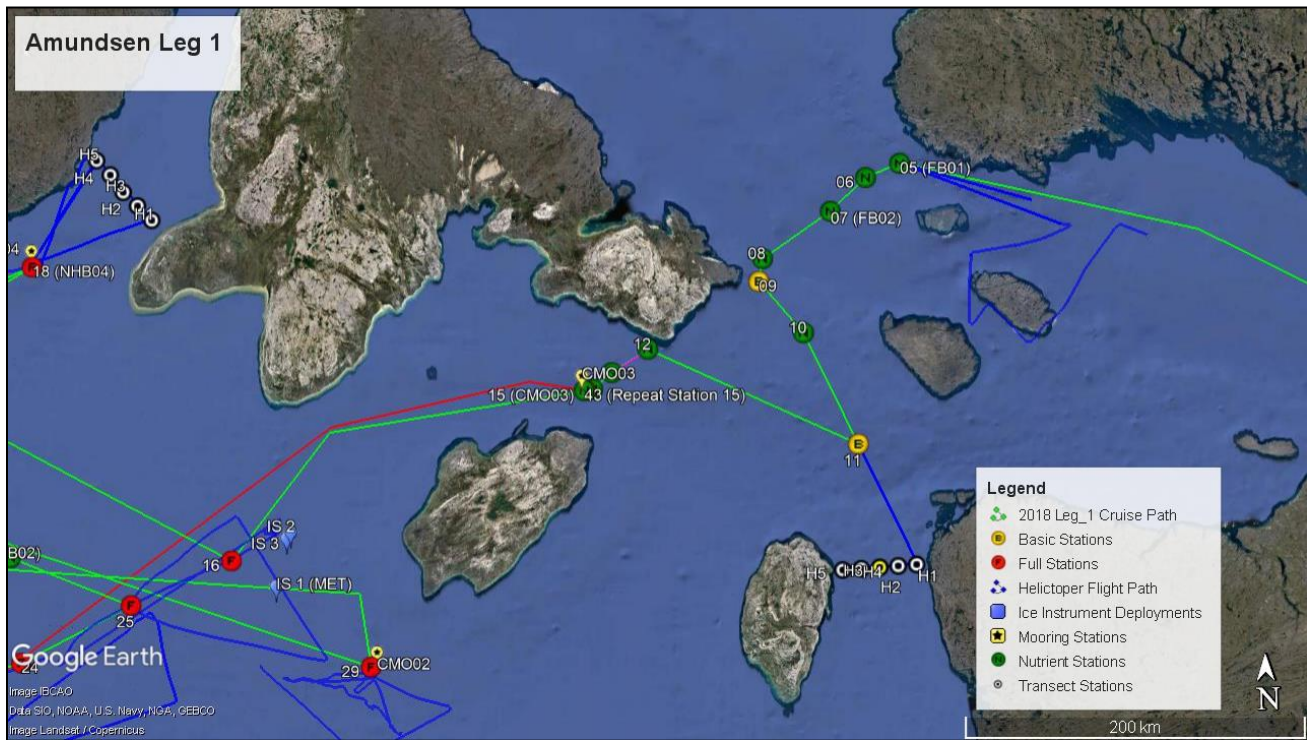


FIGURE 7.4 Northern entrance into Hudson Bay. Cruise track with all stations and remote tracks included

7.3 *Marine and Climate System - Sea Ice*

Principal Investigators: Dr. David Barber¹ (david.barber@umanitoba.ca); Dr. Jens Ehn¹ (jens.ehn@umanitoba.ca). Cruise participants: Dr. David Barber¹; Dr. Greg McCullough¹ (Leg 1B); David Babb¹ (Leg 1A); Maddison Harasyn¹; Laura Dalman¹

¹Centre for Earth Observation Science, University of Manitoba, Winnipeg, Manitoba, Canada

Introduction and Objectives

The BaySys 2018 cruise provided a unique opportunity to sample the seasonal ice cover in Hudson Bay during the melt season. Previously during February and March 2017, as part of the BaySys program, mobile sea ice was sampled near Churchill via helicopter and landfast ice near the Nelson estuary via snowmobile. Combined, these three programs provided the opportunity to sample landfast and mobile sea ice during both the winter and summer months and gain a more complete understanding of the seasonal and spatial variability in the sea ice cover of Hudson Bay.

While many other teams onboard the Amundsen were interested in collecting ice samples for carbon, mercury, contaminants, nutrients, and biology/optics our team was interested in characterizing the physical properties of the ice cover. This data will go towards our research, but also provide context on the ice conditions for the other BaySys teams. To describe the physical properties of an ice cover we were interested in describing the temperature and salinity profiles within the ice, measuring its thickness, assessing its roughness, quantifying its aerial concentration and the floe size distribution, monitoring its radiometric signatures to compare to satellite observations, and tracking its drift. To do this, we used a variety of field techniques from direct in situ physical measurements, to remote sensing and autonomous platforms that remained on the ice cover. Below is a brief description of our methods and examples of the preliminary results that we have collected.

Operations Conducted and Methodology:

Ice Sampling

Ice samples were collected using a 9 cm Mark II Kovacs core barrel. Full or partial ice cores were taken to measure the temperature and salinity throughout the sea ice. Holes were drilled to the center of the core at 10 cm intervals beginning 5 cm from the ice-air interface. A Traceable Digital Thermometer was then inserted into the drilled hole and temperature was recorded. Salinity ice cores were cut with a saw into 10 cm sections, put into buckets, melted overnight, and salinity measurements were taken with a Thermo Scientific Orion 3-star salinometer from pure melt the following day. These profiles provide information on the state of the sea ice to assess whether the ice is growing or melting. An ice core for temperature and salinity was taken at every ice station for a total of 15 stations throughout Hudson Bay. Partial ice cores were taken only in southern Hudson Bay where the ice was much thicker with ice floes >3m thick.



FIGURE 7.5 Laura Dalman measuring the ice temperature profile of an ice core

Manual measurements of ice thickness were collected at each site with a 2” Kovacs ice auger and a Kovacs ice thickness tape. Both the manual auger head and a Stihl gas-powered auger were used to drill holes at specific sites or along transects. Additional ice thickness measurements were to be collected with a towed Electromagnetic Induction System, however, both systems were malfunctioning and were therefore not used.

Remote Sensing

During the 2018 BaySys Leg 1 field season, passive microwave radiometric scans of ice floes were completed at 14 stations located in the north/northwest and southwest sectors of Hudson Bay. Scans were completed while situated beside the ice floe which would later be sampled for physical properties, at incidence angles ranging from 25 – 80° in both horizontal and vertical polarizations at 19, 37, and 89 GHz. Physical sampling was then completed after scanning on the ice, measuring snow presence/depth, wetness, and salinity within the footprint of the radiometer. Drone surveys were also completed for 11 of the 14 full stations to capture an aerial survey of the sampled floe and surrounding area. Drone surveys were completed using a DJI Phantom 4 and DraganFly Commander, which capture RGB and multispectral imagery respectively. Aerial imagery was used to classify sea ice surface features, such as melt pond size or sediment presence. As well, digital elevation models were generated using photogrammetric techniques, providing a 3D model of the surface roughness of sea ice within the survey

area. Physical and drone sampling was combined to classify the physical properties of the scanned floe, to be compared to the measured brightness temperatures from the passive microwave radiometer.

Sampled ice at each of the stations varied in melt progression, ice composition, and surface characteristics. Ice sampled during early June in the north sector of the bay showed no melt features, with all ice floes being very large with a more uniform surface elevation. Floes were covered with a layer of dry fresh snow (~10 cm) covering a deeper layer of saturated, highly saline snow (~5 cm). The radiometric signature of these floes shows uniform brightness temperatures across the range of incidence angles, with brightness temperatures residing between 170 and 270 K for each frequency/polarization.

Ice in the southwestern sector of the bay had different physical and surface properties compared to the northern ice. This ice was sampled during late June, meaning that melt features were more prominent. Ice in this area contained sediment in the surface layer, had larger ridge features, and was thicker than the northern ice. Snow on the ice was thinner (~3 cm) and was fresh. Melt ponds were often covered by a layer of ice (~1 cm thick). The radiometric signature of this ice was slightly different, showing diverging brightness temperatures at higher incidence angles. As well, brightness temperatures for the horizontal polarization varied greater than the vertical polarization over the range of incidence angles.

Autonomous Instruments:

Ice Beacons

To measure sea ice drift 10 ice beacons were deployed on large ice floes in central and southern Hudson Bay. Ice Beacons are contained within sealed PVC tubes (13 cm diameter x 50 cm length) that house a small processor, GPS, and Iridium antennae, and a battery pack. Once the units are activated they transmit their GPS location at user-defined intervals (typically 1 hour) to an online web portal. The ice beacons transmit their location until the ice floe breaks up and they sink.

TABLE 7.2 Ice drift beacon deployment details

Beacon #	IMEI	Deployment Date	Coordinates
17	607220	18-06-2018	58.61729 -89.57683
19	206980	19-06-2018	57.72522 -88.05737
23	503520	19-06-2018	57.12653 -88.35158
13	504190	20-06-2018	56.60985 -87.08107
21	300430	21-06-2018	54.40994 -85.89129
26	908870	21-06-2018	56.10707 -84.56303
25	907730	22-06-2018	57.87995 -84.22141
18	201080	22-06-2018	58.29801 -87.60599
20	300000	23-06-2018	59.26393 -87.99193
22	300440	23-06-2018	58.79762 -84.22619

Below is a map of the 10 beacon locations and near-real-time sea ice concentration (0 - 100%) from June 24th. The 10 beacons provide good spatial coverage of the ice cover and will hopefully last well into July as the ice cover melts out and breaks up. Note that the near-real-time sea ice concentration is provided by NSIDC and is based on space-borne passive microwave sensors that have known limitations during the melt season due to liquid water at the ice surface. Ice charts from the Canadian Ice Service provided higher resolution data that is more reliable, but for this exercise the near-real-time data is suitable.

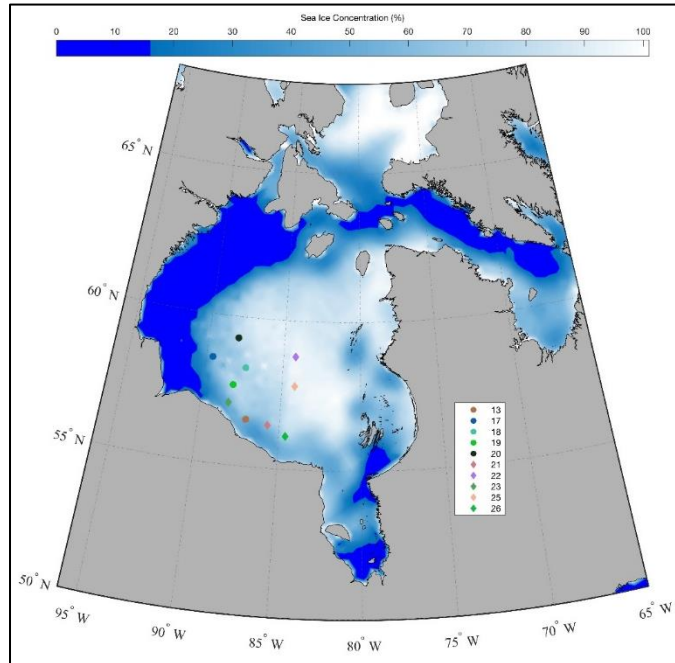


FIGURE 7.6 Ice beacon positions and sea ice concentration on June 24th, 2018

Short Deployment of on-ice Weather Station and CT Lines

Taking advantage of our multiple trips across the marginal ice zone in northwestern Hudson Bay we deployed a suite of autonomous instruments for 6 days to capture a high-resolution dataset on atmosphere-ice-ocean interactions. Two ice tethered moorings and a meteorological station were deployed on large pans of sea ice. The mooring lines contained CT sensors and an upward-looking ADCP, while the meteorological station contained an Air temperature sensor (Campbell Scientific 107 Temperature Probe), a barometer (Campbell Scientific 61302V), turbine anemometer (RM Young 05106-10 Wind Monitor, Marine), and an under-ice acoustic sounder (Teledyne Benthos 9602) to monitor sea ice melt. To correct the wind direction for floe rotation an electronic compass (R.M. Young 32500) was calibrated and set up on the tower, while an additional ice beacon was deployed ~50m from the co-located ice tethered mooring to provide two GPS positions to verify the compass measurement of floe rotation. The station was operated by a CR-1000 and powered by a Lithium-Ion Battery, both of which were located in the white weatherproof enclosure visible in Figure 7.3. The systems were deployed on June 6th and recovered on June 12th, both via helicopter. A complimentary ice core was collected during

deployment, however, no core was collected during recovery because the floe had broken up considerably and the mooring and met station were recovered while the helicopter hovered.

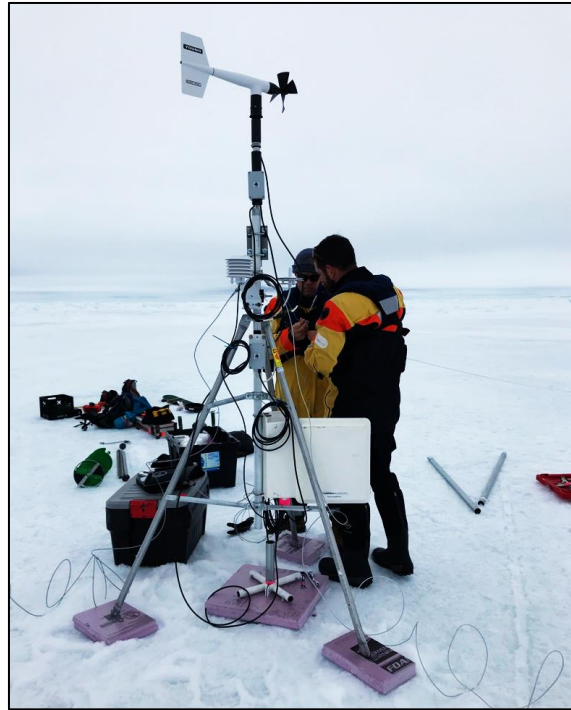


FIGURE 7.7 Photograph of the on-ice meteorological station setup



FIGURE 7.8 The surface portion of the ice-tethered mooring. There is a GPS tracker within the surface unit that allowed us to recover the unit after 6 days

Further details on the oceanographic observations and mooring operations are presented in section 7.4.

Preliminary Results:

Physical samples

Two sample profiles of the Temperature and Salinity are provided below. Overall, the sea ice was relatively warm and near isothermal at every site. The salinity varied from values typical of first-year sea ice (5 – 7) to values indicative of freshwater ice (0 – 1).

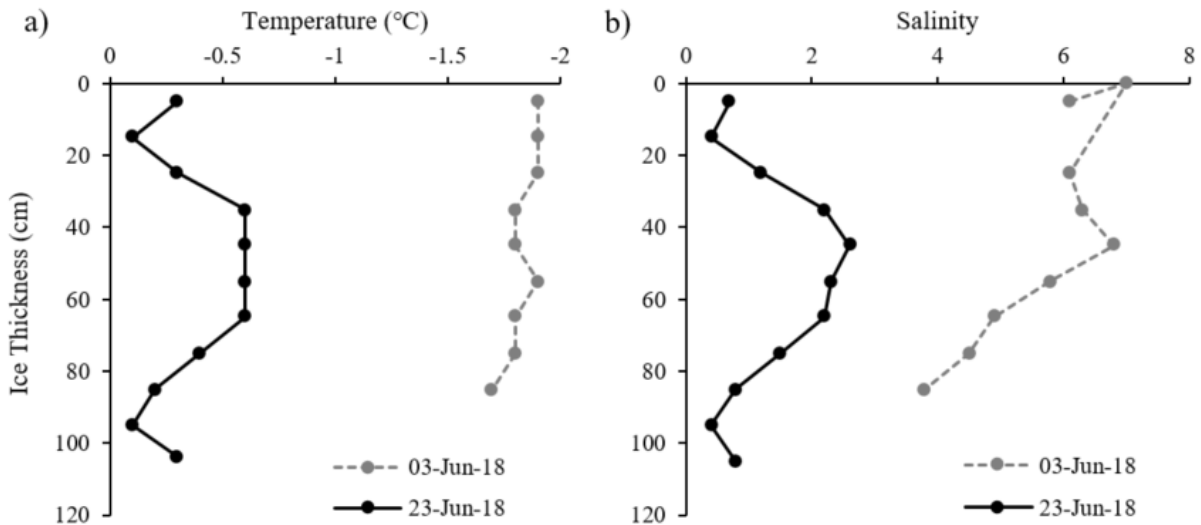


FIGURE 7.9 Temperature (a) and salinity (b) profiles for ice floes sampled in northern Hudson Bay (03-Jun-18) and southern Hudson Bay (23-Jun-18)

Ice Beacons

Below are two examples of the ice beacon data from beacons 21 and 26. A map with the points coloured by ice drift speed (km/d) and the time series of ice drift speeds are provided for each beacon. The ice is quite mobile and in near-constant motion, with frequent reversals and loops along its trajectory. The periodic loops are to the left of the trajectory and are therefore not inertial, but instead likely tidally driven. This will be explored further following the loss of all ice beacons in late-July or early-August. Note that there is a 5-day gap in the data during early July, the Iridium servers at Solara Communications were down during that time and they are in the process of retrieving this data from the Iridium servers.

BAYSYS 2018 - Amundsen - Ice Beacon: B21 - Ice Drift Speed (m/hr)
 Deployed: 21-Jun-2018 15:03:13 / Last Position: 16-Jul-2018 16:29:36

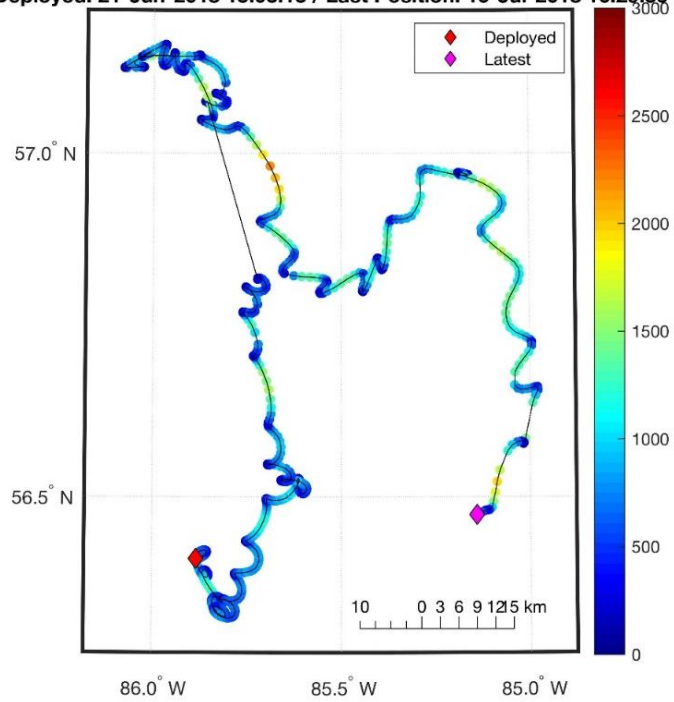


FIGURE 7.10 Ice beacon 21 position and drift speed

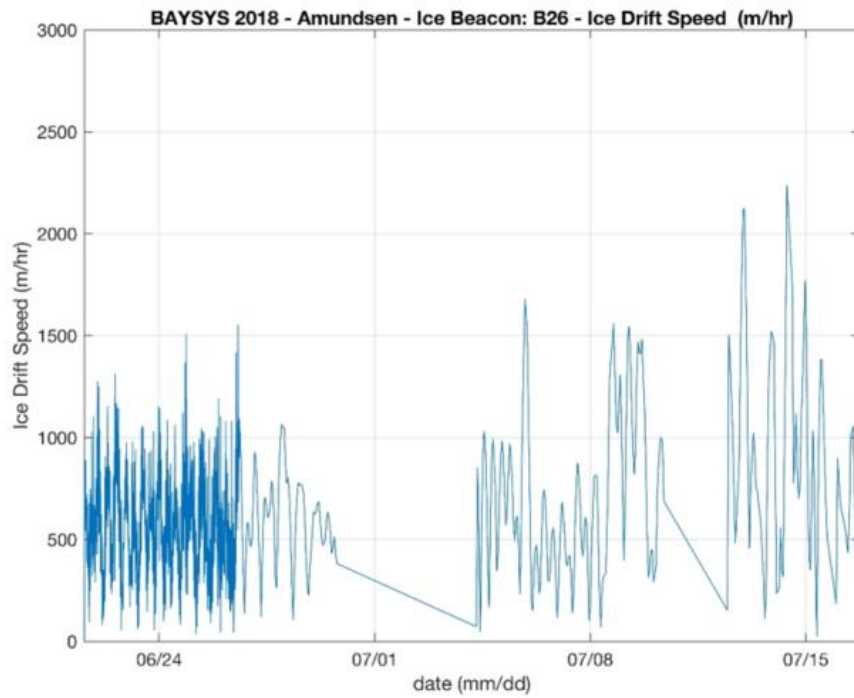


FIGURE 7.11 Ice beacon 26 drift speed

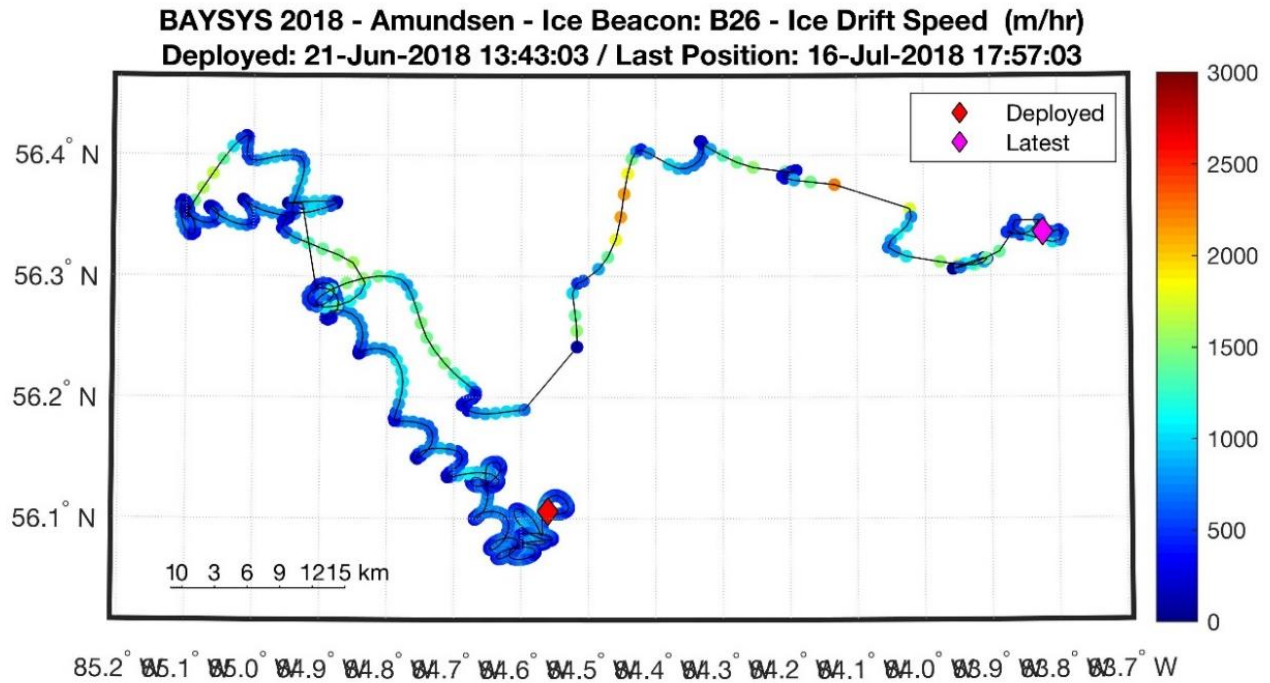


FIGURE 7.12 Ice beacon 26 position and drift speed

7.4 Mooring Operations in Hudson Bay

Principal Investigators: Jens Ehn¹; CJ Mundy¹. Cruise Participants: Sergei Kirillov¹; Keesha Peterson¹; Yanique Campbell¹

¹Centre for Earth Observation Science, University of Manitoba.

Introduction and Objectives

The initial cruise plan intended the recovery of five BaySys moorings deployed in the Hudson Bay in September 2016 (NE01 and JB02) and in October 2017 (NE02, NE03, and AN01). The change of cruise plan due to several SAR operations and heavy ice conditions in the central and southern parts of Hudson Bay did not allow us to reach the position of JB02 mooring at the mouth of James Bay. Two separate components of NE01 mooring deployed at ~30 m depth in the inner Nelson estuary zone were also not recovered. Although we were able to communicate with both acoustic releases, all our attempts to release the CT-line from the anchor and recovery pod from the bottom mount (Figure 7.13) failed. Later, the subsurface float from the CT-line was found nearby on the shoreline during one of the reconnaissance helicopter flight. Taking into account that float was initially located at ~20 m depth, we suggest that deep ice keels could have caused the damage of that mooring. Such deep keels could be associated with large

stamakhi which were formed in the Nelson region due to the extremely strong tidal dynamics resulting in ice piling at the edge of landfast ice.

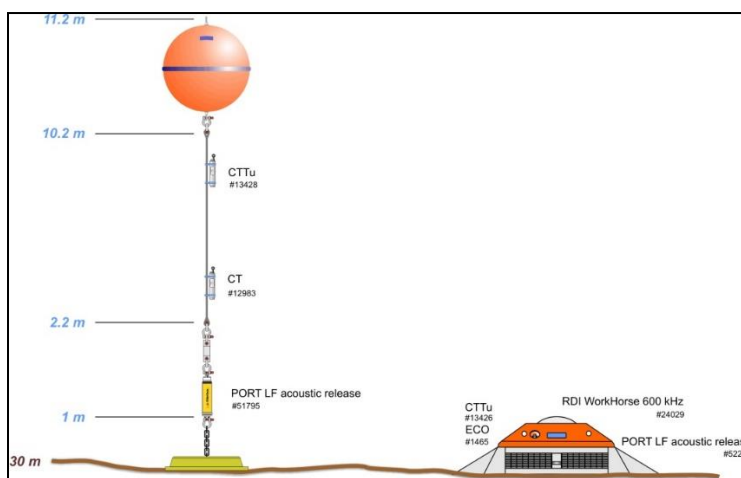


FIGURE 7.13 The configuration of the lost mooring NE01

Three other moorings deployed in October 2017 were successfully recovered on June 18, 25, and 28 (see Table 7.3). The zodiac was used at every recovery station to draw the mooring line to the ship (Figure 7.14) for further lifting with a capstan and A-frame from the foredeck.

TABLE 7.3 The positions of recovered, deployed, and short-term moorings

Date	CTD cast	ID	LAT	LONG	Operation	Time (UTC)	Depth (m)
05-Jun	AM18-015	CMO-C	63.1934	-81.9231	Mooring deployment	13:30	194
06-Jun	AM18-H06	Ice-tethered setup	62.2815	-85.9543	Mooring deployment	15:15	
06-Jun	AM18-H07	Ice-tethered setup	62.2592	-85.8273	Mooring deployment	22:00	
08-Jun	AM18-018	CMO-D	63.7137	-88.4168	Mooring deployment	12:30	119
12-Jun	AM18-H24	Ice-tethered setup	62.4396	-85.3650	Mooring recovery	15:30	
12-Jun	AM18-H25	Ice-tethered setup	62.4595	-85.5283	Mooring recovery	18:45	
16-Jun	AM18-029	CMO-B	61.7698	-84.3091	Mooring deployment	09:00	179
18-Jun	AM18-031	NE02	57.5001	-91.7953	Mooring recovery	16:15	43
25-Jun	No cast	NE03	57.8278	-90.8759	Mooring recovery	12:45	53
25-Jun	No cast	Wave buoy	57.3015	-91.4751	Mooring deployment	18:00	43
28-Jun	AM18-044	CMO-A	59.9747	-91.9506	Mooring deployment	15:00	106
28-Jun	AM18-044	AN01	59.9747	-91.9506	Mooring recovery	15:30	105
01-Jul	AM18-046	Wave buoy	57.3015	57.3015	Mooring recovery	21:40	43



FIGURE 7.14 Mooring recovery with the assistance of zodiac

Preliminary Results

Data from all instruments were examined after recovery to determine if all equipment worked properly and recorded reliable data. We also examined the pressure records from all available sensors to adjust the depths of moored instruments and prepared the final schemes for the moorings' configurations (Figure 7.15). In general, all recovered instruments worked well and 8-month time series of temperature, salinity, current velocities, ice thickness/waves, etc. were correctly recorded (see Table 7.3).

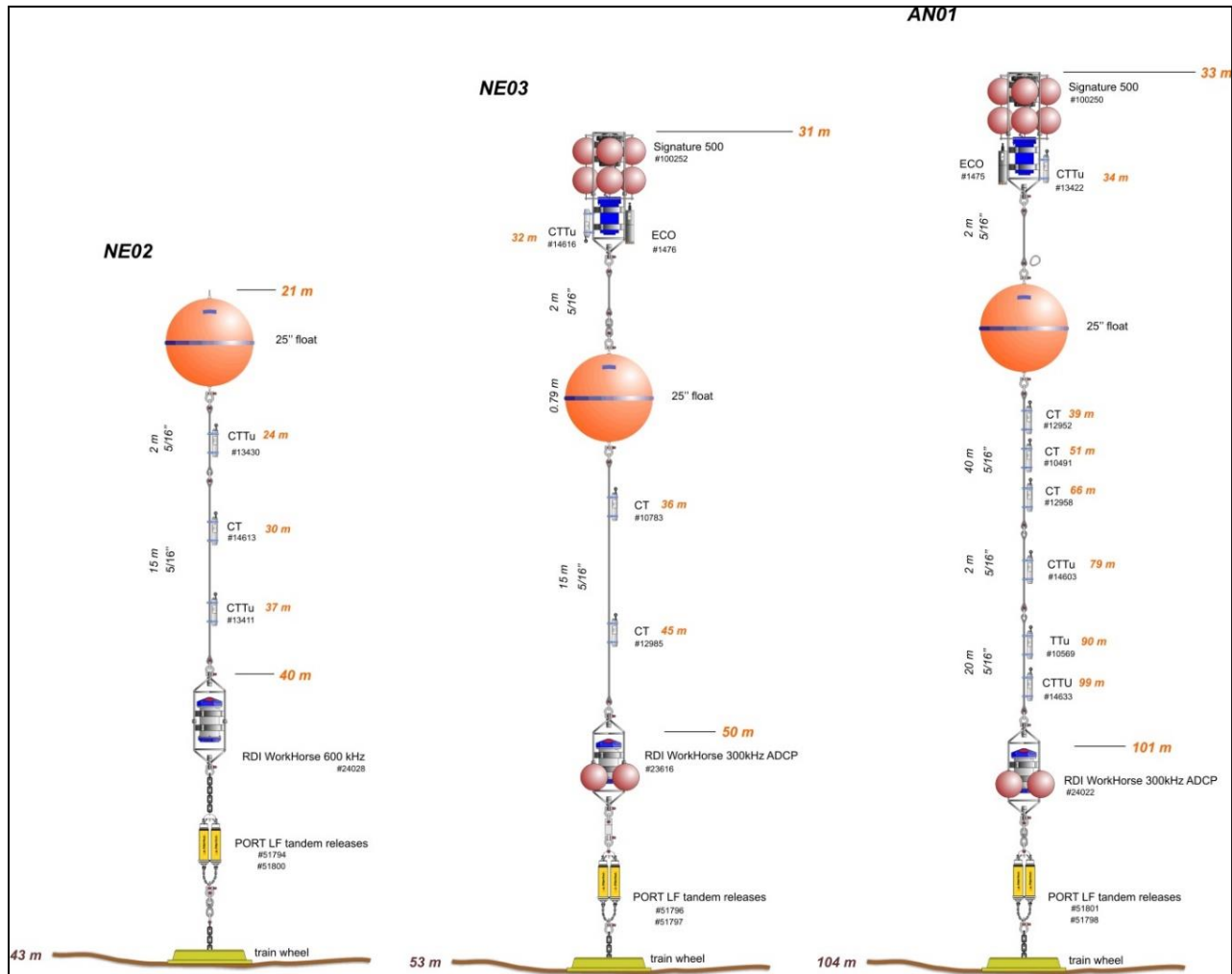


FIGURE 7.15 NE02 (Nelson Outer Estuary), NE03 (Nelson River outer shelf), and AN01 (Churchill shelf), mooring configurations as recovered.

TABLE 7.4 Status of data at recovered moorings

ID	Instrument	Depth m	Start time	End time	Period	Data status	Notes
NE02	WH600	40	29 Oct, 2017	18 Jun, 2018		OK	
	RBR CTTu	24	29 Oct, 2017	18 Jun, 2018	15 min	OK	
	RBR CT	30	29 Oct, 2017	18 Jun, 2018	15 min	OK	
	RBR CTTu	37	29 Oct, 2017	18 Jun, 2018	15 min	OK	
NE03	Signature 500	31	29 Oct, 2017	25 Jun, 2018		OK	
	WH300	50	29 Oct, 2017	25 Jun, 2018		OK	
	ECO	32	29 Oct, 2017	25 Jun, 2018	30 min		Not retrieved yet
	RBR CTTu	32	29 Oct, 2017	25 Jun, 2018	15 min	OK	
	RBR CT	36	29 Oct, 2017	25 Jun, 2018	15 min	OK	
	RBR CT	45	29 Oct, 2017	25 Jun, 2018	15 min	OK	

ID	Instrument	Depth m	Start time	End time	Period	Data status	Notes
AN01	Signature 500	33	1 Nov, 2017	28 Jun, 2018		OK	
	WH300	101	1 Nov, 2017	28 Jun, 2018		OK	
	ECO	34	1 Nov, 2017	28 Jun, 2018	30 min		Not retrieved yet
	RBR CTTu	34	1 Nov, 2017	28 Jun, 2018	15 min	OK	
	RBR CT	39	1 Nov, 2017	28 Jun, 2018	15 min	OK	
	RBR CT	51	1 Nov, 2017	28 Jun, 2018	15 min	OK	
	RBR CT	66	1 Nov, 2017	28 Jun, 2018	15 min	OK	
	RBR CTTu	79	1 Nov, 2017	28 Jun, 2018	15 min	OK	
	RBR TTu	90	1 Nov, 2017	28 Jun, 2018	15 min	OK	
	RBR CTTu	99	1 Nov, 2017	28 Jun, 2018	15 min	OK	

Mooring Deployments

Four moorings were deployed along the main shipping channels across Hudson Bay as a part of the Environmental Observing system related to the Churchill Marine Observatory project. The positions of all these moorings are shown in Figure 7.16 and also listed in Table 7.3. All deployed moorings were equipped with similar instruments except CMO-C site where 2 sediment traps (at 63 and 167 m) and a SeaFET pH sensor (at 30 m) were added to the line (see Figure 7.17). The sediment trap motors were turned on at exactly 20:00 UTC on 4 June 2018 (interval 0) and they would begin rotating the carousel in 48 hours with a 36-day interval between rotations.



FIGURE 7.16 Positions of CMO moorings deployed in the Hudson Bay in June 2018

The following set of standard instruments was used for each mooring:

- Ice Profiling Sonar (IPS5) at 30 m
- Acoustic Doppler Current Profiler (WH300 Sentinel ADCP) at 60 m
- Acoustic Zooplankton Fish Profiler (AZFP)

The depth of units varied from 75 to 90 m at different moorings a broadband underwater acoustic recorder (TR-ORCA) deployed in between 80 and 150 m depth Wetlab ECO triplet logger (measuring turbidity, chlorophyll-a, and CDOM fluorescences) at 30 m 3 SBE37 CTD (conductivity-temperature-depth) sensors at 30 m, 60 m and near the bottom.

All instruments were programmed for about 15-months deployment with the planned recovery in the fall, 2019. All moorings were deployed anchor last from the foredeck using the A-frame (Figure 7.19).

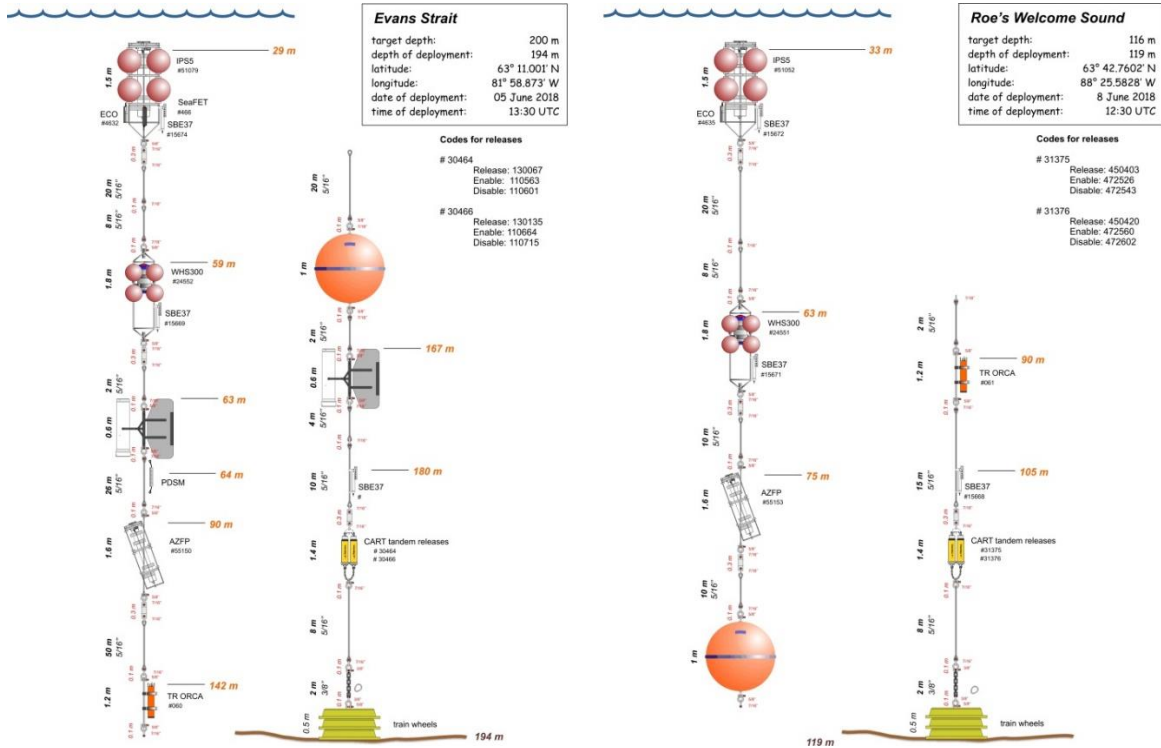


FIGURE 7.17 The configuration of CMO-C (Evans Strait) and CMO-D (Roes Welcome Sound) moorings

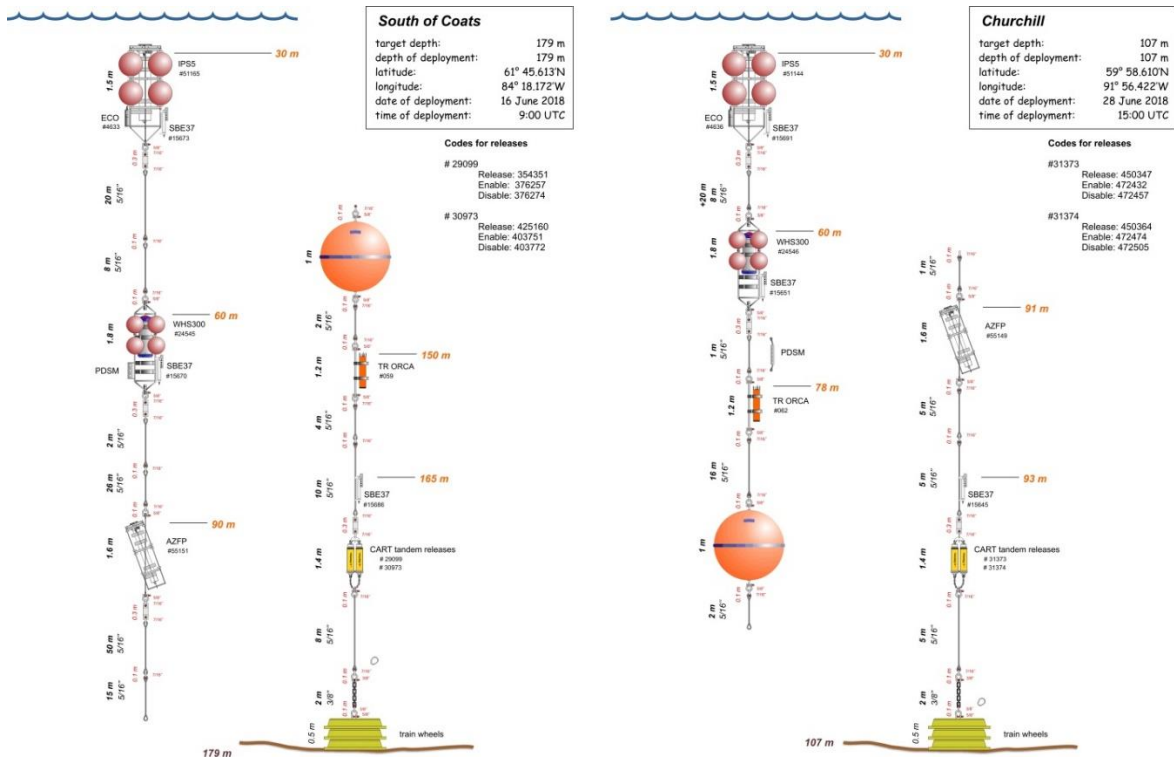


FIGURE 7.18 The configuration of CMO-B (South of Coats) and CMO-A (Churchill) moorings



FIGURE 7.19 Anchor last mooring deployment from the foredeck

Short-term moorings

Three short-term moorings were deployed during Leg 1. Two of them were ice-tethered setups that included a line of RBR CT sensors mounted between 2 and 14 meters, an upward-looking Aquadopp 600 kHz ADCP at 13 m, and a GPS beacon (Figure 7.20). The eastern mooring was additionally equipped with a basic meteorological tower measuring air temperature, pressure, wind speed and direction, and sea ice thickness.

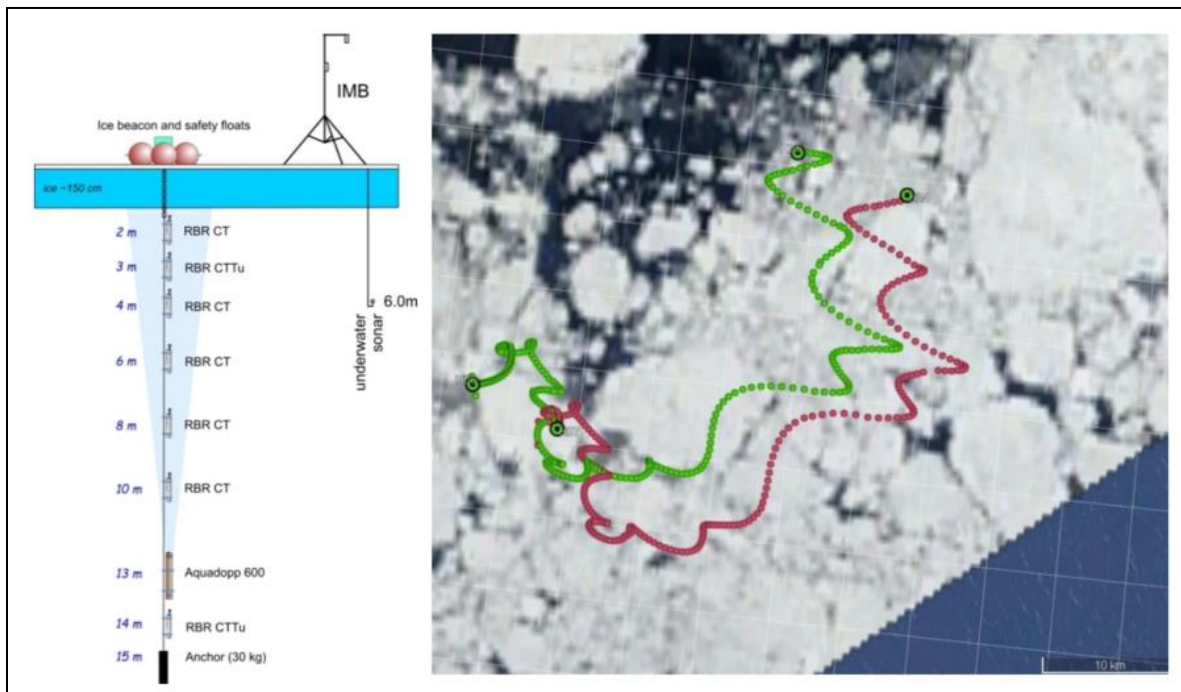


FIGURE 7.20 The configuration of the ice-tethered moorings and their trajectories between June 6 and 12

In the Nelson estuary region, a TRIAXYS wave buoy equipped with a g3 sensor was deployed between June 25 and July 1 to measure the directional pattern of surface waves. The deployment took place at the beginning of a period of high winds (>10 m/s) over the region that persisted for several days. The objective of the wave buoy was to capture storm wave conditions in the region as a function of wind and the fetch distance created by the ice edge that was receding to the east. The growth and propagation of waves as a function of these parameters will be assessed. In addition, temperature and salinity data in the upper few metres will supplement the wave measurements, allowing for insight into wind-wave mixing in the mixed layer.

The synchronous measurements carried out with Nortek Signature 500 ADCP that was deployed at TRIAXYS site at 30 m depth are aimed to validate and compare TRIAXYS and ADCP records to each other. Figure 7.21 shows the diagram of the experimental setup and Table 7.3 contains the coordinates of TRIAXYS site.

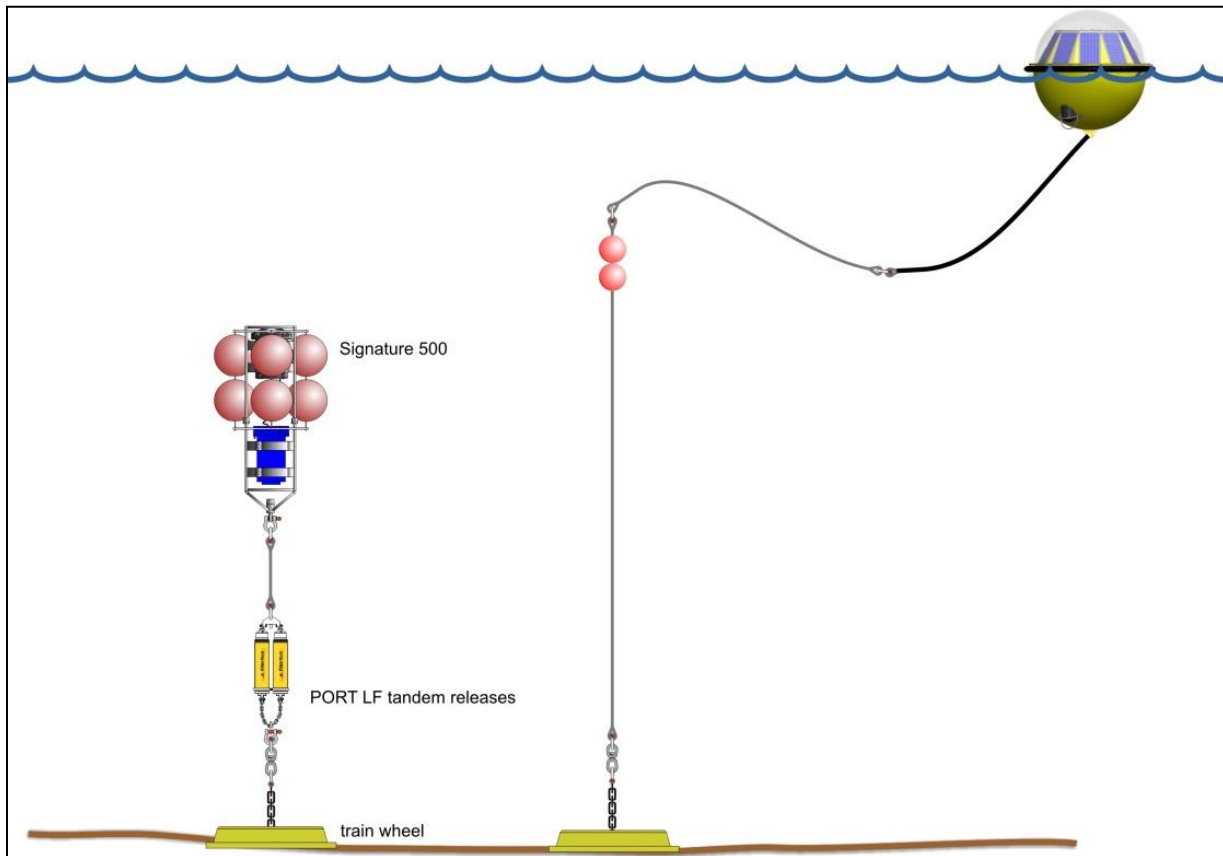


FIGURE 7.21 TRIAXYS wave buoy and Signature 500 ADCP setup for the wave measurements in the Nelson region

7.5 *BaySys Team 3 – Optical Properties of Open and Ice-covered Hudson Bay*

Principal investigators: Jens Ehn¹; C.J. Mundy¹; Simon Bélanger². Cruise participants: Atreya Basu¹; Lucas Barbedos de Freitas²; Lisa Matthes¹; Laura Dalman¹; Rachel Hussher²; Julie Mayor²

¹Centre for Earth Observation Science, University of Manitoba, 125 Dysart Rd, Winnipeg, MB R3T 2N2

²Département de biologie, chimie et géographie, Université du Québec à Rimouski, 300 allée des Ursulines, Rimouski, Quebec G5L 3A1

Introduction and Objectives

The research goal of our team was to use optical measurements accompanied by water and ice sampling for biological and oceanographic parameters to gain information about spring primary production and the distribution and concentration of freshwater, sediments, and organic matter in the Hudson Bay System (HBS). The system is influenced by a large freshwater input from rivers and sea ice melt at this time of the year. Three Ph.D. projects dealing with different aspects of the main objectives were involved in this cruise:

Team Member Projects:

Atreya Basu

To map the freshwater distribution in the Hudson Bay during the spring freshet season. This study focuses on the response of surface freshwater distribution during the open water season to climate variability and hydroelectric regulation. The approach is to use satellite-derived optical proxies and field-based observations, carried out in the fall and spring season, for the development of a Hudson Bay specific ocean color remote sensing algorithm that characterizes the freshwater distribution. One of the main challenges is the partitioning of freshwater origins such as sea ice melt and riverine components. Hudson Bay is fully ice-covered over several months and has a large number of rivers draining into the bay. The coastal waters are one of the prime geographical focus areas of the research with an emphasis on the Nelson-Hayes river estuary. The collected dataset is going to supply crucial information to fill the following objectives:

Studying the optical interdependency among CDOM and particulates in the Hudson Bay: A precursor to the freshwater tracing algorithm

Studying the distribution of runoff, sea ice melt, sea ice during spring freshet in the Hudson Bay using salinity- $\delta^{18}O$ -CDOM measurements

Tracing river plumes in the coastal Hudson Bay (Canada) using satellite remote sensing: Influence of Non-Algal Particles on Remote sensing reflectance and aCDOM retrieval

Optical delineation of the Nelson-Hayes River plume extent (Hudson Bay, Canada) using a satellite remote sensing approach (2012-2018)

Lucas Barbedos de Freitas

The dataset acquired during the BaySys 2018 Expedition will improve the satellite Net Primary Production (NPP) model developed over the last year at UQAR-Takuvik. The model is based on in situ samples of biological parameters as well as in-water and above water radiometry measurements [Babin et al., 2015; Lee et al., 2015]. Hudson Bay is characterized as a domain of optically complex waters with relatively high spatial-temporal variability in the optical properties [Xi et al., 2013, 2014, 2015], therefore, measurements have to be carried out on a high spatial resolution. The collected dataset is going to supply crucial information to fill the following objectives:

Regionalize the remote sensing depth and wavelength resolved net phytoplankton primary production model [Platt et al., 1980] through in situ radiometry, Apparent Optical Properties (AOP), satellite match-up, and water column structure in HBS

Perform a sensitivity study of the NPP algorithm to bio-optical parameters ([Chl a], photosynthetic parameters, diffuse attenuation coefficient for downwelling irradiance ($K_d(\lambda)$) and oceanographic processes to estimate the absolute model uncertainty

Assess the uncertainty of the satellite NPP model when there is evidence that the bloom occurred under ice

Evaluate the capability of the satellite NPP model to access under-ice production

Lisa Matthes

An indication for significant phytoplankton growth in late spring is the changing sea ice conditions of the Hudson Bay system during the last decades such as a significant decline of -15.1 % /decade in sea ice concentration in the western and north-western parts of the Bay [Hochheim et al. 2010]. Up to now, primary production measurements were mainly performed in open water between June and September in Hudson Bay [Legendre and Simard 1979; Grainger 1982; Ferland et al. 2011], neglecting a potential under-ice and/or ice algae spring bloom and resulting in low annual production estimates. Additionally, little is known about the photophysiological adaptation of present algae communities to these quickly changing environmental conditions in late spring. My project aims to investigate the following objects during the summer cruise:

Investigate the role of spectral light availability on the timing and location of spring primary production with a retreating sea-ice cover in Hudson Bay

Quantify the seasonal variability in spectral light attenuation in the upper water column associated with biological properties of primary producers, dissolved organic matter, and non-algal particles

Describe the variability in primary production in the Nelson estuary along a salinity gradient during the spring melt

Operations Conducted and Methodology

Sampling was conducted in the open water of Hudson Bay, on ice, and via helicopter at several rivers (Figure 7.22). Water samples for the analysis of oceanographic, optical, and biological parameters were collected from the rosette at 6 optical depths as well as at deeper depths according to stratification patterns of the water column. Simultaneously, optical instruments were deployed from the foredeck to measure the reflection of light at the water surface, the extinction of light in the water column, and the concentration and distribution of particulate and dissolved matter impacting the propagation of light

through absorption and scattering processes. Table 4 provides an overview of the sampled parameters at each station.

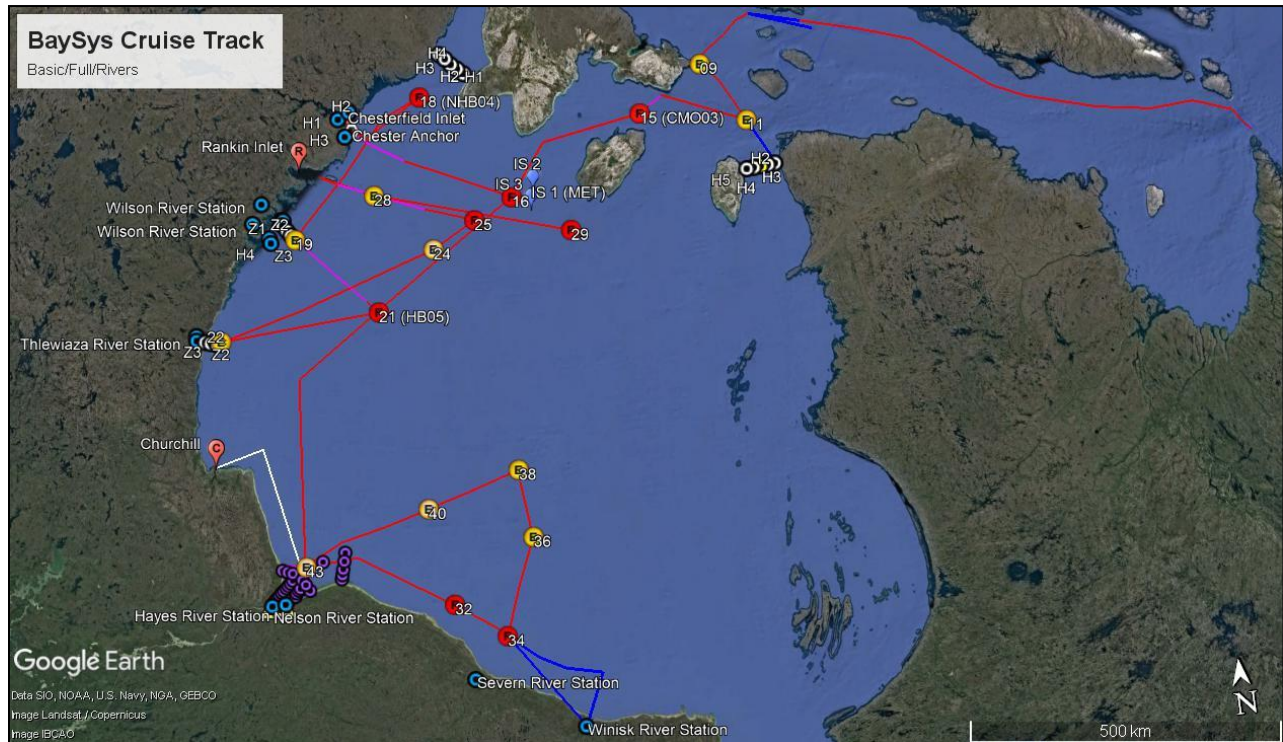


FIGURE 7.22 Water sampling and the deployment of optical instruments were performed at full and basic stations (B, F). Ice work including under-ice light measurements and the sampling of ice cores was carried out at several of these stations.

Optical Operations

From the foredeck, measurements of surface reflection were conducted with the Hyperspectral Surface Acquisition System (HyperSAS, Satlantic, USA) following the methodology of Mobley [1999]. In-water radiometric profiles of light extinction were recorded by the submersible spectroradiometer Compact Optic Profile System (C-OPS, Biospherical Instruments Inc., USA) using a similar methodology of Hooker et al., (2013). To complete dataset interpretation, Secchi disk depth was measured before the deployment of the C-OPS. Additionally, a photographic report was performed continually during each station and ship transects to monitor the sea-ice, atmospheric, and sea state.

Total atmospheric ozone, water vapor, and aerosol measurements are conducted using the handheld ozone monitor and Sun photometer Microtops II [Morys et al., 2001]. This dataset will help to improve the atmospheric correction related to ocean color satellite observations.

Measurements of the inherent optical properties such as absorption and scattering by particles (phytoplankton, sediment, detritus) and colored dissolved organic matter (CDOM) were conducted via instruments (AC-S, BB9, BB3, CTD-probe, fluorometer) attached to a metal frame. The frame was

lowered with the help of the A-frame at the foredeck to the water surface and several profiles from the water surface to the bottom were recorded. The deployment of the Laser in-situ Scatterometer/Transmissometer (LISST 100x, Sequoia Scientific Inc., USA) followed to measure particle size distribution and concentration along the same profile.

To determine the optical depths for water sampling via the rosette, a Profiling Natural Fluorometer (PNF-300, Biospherical Instruments Inc., USA) was deployed from the foredeck. The ship was positioned towards the sun so that the recorded light profile was not contaminated by the ship's shade. Afterwards, the diffuse attenuation coefficient of downwelling irradiance was calculated to determine 6 optical depths: 100 %, 30 %, 15 %, 5 %, 1 %, and 0.2 %.

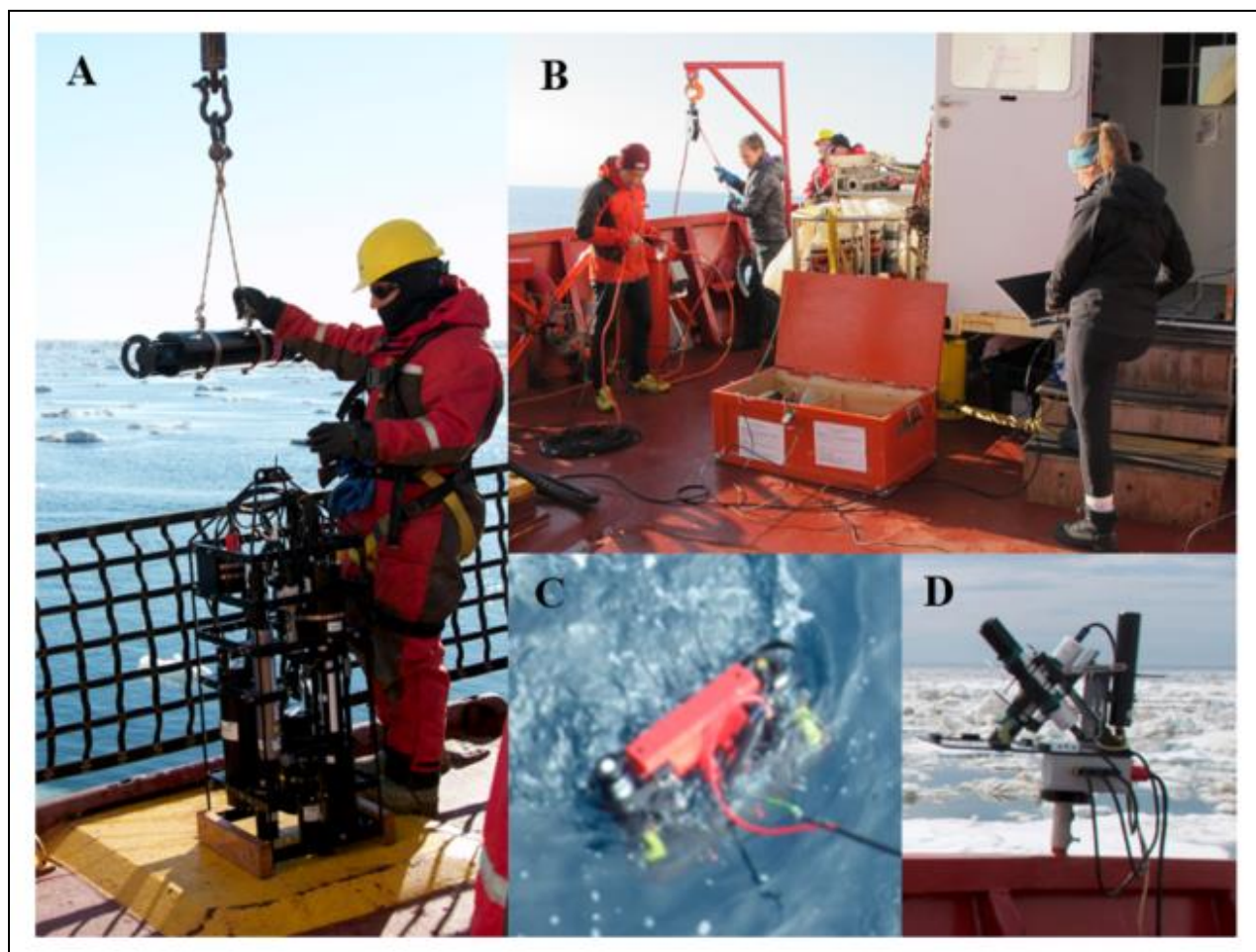


FIGURE 7.23 Optical instruments A) LISST, IOP-frame, B) PNF, C) C-OPS, D) HyperSAS (Photo Credit: Lucette Barber, Lisa Matthes, Lucas Barbedos de Freitas)

Water Sampling

14C incubations

Measurements to determine primary production in function of a light gradient were performed at 22 different locations during the cruise (see Table 4). Production vs. Irradiance (PE) curves were measured by incubating seawater, melt pond water, and melted scrapes of the bottom ice cores inoculated with ^{14}C . The incubations were conducted according to the radioactive safety guidelines in the Radvan after the protocol of Takuvik (Marcel Babin, Université Laval). The incubator is a custom-made instrument adapted after the one presented in Babin et al. 1994 (Figure 7.24).



FIGURE 7.24 General set-up for the PE incubations in the Radvan. From right to left: inoculation space, incubator, filtration ramp, clean workspace (Photo Credit: Rachel Hussherr)

Six or seven incubations were carried out at each station: either 6 optical depths (determined by PAR measurements from PNF 300) in the water column if the station was in open water, or 4 optical depths + ice bottom scrapes + melt pond/ interface water if the station was a mix of open water and sea ice floes. The seawater from each sampled depth was incubated in an individual incubation chamber for 3 to 4 hours depending on the in-situ production in the water column. After filtration, samples were placed in a Beckman Coulter LS 6500 scintillation counter to count the ^{14}C uptake of algae cells. Afterward, PE curves (Counts per minute in function of irradiance) were made for every water sample at each station.

Filtrations

Water samples, taken with the rosette from several water depths, were filtered for various parameters (Table 7.5). Thereby, sampling depths (optical depths, discrete depth levels based on stratification) were in line with the water sampling of other teams to gain a full picture of the biological, chemical, and physical processes in the water column. Filtrations took place in the aft filtration lab under green light to minimize photodamage of the studied organic matter.

TABLE 7.5 Water sampling parameters collected during Leg 1

Sampling depth	Parameter	Description
Optical depths, Ice samples	Chl a	Chlorophyll a
Optical depths, Ice samples	HPLC	High-performance liquid chromatography for pigment analysis
Optical depths, Ice samples, Discrete depths	POC/N	Particulate organic carbon and nitrogen
Optical depths, Ice samples, Discrete depths	ap	Particulate absorption

Ice samples	Taxonomy	Species identification
Discrete depths	TSS	Total suspended sediment
Discrete depths	CDOM/FDOM	Colored dissolved organic matter
Discrete depths	Salinity	Salinity
Discrete depths	δ 18O	Oxygen isotopes

Chlorophyll was analyzed on board with a Fluorometer (Turner 10AU, Turner Designs, USA) following the method described in Parsons et al. [1984]. The filters for the analysis of the remaining parameters were stored in the fridge (4°C) or freezer (-80°C) to be transported back to the lab with the crew change. Additionally, water samples were collected for δ 18O and salinity measurements at discrete depth levels. Salinity samples were analyzed using the onboard salinometer.

Ice Sampling

To complete data collection for the investigation of spring primary production in Hudson Bay, samples of algae inhabiting the ice bottom were taken at each ice station. The last 5 cm of three ice cores as well as scrapes from the bottom of another three cores were collected to be filtered onboard for the biological parameters listed in table 7.6 as well as 14C incubations (Figure 7.25B). Additionally, water from the ice interface and melt ponds were collected via pump for the same objective. However, before ice cores for ice algae biomass were sampled, optical measurements were carried out in the undisturbed area to determine light availability for primary production at the ice bottom. Spectral albedo $\alpha(\lambda)$ of different sea ice surface properties was measured prior to the under-ice light sampling with one hyperspectral radiometer (1 planar RAMSES-ACC, TriOS GmbH, Germany, Figure 7.25A). Transmitted irradiance beneath the sea ice cover was recorded via a custom-built double-hinged aluminum pole (L-arm) and 3 hyperspectral radiometers (1 planar RAMSES-ACC, 2 scalar RAMSES-ASC, TriOS GmbH, Germany). Finally, ice thickness, freeboard, melt pond depth, and snow height was measured at the ice core sampling site.



FIGURE 7.25 Measurement of surface albedo (A) and ice core sampling (B)

TABLE 7.6 Sampled parameters at each station type (Nutrient, Basic, Ice, Transect, Helicopter, River, Estuary)

Date	Station	Station type	Depth [m]	Optical	14C	Chl a	HPLC	POC/N	ap	Tax.	TSS	CDOM/FDOM	Sal	18O	Sedi. core
31-May	N01	Nutrient	386									x			
31-May	N02	Nutrient	566			x	x	x	x			x			
31-May	Brash	Random				x		x	x						
31-May	N03	Nutrient	419			x						x			
01-Jun	B04	Nutrient	283			x	x	x	x			x			
02-Jun	FB05	Nutrient	245			x	x	x	x		x	x			
02-Jun	FB07	Nutrient	274			x		x	x		x	x	x	x	
02-Jun	FB05-H	Helicopter										x	x	x	x
03-Jun	FB09	Basic	104	x	x	x	x	x	x		x	x			
03-Jun	B10	Nutrient	199			x			x			x	x	x	
04-Jun	B11	Basic	321	x	x	x	x	x	x		x	x			
04-Jun	B11-Ice	Full/Ice										x	x	x	x
04-Jun	H3	Helicopter										x	x	x	
05-Jun	B12	Nutrient	83			x			x			x	x	x	
05-Jun	B13	Nutrient	144			x			x			x	x	x	
05-Jun	B15	Basic	189	x	x	x	x	x	x		x	x			
06-Jun	B16	Full/Ice	132	x	x	x	x	x	x	x	x	x			x
07-Jun	B17	Basic	90			x	x	x	x		x				
08-Jun	B18	Full/Ice	114	x	x	x	x	x	x	x	x				x
09-Jun	B19	Full/Water	86			x	x	x	x		x	x			
09-Jun	B19-Wilson	River				x		x				x	x	x	
		Estuary													
09-Jun	B19-Ferguson	River				x		x				x	x	x	
		Estuary													
09-Jun	B19-Zodiak	Transect										x	x	x	
09-Jun	B20	Nutrient	109			x	x	x	x			x	x	x	
10-Jun	B21	Full/Ice	147	x	x	x	x	x	x	x	x	x	x	x	
11-Jun	B22	Full/Water	65	x	x	x	x	x	x		x	x	x	x	
11-Jun	B22-Thanne	River				x		x	x			x			
11-Jun	B22-Thlewiza	River				x		x	x			x			
11-Jun	B19-Zodiak	Transect										x	x	x	
11-Jun	B23	Nutrient	110			x	x	x	x			x	x	x	
12-Jun	B24	Full/Ice	185	x	x	x	x	x	x	x	x	x	x	x	

13-Jun	B25	Full/Ice	149	x		x	x	x	x	x	x	x	x	x	
14-Jun	B26	Nutrient	129										x	x	x
15-Jun	B28	Basic	160			x	x	x	x				x		
16-Jun	B29	Full/Water	175	x		x		x	x			x	x		
18-Jun	B31 (AN02)	Nutrient	46			x		x	x			x	x	x	x
18-Jun	Nelson River	River				x		x	x			x	x		
18-Jun	Hayes River	River				x		x	x			x	x		
19-Jun	B32	Full/Ice	31	x	x	x	x	x	x			x	x		x
19-Jun	Severn River	River				x		x	x			x	x		
19-Jun	B32	Full/Ice											x	x	x
20-Jun	B33	Nutrient /Ice (Bucket)				x		x	x	x	x	x	x	x	
20-Jun	Winisk River	River				x		x	x			x	x	x	x
20-Jun	B33-H(1-3)	Full/Ice							x				x	x	x
20-Jun	B34	Full/Ice	45	x	x	x	x	x	x			x	x	x	x
21-Jun	B34b	Full/Ice		x		x	x	x	x	x			x	x	x
21-Jun	B34b-Z	Full/Water				x		x	x			x	x	x	x
21-Jun	B35	Nutrient	60			x		x	x			x	x		
22-Jun	B36	Full/Ice	126	x	x	x	x	x	x	x	x	x	x	x	x
22-Jun	B36-HA	Helicopter				x							x		
22-Jun	B36-HB	Helicopter				x							x		
22-Jun	B36-HC	Helicopter				x							x		
22-Jun	B36-HD	Helicopter				x							x		
23-Jun	B38	Full/Ice	179	x	x	x	x	x	x			x	x		x
24-Jun	B39	Nutrients	180										x	x	x
24-Jun	B40	Basic/Ice	90	x	x	x	x	x	x			x	x		
27-Jun	B15-2	Nutrient	190			x	x	x	x				x	x	x
27-Jun	L1	TSG				x	x	x	x						
27-Jun	L2	TSG				x	x	x	x						
27-Jun	L3	TSG				x	x	x	x						
28-Jun	B44	Basic	104	x	x	x	x	x	x			x	x	x	x
29-Jun	Nelson-A	River	~5	x	x	x	x	x	x			x		x	x
29-Jun	N-B	River	~5	x	x	x	x	x	x			x		x	x
29-Jun	South-Transect	Estuary				x	x	x	x			x			
30-Jun	B45-R	Water				x	x	x	x			x		x	x
30-Jun	N-C	River		x	x	x	x	x	x			x		x	x
30-Jun	N-D	River		x	x	x	x	x	x			x		x	x
01-Jul	B46-R	Water		x	x	x	x	x	x			x		x	x
01-Jul	West-Transect	Estuary	15											x	x

Preliminary results:

Location of the Highest Chlorophyll-a Concentration

The surface chlorophyll maximum (SCM) is shallower in low productive areas (close to the coast, ice edge, and eastern entrance to Hudson Bay) compared to the very productive area in the center of the open water in the north-west of the bay (Figure 7.26). In this area, nutrients must have been completely depleted in the surface water column, so that a high phytoplankton abundance is only visible on top of the pycnocline through which nutrients diffuse from the richer bottom water layer. The southern part also showed a shallow SCM and a low phytoplankton concentration which could be related to the high ice coverage and an existing light limitation.

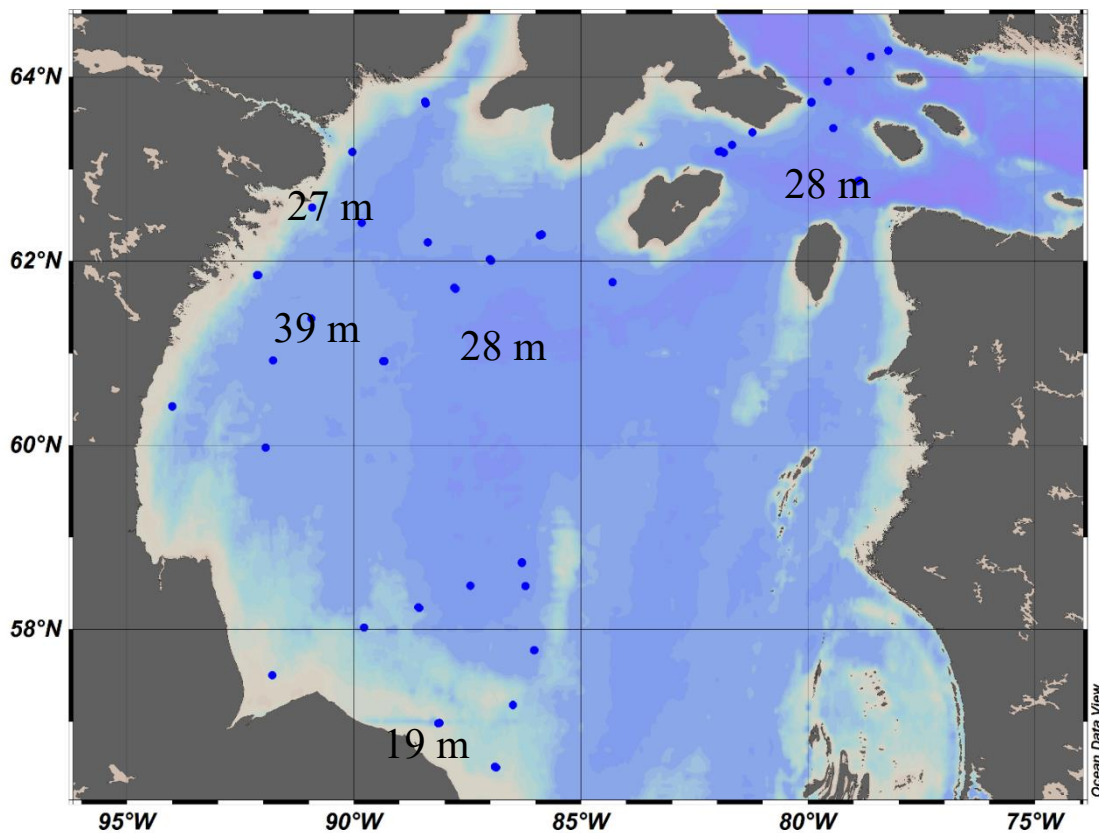


FIGURE 7.26 Depth of the surface chlorophyll maximum

Chlorophyll Concentration in the Water Column and Ice Bottom

The concentration of chlorophyll-a as a proxy for phytoplankton and ice algae abundance was measured at 6 optical depths in open and ice-covered water column, at the ice bottom, and upstream of several rivers (Figure 7.27). Chlorophyll-a concentration was higher at the SCM compared to the surface water layer. At the ice bottom, chlorophyll-a concentration was much higher than expected. This is probably related to the large observed abundance of filamentous algae (genus *Melosira*) hanging down from the ice

bottom in northern Hudson Bay. In southern Hudson Bay, a lower ice algae abundance was observed which could be related to the late sampling time (bloom terminated) and/or a higher freshwater concentration in the surface water layer. Chlorophyll a concentration of sampled rivers was lower at the north-west coast compared to the south coast. The highest concentration was measured in the Hayes River.

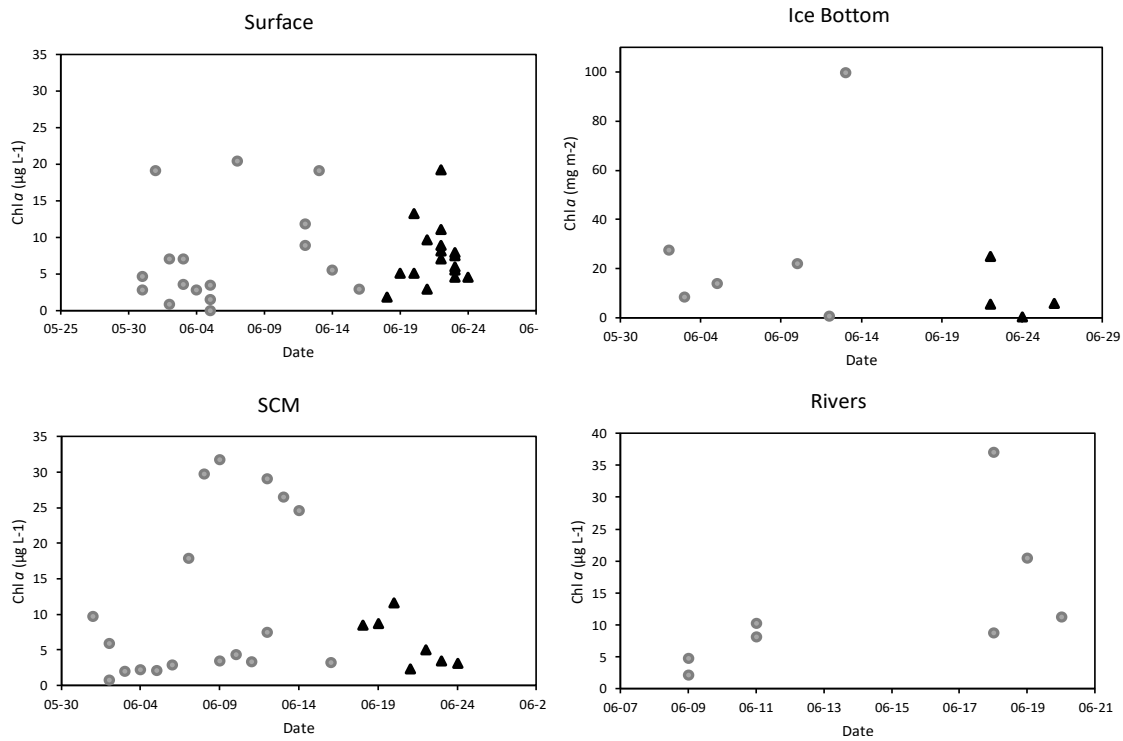


FIGURE 7.27 Chlorophyll-a concentration sampled at the water surface in north-west Hudson Bay (grey) and south Hudson Bay (black), at the depth of the surface chlorophyll maximum (SCM), the ice bottom and upstream of rivers at the west and south coast of Hudson Bay

Additional Observations in the Nelson-Hayes Estuary

Ship- and ice-based observations described above were supplemented using the ship's barge and Zodiac to sample across salinity gradients in the Nelson-Hayes estuary (Figure 7.28). Stations NA, NB (barge), and S1–S3 (Zodiac) were visited on 29 June; NC, NC (Zodiac), and BN3–BN7 (barge) and were visited on 30 June. W1–W3 was sampled on 1 July by rosette from the Amundsen. Stations NA and BN3 were in freshwater. At stations S1-S3, water was collected for Team Optics/Biology by the carbon and mercury teams.

Surface water samples collected at each station were filtered for TSS, ap, chlorophyll a, and CDOM. The frame with attached inherent optical properties instruments (Wetlabs AC-S, BB9, BB3, CTD-probe, fluorometer) and the LISST instrument was deployed at stations NA and NB only (Atreya Basu). The

Compact Optic Profile System was used to record radiometric profiles of light extinction at stations NA, NB, and BN3–BN7 (Lucas Barbedos De Freitas). An Idronaut CTD was deployed at all Zodiac stations to record profiles of conductivity, temperature, and optical backscatter. A Seabird 19+ CTD was deployed at barge stations to record conductivity, temperature, oxygen, chlorophyll fluorescence, CDOM fluorescence, beam transmission, and photosynthetically-active radiation through the water column. (The Seabird 19+ was also deployed from the Zodiac and/or from the ice at stations 32, 33, 34, 36, 38, and 40 in southern and south-central Hudson Bay to record profiles away from upper water column disturbance by the ship’s thrusters.) Figure 7.22 also shows locations of sediment samples MF1–MF4, collected from the tidal mudflats on 30 June. Samples were collected at 0–5 and 10–15 cm depth at each location.



FIGURE 7.28 Stations sampled by barge or Zodiac in the Nelson-Hayes estuary. The map on the right shows station locations in the area bounded by the box on the map on the left. Waypoints were recorded at the beginning and end of the period of observations and sampling at stations BN3–BN7. A similar drift at other stations in the estuary was not recorded.

References

Babin, M., S. Bélanger, I. Ellingsen, A. Forest, V. Le Fouest, T. Lacour, M. Ardyna, and D. Slagstad (2015). Estimation of primary production in the Arctic Ocean using ocean colour remote sensing and coupled physical-biological models: strengths, limitations and how they compare, *Prog. Oceanogr.*, doi:10.1016/j.pocean.2015.08.008.

Ferland J, Gosselin M, Starr M (2011) Environmental control of summer primary production in the Hudson Bay system: The role of stratification. *J Mar Syst* 88:385–400.

Grainger E (1982) Factors affecting phytoplankton stocks and primary productivity at the Belcher Islands, Hudson Bay. *Le Naturaliste canadien*.

Hochheim K, Barber DG, Lukovich JV (2010) Changing sea ice conditions in Hudson Bay, 1980–2005. In: *A little less Arctic*. Springer, pp 39–52

Hooker, S. B., J. H. Morrow, and A. Matsuoka (2013), Apparent optical properties of the Canadian Beaufort Sea - Part 2: The 1% and 1 cm perspective in deriving and validating AOP data products, *Biogeosciences*, 10(7), 4511–4527, doi:10.5194/bg-10-4511-2013.

Lee, Y. J. et al. (2015), An assessment of phytoplankton primary productivity in the Arctic Ocean from satellite ocean color/in situ chlorophyll-a based models, *J. Geophys. Res. Ocean.*, 120(9), 6508–6541, doi:10.1002/2015JC011018.Received.

Legendre L, Simard Y (1979) Océanographie biologique estivale et phytoplancton dans le sud-est de la baie d'Hudson. *Mar Biol* 52:11–22.

Mobley, C. D. (1999), Estimation of the remote-sensing reflectance from above-surface measurements, *Appl. Opt.*, 38(36), 7442, doi:10.1364/AO.38.007442.

Morrow, J. H., C. R. Booth, R. N. Lind, and S. B. Hooker (2010), Advances in Measuring the Apparent Optical Properties (AOPs) of Optically Complex Waters: The Compact-Optical Profiling System (C-OPS), Greenbelt, Maryland.

Morys, M., F. M. Mims, S. Hagerup, S. E. Anderson, A. Baker, J. Kia, and T. Walkup (2001), Design, calibration, and performance of MICROTOPS II handheld ozone monitor and Sun photometer, *J. Geophys. Res. Atmos.*, 106(D13), 14573–14582, doi:10.1029/2001JD900103.

Xi, H., P. Larouche, S. Tang, and C. Michel (2013), Seasonal variability of light absorption properties and water optical constituents in Hudson Bay, Canada, *J. Geophys. Res. Ocean.*, 118(6), 3087–3102, doi:10.1002/jgrc.20237.

Xi, H., P. Larouche, S. Tang, and C. Michel (2014), Characterization and variability of particle size distributions in Hudson Bay, Canada, *J. Geophys. Res. Ocean.*, 119(6), 3392–3406, doi:10.1002/2013JC009542.

Xi, H., P. Larouche, C. Michel, and S. Tang (2015), Beam attenuation, scattering and backscattering of marine particles in relation to particle size distribution and composition in Hudson Bay (Canada), *J. Geophys. Res. Ocean.*, 120(5), 3286–3300, doi:10.1002/2014JC010668.

7.6 *Zooplankton and Fish Ecology/Acoustics*

Principal Investigator: Louis Fortier¹. Cruise participants: Cyril Aubry¹, Sarah Schembri¹ and Tommy Pontbriand¹

¹Québec-Océan, Université Laval, 1045 avenue de la Médecine, Québec, QC, G1V 0A6

Introduction and Objectives

The main objective of our team during Leg 1 was the monitoring of key parameters (abundance, diversity, biomass, and distribution) for zooplankton and fish using various sampling devices and the EK60 echosounder. The specific objectives were to:

Compare zooplankton and fish species assemblages in different areas of the Hudson Bay system: comparison of coastal species assemblages with off-shore ones; comparison between the West, South, and East coasts of the Hudson Bay. Find out which fish species develop in estuaries and along the ice-edge during the spring-melt season, and capture adult fish in Hudson Bay for the first time.

Operations Conducted and Methodology:

Double Square Net (DSN) (1 × 750µm, 1 × 500µm, 1 × 50µm)

The Ichtyoplankton net is a rectangular frame carrying two 4.5 m long, 1 m² mouth aperture, square-conical nets, and an external 10 cm diameter, 50 µm mesh net (to collect microzooplanktonic prey of the fish larvae). The DSN was equipped with three KC® flowmeters; one for the 750 µm net, one for the 500 µm net, and a control flowmeter between the two nets. The sampler was towed obliquely from the side of the ship at a speed of ca. 2-3 knots to a maximum depth of 90m (depth estimated during deployment from cable length and angle; real depth obtained afterward from a Star-Oddi® mini-CTD attached to the frame).

For onboard analysis, all fish larvae collected with the DSN were identified, measured, and preserved individually in 95% ethanol + 1% glycerol. Zooplankton samples from the 500 µm mesh and the 50 µm mesh nets were preserved in 10% formalin solution for further taxonomic identification. The zooplankton from the 750 µm mesh net was given to the contaminant team (Ainsleigh Loria, PI: Gary Stern) for mercury and pollutant analysis.

5 Net Vertical Sampler (5NVS) (3 × 200µm, 1 × 500µm, 1 × 50µm)

The zooplankton sampler is made up of four 1 m² metal frames attached and rigged with four 4.5 m long, conical-square plankton nets, an external 10 cm diameter, 50 µm mesh net. The 5NVS was equipped with five KC Denmark ® flowmeters – each of the nets with a mesh size larger than 50 µm was equipped with a flowmeter and a control flow meter was attached to the centre of the frame. The sampler was deployed vertically from 10 meters off the bottom to the surface. After removal of any fish larvae/juveniles (identified, measured, and preserved separately in 95% ethanol + 1% glycerol), zooplankton samples

from the 500 μm , 50 μm and one of the 200 μm mesh nets were preserved in 10% formaldehyde solution for abundance measurements. The zooplankton from the second 200 μm mesh net was split into fractions (depending on the size of the sample); one fraction was preserved in alcohol for genetic analysis and a second fraction was divided into zooplankton smaller and larger than 1000 μm , dried and frozen for biomass analysis. The third 200 μm mesh net was given to Ainsleigh Loria (PI: Gary Stern) for contaminant analysis.

Hydrobios (9 × 200 μm)

The hydrobios is a multi-net plankton sampler. The hydrobios is equipped with nine 200 μm mesh nets (opening 0.5 m²). This allows for depth-specific sampling of the water column. The Hydrobios is also equipped with a CTD to record water column properties while collecting biological samples. The deployment is vertical from 15 m off the bottom to the surface. The nets open and close one by one as the pressure decreases while the net is going up in the water column. The depth at which the different nets open and close is programmed prior to deployment. The zooplankton samples were preserved in 10% formalin solution for further taxonomic identification.

Benthic Beam Trawl

This trawl includes a Demersal fish sampler. It is a rectangular net with a 3 m² mouth aperture, 32 mm mesh size in the first section, 16mm in the last section, and a 10 mm mesh liner. The net was lowered on the seafloor and towed for 5 to 20 minutes at a speed of 3 knots. Adult fish collected with this sampler were identified, measured, and stored at -200C while larvae were preserved in 95% ethanol + 1% glycerol.

Ring Net

Small ichthyoplankton net, 3.25 m long conical net with a circular 65 cm diameter opening and 500 μm mesh size. A TSK flowmeter is attached to the opening. The ring net was deployed from the zodiac or barge in river estuaries or when heavy ice cover prevented the use of the DSN. The net is towed from the back of the zodiac at about 2 to 3 kts, about 30 m of rope is deployed. All fish larvae collected were identified, measured, and preserved individually in 95% ethanol + 1% glycerol.

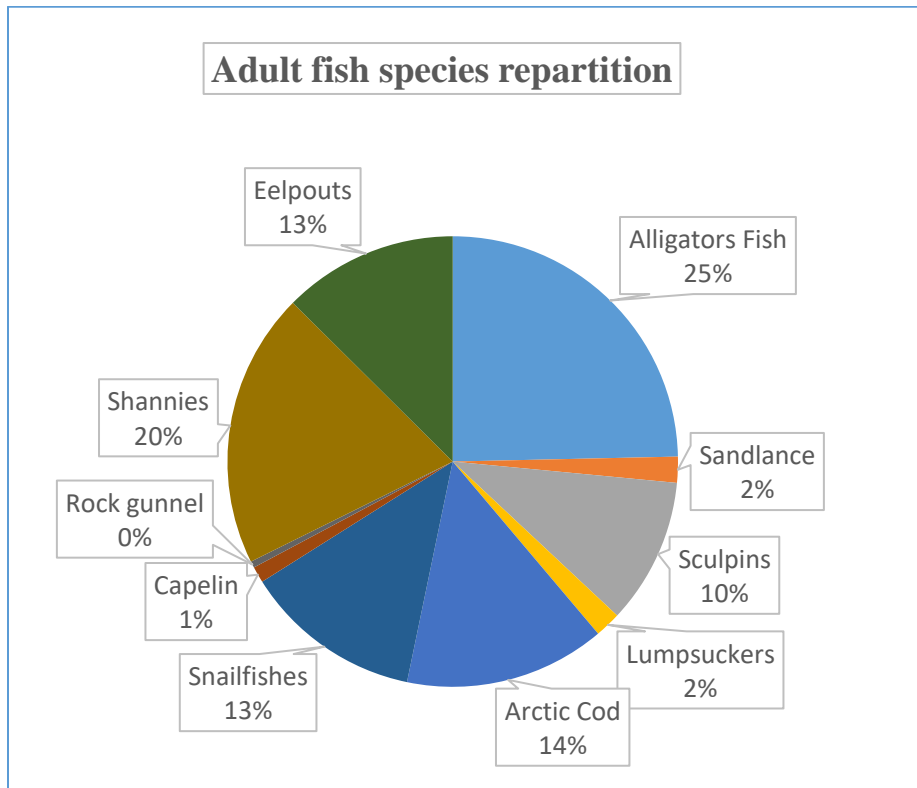
Acoustic Monitoring

The Simrad® EK60 echosounder of the CCGS Amundsen allows our group to continuously monitor the spatial and vertical distribution and biomass of zooplankton and pelagic fish that have a swim bladder such as cod (*Boreogadus saida*) and capelin (*Mallotus villosus*). The hull-mounted transducers are in operation 24h a day thus providing an extensive mapping of where the fishes are along the ship track.

Preliminary Results

TABLE 7.7 Summary of fish catches

Fish Family	Common Name	Adult	Larvae
Agonidae	Alligators Fish	106	62
Ammodytidae	Sandlance	8	274
Cottidae	Sculpins	45	742
Cyclopteridae	Lumpsuckers	8	3
Gadidae	Arctic Cod	62	43
Gasterosteidae			1
Liparidae	Snailfishes	55	149
Osmeridae	Capelin	5	13
Pholidae	Rock gunnel	2	3
Stichaeidae	Shannies	85	1066
Unidentified			73
Zoarcidae	Eelpouts	54	5



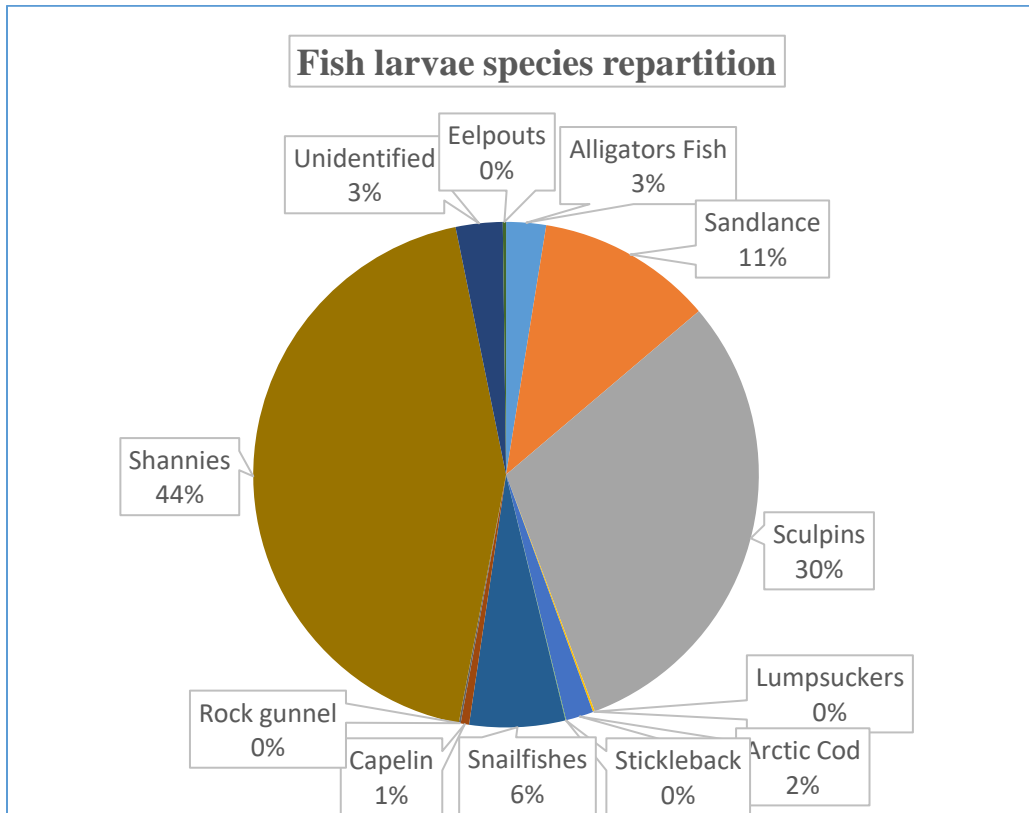


TABLE 7.8 Summary of net operations

Station	Sampling Date	4x1m2 (vertical)	2x1m2 (oblique)	Beamtrawl	Hydrobios	Ringnet 0.60m	Ringnet 1m
04	01 Jun 2018	X					
05	02 Jun 2018	X					
09	03 Jun 2018	X	X	X			
10	04 Jun 2018	X	X	X			
11	04 Jun 2018	X					
15	05 Jun 2018	X	X	X			
16	06 Jun 2018	X	X	X			
17	07 Jun 2018	X					
17a	07 Jun 2018					X	
17b	07 Jun 2018					X	
18	08 Jun 2018	X	X	X	X		
19	09 Jun 2018	X	X	X			
19c	09 Jun 2018					X	
21	10 Jun 2018	X	X	X	X		
22	11 Jun 2018	X	X	X			
22a	11 Jun 2018					X	
24	12 Jun 2018	X			X		

Station	Sampling Date	4x1m2 (vertical)	2x1m2 (oblique)	Beamtrawl	Hydrobios	Ringnet 0.60m	Ringnet 1m
25	13 Jun 2018		X		X		
28	15 Jun 2018	X	X	X			
29	16 Jun 2018	X	X	X			
32	19 Jun 2018	X					
32a	19 Jun 2018					X	
34	21 Jun 2018		X				
36	22 Jun 2018	X			X		
38	23 Jun 2018		X				
40	24 Jun 2018	X					
43	27 Jun 2018		X	X			
44	28 Jun 2018		X	X	X		
45	30 Jun 2018			X			
46	01 Jul 2018	X	X	X			
BN3	30 Jun 2018						X
BN5	30 Jun 2018						X
BN7	30 Jun 2018						X

7.7 *Marine Productivity: Carbon and Nutrients Fluxes*

Principal Investigator: Jean-Éric Tremblay¹. Cruise Participants: Jonathan Gagnon¹, Janghan Lee¹, Kasey Cameron-Bergeron¹

¹Department of Biology, Laval University

Introduction and Objectives

The Arctic climate displays high inter-annual variability and decadal oscillations that modulate growth conditions for marine primary producers. Much deeper perturbations recently became evident in conjunction with globally rising CO₂ levels and temperatures (IPCC 2007). Environmental changes already observed include a decline in the volume and extent of the sea-ice cover (Johannessen et al. 1999, Comiso et al. 2008), an advance in the melt period (Overpeck et al. 1997, Comiso 2006), and an increase in river discharge to the Arctic Ocean (Peterson et al. 2002, McClelland et al. 2006) due to increased precipitation and terrestrial ice melt (Peterson et al. 2006). Consequently, a longer ice-free season was observed in both Arctic (Laxon et al. 2003) and subarctic (Stabeno & Overland 2001) environments. These changes entail a longer growth season associated with a greater penetration of light into surface waters, which is expected to favoring phytoplankton production (Rysgaard et al. 1999), food web productivity, and CO₂ drawdown by the ocean. However, phytoplankton productivity is likely to be

limited by light but also by allochthonous nitrogen availability. The supply of allochthonous nitrogen is influenced by climate-driven processes, mainly the large-scale circulation, river discharge, upwelling, and regional mixing processes. In the global change context, it appears crucial to improve the knowledge of the environmental processes (i.e. mainly light and nutrient availability) interacting to control phytoplankton productivity in the Canadian Arctic. Also, changes in fatty acid proportions and concentrations will reflect shifts in phytoplankton dynamics including species composition and size structure and will reveal changes in marine energy pathways and ecosystem stability¹²³.

The main goals of our team were to establish the horizontal and vertical distributions of phytoplankton nutrients and to measure the primary production located at the surface of the water column using O₂/Ar ratios and tracers incubations. The auxiliary objective was to calibrate the ISUS nitrate probe attached to the Rosette.

Operations Conducted and Methodology

Samples for inorganic nutrients (ammonium, nitrite, nitrate, orthophosphate, and orthosilicic acid) were taken at all NUTRIENTS/BASIC/FULL stations (Table 7.8) to establish detailed vertical profiles at standard depths (5, 10, 20, 30, 40, 50, 60, 70, 80, 100, 125, 150, 175, 200, 250 meters, and near the bottom). Samples were collected in acid-cleaned polyethylene tubes after thorough rinsing and filtration through a GF/F filter and stored at 4°C in the dark. Concentrations of nitrate, nitrite, orthophosphate, and orthosilicic acid were determined within a few hours on a Bran+Luebbe AutoAnalyzer 3 using standard colorimetric methods adapted for the analyzer (Grasshoff et al. 1999). Additional samples for ammonium determination were taken at stations where incubations were performed and processed immediately after collection using the fluorometric method of Holmes et al. (1999). Urea samples were analyzed using the method of Mulveena and Savidge [1992] and Goeyens et al. [1998]. Samples for total dissolved nitrogen (TDN) will be analyzed by high-temperature catalytic combustion. DON will be calculated by the difference between TDN and inorganic N. A quadrupole mass spectrometer (PrismaPlus, Pfeiffer Vacuum) was used to measure the dissolved gases (N₂, O₂, CO₂, Ar) coming from the underway seawater line located in the 610 laboratory. O₂ to Ar ratios will later be analyzed to measure primary production that occurred up to 10 days prior to the ship's passage in all the areas visited.

To examine the potential effects of environmental conditions (e.g. acidity, alkalinity, free CO₂) on energy transfer through the food chain, we realized at Full and Basic stations, 3L filtration in duplicate from the water surface and SCM with pre-combusted GF/C, to analyse the lipids composition, which is the densest form of energy, in particulate organic matter. Samples of 100 to 1000 mg of earlier and adult stage of copepods were also realized and stored on GF/F filters by -80°C to aims our objectives. Moreover, the pH of SCM and surface water has been measured by spectrophotometer by using red phenol and cresol purple colorants. Then we stored 500 ml of water from each depth to determine the alkalinity in laboratory as soon as possible after the end of the mission. Finally, we continue the long-term analysis conducted during the previous year such as filtration of POC/PN, POP, BSi, and incubation of phytoplankton with ¹⁵N. To determine nitrate, ammonium, and urea uptake rates and primary production, water samples from the surface were incubated with ¹⁵N and ¹³C tracers. The bottles were then incubated for 24 h using on deck incubator and light controlled incubators to establish the relationship between photosynthesis and irradiance. After 24 h, the water samples were filtered through pre-combusted GF/F filters and the filters

dried for 24 h at 60°C for further analyses. Nutrients at T0 were measured with the Auto-Analyzer. Incubations were then terminated by filtration through a pre-combusted GF/F filter and stored for further analyses. Isotopic ratios of nitrogen and carbon from all GF/F filters will further be analyzed using mass spectrometry.

References

- Arts, M. T., Brett, M. T., Kainz, M. J. Lipids in aquatic ecosystems. *Journal of Chemical Information and Modeling* 53, (2013).
- Wynn-Edwards, C. King, R., Davidson, A., Wright, S., Nichols, P.D., Wotherspoon, S., Kawaguchi, S., Virtue, P. Species-specific variations in the nutritional quality of southern ocean phytoplankton in response to elevated pCO₂. *Water (Switzerland)* 6, 1840–1859 (2014).
- Lee, R. F., Hagen, W., Kattner, G. Lipid storage in marine zooplankton. *Marine Ecology Progress Series* 307, 273–306 (2006).
- Comiso (2006) *Geophys Res Lett* 33, L18504, doi:10.1029/2006GL027341
- Comiso et al. (2008) *Geophys Res Lett* 35, L01703, doi:10.1029/2007GL031972
- Grasshoff et al. (1999) *Methods of seawater analyses*, Weinheim, New-York
- Holmes et al. (1999) *Can J Fish Aquat Sci* 56:1801–1808
- IPCC (2007) *Climate change 2007: The physical science basis*. Cambridge University Press, Cambridge, and New York
- Johannessen et al. (1999) *Science* 286:1937–1939
- Laxon et al. (2003) *Nature* 425:947–950
- McClelland et al. (2006) *Geophys Res Lett* 33, L06715, doi:10.1029/2006GL025753
- Overpeck et al. (1997) *Science* 278:1251–1256
- Peterson et al. (2002) *Science* 298:2171–2174
- Peterson et al. (2006) *Science* 313:1061–1066
- Rysgaard et al. (1999) *Mar Ecol Prog Ser* 179:13–25
- Stabeno & Overland (2001) *EOS* 82:317–321

TABLE 7.9 List of sampling stations and measurements during Leg 1

Station	Cast	Nutrient	NH4	15N-N03	Urea	Filtrations									Incubations			
						Ab. Nat.POM	Total Sele.	POP	Bsi	PIC	POC PN	Lipids POMM	Taxo	Upt. NH4	Upt. N03	Upt. Urea	N2 Fix	
1	1	X		X														
2	2	X		X														
3	3	X		X														
4	4	X	X		X	X	X	X	X	X	X	X	X	X	X	X	X	X
5	5	X		X														
6	6	X		X														
7	7	X		X														
8	8	X		X														
9	9	X	X		X	X	X	X	X	X	X	X	X	X	X	X	X	X
9	10	X		X														
10	11	X		X														
11	12	X	X		X	X	X	X	X	X	X	X	X	X	X	X	X	X
11	13	X		X														
12	14	X		X														
13	15	X		X														
15	17	X		X														
15	18	X		X														
16	19	X	X		X	X	X	X	X	X	X	X	X	X	X	X	X	X
16	20	X		X														
17	21	X	X		X	X	X	X	X	X	X	X	X	X	X	X	X	X
18	22	X		X														
18	23	X	X		X	X	X	X	X	X	X	X	X	X	X	X	X	X
19	24	X	X		X	X	X	X	X	X	X	X	X	X	X	X	X	X
19	25	X		X														
20	26	X		X														
21	27	X	X		X	X	X	X	X	X	X	X	X	X	X	X	X	X
21	28	X		X														
22	29	X	X		X	X	X	X	X	X	X	X	X	X	X	X	X	X
22	30	X																
23	31	X	X		X	X		X	X	X	X		X					
24	32	X	X		X	X	X	X	X	X	X	X	X	X	X	X	X	X
24	33	X		X														
25	34	X		X														
25	35	X	X		X	X	X	X	X	X	X	X	X	X	X	X	X	X
26	36	X		X														
27	37	X		X														
28	38	X	X		X	X		X	X	X	X		X					
29	39	X		X														
31	40	X		X														
32	41	X	X		X	X	X	X	X	X	X	X	X	X	X	X	X	X
32	42	X																
34	43	X	X		X	X		X	X	X	X		X	X	X	X	X	X
34	44	X		X														
35	45	X		X														
36	46	X		X														
36	47	X	X		X	X		X	X	X	X		X	X	X	X	X	X
37	48	X		X														
38	49	X	X		X	X		X	X	X	X		X	X	X	X	X	X
38	50	X		X														
39	51	X		X														
40	52	X	X		X	X		X	X	X	X		X	X	X	X	X	X
40	53	X		X														

41	54	X		X													
15B	55	X															
44	56	X	X		X	X		X	X	X	X		X	X	X	X	X
44	57	X		X													
45	58	X	X		X	X		X	X	X	X		X	X	X	X	X
45	59	X	X		X	X		X	X	X	X		X	X	X	X	X
W-T01	60	X		X													
W-T02	61	X		X													
W-T03	62	X		X													
46	63	X	X		X	X		X	X	X	X		X	X	X	X	X
46	64	X		X													
9	Ice	X	X			X	X	X	X	X	X	X	X				
H3	Ice	X	X			X	X	X	X	X	X	X	X				
16	Ice	X	X			X	X	X	X	X	X	X	X				
NE01	Barge	X	X	X	X	X		X	X	X	X		X	X	X	X	X
NE02	Barge	X	X	X	X(?)	X		X	X	X	X		X				
NE03	Zodiac	X	X	X	X	X		X	X	X	X		X	X	X	X	X
NE04	Zodiac	X	X	X	X	X		X	X	X	X		X	X	X	X	X
Wilson	Helicopter	X	X	X	X	X		X	X	X	X		X	X	X	X	X
Ferguson	Helicopter	X	X	X	X	X		X	X	X	X		X	X	X	X	X
Tha-Anne	Helicopter	X	X	X	X	X		X	X	X	X		X	X	X	X	X
Thiewiaza	Helicopter	X	X	X	X	X		X	X	X	X		X	X	X	X	X
Nelson	Helicopter	X	X	X	X	X		X	X	X	X		X	X	X	X	X
Hayes	Helicopter	X	X	X	X	X		X	X	X	X		X	X	X	X	X
Severn	Helicopter	X	X	X	X	X		X	X	X	X		X	X	X	X	X
Winisk	Helicopter	X	X	X	X	X		X	X	X	X		X	X	X	X	X
Seal	Helicopter	X	X	X	X	X		X	X	X	X		X	X	X	X	X
Knife	Helicopter	X	X	X	X	X		X	X	X	X		X	X	X	X	X
Churchill	Helicopter	X	X	X	X	X		X	X	X	X		X	X	X	X	X
Churchill	Zodiac	X	X	X	X			X	X	X	X		X	X	X	X	

7.8 *Macrofauna Diversity Across Hudson Bay Complex*

Principal Investigator: Philippe Archambault¹; Cruise Participant: Marie Pierrejean¹; Catherine Van Doorn¹

¹Laboratoire d'écologie benthique, Université Laval, Pavillon Vachon 1045 Avenue de la Médecine, G1V0A6 Québec (QC), Canada

Introduction and Objectives

Most epibenthic (i.e. benthic organisms living at the surface of sediments) and endobenthic (i.e. living inside the sediments) are either sessile or have low mobility. They are therefore directly affected by changes in their environment. For instance, global change affects physical parameters such as sea ice extent and thickness but also impacts ecosystem functioning and the structure of food webs including those of benthic communities (Darnis et al. 2012, Kedra et al. 2015). Benthic invertebrates of the Hudson Bay Complex are exposed to two major stresses in space and time: climate change and freshwater discharge from several rivers (Grant Ingram and Prinsenberg 1998). These stressors will also likely cause an increase in shipping transport (Arctic-Council 2009) through the expansion of fisheries in the Hudson Bay Complex or shipping activities (e.g. Churchill and Deception Bay ports) and the establishment of aquatic invasive species because of ballast water (Goldsmid et al. 2017). The RCP8.5 emission scenario predicts a salinity anomaly greater than or equal to -0.5 PSU along coastlines (NOAA-ESRL). In addition to climate-induced changes, freshwater discharge along the coastlines will show notable increase in the southeastern portion of the Nelson basin (Clair et al. 1998, McCullough et al. 2012). This could have great consequences on ecological communities, as salinity gradients control species richness (Witman et al. 2008) and can influence the distribution of species.

Many studies have shown a temporal shift in Arctic benthic communities (Cusson et al. 2007; Renaud et al. 2007; Taylor et al. 2017), but data for the Hudson Bay Complex are scarce and few recent data are available. However, knowledge on benthic biodiversity in the Hudson Bay Complex has increased during the past decade thanks to scientific programs like MERICA (2003), ArcticNet (2010), CHONe (Snelgrove et al. 2012), BaySys (2016), and BriGhT (Bridging Global Change, Inuit Health, and the Transforming Arctic Ocean) (2017). The main objective is to describe benthic communities in the Hudson Bay Complex and to determine the relationship between the distribution of organisms and environmental parameters. In the second time, to link the presence of a given community with environmental parameters, a community distribution model will be developed.

Operations Conducted and Methodology

At 22 stations, the Agassiz trawl (Figure 29) was deployed to collect macrofauna (Table 7.10). Catches were passed through a 2 mm mesh sieve. When possible, specimens were identified to the lowest taxonomic level, then count and weight. The unidentified specimens were preserved in a 4% seawater-formalin solution. Fishes collected and some benthic organisms were kept for Fortier's laboratory and contaminants. Corals and sponges were preserved.

At 21 stations, the box core was deployed to quantitatively sample diversity, abundance, and biomass of infauna and to sample sediment. Unfortunately, the bottom of XX sites was sandy or rocky and the sampling was not possible. Sediments of a surface area of 0.125 m² and 10-15 cm in depth were collected and sieved through a 0.5 mm mesh and preserved in a 4% formaldehyde solution for further identification in the laboratory (Table 7.9). Sub-cores of sediment were collected for sediment pigment content, organic matter, and sediment grain size; for sediment pigments, the top 1 cm was collected, although for sediment grain size, the top 5 cm was collected. Sediment pigment samples were frozen at -80°C, and organic matter and sediment grain size samples were frozen at -20°C.



FIGURE 7.29 Sampling with the agassiz trawl

The small benthic trawl was deployed at 4 stations and one time from the barge. It was deployed at a depth of 15 m at station 17 but did not seem to reach the bottom according to the species found. At station 22, the trawl stayed stuck and got ripped: we were not able to sample. It was fixed for the next station. It was deployed in the Nelson River but we were not able to sample due to the weather. In total, 3 samples were taken at station 17, 19, and 34.

At each sampling station, a conductivity-temperature-depth probe (CTD) recorded bottom temperature (°C), bottom dissolved oxygen (μM), and bottom salinity (PSU). Surface particulate organic carbon content (POC; mg m^{-3}) and mean annual surface primary production (PP; $\text{mg C m}^{-2} \text{y}^{-1}$) were extracted from interpolated environmental data layers generated at the global scale as well as in the Eastern Canadian Arctic and Sub-Arctic regions [Basher et al., 2018; Beazley et al., 2019]. The substratum type was classified into three separate classes based on substratum data presented by Henderson [1989] and Pelletier [1986]. The three classes of the substrate are: “coarse” refers to stations mostly composed of gravel, sandy gravel, and cobbles; “mixed” refers to stations composed of a mix between silt and gravel; and “mud” refers to stations characterized by fine-grained sediment.

To define distinct communities from the co-distributions of individual species, Bray–Curtis dissimilarity measures were used to build a community dissimilarity matrix. This matrix was subjected to a hierarchical cluster analysis using Ward's minimum variance agglomeration method to detect compact, spherical clusters [Ward, 1963]. Several well-defined clusters corresponding to the dissimilarity between communities of less than 20% were selected. The relationship between epibenthic community composition and the environmental variables was evaluated using canonical correspondence analysis (CCA) [ter Braak and Verdonschot, 1995].

7.9 *Freshwater Influence on Microbial Communities of the Hudson Bay System*

Principal Investigators: Connie Lovejoy¹; Cruise Participant: Loïc Jacquemot¹

¹Departement de Biologie and Institut de Biologie Integrative et des Systemes, Universite Laval, Quebec, Canada

Introduction and Objectives

Freshwater is a major component of the Hudson Bay System and influences physical, biogeochemical, and biological processes within the bay. As part of the BaySys Team 3, my project aims to understand the influence of freshwater marine coupling on the microbial communities (protists, bacteria, and archaea). My objectives are to identify key environmental factors (salinity, nutrients, temperature, pH) influencing the diversity, distribution, and interactions within microbial assemblages at different scales, from the entire Hudson Bay System to local coastal regions of the bay. We will particularly focus on the salinity gradient observed on the surface at the ice edge and between the river and coastal ocean in estuarine systems. In estuaries, combining effects of upstream and downstream processes are known to structure microbial plankton communities and to induce a clear taxonomic transition from river to ocean (Harvey et al., 1997), as they regulate the balance between advection of organisms from adjacent ecosystems (here river and coastal ocean) and selection by local-environmental conditions, predation or competition (Crump et al., 2004; Niño-García et al., 2016; Ruiz-González et al., 2015). Recent molecular techniques such as 16S/18S amplicons sequencing and shotgun metagenomic will allow us to gain further into the structure of plankton communities and the potential genetic adaptations to salinity gradients. We

hypothesize that microbial communities' distribution in the Hudson Bay will be driven by freshwater circulation in the surface. Some species will present genetic adaptations to these freshwater gradients.

Operations Conducted and Methodology

156 water samples were collected during the mission onboard the CCGS Amundsen (Figure 7.30). We collected oceanic vertical profiles at 4 depths (surface, SCM, 70m, and bottom) with the rosette and surface river water using the zodiac and the helicopter. We also use the zodiac to collect water at the ice edge or under the ice using a pump. Water for environmental DNA was collected into clean acid rinsed carboys of 10L. We immediately filtered 6 litres of water through a 50 µm nylon mesh, a 47-mm diameter 3-µm polycarbonate filter, and finally through a 0.2 µm Sterivex unit (Millipore Canada Ltd, Mississauga, ON, Canada). 3-µm filters were folded and placed in 15 ml tubes with RNA-later buffer. RNA-later buffer was added to the Sterivex units and the samples were stored at -80°C until nucleic acid extraction as in Potvin and Lovejoy (2009). Additional water was used to fix cells for flow cytometry, DAPI visualization on an inverted microscope, and fish analysis. All samples were stored at -80°C.

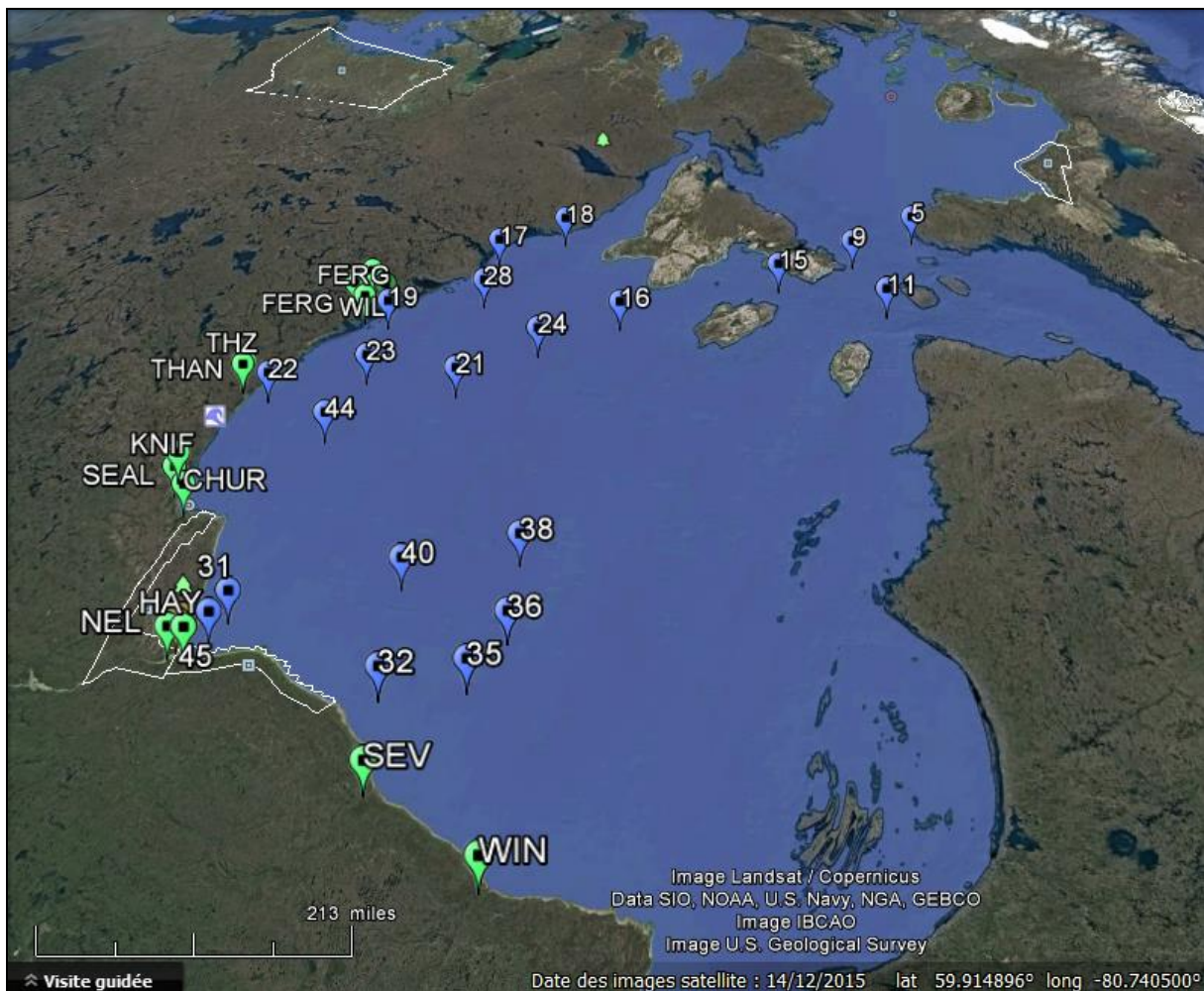


FIGURE 7.30 Locations of samples obtained during the BaySys mission (Leg 1). Blue waypoints were collected with the rosette and green waypoints were collected from rivers via helicopter.

The biodiversity and distribution of pelagic microbes were assessed with molecular techniques following the approach of Comeau et al. [2011]. All laboratory work was carried out at Université Laval, DNA and RNA were extracted from filters using commercial kits (e.g., Qiagen All-Prep) and RNA was immediately converted to cDNA. The DNA and cDNA samples were prepared for high-throughput amplicon sequencing using the Illumina MySEQ platform at the IBIS/Université Laval Plateforme d'Analyses Génomiques. The resulting reads were analyzed using a combination of BBMerge (v37.36, Bushnell et al., 2017), USEARCH [Edgar, 2010], and mothur (v1.39) [Schloss et al., 2009; Comeau et al., 2011; Mohit et al., 2014]. Taxa were classified based on NCBI taxonomy and specialized reference databases (Silva, PR2 database) and verified when needed by BLAST searches on NCBI. All raw reads are publicly available on the NCBI Sequence Read Archive (SRA). The Bacteria, Archaea, and Eukarya from different river systems and offshore waters were compared. Our high throughput sequencing provided the sensitivity needed to identify populations of microbes and infer generalist and specialist taxa from different freshwater signals. Sorting flow cytometry and metagenomics were employed to reconstruct metagenome assembled genome (MAGs) of targeted indicator species. These MAGs were employed to recruit reads from public metagenomes to infer the distribution of these microbes in temperate versus Arctic seas (Vannier et al., 2016).

7.10 Carbon Exchange Dynamics, Air-Surface Fluxes and Surface Climate

Principal Investigator: Tim Papakyriakou¹; Cruise Participants: Tim Papakyriakou¹ (Leg 1a); Dave Capelle¹; Mohamed Ahmed²; Rachel Mandryk¹ Yekaterina (Kate) Yezhova¹

¹Centre for Earth Observation Science, University of Manitoba, R3T 2N2Winnipeg, Manitoba, Canada

²Geography Department, University of Calgary, T2N 1N4 Calgary, Alberta, Canada

Introduction and Objectives

The biogeochemical cycling of carbon is continually changing within the Arctic Ocean as a consequence of climate change. In particular, Arctic Seas appear to be fresher, and freshwater in the system strongly impacts seawater carbonate chemistry, including air-sea exchange and rates and patterns of acidification. Of all the Arctic Seas, Hudson Bay receives disproportionately large amounts of river input, and many of the largest rivers are regulated for hydroelectric production. The impact of river water on the carbon system depends on water properties, which are closely tied to watershed characteristics and season. Our cruise objectives were to measure principal components of the carbon system across Hudson Bay, including those variables deemed most influential at moderating the transformation, transport, and distribution of carbon. Central to the cruise objectives were to include freshwater from the Bay's major rivers. Measurements were made within the water column, at the air-sea (or air-ice) interface, and in the atmosphere.

Operations Conducted and Methodology

Multiple observation platforms have been utilized throughout the cruise to collect data pertaining to the atmosphere and the surface ocean, such as a meteorological tower on the ship's foredeck, an underway pCO₂ system in the engine room, an underway FDOM system in the engine room, an underway optode / GTD (PIGI) system in the forward lab, and radiation sensors above the wheelhouse of the ship (Figure 7.31), the ship's rosette, and distributed sampling by helicopter, small boat and on sea ice.

Automated Systems

Table 7.9 lists the variables that are monitored, the location where the sensor is installed, and height, along with the sampling and averaging frequency (if applicable).

TABLE 7.10 Summary of variable inventory and instrumentation. Deck height above sea surface was measured on 27-May at 6.4 m

Variable	Instrumentation	Location	Ht above Main Deck (m)	Ht above sea srfc	Sample/Ave Frequency (s)
Air temperature (Ta)	HMP155A	foredeck tower	8.74	15.14	1 / 60
relative humidity (RH)	HMP155A	foredeck tower	8.74	15.14	1 / 60
wind speed (ws-2D)	RM Young 05106-10	foredeck tower	10.45	16.85	1 / 60
barometric pressure (P _{atm})	RM Young 61302V	foredeck tower			
incident solar radiation	Eppley Pyranometer (model PSP)	wheel-house platform	On top of the wheelhouse		2 / 60
incident long-wave radiation	Eppley Pyrgeometer (model PIR)	wheel-house platform	On top of the wheelhouse		2 / 60
photosynthetically active radiation (PAR)	Kipp & Zonen PARLite	wheel-house platform	On top of the wheelhouse		2 / 60
UVA&B	Kipp & Zonen UVS-AB-T	wheel-house platform	On top of the wheelhouse		2 / 60
wind speed 3D (u, v, w)	CSAT3 Sonic	foredeck tower	9.29	15.69	0.1 (10 Hz)/60
wind speed 3D (u, v, w, Ts)	Gill Wind Master Pro	foredeck tower	7.68	14.08	0.1 (10 Hz)/60
Atm CO ₂ and H ₂ O	LICOR LI7500A	foredeck tower	9.06	15.46	0.1 (10 Hz)/60
Atm CO ₂ and H ₂ O	LICOR LI7200	foredeck tower	9.06	15.46	0.1 (10 Hz)/60
Atm CO ₂ , CH ₄ , and H ₂ O	LGR	foredeck tower	9.06	15.46	0.1 (10 Hz)/60
rotational motion (acc _x , acc _y , acc _z , r _x , r _y , r _z)	Systron Donner MotionPak	foredeck tower	9.15	15.55	0.1 (10 Hz)/60

Variable	Instrumentation	Location	Ht above Main Deck (m)	Ht above sea srfc	Sample/Ave Frequency (s)
Underway seawater pCO ₂ , O ₂ , temperature (T _{sw}), and salinity	General Oceanics 8050 pCO ₂	underway system, forward engine room	~-5 m		3 / 60
Weather conditions	Campbell digital camera (CC5MPX)	wheelhouse platform	meteorological parameter		2 min

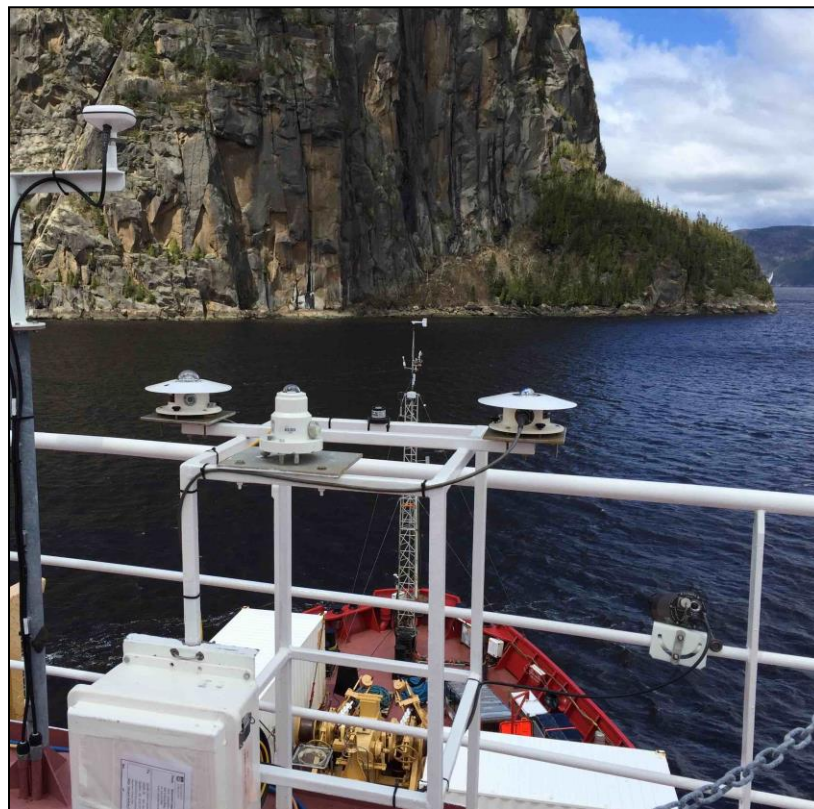


FIGURE 7.31 The radiation sensors and a digital camera located above the wheelhouse of the Amundsen. Shown are the pyrgometer (right), pyranometer (left), and PAR sensor (centre back), and UV sensor (centre front). The automated digital camera is mounted on the rail below and to the right of the pyrgometer.

The micrometeorological tower located on the front deck of the Amundsen provides continuous monitoring of meteorological variables and eddy covariance parameters (Figure 7.32). The tower consists of slow response sensors that record bulk meteorological conditions (air temperature, humidity, wind speed/direction) and fast response sensors that record the eddy covariance parameters (CO₂/H₂O/CH₄

concentration, 3D wind velocity, 3D ship motion, air temperature). All data was logged to Campbell Scientific dataloggers; a model CR3000 logger was used for the eddy covariance data, a CR1000 logger for the slow response met data. Eddy covariance data were sampled at 10 Hz while slow response sensors were scanned every 2 s and saved as 1-minute averages. All loggers were synchronized to UTC using the ship's GPS as a reference. The set-up includes two closed path eddy-covariance systems: i) LI-7200 based system (CO₂ and H₂O) and ii) LGR (model) based system (CO₂, H₂O, and CH₄). In both systems air was drawn through ½" Synflex® tubing at 10 L/m and ~ 25 L/m, respectively for the LI7200 and LGR systems. Some connections in both systems were ¼". Pressure in the LI7200 was kept within 8%-9% of barometric pressure using a by-pass system that allowed higher flow rates upstream of the gas analyzer, thus allowing for turbulent flow. The LI7200 closed-path system was situated at the base of starboard rail inside a weatherproof enclosure, approximately 3 m from the tower base and approximately 13 m from the intake. Air was partially dried upstream of the gas analyzer using a nafian drier (Perma Pure PD-100T-48SS) and zero gas generator (Aadco model 747-30). Counter flow through the nafian drier was maintained between 13 and 14 l pm. Periodically, zero and span gas were introduced to the LI7200.



FIGURE 7.32 The metrological tower located on the foredeck of the Amundsen with EC flux system (inset)

A digital camera (Campbell CC5MPX) was mounted on the forward rail above the bridge and pointed forward to record the ice cover and sea-state in front of the ship at 2-minute intervals. The camera has a resolution of 5 megapixels and is housed in an enclosure to protect it from the elements. An internal

heater keeps the temperature of the enclosure above 15degC, which helps prevent ice and moisture buildup on the lens. The camera was connected by a 100' long inverted Ethernet cable to the ship's network via a switch in the Met-Ocean container beside the wheelhouse, allowing pictures to be automatically backed up to a data server in the acquisition room.

A General Oceanics 8050 pCO₂ system has been installed on the ship to measure dissolved CO₂ within the upper 5-7 m of the sea surface in near-real-time (Figure 7.33). The system is located in the engine room of the CCGS Amundsen and draws sample water from the ship's clean water intake. The water is passed into a sealed container through a showerhead, maintaining a constant headspace. This set up allows the air in the headspace to come into equilibrium with the CO₂ concentration of the seawater, and the air is then cycled from the container into an LI-7000 gas analyzer in a closed loop. The system also passes a subsample of the water stream through an Idronaut Ocean Seven CTD, which measured this cruise temperature, conductivity, pressure, and dissolved oxygen. All data was sent directly to a computer using software customized to the instrument. Zero and span were set on the LI-7000 every 8 h using ultra-high purity N₂ as a zero gas, and a gas with known CO₂ concentration as a span gas (474.98 ppm). Additionally, air at two different CO₂ concentrations (315.58 ppm, and 585.20 ppm) was run through the system and are traceable to the World Meteorological Organization (WMO) standards. Discrete water samples were collected from the water inlet line periodically (~weekly) to calibrate pCO₂, salinity, and Oxygen.



FIGURE 7.33 The underway system located in the engine room of the Amundsen

An underway FDOM sensor has been installed on the ship to measure fluorescence within the upper 7m in response of dissolved organic matter in the water (Figure 7.34). This system located in the engine room on the same intake line that the ship's thermal-salinograph system (TSG) system is using for data

matching later. The FDOM sensor recording the measurements every 30 sec with FDOM water samples were collecting every 12h for calibrations. The TSG system recording continuous measurements every second for the seawater temperature, salinity, fluorescence, and sound velocity.

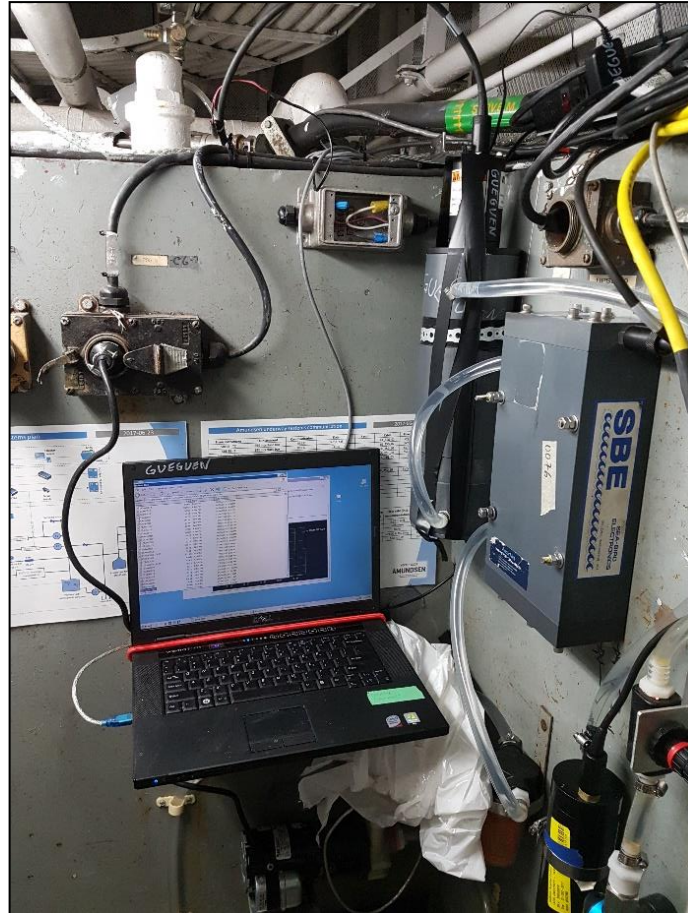


FIGURE 7.34 The FDOM underway system located in the engine room beside the ship TSG system

The PIGI (Pressure of In-situ Gases Instrument) has been installed in the forward lab and consists of a 2-stage chamber setup (Figure 7.35). The first chamber (primary chamber) consists of a debubbler that allows bubbles to exist from the top and bubble-free water to exist via the bottom. The bubble-free water goes to the second chamber, via a downstream pump, that contains two instruments: an Optode and Gas Tension Device (GTD). The optode measures O₂ concentration, and the GTD measures total dissolved gas pressure (which can be used to drive N₂ concentrations).



FIGURE 7.35 The underway optode / GTD (PIGI) system installed in the forward lab

Discrete Water Sampling

i) Ship Rosette

Additionally, water samples were collected from the rosette for the analysis of dissolved inorganic carbon (DIC), total alkalinity (TA), stable oxygen and carbon isotopes ($\delta^{18}\text{O}$, $\text{C}^{13}\text{-DIC}$; $\text{C}^{13}\text{-CH}_4$), Ba^+ and other ions, methane (CH_4), dissolved organic carbon (DOC), total dissolved nitrogen (TDN), and salinity. These measurements will allow us to study the carbon chemistry of various water mixtures across the cruise track. The salinity samples were analyzed onboard in the salinometer room by using the AUTOSAL machine to compare it with the salinity log obtained from the CTD rosette and ensure accurate salinity measurements are available for deriving solubility constants for our discrete samples. Other analyses will occur at various labs after the cruise.

ii) Surface Water Sampling (ship bow, zodiac, skippy boat)

Additional discrete surface samples were collected using a submersible pump and/or horizontal Niskin bottle to measure unmixed surface water which is not possible with the ship's rosette. Ideally, samples were collected from the zodiac or skippy boat more than 100m from the ship, but less than 500m. When this wasn't possible, samples were collected from the foredeck immediately upon arrival at the station, to maximize the chance of collecting undisturbed water. Three depths were sampled, 0m, 1m, and 7m, and a CTD (Idronaut or Cast-Away) was performed immediately after water sampling.

iii) Helicopter Sampling

The helicopter was used to sample from ice floes, rivers, and landfast ice. At each site, ice-water interface water samples were collected, and occasionally a second, deeper sample (7 m), using a submersible pump (Waterra Cyclone pump) powered by a 12V battery. Water was pumped through 3/8" ID vinyl tubing into 250 mL BOD glass bottles with sintered glass stoppers, and 4 L glass jars with narrow mouth plastic screw caps. Samples were stored in the dark and processed/preserved upon return to the ship within 4 hours of sampling, for DIC, TA, 18O, Ba, CH₄, 13C-DIC, 13C-CH₄, salinity, DOC, TDN. Subsampling from the 4L glass bottle was done using a 50 mL glass syringe with a 15 cm long 1/8" ID vinyl tube attached to the end. The syringe was rinsed 3x with sample water and filled without bubbles before rinsing and filling sample bottles, also without bubbles.

CTDs were always performed when water samples were collected by helicopter, up to 50 m depth using an Idronaut.

iv) Ice and Under-ice Water

Ice cores were collected at select ice stations accessed either by the ship's cage or helicopter. Up to 5 x 10cm sections were vacuum-sealed from each core and melted at room temperature before subsampling for 18O, Ba, Salinity, DIC, and TA. In many cases, only the upper 1m of ice was sampled due to the very thick ice cover and time constraints. Where possible, under ice water was collected by a submersible pump and subsampled in the same way as under-ice water collected by helicopter (see above).

Preliminary Results

The data at this time are very preliminary and require additional processing before making reliable inferences, but it appears that the bay is overall under-saturated in pCO₂, suggesting the bay is net autotrophic and a net sink for atmospheric CO₂ during the spring. Unfortunately, no preliminary results from discrete water samples are available at this time.

7.11 Contaminants

Team Leads: Fei Wang¹, Allison Zacharias², Sarah Wakelin²; Team Members: Zou Zou Kuzyk¹, David Lobb¹, Philip Owen³, Ellen Petticrew³, Robie Macdonald¹, Gary Stern¹; Cruise Participants: Kathleen Munson¹, James Singer¹, Zhiyuan (Jeff) Gao¹, Samantha Huyghe¹, Ainsleigh Loria¹; Punarbasu Chaudhuri⁴

¹Center for Earth Observation Science, Department of Environment and Geography, University of Manitoba, Winnipeg, MB, R3T 2N2, Canada; ²Manitoba Hydro, Winnipeg MB. ³University of Northern British Columbia, ⁴University of Calcutta, Kolkata.

Part I: Water and Ice

Principal Investigator: Feiyue Wang¹; Cruise Participants: Kathleen Munson¹, James Singer¹, Zhiyuan Gao¹

¹Center for Earth Observation Science, Department of Environment and Geography, University of Manitoba, Winnipeg, MB, R3T 2N2, Canada

Introduction and Objectives

Mercury is a containment of global concern. Away from industrialized areas, mercury is observed to accumulate through food webs in the Arctic marine ecosystem, which provokes concern from northern communities whose daily diet is heavily dependent on Arctic marine biota. The speciation of mercury determines its toxicity, the methylated species are known as a neurotoxin and can cause adverse effects on living organisms. On the other hand, dissolved organic matter (DOM) in the water column plays an important role in regulating mercury redox chemistry and mediating methylation/demethylation capability (Luo et al. 2017; Soerensen et al. 2017). However, the mechanism behind the seawater is not well understood due to the lack of structural and molecular information of marine DOM.

The Canadian Arctic is experiencing a period with extensive influence caused by climate change, which may greatly affect the fate of mercury (Stern et al. 2012). These changes include increased freshwater inputs and changing sea ice conditions.

The objective of this cruise is to build a mercury (total mercury and methylmercury) budget in Hudson Bay by seawater samples collected from the rosette, ice sampling, zodiac, barge, and helicopter sampling for rivers and sediment core sampling. Selected water and ice samples will be analyzed for DOM characterization, which may assist in interpreting the fate of mercury in the Arctic. Incubation experiments were conducted using seawater samples from subsurface chlorophyll maximum, oxygen minimum, and bottom, as well as in sediment cores to determine the net methylation capability in different Hudson Bay reservoirs to determine their impact on the mass budget of mercury.

Operations Conducted and Methodology

To assess the ability to collect contamination-free water samples during Leg 1, we cleaned the Amundsen rosette Niskin bottles in the rosette shack by soaking 0.1% citronax overnight in the bottle. We then rinsed then bottles several times. Random Niskin bottles were tested for contamination by adding reagent grade water (Milli Q) to the bottles and collecting blank tests after allowing the MQ to sit in the bottle for an hour. Total mercury (THg) was analyzed from each bottle in the Portable In-Situ Laboratory for Mercury Speciation (PILMS). Every bottle tested was found to be clean (below detection limit defined as three times the standard deviation of reagent blank values) for THg analysis.

During the rosette sampling, the door to the rosette shack was closed all the time, both unfiltered and filtered seawater samples were collected from targeted depths, including 10 m, 20 m, 30 m, subsurface chlorophyll maximum, 50 m, 60 m, 80 m, 100 m, 140 m, 160 m, 200 m, and bottom. Filtered samples were collected by directly attaching a capsule filter (0.45 μm , Acropak) to the Niskin spigot. Samples were collected in both 250mL amber glass bottles and 50 mL Falcon tubes. Amber glass bottles were preserved with 0.5% HCl and will be transported back to the University of Manitoba for methylmercury and total mercury analysis. Samples collected in Falcon tubes were brominated (0.5 % BrCl) for 8 hours and analyzed onboard in PILMS for total mercury analysis on a Tekran 2600 using manufacturer-based adaptations of standard protocols (EPA 1631). A full list of stations collected for mercury analysis is noted in Table 7.11.

TABLE 7.11 Amundsen 2018 Leg 1 rosette water sample collection (HgT: total mercury; MeHg: methylmercury)

Time	Station ID	Latitude	Longitude	Cast type	Depth (m)	deep bottle (m)	Samples collected
18:00:01 31/05/2018	N01 (356)	60.813 26	- 64.53336	Nutrients	328.75	378	HgT, MeHg
21:56:38 31/05/2018	N02 (354)	60.973 50	- 64.77335	Nutrients	571.13	555	HgT, MeHg
00:55:43 01/06/2018	N03 (352)	61.150 20	- 64.80869	Nutrients	430.12	408	HgT, MeHg
21:32:25 02/06/2018	05 (FB01)	64.286 52	- 78.23075	Nutrients	233.03	228	HgT, MeHg
03:27:11 03/06/2018	07 (FB02)	64.065 26	- 79.06239	Nutrients	270	259	HgT, MeHg
20:22:26 03/06/2018	09 (FB03)	63.720 14	- 79.92091	Chem	94.15	91	HgT, MeHg
18:57:02 04/06/2018	11	62.876 49	- 78.86373	Chem	315.56	300	HgT, MeHg
07:47:48 05/06/2018	12	63.395 75	- 81.22443	Nutrients	85.78	74	HgT, MeHg
17:40:55 05/06/2018	15	63.175 18	- 81.84978	Chem	189.97	179	HgT, MeHg
21:28:57 06/06/2018	16	62.288 97	- 85.85817	Chem	134.24	122	HgT, MeHg, DOM characterization
21:52:02 07/06/2018	17	63.184 64	- 90.03573	Bio- Chem	88.43	80	HgT, MeHg
08:34:38 08/06/2018	18	63.713 67	- 88.41683	Chem	115.61	104	HgT, MeHg
15:26:46 09/06/2018	19	61.846 52	- 92.13222	Chem	78.33	69	HgT, MeHg
17:40:14 10/06/2018	21	60.910 36	- 89.32936	Chem	149.3	135	HgT, MeHg
14:35:02 11/06/2018	22	60.420 76	1000.650 00	Chem	63.56	53	HgT, MeHg
22:43:44 12/06/2018	24	61.710 82	- 87.78786	Chem	188.81	177	HgT, MeHg, DOM characterization
01:19:37 15/06/2018	28	62.415 52	- 89.83392	Nuts- Chem	163.63	150	HgT, MeHg
13:05:13 16/06/2018	29	61.769 78	- 84.30910	Chem	176.99	164	HgT, MeHg
18:19:26 18/06/2018	31	57.500 09	- 91.79532	Nutrients	47.4	37	HgT, MeHg
19:26:14 19/06/2018	32	56.982 03	- 88.14683	Chem	35.03	24	HgT, MeHg, DOM characterization
01:09:36 21/06/2018	34	56.499 83	- 86.86875	Chem	43.78	33	HgT, MeHg, DOM characterization
02:42:34 22/06/2018	35	57.179 78	- 86.49995	Nutrients	61.46	51	HgT, MeHg, DOM characterization

15:19:45 22/06/2018	36	57.774 13	- 86.03131	Chem	128.34	116	HgT, MeHg, DOM characterization
03:07:08 23/06/2018	37	58.468 92	- 86.22553	Nutrients	169.68	157	HgT, MeHg, DOM characterization
19:17:04 23/06/2018	38	58.730 43	- 86.30196	Chem	180.99	168	HgT, MeHg, DOM characterization
18:47:11 24/06/2018	40	58.239 79	- 88.58159	Chem	87.07	75	HgT, MeHg, Methylation incubation
	43 (15 rep)			Chem	189.97	100	HgT, MeHg
	44			Chem		91	HgT, MeHg, DOM characterization
	45			Bio- Chem	18	10	HgT, MeHg, Methylation incubation

To determine the magnitude of the sea ice mercury reservoir in Hudson Bay, ice cores were collected at selected ice stations and sectioned in situ on the ice floes. Cores were collected using a core barrel (9 cm ID, Kovac Mark II). In order to keep samples free of contamination, ice sections were trimmed using a ceramic knife to remove the outer ice layer that came into contact with the core barrel. Trimmed sections were transported in double Ziploc bags and melted at room temperature in PILMS. Unfiltered ice melts were poured off for methylmercury and total mercury analysis and filtration (0.45 µm Pall filter, Nalgene filter cups) under low pressure (~10 psi) using a vacuum pump in PILMS. Both filtered and unfiltered ice melts were preserved according to the same method as seawater samples. Ice interface waters and melt pond waters were collected in some stations. The details of the ice samples are noted in Table 7.12.

TABLE 7.12 Stations sampled for ice

Time	Station ID	Latitude	Longitude	Sampled by
	5			Helicopter
	9_H3			helicopter
18:44:48 06/06/2018	16	62.27823	-85.89189	Ice cage
20:10:02 08/06/2018	18	63.72603	-88.32335	Ice cage
14:36:36 13/06/2018	25	61.99977	-86.97196	Ice cage
18:27:09 23/06/2018	38	58.72937	-86.30572	Ice cage

Additional samples were collected from surface waters during helicopter and zodiac deployments to ice and open water stations. Because the upper water is both subject to mixing and mercury contamination

from the ship, surface (< 10 m) samples cannot be collected from the rosette. Instead, surface water, including interface water under ice floes, was collected using a battery-powered submersible cyclone pump (Proactiv, 12V). The pump and tubing were tested for total mercury contamination prior to sample collection and compared to values obtained using a Go-Flo bottle. For each station, blanks were collected on-site to test the sampling environment.

TABLE 7.13 River estuary sampling by Barge and Zodiac

Date	Time (UTC)	Name	Latitude	Longitude
2018-06-7?	After visit hydr	River 1 ice edge (chesterfield inlet) St17	63.3738	-90.630833
2018-06-7	After visit hydr	River 1 intermediate St17	63.285	-90.353333
2018-06-7	After visit hydr	River 1 rosette St17	61.191666	-90.541666
2018-06-8	19:29	St18 skippy	63.7313862	-88.3224324
2018-06-10	19:39	St19	61.9570016	-92.2719114
2018-06-11	17:17	St22 estuary	60.479666	-94.563833
2018-06-11	18:15	St22 intermediate	60.475833	-94.527683
2018-06-11	18:53	St22 rosette	60.446666	-94.005
2018-06-19	17:10	St32 Rosette open water near dirty ice	56.9866728	-88.1352983
2018-06-19	16:40	St 32 Under dirty ice	56.9839734	-88.120189
2018-06-20	18:20	St34 5m from ice	56.506166	-90.883166
2018-06-20	19:12	St34 open water area	56.496266	-86.878433
2018-06-29	Afternoon	Nelson southern transect st1	57.1842333	-91.81105
2018-06-29	Afternoon	Nelson southern transect st2	57.2081	-91.8711
2018-06-29	14:20	Nelson 1(barge)	57.0533682	-92.5321723
2018-06-29	18:50	Nelson 2 (barge)	Greg, gps not on cw	
2018-06-30	14:21	Nelson water 3	57.2059296	-92.2824796
2018-06-30	19:48	Nelson water 4	57.22215	-92.29395

To determine the magnitude of the riverine mercury and methylmercury inputs into Hudson Bay, surface water samples were collected from rivers reached by helicopter at stations targeting freshwater (salinity = 0). River water was collected using a submersible pump (Proactiv, 12 V) attached to an extendable painter pole the end of which was kept afloat with an empty 4 L plastic acid bottle to keep the pump near the water surface. Filtered and unfiltered water samples were collected from the pump.

TABLE 7.14 River sampling by helicopter

Date	Time (UTC)	Name	Latitude	Longitude
2018-06-10	14:08	Thlewiaza River	60.4851	-94.8167
2018-06-10	13:15	Tha-anne River	60.5461	-94.8292
2018-06-18	18:55	Nelson River	56.9659	-92.6305
2018-06-18	20:50	Hayes River	56.9955	-92.2924
2018-06-19	18:42	Severn River	55.9603	-87.7081
2018-06-20	17:15	Winisk River	55.2275	-85.2114
2018-06-28	19:08	Seal River	59.0739	-94.8425
2018-06-28	20:06	Knife River	58.8831	-94.7031
2018-06-28	20:42	Churchill River	58.6781	-94.2033

In selected stations, water and ice samples were collected for DOM characterization. For the rosette sampling, targeted depth included 10 m, subsurface chlorophyll maximum, and bottom. Ice cores were sectioned into a size of 10 to 15 cm from the top, middle, and bottom parts. Only filtered water samples were used for DOM, it can be either a capsule filter directly from the Niskin bottle or filtration using a vacuum pump. For both seawater samples and ice melts collected for DOM, 200 mL was stored in an amber glass bottle in the chest freezer, and up to 500 mL was loaded through a solid phase extraction (SPE) setup using Bond Elut PPL cartridges from Agilent. The volume of ice melts loaded on the cartridges varied depending on the size of the ice section. The loaded cartridges were stored in Ziploc bags separately and in the freezer until further treatment.

References

Luo HW, Yin X, Jubb AM, et al (2017) Photochemical reactions between mercury (Hg) and dissolved organic matter decrease Hg bioavailability and methylation. *Environ Pollut* 220:1359–1365 . DOI: 10.1016/j.envpol.2016.10.099

Soerensen AL, Schartup AT, Skrobonja A, Björn E (2017) Organic matter drives high interannual variability in methylmercury concentrations in a subarctic coastal sea. *Environ Pollut* 229:531–538 . DOI: 10.1016/j.envpol.2017.06.008

Stern GA, Macdonald RW, Outridge PM, et al (2012) How does climate change influence arctic mercury? *Sci Total Environ* 414:22–42 . DOI: 10.1016/j.scitotenv.2011.10.039

Part II: Sediment

Principal Investigators: Zou Zou Kuzyk¹, David Lobb¹; Cruise Participants: Samantha Huyghe¹, Punarbasu Chaudhuri¹

Introduction and Objectives

The objectives of the sediment collection were, 1) To revise and update the estimate of the total sediment sink for Hudson Bay in consideration of both oceanographic and geologic domains using a combination of geophysical and geochemical data, and 2) To investigate the processes contributing to sedimentation patterns and rates using approximately monthly sediment trap samples spanning a year to document seasonal distribution of fluxes. The samples collected on this cruise will go towards objective 1 and filling the gaps in the data from archived and previously published data. The cores are also being supplemented by subbottom data, collected on Leg 1, to compare the geophysical data from each coring location with the geochemical data that will be obtained from the cores.

Operations Conducted and Methodology:

Sediment Sampling

A box corer was used to collect sediment cores at basic and full stations where there were not too many rocks (the Agassiz trawl was used to assess the presence of large rocks that could damage the box corer). The box corer was deployed using the a-frame and winch on the port side of the ship. If the bottom of the box corer was sealed and the sediment inside was not slumped, a core tube was then pressed into the sediment. The sediment core was then taken to the lab onboard the ship, measured, and sectioned into whirlpacks in intervals of 1 cm until 10 cm, 2 cm until 20 cm, and 5 cm after 20 cm. There were a couple of exceptions to these intervals in the cases of cores (Stations 17, 18, and 19) where there were still visible colour or textural changes past 20 cm. In these cases, the cores were sectioned 1 cm until 10 cm and 2 cm after 20 cm for higher resolution during analysis. The whirlpacks were then placed into a refrigerator and sent to the University of Manitoba for radioisotope, contaminants, and organic matter analyses.

TABLE 7.15 Locations and dates of the cores taken on Leg 1 of the 2018 Amundsen cruise

Station Number	Date	UTC	Latitude	Longitude	Depth (m)
10	04-Jun-18	5:32:39	63.45071	-79.4452	202.73
17	08-Jun-18	0:08:20	63.18458	-90.0337	91.62
18	08-Jun-18	6:10:20	63.71968	-88.4021	122.15
19	09-Jun-18	17:21:36	61.84316	-92.1328	86.18
21	10-Jun-18	21:08:18	60.91407	-89.3385	148.93
24	13-Jun-18	0:04:24	61.70548	-87.7845	N/A
28	15-Jun-18	4:10:07	62.41676	-89.8175	161.79
29	16-Jun-18	9:58:48	61.74867	-84.2958	177.46
32	19-Jun-18	21:01:05	56.97127	-88.1301	33.6
36	22-Jun-18	20:16:31	57.77581	-86.0279	127.07
38	23-Jun-18	23:21:16	58.72343	-86.2957	179.9
40	24-Jun-18	19:52:17	58.24775	-88.5965	90.08

Water Filtration

At stations near and in the Nelson River estuary, a water filtration system was run to collect suspended sediment. The filtration system was run using a pump on the ship allowing the system to draw seawater from the ship's plumbing for the duration of the station. At the end of the station, the filters were removed, refrigerated, and then sent back to the University of Manitoba for further analysis.

TABLE 7.16 The location and duration of each filtration for suspended sediment

Station Number	Date	Latitude	Longitude	Duration of Filtering
40	24-Jun-18	58.24337	-88.589	8 hrs, 50 min
45	29-Jun-18	57.25124	-91.9629	7 hrs, 55 min
45	30-Jun-18	57.22999	-91.9536	11 hrs, 5 min
46	01-Jul-18	57.39829	-92.0727	7 hrs, 40 min

Part III: Mercury and Organic Contaminants Sampling and Deployments

Principal Investigator: Gary A. Stern¹; Liisa Jantunen²; Cruise Participants: Ainsleigh Loria¹

¹Centre for Earth Observation Science, Department of Environment and Geography, Clayton H. Riddell Faculty of Environment, Earth and Resources, University of Manitoba, Winnipeg, MB

²Environment and Climate Change Canada, Burlington, ON,

Introduction and Objectives

As the average global temperature increases, the sea ice cover in the Arctic is declining. With a reduced ice cover throughout the year, the amount of cargo traffic and oil exploration and exploitation throughout the Arctic is expected to increase, putting this pristine environment at a higher risk of cargo-related pollution.

As a part of Arctic Net and BaySys, our group aims to collect baseline contaminant data in a variety of media in the Arctic. More specifically, we collect biological samples (zooplankton and invertebrates) to determine mercury concentrations within the food web. This year, I also collected water samples and surface sediment (sediment collected by Diana Saltymakova and Teresinha Wolfe) for organic contaminants for Liisa Jantunen. Moreover, the deployment of organic contaminant passive samplers on moorings along the primary shipping route to Churchill will help us generate an idea of the existing organic contaminant concentrations within the Bay.

Operations Conducted and Methodology

Onboard the CCGS Amundsen, we collected zooplankton alongside the Fortier group with the Tucker (1 m² 750 µm mesh) and the Monster (1 m² 200 µm mesh) nets. Benthic invertebrate samples were also collected using the Beam Trawl and the Agassiz trawl. The samples from the Agassiz trawl were collected and identified by Marie Pierrejean. Water samples for organic contaminants were collected from the rosette. 4 liters of surface water was collected for OPEs on the west/mid-Hudson Bay, while 1-liter water samples were collected at the surface, above the thermocline, and below the thermocline at passive sampler mooring sites for PFC analysis.

Organic contaminant passive samplers were deployed on moorings at 3 sites along the primary shipping route in Hudson Bay.

The following tables summarize the samples collected and the deployments that occurred related to contaminants during Leg 1 of the 2018 Amundsen cruise.

TABLE 7.17 Zooplankton samples collected during the BaySys 2018 cruise.

Station	Tow	Bottom Depth (m)	Sampler Depth (m)	Species
04	Vertical	287	276	Calanus sp., Chaetognata, Clione limacina (2 cm), Hydromedusae, Bulk
05	Vertical	220	212	Calanus hyperboreus CV adult female, Ctenophora, Hydromedusae, Chaetognata, Bulk
09	Vertical	104	94	Chaetognata, Ctenophora, Bulk
09	Oblique	106	80	Chaetognata, Clione limacina (3.0-3.5 cm), Ctenophora, Bulk
10	Oblique	196	92	Calanus hyperboreus CV adult female, Clione limacina (5 cm), Ctenophora, Hydromedusae, Thysanoessa sp., Bulk
10	Vertical	199	189	Chaetognata, Themisto libellula (2.5-3.0 cm), Thysanoessa sp., Bulk
11	Vertical	320	310	Calanus hyperboreus CV adult female, Chaetognata, Ctenophora, Hydromedusae, Themisto libellula (2.5-3.0 cm, 3.5-4.0 cm), Thysanoessa sp., Bulk
15	Oblique	190	90	Ctenophora, Hyperoche medusarum, Themisto libellula (1.5-2.0 cm), Bulk
15	Vertical	191	181	Chaetognata, Ctenophora, Thysanoessa sp., Bulk
16	Oblique	135	95	Calanus hyperboreus CV adult female, Chaetognata, Ctenophora, Themisto libellula (2.0-2.5 cm), Bulk
16	Vertical	135	125	Calanus hyperboreus CV adult female, Chaetognata, Clione limacina, Bulk
17	Vertical	94	84	Chaetognata, Themisto libellula (2.0 cm), Bulk
18	Oblique	112	88	Chaetognata, Clione limacina (4.0-4.5 cm), Ctenophora, Themisto libellula (2.0-2.5 cm, 2.5-3.0 cm, 3.0-3.5 cm), Thysanoessa sp., Bulk
18	Vertical	115	105	Chaetognata, Clione limacina (4.0-4.5 cm), Ctenophora, Bulk
19	Vertical	76	66	Chaetognata, Bulk
19	Oblique	77	60	Chaetognata, Clione limacina (3.0 cm), Ctenophora, Themisto libellula (0.5-1.0 cm), Thysanoessa sp., Bulk

21	Vertical	163	133	Bulk
21	Oblique	147	92	Chaetognata, Ctenophora, Themisto libellula (0.5-1.0 cm, 2.5-3.0 cm, 3.0-3.5 cm), Bulk
22	Oblique	61	45	Clione limacina (2 cm), Ctenophora, Limacina helicina, Themisto libellula (0.0-0.5 cm, 0.5-1.0 cm, 1.0-1.5 cm, 1.5-2.0 cm), Bulk
22	Vertical	58	48	Bulk
24	Vertical	187	177	Calanus hyperboreus CV adult female, Chaetognata, Themisto libellula (2.5-3.0 cm), Thysanoessa sp., Bulk
25	Oblique	148	95	Calanus hyperboreus CV adult female, Chaetognata, Ctenophora, Clione limacina (2.0 cm, 4.0 cm), Bulk
25	Vertical	148	138	Calanus hyperboreus CV adult female, Chaetognata, Themisto libellula (2.5-3.0 cm), Thysanoessa sp., Bulk
28	Oblique	161	89	Chaetognata, Ctenophora, Themisto libellula (2.0-2.5 cm, 2.5-3.0 cm, 3.0-3.5 cm, 3.5-4.0 cm), Bulk
28	Vertical	161	89	Chaetognata, Thysanoessa sp., Bulk
29	Vertical	178	168	Calanus hyperboreus CV adult female, Chaetognata, Themisto libellula (1.5-2.0 cm, 2.0-2.5 cm, 2.5-3.0 cm), Bulk
29	Oblique	177	98	Calanus hyperboreus CV adult female, Chaetognata, Ctenophora, Themisto libellula (1.5-2.0 cm, 2.0-2.5 cm, 2.5-3.0 cm), Bulk
32	Vertical	32	22	Bulk
34	Oblique	44	34	Chaetognata, Hyperia galba, Bulk
34	Vertical	44	34	Bulk
36	Vertical	127	117	Chaetognata, Limacina helicina, Bulk
38	Oblique	178	75	Chaetognata, Ctenophora, Themisto libellula (2.5-3.0 cm, 3.5-4.0 cm), Bulk
38	Vertical	178	168	Chaetognata, Hydromedusae, Limacina helicina, Bulk
40	Vertical	86	76	Chaetognata, Bulk
43	Vertical	190	180	Chaetognata, Limacina helicina, Themisto libellula (0.5-1.0 cm, 2.0-2.5 cm, 2.5-3.0 cm), Thysanoessa sp., Bulk
43	Oblique	191	92	Chaetognata, Ctenophora, Limacina helicina, Themisto libellula (0.5-1.0 cm, 1.0-1.5 cm, 1.5-2.0 cm, 2.0-2.5 cm, 2.5-3.0 cm), Bulk
44	Oblique	106	90	Chaetognata, Hyperia galba, Limacina helicina, Themisto libellula (0.5-1.0 cm, 1.0-1.5 cm, 3.0-3.5 cm), Bulk
BN5	Reverse	14	10	Mysis sp.
45	Oblique	44	31	Bulk
45	Vertical	44	34	Bulk

Vertical tow = 1 m², 200 µm mesh net, oblique tow = 1 m², 750 µm mesh net and reverse tow = 1 m², 500 µm mesh net.

TABLE 7.18 Benthic invertebrate samples collected during the BaySys 2018 cruise

Station	Trawl	Depth	Species
04	Agassiz	274	Eualus gaimardii gaimardii, Gorgonocephalus sp.
09	Agassiz	237	Crossaster papposus, Rossia sp.
09	Beam Trawl	218	Anonyx sp., Argis dentata, Eualus gaimardii gaimardii, Henricia sp., Pandalus borealis, Rossia sp., Sclerocrangon boreas, Strongylocentrotus droebachiensis
15	Agassiz	189	Strongylocentrotus droebachiensis

15	Beam Trawl	200	<i>Sclerocrangon boreas</i>
16	Beam Trawl	135	<i>Heliometra glacialis</i> , <i>Ophiacantha bidentata</i> , <i>Sclerocrangon boreas</i>
17	Agassiz	94	<i>Gorgonocephalus arcticus</i> , <i>Pandalus borealis</i>
18	Beam Trawl	114	<i>Argis dentata</i> , <i>Eualus gaimardii gaimardii</i> , <i>Heliometra glacialis</i> , <i>Ophiacantha bidentata</i>
19	Agassiz	83	<i>Argis dentata</i> , <i>Hyas coarctatus</i> , <i>Poraniomorpha</i> sp., <i>Strongylocentrotus droebachiensis</i>
21	Agassiz	152	<i>Ctenodiscus crispatus</i>
21	Beam Trawl	152	<i>Argis dentata</i>
22	Agassiz	63	<i>Chlamys islandica</i> , <i>Hyas coarctatus</i> , <i>Strongylocentrotus droebachiensis</i>
25	Agassiz	145	<i>Ophiura</i> sp., <i>Strongylocentrotus droebachiensis</i>
28	Agassiz	162	<i>Argis dentata</i> , <i>Sabinea septemcarinata</i> , <i>Spirotocaris intermedia</i>
29	Agassiz	180	<i>Ophiura sarsii</i>
32	Agassiz	32	<i>Strongylocentrotus droebachiensis</i>
38	Agassiz	180	<i>Ophiura sarsii</i> , <i>Pontaster tenuispinus</i>
43	Beam Trawl	193	<i>Argis dentata</i> , <i>Eualus gaimardii belcheri</i> , <i>Spirotocaris</i> sp.
44	Agassiz	104	<i>Argis dentata</i> , <i>Crossaster</i> sp., <i>Sabinea septemcarinata</i> , <i>Strongylocentrotus droebachiensis</i>

TABLE 7.19 Water samples collected during the BaySys 2018 cruise.

Sampling Variable	Station	Station Depth (m)	Sampling Depth	Water T (oC)	Salinity
PFCs	15	189	Surface	-0.9931	32.2388
			30 m	-1.1237	32.3298
			140 m	-1.6181	32.6255
PFCs	29	175	Surface	-1.5223	30.7520
			20 m	-1.5437	30.7590
			50 m	-1.4613	31.6827
PFCs	44	98	Surface	1.4835	29.9287
			10 m	1.6668	30.6000
			40 m	-1.6588	32.6680
OPEs	22	63	Surface	0.9763	32.2266
OPEs	26	129	Surface	1.2516	31.7071
OPEs	31	46	Surface	1.4007	28.5423
OPEs	38	177	Surface	-1.3730	31.7004

TABLE 7.20 Sediment samples collected during the BaySys 2018 cruise

Station	Date	Depth	End Latitude (N)	End Longitude (W)	Section
10	04-Jun-18	203	63.45098	79.44622	Surface

11	04-Jun-18	319	62.87041	78.85538	Surface
15	05-Jun-18	190	63.18558	81.86553	Surface
17	08-Jun-18	92	63.18437	90.03285	Surface
18	08-Jun-18	122	63.7196	88.40239	Surface
19	09-Jun-18	88	61.84331	92.13279	Surface
21	10-Jun-18	150	60.91368	89.33957	Surface
24	13-Jun-18	189	61.70507	87.78463	Surface
29	16-Jun-18	179	61.74696	84.29496	Surface
36	22-Jun-18	127	57.77598	86.02764	Surface
38	23-Jun-18	180	58.72420	86.29730	Surface

TABLE 7.21 Organic contaminant passive samplers deployed during the BaySys 2018 cruise

Name	Cage Style	Station	Date	Station depth (m)	Cage depth (m)
Hudson Bay 1	Large stainless steel	15 Mooring 1	05-Jun-18	195	60
Hudson Bay 2	Small plastic/aluminum	29	16-Jun-18	179	40
Hudson Bay 3	Large stainless steel	44 CMO01	28-Jun-18	105	62

TABLE 7.22 List and coordinates of stations sampled.

Station	Samples	Latitude (surface water)	Longitude (surface water)	Latitude (bottom water)	Longitude (bottom water)	Latitude (Box Core)	Longitude (Box Core)	Date	Depth (m)
4	SSW, BSW	62.15139	69.64583	62.15639	69.84778	NA	NA	01-Jun	283
9	SSW, BSW, Ice	63.92056	80.10722	63.78556	80.01722	NA	NA	03-Jun	91
10	Box cores (single Core)	NA	NA	NA	N/A	63.451	079.445	04-Jun	100

11	Box cores, Ice, SSW, BSW	63.04639	78.93306	63.03389	79.08944	62.870	078.856	04-Jun	3 0 9
15	Box Cores, SSW, BSW, SSW Virus	63.30889	82.10639	63.30889	82.10639	63.184	081.860	05-Jun	
16	Box Cores, SSW, BSW, Ice	62.35639	85.88028	62.39278	85.975	NA	NA	06-Jun	1 3 5
17	SSW, Box Cores, BSW	63.20278	90.05	63.20278	90.03972	63.183	090.033	07-Jun	9 0
18	SSW, SSW virus, BSW, Ice, Box Cores	63.94194	88.57389	63.93056	88.42222	63.720	088.399	08-Jun	1 2 0
19	SSW, BSW, Sediment	62.065	92.38389	62.065	92.38389	61.843	092.131	09-Jun	7 0
21	SSW,BSW, Sediment, Ice	61.07917	89.53917	61.09111	89.53917	60.910	089.339	10-Jun	1 4 4
22	SSW, BSW,	60.49722	94.05389	60.49222	94.05389	NA	NA	11-Jun	6 3
28	Sediment, SSW, BSW	62.64278	84.43611	62.68278	90.06194	62.416	089.820	14-Jun	1 6 0
29	Sediment, SSW, BSW	61.99222	84.43611	61.81722	84.43611	61.747	84.29308	16-Jun	1 7 5
32	SSW, BSW, Ice, Sediment	57.20389	88.34139	57.20083	88.33972	NA	NA	19-Jun	3 4

34	SSW, BSW,	56.50222	86.88111	56.50167	87.11972	NA	NA	20-Jun	4 3
36	SSW, Sediment, BSW	57.88944	86.25694	57.88944	86.25194	57.776	086.027	22-Jun	1 2 6
38	SSW, BSW, Ice, Sediment	58.94583	86.31806	58.95194	86.31806	58.724	086.298	23-Jun	1 7 7
40	SSW,BSW, Sediment	58.34639	88.84333	58.35083	88.84333	58.244	088.591	24-Jun	8 5
44	SSW, BSW	60.10944	91.95444	60.12861	92.19389	NA	NA	28-Jun	9 8
45	SSW, BSW, Sediment	57.28528	92.00917	57.26222	92.06861	57.252	91.963	30-Jun	1 6
46	SSW, BSW, Sediment	57.65972	91.825	57.65833	91.83833	57.503	091.805	01-Jul	4 5

7.12 Amundsen Science – Seabed Mapping, MVP & Sub-Bottom Profiling

Principal Investigator: Amundsen Science; Cruise Participants: Matt Downton¹; Collaborators: Catherine Van Doorn², Samantha Huyghe³, Sergei Kirillov⁴

¹School of Ocean Technology, Fisheries and Marine Institute of Newfoundland and Labrador, St. John's, Canada

²Department of Biology, Laval University, Quebec City, Quebec, Canada

³Department of Geological Sciences, University of Manitoba, Winnipeg, Manitoba, Canada

⁴Centre for Earth Observation Science, University of Manitoba, Winnipeg, Manitoba, Canada

Introduction and Objectives

The BaySys 2018 Amundsen Leg 1 cruise took place from May 25th to July 5th, 2018. The Marine Geosciences Lab. (MGL – Université Laval) was onboard and responsible for multibeam and sub-bottom data acquisition. The MGL has been mainly involved in mapping the seabed morphology and in acquiring sub-bottom stratigraphy during transits, choosing appropriate coring sites, assisting mooring deployment and recovery as well as deploying the Moving Vessel Profiler (MVP). This cruise report presents the instruments, methods, and preliminary results for Leg 1.

Operations Conducted and Methodology

The Amundsen is equipped with an EM302 multibeam sonar operated with the Seafloor Information System (SIS). Attitude is given by an Applanix POS-MV receiving RTCM corrections from a CNAV 3050 GPS receiver. Position accuracies were approximately < 0.8 m in planimetry and < 1 m in altimetry. Beam forming at the transducer head was done by using an AML probe. CTD-Rosette casts, when available, were used for sound speed corrections. During long periods without CTD casts, the WOA09 model was used.

Knudsen 3260 CHIRP Sub-Bottom Profiler

Since May 2016, a new Knudsen 3260 deck unit has been installed onboard the Amundsen. It was acquired to replace the old 320-BR system that shows signs of high degradation at the end of the 2015 field season. The new system now operates using a USB connector instead of an SCSIII communication port. We also installed a new operating computer (HP EliteDesk). Sub-bottom profiles were acquired all along transits at a frequency of 3.5 kHz to image sub-bottom stratigraphy of the seafloor.

Moving Vessel Profiler (MVP) 300

During Leg 1, four MVP transects were performed using a Moving Vessel Profiler (MVP 300) towed behind the ship at 8-10 kts. The MVP measures temperature, salinity, transmissivity, dissolved O₂, fluorescence, and sound velocity. Mainly, our team used MVP data to correct for sound velocity during transit mapping, but these transects were also used to visualize water column properties for physical and biological purposes.

Preliminary Results

All the data acquired during the cruise was post-processed in real-time using the CARIS HIPS&SIPS 10.4 software. This post-processing phase is essential to rapidly detect any anomaly in the data collection. The final addition of the 2018 data will be done upon the return of the ship in Quebec City.

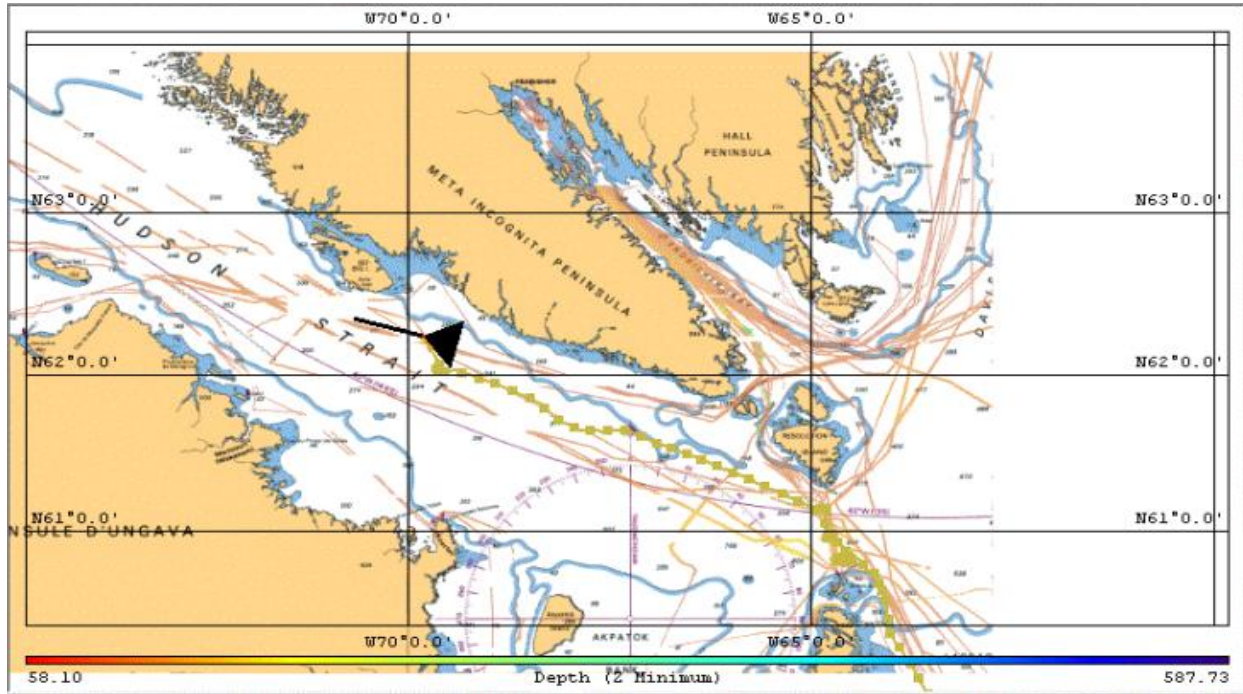


FIGURE 7.36 Example of opportunistic mapping in Hudson Strait

Transit Mapping

The mapping of the Arctic seabed is an important objective of the BaySys program. Transit routes were surveyed systematically to increase the multibeam dataset. These data will be shared with the Canadian Hydrographic Service (CHS) to update marine charts and might be useful for future work with Amundsen Science (Figure 7.36). Overall, the multibeam worked well and generated new data in previously poorly charted areas.

Since 2016, our team has been developing a bathymetry database to easily access all the bathymetry data acquired since the beginning of the ArcticNet program. This ArcMap based database is a raster catalog of more than 3500 data grids (15'x30' spatial extent) that can be rapidly added to navigation charts to improve the multibeam coverage of the Arctic (Figure 7.37). In 2017, the sub-bottom profiles acquired since 2003 were added to this database, making it easier to choose alternative coring sites during the cruise depending on ice conditions.

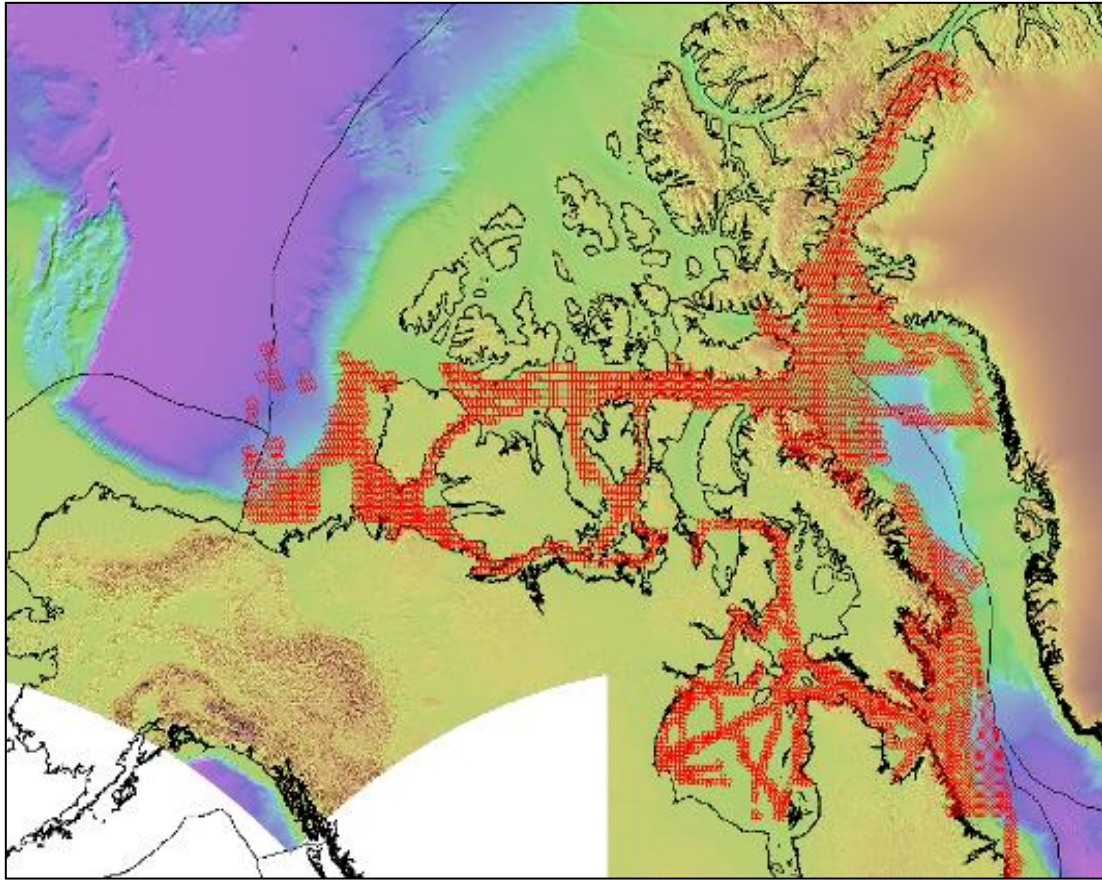


FIGURE 7.37 Image of the Amundsen Bathy-CHIRP Database for bathymetric and sub-bottom data collection

MVP transects

During Leg 1, six MVP transects were performed. Due to ice and sheave issues, only four MVP transects provided useful data (1801003 – 1801006). The casts (Table 7.23) were performed as part of the BaySys program. Figures 7.38 – 7.41 shows the preliminary data.

TABLE 7.23 Description of the relevant MVP transects performed during Leg 1

MVP transect	Location	Speed (kts)	Nb. of casts
1801003	62.86859°N 88.92363°W – 63.29666°N 90.38346°W	8-10	124
1801004	61.84291°N 92.13785°W – 61.37693°N 90.9538°W	8-10	113
1801005	61.38983°N 90.95297°W – 61.00155°N 90.07916°W	8-10	93
1801006	62.20248°N 88.39438°W – 62.5818°N 90.91398°W	8-10	247

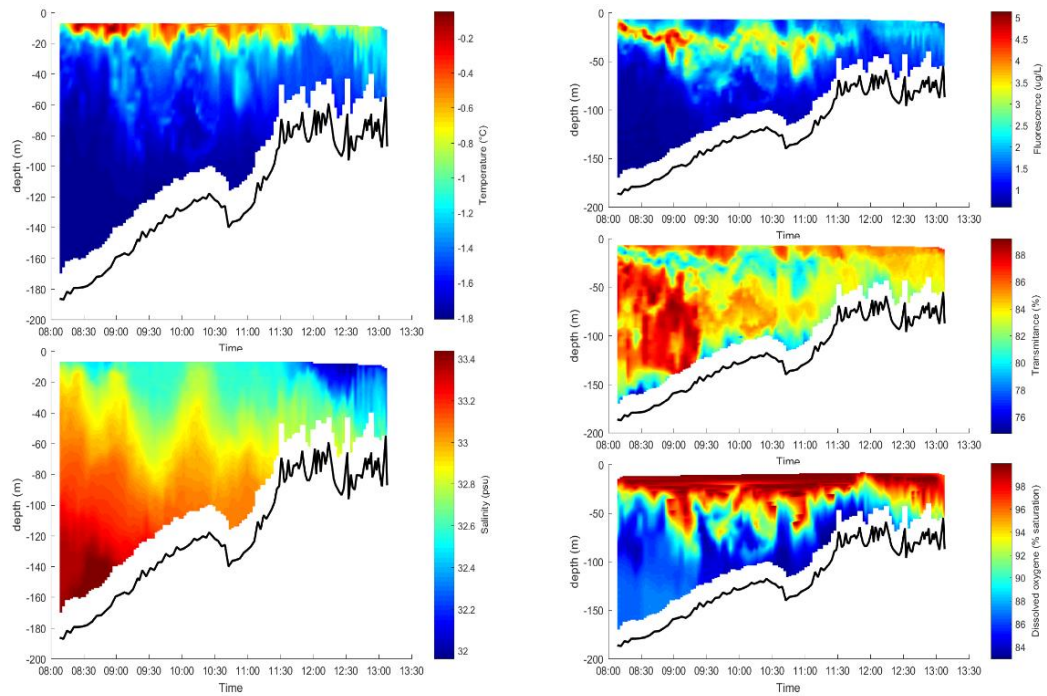


FIGURE 7.38 Preliminary results of the MVP transect 1801003 performed during Leg 1 displaying Temperature, Salinity, Fluorescence, Transmittance, and Dissolved Oxygen

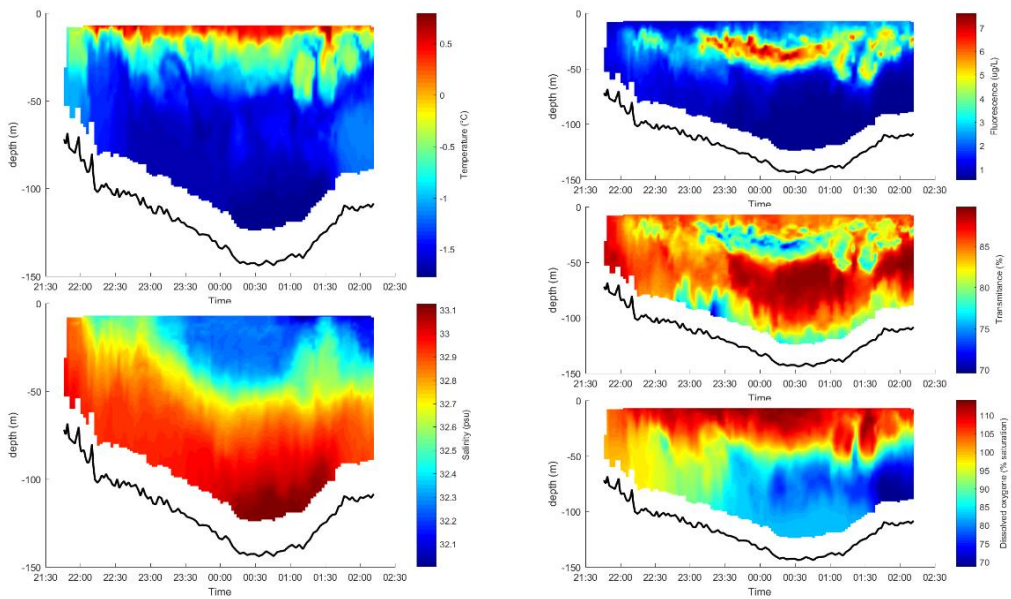


FIGURE 7.39 Preliminary results of the MVP transect 1801004 performed during Leg 1 displaying Temperature, Salinity, Fluorescence, Transmittance, and Dissolved Oxygen

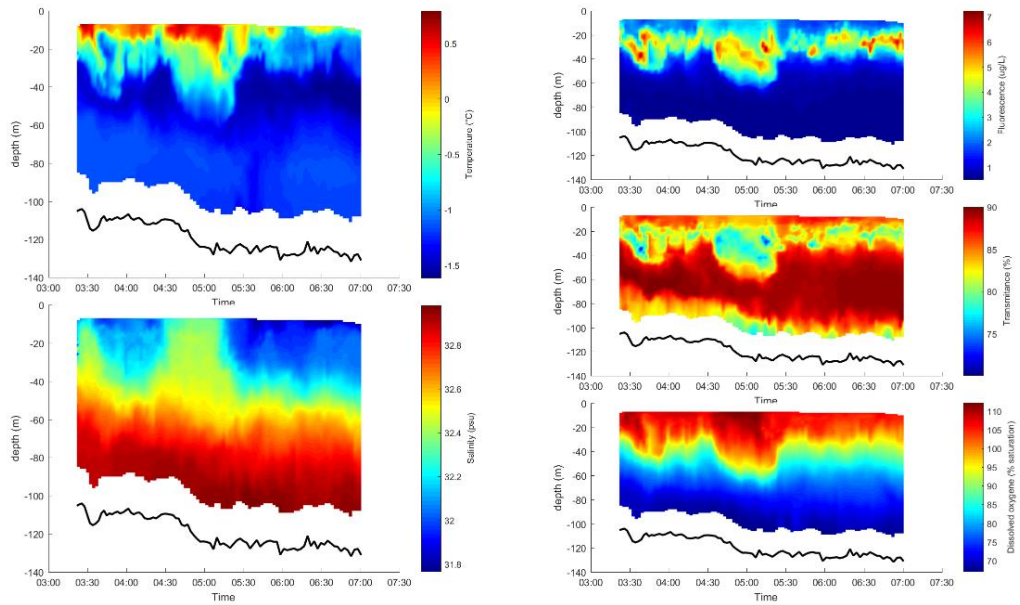


FIGURE 7.40 Preliminary results of the MVP transect 1801005 performed during Leg 1 displaying Temperature, Salinity, Fluorescence, Transmittance, and Dissolved Oxygen

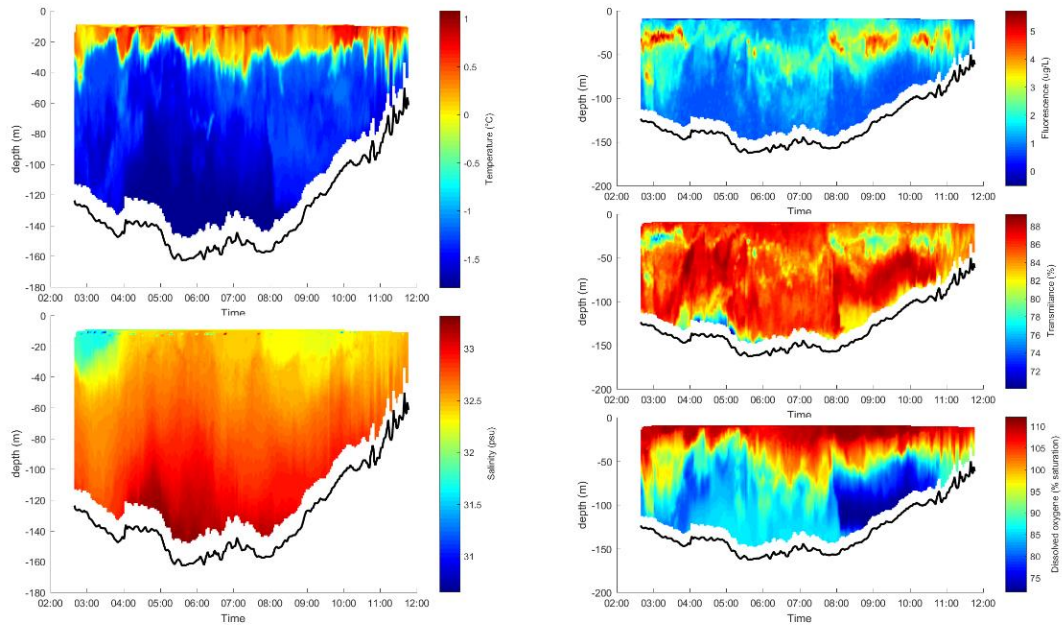


FIGURE 7.41 Preliminary results of the MVP transect 1801006 performed during Leg 1 displaying Temperature, Salinity, Fluorescence, Transmittance, and Dissolved Oxygen

Mooring Deployment and Recovery

The role of the mapping team during mooring deployment and recovery was to 1) ensure the mooring was still in its position (identify the buoys and the exact position), 2) validate the depths of the deployment sites, 3) map the surface morphology of the sites and 4) determine the verticality of the moorings after deployment.

The survey lines from the mooring were processed in CARIS HIPS&SIPS after the survey to find the exact position of the mooring. The procedure started with the visualization of the water column data to find the buoys (Figure 7.42). The buoys scattering was added to bathymetry to find the final position of the deployment.

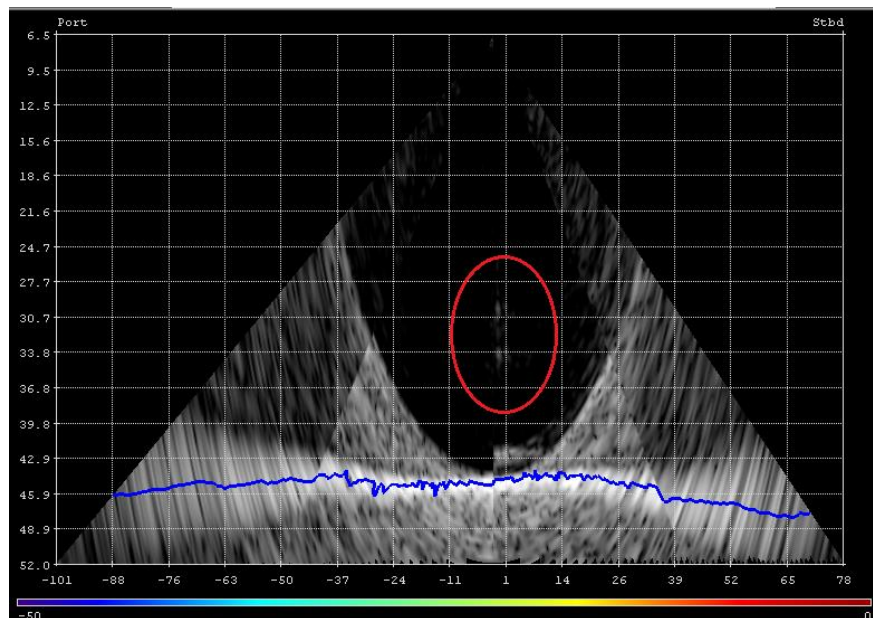


FIGURE 7.42 SIS water Column display of Mooring on July 25th before recovery. The red circle shows the buoys

Sediment Cores

During Leg 1, many box cores were sampled. Coring sites were chosen in real-time while doing a seismic survey, or by analyzing sub-bottom profiles of previous years. Details of the cores, their location, and length of recovery, as well as the targeted type of sediment/feature, are presented in the coring team report (see section 7.11).

Figures were produced by the mapping team for every coring sites to indicate the target on the acoustic sub-bottom profile (Figure 7.43).

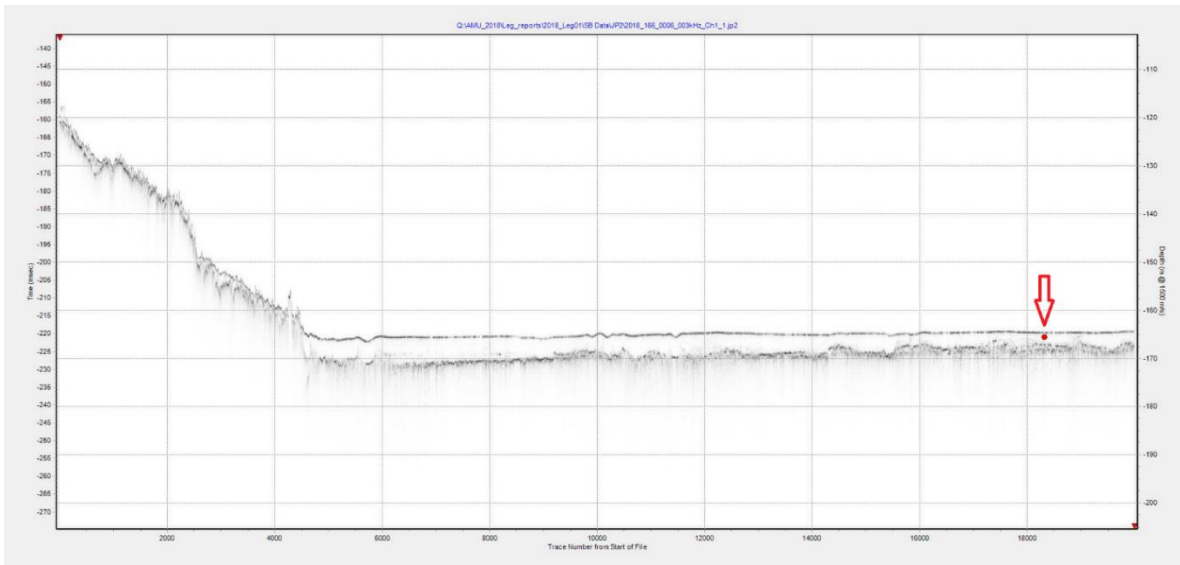


FIGURE 7.43 Location of the core site of near Rankin Inlet on the acoustic subbottom profile

7.13 LEG 2a – Eastern Hudson Bay Sampling and Rivers

Chief Scientist: Jean-Éric Tremblay¹ Cruise Participants: Jean-Éric Tremblay¹, Gabrièle Deslongchamps¹, Gabrielle Fortin¹, Kasey Cameron-Bergeron¹, Janghan Lee¹, Vincent Marmillot¹

¹Department of Biology, Laval University

Date: July 5, 2018 – July 13, 2018

Introduction and Objectives

The Arctic climate displays high inter-annual variability and decadal oscillations that modulate growth conditions for marine primary producers. Much deeper perturbations recently became evident in conjunction with globally rising CO₂ levels and temperatures (IPCC 2007). Environmental changes already observed include a decline in the volume and extent of the sea-ice cover (Johannessen et al. 1999, Comiso et al. 2008), an advance in the melt period (Overpeck et al. 1997, Comiso 2006), and an increase in river discharge to the Arctic Ocean (Peterson et al. 2002, McClelland et al. 2006) due to increased precipitation and terrestrial ice melt (Peterson et al. 2006). Consequently, a longer ice-free season was observed in both Arctic (Laxon et al. 2003) and subarctic (Stabeno & Overland 2001) environments. These changes entail a longer growth season associated with a greater penetration of light into surface waters, which is expected to favoring phytoplankton production (Rysgaard et al. 1999), food web productivity, and CO₂ drawdown by the ocean. However, phytoplankton productivity is likely to be limited by light but also by allochthonous nitrogen availability. The supply of allochthonous nitrogen is

influenced by climate-driven processes, mainly the large-scale circulation, river discharge, upwelling, and regional mixing processes. In the global change context, it appears crucial to improve the knowledge of the environmental processes (i.e. mainly light and nutrient availability) interacting to control phytoplankton productivity in the Canadian Arctic. Also, changes in fatty acid proportions and concentrations will reflect shifts in phytoplankton dynamics including species composition and size structure and will reveal changes in marine energy pathways and ecosystem stability¹²³.

The main goals of our team for LEG 2a of ArcticNet 2018 were to establish the horizontal and vertical distributions of nutrients, to measure the primary production and nitrogen uptake in the water column, and to assess the concentrations of fatty acids in phytoplankton as well as zooplankton. The auxiliary objective was to assess the effects of acidification and temperature on lipids.

Methods

Samples for inorganic nutrients (ammonium, nitrite, nitrate, orthophosphate, and orthosilicic acid) were taken at all stations (Table 7.24) to establish detailed vertical profiles. Samples were stored at 4°C in the dark and analyzed for nitrate, nitrite, orthophosphate, and orthosilicic acid within a few hours on a Bran+Luebbe AutoAnalyzer 3 using standard colorimetric methods adapted for the analyzer (Grasshoff et al. 1999). Samples for ammonium determination were collected at all depths and processed immediately after collection using the fluorometric method of Holmes et al. (1999). Additional samples for urea, particulate organic phosphate (POP), biogenic silica (BSi), particulate carbon and nitrogen (POC/PN), pigments (chl a and HPLC), taxonomy, lipids (phytoplankton and zooplankton), carbon and nitrogen natural abundances, and total selenium were taken at surface and scm at all marine stations and the surface only at river and zodiac stations. To determine nitrate, ammonium, and urea uptake, primary production and nitrogen fixation rates water samples from 6 optical depths were incubated with ¹⁵N and ¹³C tracers. The bottles were then incubated for 24 h using on deck light controlled incubators to establish the relationship between photosynthesis and irradiance. After 24 h, the water samples were filtered through pre-combusted GF/F filters and the filters dried for 24 h at 60°C for further analyses. Incubations were then terminated by filtration through a pre-combusted GF/F filter and stored for further analyses. Isotopic ratios of nitrogen and carbon from all GF/F filters will further be analyzed using mass spectrometry.

A quadrupole mass spectrometer (PrismaPlus, Pfeiffer Vacuum) was used to measure the dissolved gases (N₂, O₂, CO₂, Ar) coming from the underway seawater line. O₂ to Ar ratios will later be analyzed to measure primary production that occurred up to 10 days prior to the ship's passage in all the areas visited.

TABLE 7.24 List of sampling stations and parameters measured during LEG 2a

	NO3, NO2, Si, PO4, NH4 (full profile)	NO3 natural abundance (full profile)	POP, BSi, POC/PN, lipids phyto, C and Natural abundance, HPLC, taxo, total selenium (surface and scm)	15N-tracers uptake experiments (optical depths)	Urea, chla (optical depths)	Lipids zoo (nets)
Station						
731	X	X	X	X	X	
730	X	X	X	X	X	
736	X	X	X	X	X	X
736Z	X	X	X	X	X	
689	X	X	X	X	X	
689Z	X	X	X	X	X	
341	X	X	X	X	X	X
River						
Puvurnituq	X	X	X	X	X	
Deception Bay	X	X	X	X	X	
Salluit	X	X	X	X	X	

References

Arts, M. T., Brett, M. T., Kainz, M. J. Lipids in aquatic ecosystems. *Journal of Chemical Information and Modeling* 53, (2013).

Wynn-Edwards, C. King, R., Davidson, A., Wright, S., Nichols, P.D., Wotherspoon, S., Kawaguchi, S. Virtue, P. Species-specific variations in the nutritional quality of southern ocean phytoplankton in response to elevated pCO₂. *Water (Switzerland)* 6, 1840–1859 (2014).

Lee, R. F., Hagen, W., Kattner, G. Lipid storage in marine zooplankton. *Marine Ecology Progress Series* 307, 273–306 (2006).

Comiso (2006) Abrupt decline in the Arctic winter sea ice cover. *Geophys Res Lett* 33, L18504, doi:10.1029/2006GL027341

Comiso et al. (2008) Accelerated decline in the Arctic sea ice cover. *Geophys Res Lett* 35, L01703, doi:10.1029/2007GL031972

- Grasshoff et al. (1999) *Methods of seawater analyses*, Weinheim, New-York
- Holmes et al. (1999) *Can J Fish Aquat Sci* 56:1801–1808
- IPCC (2007) *Climate change 2007: The physical science basis*. Cambridge University Press, Cambridge, and New York
- Johannessen et al. (1999) *Science* 286:1937–1939
- Laxon et al. (2003) *Nature* 425:947–950
- McClelland et al. (2006) A pan-arctic evaluation of changes in river discharge during the latter half of the 20th century. *Geophys Res Lett* 33, L06715, doi:10.1029/2006GL025753
- Overpeck et al. (1997) *Science* 278:1251–1256
- Peterson et al. (2002) *Science* 298:2171–2174
- Peterson et al. (2006) *Science* 313:1061–1066
- Rysgaard et al. (1999) *Mar Ecol Prog Ser* 179:13–25
- Stabeno & Overland (2001) *EOS* 82:317–321

Appendix 7A – Station Type Definitions

Nutrient

Station with 1 Rosette Cast for nutrient sampling

May include 1 or 2 additional on-deck operations if time permitted (ex., Niskin bottle sampling; vertical or horizontal nets, etc.)

Basic

Station with open water-based sampling operations

2 Rosettes

Horizontal Nets

Vertical Nets

Beam Trawls

Agassiz Trawls

Box Cores

Optical Instrument Suite

Some ice operations were conducted where possible.

Full

Station with all sampling operations including open water, ice, and remote.

2 Rosettes

On-ice Operations via Cage

Skippy Boat/Zodiac Operations

Helicopter Survey and Sampling Operations

Vertical Nets

Horizontal Nets

Beam Trawl

Agassiz Trawl

Box Cores

Optical Instrument Suite

Appendix 7B – Complete Station List

Station ID	Alt. ID	Activity Collection Start Date	Site Description	Sample Depth (m)	Lat. Decimal Degrees	Long. Decimal Degrees
1	356	31/05/2018	Nutrient	328.75	60.8133	-64.5334
2	354	31/05/2018	Nutrient	571.13	60.9735	-64.7734
3	352	01/06/2018	Nutrient	430.12	61.1502	-64.8087
4	HN01	01/06/2018	Nutrient	285	62.0405	-69.6133
5	FB01(A)	02/06/2018	Nutrient	233.03	64.2865	-78.2308
6	FB01(B)	03/06/2018	Nutrient	276.08	64.2236	-78.6244

7	FBO 2	03/06/2018	Nutrient	270	64.0653	-79.0624
8	M19	03/06/2018	Nutrient	320.34	63.9494	-79.5646
9	FBO 3	03/06/2018	Basic	103	63.7302	-79.9264
10		04/06/2018	Nutrient	201.58	63.4474	-79.4428
11		04/06/2018	Full/Ice	320.87	62.8651	-78.8984
12		05/06/2018	Nutrient	85.78	63.3958	-81.2244
13		05/06/2018	Nutrient	148.03	63.2646	-81.6708
14		05/06/2018	Nutrient	-9999	63.1967	-81.8557
15	CM O-C	05/06/2018	Basic	187.93	63.1934	-81.9231
16		06/06/2018	Full/Ice	136.81	62.2794	-85.9089
17		07/06/2018	Basic	88.43	63.1846	-90.0357
18	CM O-D	08/06/2018	Full/Ice	115.61	63.7137	-88.4168
19		09/06/2018	Full/Water	74.89	61.8468	-92.1129
20		10/06/2018	Nutrient	112.15	61.3743	-90.9420
21		10/06/2018	Full/Ice	149.58	60.9102	-89.3595
22		11/06/2018	Full/Water	239.9	60.4231	-94.0023
23	M6	12/06/2018	Nutrient	110.52	60.9221	-91.7809
24		12/06/2018	Full/Ice	189.39	61.6960	-87.7618
25		13/06/2018	Full/Ice	148.19	62.0218	-87.0086
26		14/06/2018	Nutrient	131.46	62.2042	-88.3775
27		14/06/2018	Nutrient	61.02	62.5836	-90.9228
28		15/06/2018	Basic	163.63	62.4155	-89.8339
29	CM O-B	16/06/2018	Full	176.99	61.7698	-84.3091
31	NEO 2	18/06/2018	Nutrient	47.4	57.5001	-91.7953
32		19/06/2018	Full/Ice	32.97	56.9840	-88.1158
33		20/06/2018	Ice Sampling	47.49	56.6114	-87.0904
34		21/06/2018	Full/Ice	43.78	56.4998	-86.8688
35		22/06/2018	Nutrient	61.46	57.1798	-86.4995
36		22/06/2018	Full/Ice	128.34	57.7741	-86.0313
37		23/06/2018	Nutrient	169.68	58.4689	-86.2255
38		23/06/2018	Full/Ice	181.31	58.7224	-86.3050
39		24/06/2018	Nutrient	182.66	58.4748	-87.4385
40		24/06/2018	Basic	90.62	58.2326	-88.5635
41		25/06/2018	Nutrient	71.08	58.0189	-9999
42	NEO 3	25/06/2018	Mooring Recovery	53.82	57.8278	-90.8759
43	Repe at 15	27/06/2018	Basic	192.62	63.1917	-81.9668
44	CM O-A	28/06/2018	Basic	106.59	59.9747	-91.9506

	ANO 1					
45		30/06/2018	Basic	16.66	57.2230	-91.9554
46		01/07/2018	Basic	41.2	57.5032	-91.8129
731		08/07/2018	Basic	124	55.408	-77.928
730		08/07/2018	Basic	138	56.184	-76.723
736Z		09/07/2018	Basic	99	58.423	-78.312
689		11/07/2018	Basic	120	62.342	-75.535
341		12/07/2018	Basic	307	61.958	-70.755
Remote Stations	Alt. ID	Activity Collection Start Date	Site Description	Sample Depth (m)	Lat. Decimal Degrees	Long. Decimal Degrees
FB05-H		02/06/2018	Hudson Strait Heli			
M.I. H1		04/06/2018	Mansel Island Heli		62.2439	-78.3126
M.I. H2		04/06/2018	Mansel Island Heli		62.2429	-78.5166
M.I. H3		04/06/2018	Mansel Island Heli		62.2419	-78.7206
M.I. H4		04/06/2018	Mansel Island Heli		62.2408	-78.9246
M.I. H5		04/06/2018	Mansel Island Heli		62.2398	-79.1286
Northwest HB 1		06/06/2018	Northwest HB Heli		62.0798	-85.3600
Northwest HB 2		06/06/2018	Northwest HB Heli		62.3279	-85.2619
Northwest HB 3		06/06/2018	Northwest HB Heli		62.3604	-85.2203
R.W.S H1		08/06/2018	Roes Welcome Sound Heli		64.0049	-87.0154
R.W.S H2		08/06/2018	Roes Welcome Sound Heli		64.0739	-87.1999
R.W.S H3		08/06/2018	Roes Welcome Sound Heli		64.1391	-87.3856
R.W.S H4		08/06/2018	Roes Welcome Sound Heli		64.2236	-87.5592
R.W.S H5		08/06/2018	Roes Welcome Sound Heli		64.2920	-87.7409
C.I. H1		08/06/2018	Chesterfield Inlet Heli		63.4752	-90.8744
C.I. H2		08/06/2018	Chesterfield Inlet Heli		63.5688	-90.5472
C.I. H3		08/06/2018	Chesterfield Inlet Heli		63.2368	-90.6563
F.R. River Station		09/06/2018	Ferguson River Heli		62.0723	-93.351
F.R. Landfast 1		09/06/2018	Ferguson River Heli		61.8796	-92.8451
F.R. Landfast 2		09/06/2018	Ferguson River Heli		61.8173	-92.7918
Wil.R. River Station		09/06/2018	Wilson River Heli		62.3380	-93.1128
Wil.R. Landfast 1		09/06/2018	Wilson River Heli		62.1260	-92.4869

Wil.R. Landfast 2		09/06/2018	Wilson River Heli		62.1183	-92.4522
Wil.R. Z1		09/06/2018	Wilson River Zodiac		62.0574	-92.4729
Wil.R. Z2		09/06/2018	Wilson River Zodiac		61.9853	-92.3349
Wil.R. Z3		09/06/2018	Wilson River Zodiac		61.9211	-92.2151
T.R. River Station		11/06/2018	Thlewiaza River Heli		60.4851	-94.8167
T-A.R. River Station		11/06/2018	Tha-anne River Heli		60.5461	-94.8292
T-A.R. Z1		11/06/2018	Tha-anne River Zodiac		60.4712	-94.5673
T-A.R. Z2		11/06/2018	Tha-anne River Zodiac		60.4592	-94.4156
T-A.R. Z3		11/06/2018	Tha-anne River Zodiac		60.4434	-94.2228
Seal.R. River Station		28/06/2018	Seal River Heli		59.0739	-94.8344
K.R. River Station		28/06/2018	Knife River Heli		58.8831	-94.7031
C.R. River Station		28/06/2018	Churchill River Heli		58.6781	-94.2033
N.R. River Station		18/06/2018	Nelson River Heli		56.9659	-92.6305
H.R. Station		18/06/2018	Hayes River Heli		56.9955	-92.2924
Sev.R. River Station		19/06/2018	Severn River Heli		55.9603	-87.7081
Win.R. River Station		21/06/2018	Winisk River Heli		55.2218	-85.2068
34_HeliA		20/06/2018	Helicopter Ice Sampling		56.6833	-86.9083
34_HeliB		20/06/2018	Helicopter Ice Sampling		56.5867	-86.8968
34_HeliC		21/06/2018	Helicopter Ice Sampling		56.1072	-84.5633
34_HeliD		21/06/2018	Helicopter Ice Sampling		56.4099	-85.8918
36_HeliA		22/06/2018	Helicopter Ice Sampling		57.8781	-84.22
36_HeliB		22/06/2018	Helicopter Ice Sampling		57.8291	-85.1337
36_HeliC		22/06/2018	Helicopter Ice Sampling		58.2978	-87.6056
36_HeliD		22/06/2018	Helicopter Ice Sampling		58.0513	-86.8623
38_HeliA		23/06/2018	Helicopter Ice Sampling		58.7909	-84.2376

38_HeliB		23/06/2018	Helicopter Ice Sampling		58.7916	-85.1604
38_HeliC		23/06/2018	Helicopter Ice Sampling		59.2654	-87.9881
38_HeliD		23/06/2018	Helicopter Ice Sampling		59.0165	-87.1095
N.E. South Tran 1		29/06/2018	Nelson Estuary		57.1842	-91.811
N.E. South Tran 2		29/06/2018	Nelson Estuary		57.2081	-91.8711
N.E. South Tran 3		29/06/2018	Nelson Estuary		57.2176	-91.9585
N1a		29/06/2018	Nelson River		57.0543	-92.5351
N1b		29/06/2018	Nelson River		57.0558	-92.5313
N2		29/06/2018	Nelson River		57.1191	-92.4165
BN3a		29/06/2018	Nelson River		57.1358	-92.4118
BN3b		30/06/2018	Nelson River		57.1311	-92.4174
BN4a		30/06/2018	Nelson River		57.1660	-92.3519
BN4b		30/06/2018	Nelson River		57.1615	-92.3673
BN5a		30/06/2018	Nelson River		57.1731	-92.3411
BN5b		30/06/2018	Nelson River		57.1628	-92.3574
BN6a		30/06/2018	Nelson River		57.2078	-92.2868
BN6b		30/06/2018	Nelson River		57.2019	-92.308
BN7a		30/06/2018	Nelson River		57.2500	-92.2216
BN7b		30/06/2018	Nelson River		57.2579	-92.237
N3		30/06/2018	Nelson River		57.2059	-92.2825
N4		30/06/2018	Nelson River		57.2221	-92.2939
IB13		19/06/2018	Ice Beacon Deployment Via Heli		56.6173	-87.4002
IB17		18/06/2018	Ice Beacon Deployment Via Heli		58.4802	-89.2547
IB18		22/06/2018	Ice Beacon Deployment Via Heli		58.3499	-87.4718
IB19		19/06/2018	Ice Beacon Deployment Via Heli		57.7233	-88.2824
IB20		23/06/2018	Ice Beacon Deployment Via Heli		59.3507	-87.8543
IB21		21/06/2018	Ice Beacon Deployment Via Heli		56.4220	-85.4002
IB22		23/06/2018	Ice Beacon Deployment Via Heli		58.8122	-84.3463

IB23		19/06/2018	Ice Beacon Deployment Via Heli		57.0884	-88.4002
IB25		22/06/2018	Ice Beacon Deployment Via Heli		57.8789	-84.1463
IB26		21/06/2018	Ice Beacon Deployment Via Heli		56.2193	-84.5491
736		09/07/2018	Zodiac	15	58.4408	-78.1081
689Z		11/07/2018	Zodiac	20	62.2852	-75.5220
Riviere Puvirnitug		10/07/2018	Riviere Puvirnitug		60.0725	-77.2469
Riviere Foucault		11/07/2018	Riviere Foucault		62.1081	-75.7583
Riviere Deception		11/07/2018	Riviere Deception		62.0975	-74.4956

CHAPTER 8 - MOORING PROGRAM – WILLIAM KENNEDY

FIELDWORK PARTICIPANTS PIs: David Barber¹, Jens Ehn¹, Jean-Éric Tremblay², Tim Papakyriakou¹, Celine Gueguen², Zou Zou Kuzyk¹, CJ Mundy¹, Fei Wang¹, David Lobb¹; Field/Ship Coordination: Jens Ehn, David Landry¹, CJ Mundy, Zou Zou Kuzyk; Mooring Operations: Vladislav Petrusevich¹, Keesha Peterson¹, Sergei Kirillov¹, Michelle Kamula¹; Water Sampling Team: Keesha Peterson, Nicole Pogorzelec¹, Samantha Huyghe¹; Report Authors: Vladislav Petrusevich and Jens Ehn

RESEARCH VESSEL R/V William Kennedy (formerly White Diamond)

DATE OF FIELDWORK September 1 -14, 2018

1 Centre for Earth Observation Science, University of Manitoba, 535 Wallace Building, Winnipeg, MB
2 Québec-Océan, Department of Biology, Pavillon Alexandre-Vachon, 1045, Avenue de la Médecine, Local 2078, Université Laval, Québec, QC

CITE CHAPTER AS Petrusevich, V., Ehn, J., Mundy, CJ. 2019. Mooring Program – William Kennedy. Chapter 8 in, *Hudson Bay Systems Study (BaySys) Phase 1 Report: Campaign Reports and Data Collection*. (Eds.) Landry, DL & Candlish, LM. pp. 214-223.

8.1 Fieldwork Objectives

BaySys is a 4-year collaborative project between industry partner Manitoba Hydro (Hydro Québec and Ouranos) and the Universities of Manitoba, Northern British Columbia, Québec à Rimouski, Alberta, Calgary, Laval, and Sherbrooke. The overarching goal of the project is to understand the role of freshwater in Hudson Bay marine and coastal systems, and in particular, to create a scientific basis distinguishing the impacts of climate change from those of hydroelectric freshwater regulation on the physical, biological and biogeochemical conditions in Hudson Bay.

In late September 2016, five oceanographic moorings were deployed (see Chapter 1) in the eastern Hudson Bay and at the entrance to James Bay (Figure 8.1). These moorings were planned to be recovered during the summer of 2017 from onboard the CCGS Amundsen or R/V William Kennedy. A decision was made, however, to use the R/V William Kennedy to turn the mooring instead of conducting a recovery. Due to delays in the ship's inspection from Transport Canada, the 2017 cruise was canceled. An opportunistic cruise onboard CCGS Henry Larsen was successfully conducted on October 26 – November 1, 2017, for retrieval and re-deployment of some of BaySys moorings accompanied by the concurrent CTD and water sampling (see Chapter 2, Kirillov et al., 2018, 2020; Petrusevich et al., 2020). Unfortunately, mooring JB02 could not be recovered during that operation and was ultimately recovered during the MV William Kennedy field operations in 2018. On September 1-14, 2018, the MV William Kennedy embarked with the main goal of recovery of the mooring JB02 and conducting additional bathymetry surveys, water sampling and CTD casts during transects and in the Nelson River estuary.

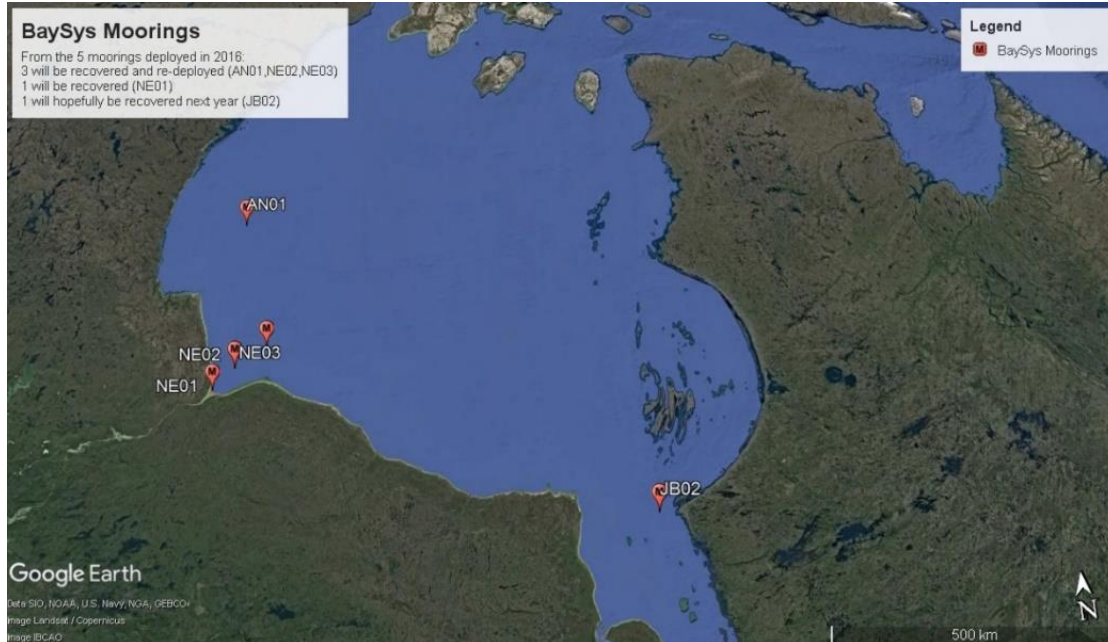


FIGURE 8.1 The array of BaySys mooring deployed in September 2016 and the initial turnaround plan for 2017-2018.

The science crew (Vladislav Petrusevich, Nicole Pogorzelec, and Samantha Huyghe) arrived in Churchill on September 1, 2018, and departed following familiarization with the vessel and crew, and a safety briefing. On September 2 we arrived at the Nelson River estuary. The morning conditions were not suitable for operations, but by the afternoon the wind decreased to 15 knots and we started water sampling and CTD casts using rosette following the proposed sampling stations plan (Figure 8.2). By the end of the day, we finished a transect in the Nelson River estuary. By the following morning, we planned to arrive at Cape Tatnam and conduct multibeam mapping of the slope and seabed, looking for the features like ice scours and ridges.



FIGURE 8.2 Proposed sampling stations on the route to the mooring JB02-16 recovery.

On September 3, we nearly ran aground while during multibeam bottom mapping, damaging one of the stabilizers. The weather worsened and the decision was made to return to Churchill when possible. Unfortunately, gale warnings for Churchill and Eastern Hudson Bay delayed any action for our vessel, therefore we decided to stay in the Nelson River estuary until better weather. The winds were 30-36 knots during this time and lost our anchor due to the storm. On September 7, with better weather, we were able to return to Churchill. We remained in Churchill until we could ensure 4 to 5 days of good weather needed for a transect from Churchill to Kuujjuarapik for the mooring recovery.

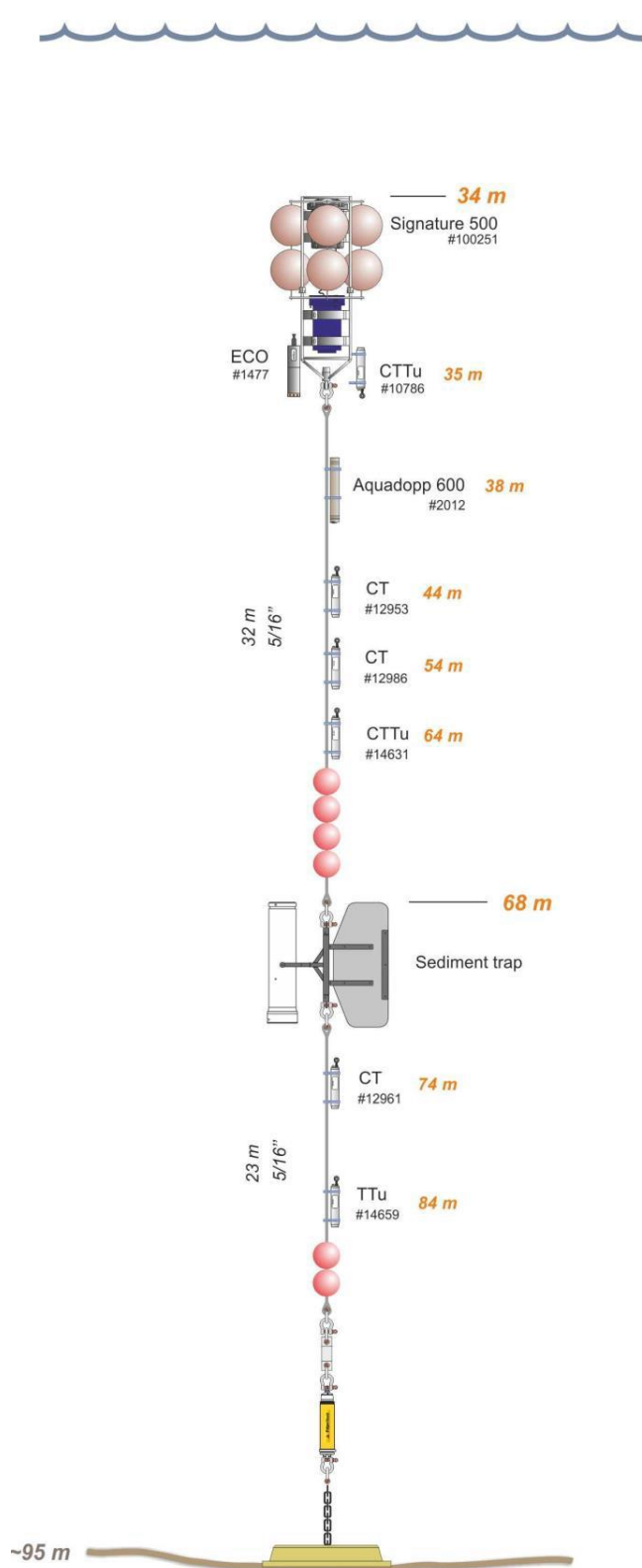
8.2 Mooring Operations

R/V William Kennedy left Churchill again on September 10, heading towards the mooring location of JB02. We arrived on site on the afternoon of September 13. The acoustic release on the mooring functioned properly, and the mooring was afloat (Figure 8.3a). Using a grapnel, the floats were dragged to the aft section of the ship with the diving platform being lowered and then connected to the A-frame winch for retrieval (Figure 8.3b).



FIGURE 8.3 a) Acoustically released mooring with floats being recovered using a grapnel from R/V William Kennedy, b) Mooring being recovered using the aft winch.

A bottom-anchored oceanographic mooring JB02-16 (Figure 8.4) was deployed at 95 m depth ~165 km south-west from Kuujjuarapik, QC ($54^{\circ}40.973'N$ $80^{\circ}11.226'W$) on 1 October 2016 and recovered on 13 September 2018. The mooring setup consisted of (i) one upward-looking 5-beam Signature 500 ADCP by Nortek placed at 35 m depth, one (ii) downward-looking 3-beam 600 kHz Aquadopp ADCP by Nortek placed at 38 m depth, and (iii) one Gurney Instrument “Baker Type” sequential sediment trap (Baker & Milburn, 1983) at 68 m with a collection area of 0.032 m². Several conductivity-temperature, conductivity-temperature-turbidity, and temperature-turbidity sensors were also deployed at various depths on the mooring.



JB02	
target depth:	100 m
depth of deployment:	101 m
latitude:	54° 40.973' N
longitude:	80° 11.226' W
date of deployment:	Oct 1, 2016
time of deployment:	17:03 UTC

FIGURE 8.4 Schematic illustration of the mooring JB02-16 configurations as recovered. Signature 500 ADCP placed at 35 m depth was covered by hydroid (possibly seapen or sponge) species (Figure 8.5).



FIGURE 8.5 Biofouling of Signature 500 ADCP.

The objective of the sediment trap program, as part of BaySys Team 4/5, was to determine the sinking fluxes of particulates (organic and lithogenic) through the water column. Four Gurney Instrument “Baker Type” sequential type sediment traps were deployed from the CCGS Des Groseilliers in 2016 fixed to moorings AN01, NE02, NE03, and JB02 at depths ranging from 28 to 85 m below the water surface. All four sediment traps were programmed to start a collection on 4 October 2016 at 0:00 CST with intervals of 35 days for each vial collected. The Sediment traps on moorings AN01, NE02, and NE03 were successfully recovered during the 2017 fall cruise and JB02 during the current 2018 fall cruise.

Once onboard (Figure 8.6a), the trap was dismantled, first removing the PVC tube that houses an asymmetrical funnel, the stabilizing fins, and then the sample vials from the rosette.



FIGURE 8.6 a) Sediment trap from mooring JB02-16 being hoisted onboard R/V William Kennedy. b) The vials from the sediment traps in the vial rack.

The samples were placed into a vial rack numbered from 1 to 10 (Figure 8.6b). The vials were then emptied into labeled amber jars which were then packed and stored in a cooler on the deck. The sediment traps were then reassembled, cleaned with fresh water, and then packed in their respective boxes for

transport. The samples collected have been placed in cold storage (-4°C) and are yet to be analyzed for captured sediments and zooplankton taxonomy identification (Petrusevich et al., 2020).

8.3 Early Results

The CT sensors deployed at different depths captured the seasonal changes in vertical thermohaline structure at the mooring location. These changes correspond to the impact of different processes such as the vertical mixing and redistribution of heat from the surface to the deeper layers in autumn; cooling of the water column and the following salinity increase due to the sea ice growth in winter; the freshening and warming associated with sea ice melting/river runoff and solar heating in summer (Figure 8.7).

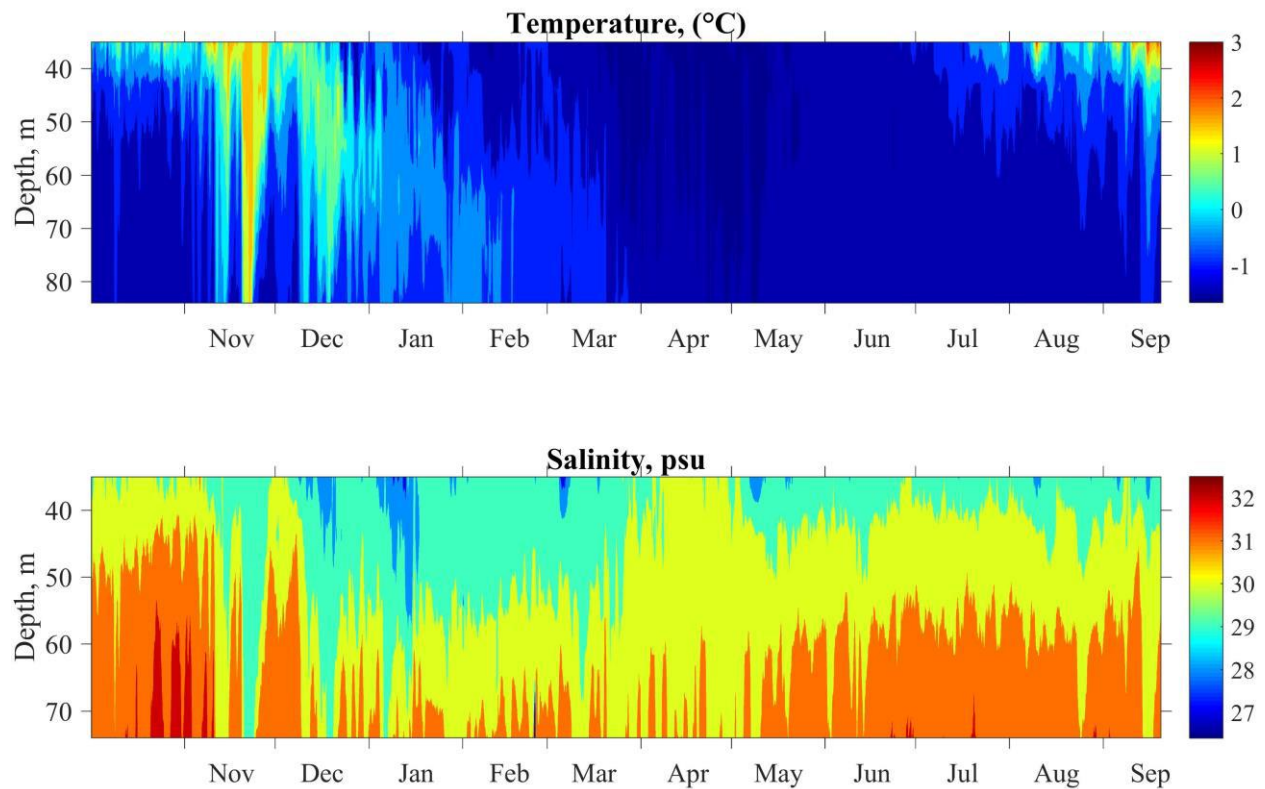


FIGURE 8.7 The one-year evolution of vertical thermohaline structure at JB02-16 mooring

The mooring carried an upward-looking five-beam acoustic Doppler current profiler (ADCP, Nortek Signature 500), which in addition to currents measured the distance from the instrument to either the sea surface or the ice bottom when sea ice floes drifted over the profiler during the ice-covered period. The thickness of sea ice at the mooring location was estimated from the ice draft evaluated from the distance to the ice-ocean interface measured by the ADCP. The acoustic-derived thicknesses were corrected for ADCP tilt, sea surface height, and atmospheric pressure (Krishfield et al., 2014), and the speed of sound.

The extreme outliers were excluded, and the mean daily ice thicknesses were calculated for further analysis (Figure 8.8) (Kirillov et al., 2020).

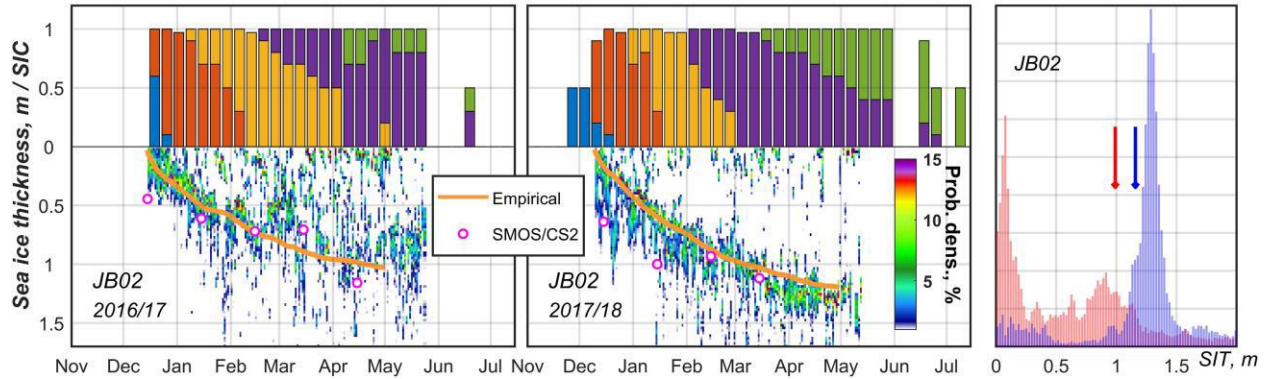


FIGURE 8.8 Evolution of sea ice thickness (SIT) recorded by upward-looking Nortek ADCP and ice types at JB02-16 during winters 2017 and 2018. The measured SITs are shown as a percent occurrence, and those maxima (from green to red colours) correspond to the peak probability of daily SIT at 2-cm bin spacing. The monthly mean CS2/SMOS data are presented as magenta circles at the center of every month. Daily mean SIT estimated from empirical thermodynamic growth is shown with an orange line. CIS data on the partial concentration of different types of sea ice is shown with colour bars (new < 10 cm, young < 10–30 cm, FYI thin 30–70 cm, FYI medium 70–120 cm, and FYI thick > 120 cm). The availability of OSI-405-c ice drift data is shown with pink horizontal bars at the top of the figure. The normalized frequency distributions of measured SIT at 2-cm bin spacing in April 2017 and 2018 are shown in the right panels together with arrows indicating the April-averaged empirical SITs (Kirillov et al., 2020).

8.4 CTD Sampling

For the hydrological measurements, we used the ship’s CTD-rosette fitted with twelve 5L Niskin bottles and Seabird CTD (Figure 8.9). Sensors on the CTD allowed it to take profiles of water temperature and salinity (Figure 8.9b and 8.9c) at JB02-16 mooring location and additionally chlorophyll fluorescence, photosynthesis-active radiation (PAR), and dissolved oxygen concentration.

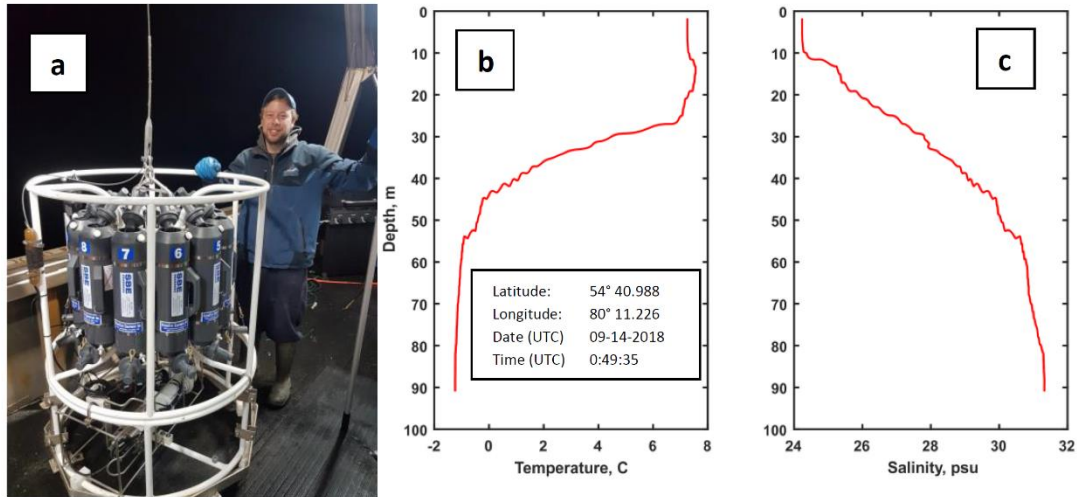


FIGURE 8.9 a) CTD Rosette onboard R/V William Kennedy, b) Temperature, and c) salinity profiles collected at the mooring location.

8.5 Water Sampling

The water samples were collected using CTD rosette at the mooring location. The initial plan included water sampling for CDOM, O18, NO₃, NO₂, Si, PO₄ at the multiple sites along the ship's track on route to the mooring location (Table 8.1), but it was canceled due to the weather/logistics issues. The results of the water sampling from the mooring location are not yet available.

TABLE 8.1 List of stations where CTD and water sampling was conducted.

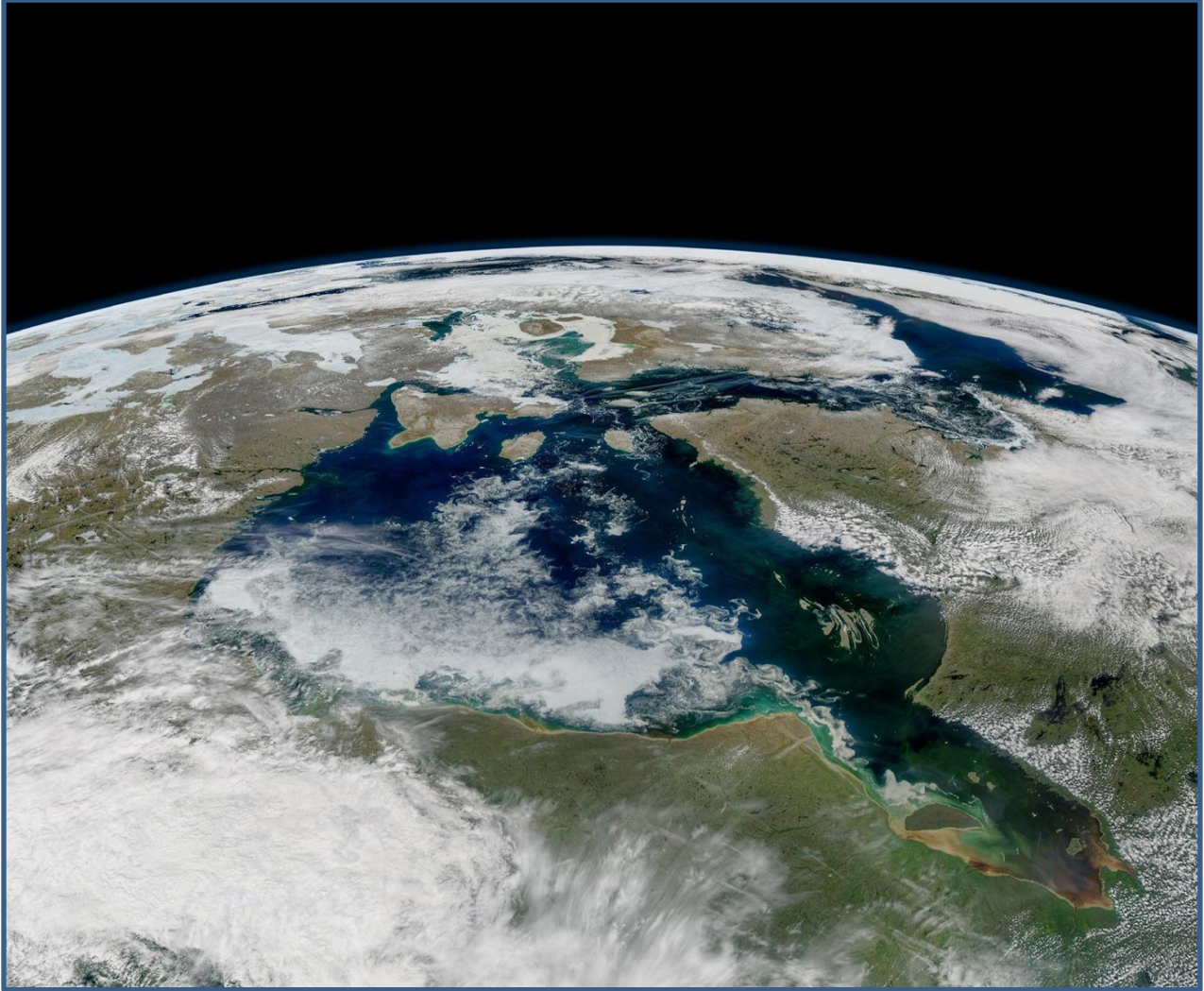
Station Name	Latitude	Longitude	Cast	Date (UTC)	Time (UTC)	Bottom Depth (m):
SH_1	57.26895	-92.1346	1	09-02-2018	21:34:42	24
SH_2	57.66983	-91.6084	1	09-02-2018	n/a	n/a
JAMES BAY MOORING	54.68313	-80.1871	1	09-14-2018	0:49:35	100

References

- Baker, E. T., & Milburn, H. B. (1983). An instrument system for the investigation of particle fluxes. Continental Shelf Research. Oxford: Elsevier Science. [https://doi.org/10.1016/0278-4343\(83\)90006-7](https://doi.org/10.1016/0278-4343(83)90006-7)
- Hornby, C., Ehn, J., Matthes, L., Blondeau, S., Basu, A., Goharrokhi, M., et al. (2016). BaySys 2016 Mooring Program Cruise Report. Winnipeg. Retrieved from <http://hdl.handle.net/1993/33754>
- Kirillov, S., Peck, C., & Petrusevich, V. (2018). BaySys 2017 Fall Cruise Report. Turnaround of Moorings. Winnipeg. Retrieved from <http://hdl.handle.net/1993/33757>
- Kirillov, S., Babb, D., Dmitrenko, I., Landy, J., Lukovich, J., Ehn, J., et al. (2020). Atmospheric Forcing

- Drives the Winter Sea Ice Thickness Asymmetry of Hudson Bay. *Journal of Geophysical Research: Oceans*, 125(2), e2019JC015756. <https://doi.org/10.1029/2019JC015756>
- Krishfield, R. A., Proshutinsky, A., Tateyama, K., Williams, W. J., Carmack, E. C., MaLaughlin, F. A., & Timmermans, M.-L. (2014). Deterioration of perennial sea ice in the Beaufort Gyre from 2003 to 2012 and its impact on the oceanic freshwater cycle. *Journal of Geophysical Research: Oceans*, 119(2), 1271–1305. <https://doi.org/10.1002/2013JC008999>
- Petrusevich, V. Y., Dmitrenko, I. A., Niemi, A., Kirillov, S. A., Kamula, C. M., Kuzyk, Z. Z. A., et al. (2020). Impact of tidal dynamics on diel vertical migration of zooplankton in Hudson Bay. *Ocean Science*, 16(2), 337–353. <https://doi.org/10.5194/os-16-337-2020>

HYPE AND NEMO MODELING



CHAPTER 9 FRESHWATER HYDROLOGIC MODELING

PROJECT CONTRIBUTORS ¹T.A. Stadnyk, ²K.A. Koenig, ^{1,3}S.J. Déry, ⁴C. Guay, ⁵G. Ali, ⁶M. Braun, ¹M.K. MacDonald, ¹A.A.G. Tefs, ¹S. Pokorny, ³R. Lilhare, ¹M. Broesky, ¹M. Hamilton, ¹R. Sologna

COLLABORATORS ²P. Slota, ²M. Vieira, ²S. Wruth, ²M. Gervais, ²J. Crawford, ³B. Gaudi-Sharma, ⁴N. Thiemonge, ⁴F. Guay, ⁴V. Fortin, ⁷D. Gustafsson, ⁷K. Isberg, ⁷B. Arheimer, ⁸A. Shiklomanov

¹Department of Civil Engineering, University of Manitoba, Winnipeg, Manitoba, Canada

²Hydroclimatic Studies Division, Manitoba Hydro, Winnipeg, Manitoba, Canada

³Department of Civil and Environmental Engineering, University of Northern British Columbia, Prince George, British Columbia, Canada

⁴Institut de recherche d'Hydro-Québec (IREQ), Hydro-Québec, Varennes, Québec, Canada

⁵Department of Geology, University of Manitoba, Winnipeg, Manitoba, Canada

⁶Groupe pour scénarios et services climatiques, Ouranos, Sherbrooke, Québec, Canada

⁷Hydrologic Research Unit, Swedish Meteorological and Hydrological Institute, Norrköping, Östergötlands, Sweden

⁸Institute for the Study of Earth, Oceans and Space, University of New Hampshire, Durham, New Hampshire, U.S.A.

CITE CHAPTER AS Stadnyk, T. 2019. Freshwater Hydrological Modeling. Chapter 9 in, *Hudson Bay Systems Study (BaySys) Phase 1 Report: Campaign Reports and Data Collection*. (Eds.) Landry, DL & Candlish, LM. pp. 225-259.

9.1 Objectives and Background

The timing and volume of freshwater delivered to Hudson Bay has a significant impact on the formation and dynamics of Hudson Bay sea-ice. Terrestrial runoff of the Hudson Bay Drainage Basin (HBDB) is a major contributor (along with sea-ice melt and precipitation) of freshwater to Hudson Bay (Granskog et al., 2011).

Over the previous five decades, major hydroelectric complexes in the Nelson Churchill River Basin (NCRB, including the heavily regulated Lower Nelson River Basin; LNRB) and the La Grande Rivière Complex (LGRC) have had effects not only on the timing of freshwater discharge but also on the volume by location (due to diversions). Changes to this water entering western Hudson Bay (from the NCRB) and eastern James Bay (from the LGRC) is a possible driver of changes to sea-ice distribution and thickness (Anctil & Couture, 1994). This regulation aims to impound spring and summer flows to be used to generate power over the winter, when power-demand is highest, resulting in a “flattening” of the annual hydrograph (Déry et al., 2011).

Coinciding with an increased number of regulated reservoirs, freshwater regimes of the HBDB are being affected by a changing climate. Shorter, warmer winters have increased winter runoff with a less significant spring freshet, seen in northwestern Canada (DeBeer et al., 2016), and the Arctic as a whole (Gelfan, et al., 2017; Bring et al., 2017). The effect of this change on discharge is seen in inter-annual and inter-decadal variability of freshwater discharge to Hudson Bay, both regulated and unregulated (Déry et al., 2011).

Distinguishing the effects of regulation and climate change on freshwater and predicting their long-term effects is a scientific priority among northern, hydroelectrically-developed countries (Arheimer et al., 2017), but has yet to be attempted for Hudson Bay and other high-latitude Canadian basins due to data-sparsity and difficulties associated with incorporating reservoir controls into continental-scale hydrologic models (Wada et al., 2017).

Beyond the challenges of accurate (or even sufficient) modeling in an environment as large and heterogeneous as the HBDB, uncertainty in long-term, large-scale climate studies is a pressing concern, particularly when projecting results into the future (Beven, 2007). To quantify and allocate uncertainty, multi-model studies (Chen et al., 2011) using climate-ensembles (Tebaldi & Knutti, 2007) and robust uncertainty analyses (Ajami et al., 2007) are necessary to report results with any confidence or authority.

To address the challenges (and opportunities) discussed above, the overall goal of this work is to produce (as much as is feasible) a complete dataset of terrestrial hydrology, discharge records, and discharge uncertainty bounds for the Hudson Bay Complex (HBC; shown in Figure 9.1) from 1981 to 2070. These records will be used to complement historic fieldwork studying sea-ice and bio-geo-chemical processes in the HBC. They will further be used to analyze projected hydrologic change for the HBDB as well as making up the input for oceanographic modeling describing current dynamics and sea-ice formation in Hudson Bay. To achieve this, the work of the freshwater modeling group falls into four primary objectives (below) corresponding to (but with scope changes from) the four BaySys tasks assigned to Team 2 (Barber et al., 2014).

- 2.1) Development of continental-scale hydrologic model(s)
- 2.2) Uncertainty assessment of LNRB discharge
- 2.3) Discharge modeling of regulated basins in the HBDB
- 2.4) Uncertainty assessment of HBDB discharge

These goals and the inter-connected steps required to complete them are summarized in the work-flow diagram shown in Figure 9.2 and detailed in Table 9.1. The methods and processes used to generate the data are explained in Section 9.2, with a summary of progress to-date in Section 9.3 and those available results are shown in Section 9.4. Note that Task 2.4 has only recently begun (January 2019) and will not be discussed further in this report except for inclusion in the overall workflow of Team 2 (Figure 9.2 and Table 9.1).

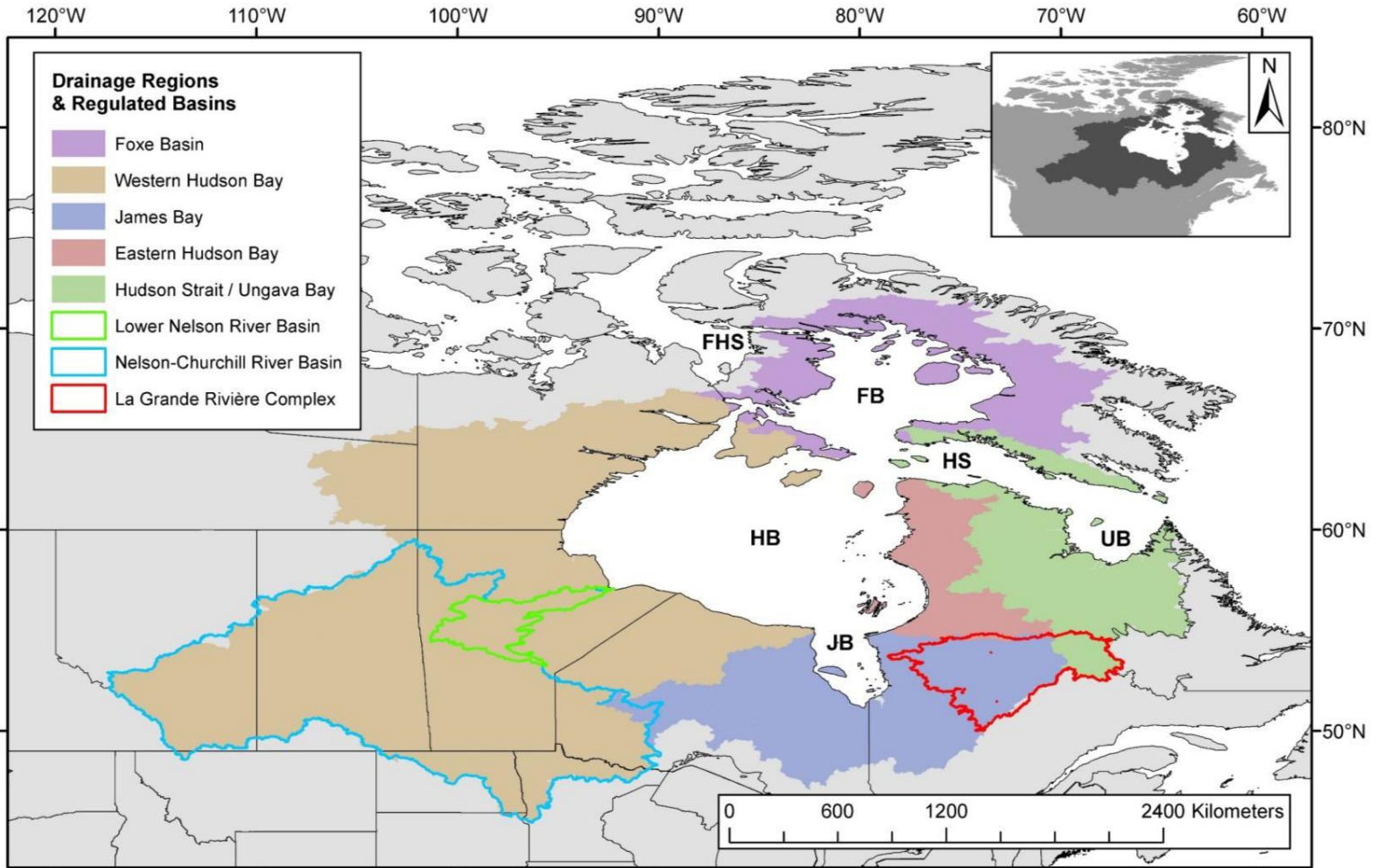


FIGURE 9.1 Major drainage regions of the HBDB contributing discharge to HBC regions: Hudson Bay (HB), James Bay (JB), Ungava Bay (UB), Hudson Strait (HS), Foxe Basin (FB), and Fury and Hecla Strait (FHS).

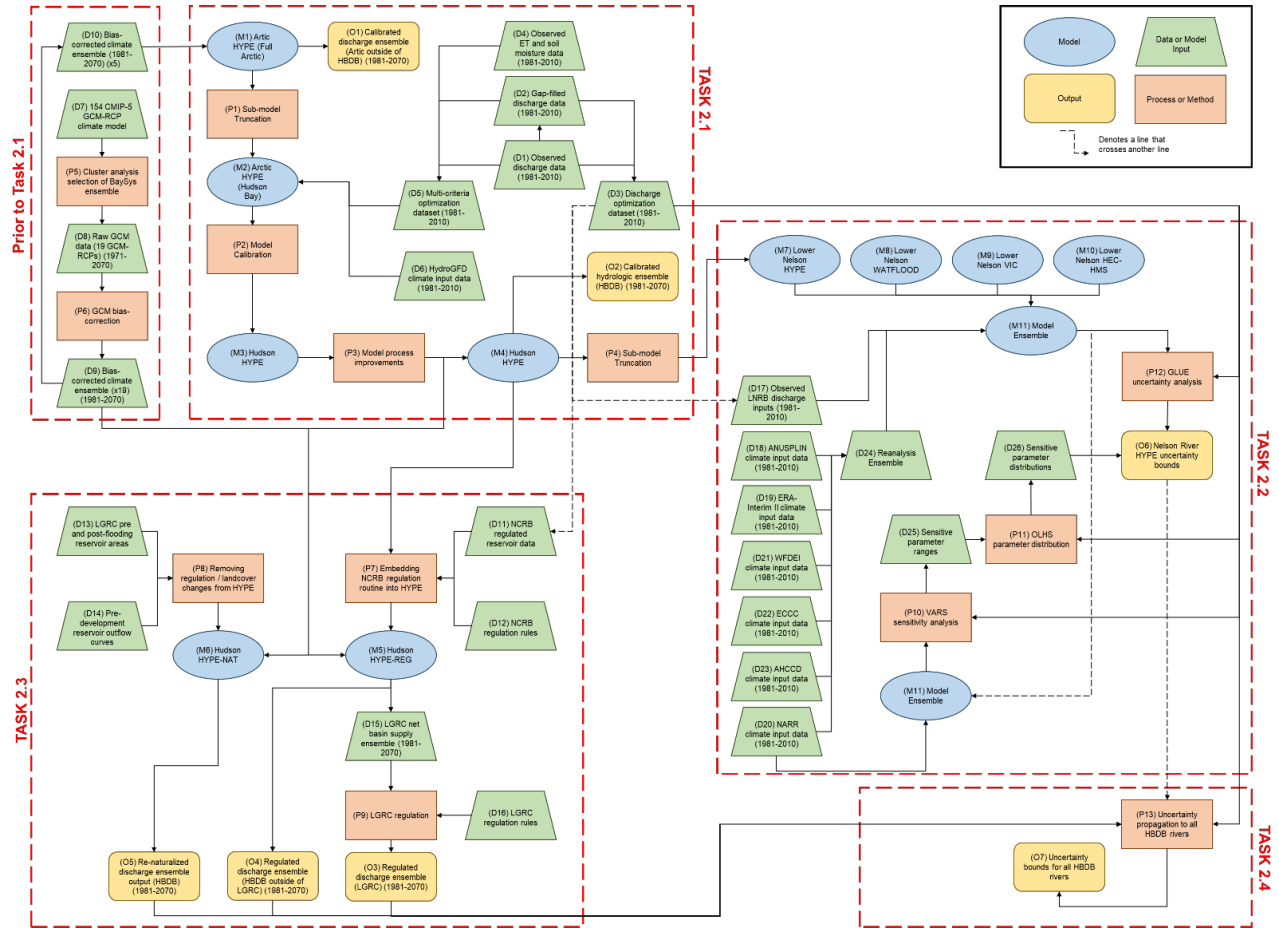


FIGURE 9.2 Team 2 workflow diagram. Tasks correspond to BaySys proposal (Barber et al., 2014) with detailed descriptions and sources in Table 5-1, codified according to D, trapezoid: input dataset; P, rectangle: method or process; M, oval: model selected or developed; O, rounded rectangle: output dataset. Note that outputs listed only pertain to critical-path BaySys tasks and datasets to be distributed between Teams.

TABLE 9.1 Team 2 workflow details and references. Items correspond to Figure 5-2. Asterisks denote publications outside of BaySys used where no published results can be consulted for details on methodology and results.

Element	Detailed Explanation	BaySys Publication
M1	Arctic HYPE (full Arctic domain, known as AHYPE)	*Andersson et al., 2015; *Lindström et al., 2010
M2	AHYPE (Hudson Bay drainage basin domain)	MacDonald et al., in revision
M3	AHYPE (HBDB domain, calibrated version known as HHYPE)	
M4	HHYPE (calibrated with process improvement)	

M5	HHYPEREG (embedded regulation)	Tefs et al., in preparation (a)
M6	HHYPENAT (re-naturalized landcover/reservoirs)	Tefs et al., in preparation (b)
M7	HHYPE (Lower Nelson River Basin domain)	MacDonald et al., in revision; Pokorny et al., (2020)
M8	WATFLOOD (Lower Nelson River Basin domain)	Pokorny et al., (2020)
M9	VIC (Lower Nelson River Basin domain)	Lilhare et al., in revision
M10	HEC-HMS (Lower Nelson River Basin domain)	Pokorny et al., (2020)
M11	Ensemble of Lower Nelson River Basin (LNRB) models	Pokorny et al., (2020); Lilhare et al., in revision
D1	Observed discharge records (1961-2018)	*Water Survey of Canada, *Manitoba Hydro, *Hydro-Québec, *Ontario Power Generation
D2	Gap-filled HBDB outlet (drainage area corrected) discharge record	*Déry et al., 2011
D3	Discharge optimization dataset (contains upstream points and outlets (1981- 2010))	
D4	Observed evapotranspiration and soil moisture data	*fluxnet.ornl.gov
D5	Multi-criteria (ET, Q, θ) optimization parameter set (1981-2010)	see D2 and D4
D6	HydroGFD climatic forcing data set (Total daily precipitation, max daily temperature, min daily temperature) (1981-2015)	*Berg et al., 2018
D7	Full suite of 154 CMIP-5 global climate models	*Taylor et al., 2012
D8	19 global climate models selected for maximum HBDB variability	Stadnyk et al., 2019
D9	19 climate models daily quantile mapping bias-corrected to HydroGFD	*Chen, et al., 2013
D10	5 climate models selected from BaySys 19 climate models (based on variables generated by individual models)	Ridenour et al., 2019
D11	NCRB regulated reservoir data selected from optimization discharge (D3)	Tefs et al., in preparation (a)
D12	NCRB regulated reservoir operational data and regulation reports	
D13	Flooded reservoir areas before and after LGRC development	*Proprietary Hydro-Québec data
D14	Pre-development stage/discharge data to develop stage-discharge reservoir outflow curves (re-naturalized model)	Tefs et al., in preparation (b)
D15	Net basin supply timeseries of 12 LGRC regulated sub-basins	*Proprietary Hydro-Québec data
D16	LGRC regulation rules	
D17	LNRB inflows (Notigi CS and Jenpeg GS) taken from larger discharge dataset (D3) (1981-2010)	See D3

D18	ANUSPLIN reanalysis data truncated to NCRB	Pokorny et al., in preparation
D19	ERA Interim II reanalysis data truncated to NCRB	Lilhare et al., (2019); Lilhare et al., in revision
D20	NARR data truncated to NCRB	
D21	WFDEI data truncated to NCRB	
D22	Observed ECCC climatic data gridded by interpolation with NCRB	
D23	Observed AHCCD climatic data gridded by interpolation with NCRB	
D24	Ensemble of reanalysis climate data over the NCRB (1981-2010)	
D25	Sets of sensitive parameters for all models in the model ensemble in the LNRB (1981-2010)	Lilhare et al., in revision
D26	Sets of sensitive parameter distributions for all models in the model ensemble in the LNRB (1981-2010)	
P1	Truncation of AHYPE to Hudson bay domain	MacDonald et al., in revision
P2	Calibration of Hudson Bay domain AHYPE model (HHYPE)	
P3	Addition of prairie NCA and frozen soil processes and lake cluster parameterization for HHYPE	
P4	Truncation of HHYPE model to LNRB domain	Pokorny et al., 2020
P5	K-means cluster analysis used to select 19 GCM-RCP combinations from CMIP-5 154 model-ensemble	Stadnyk et al., 2019
P6	Bias correction of CMIP-5 GCM-RCP combinations using HydroGFD as reference product over 1981-2010 using quantile mapping	*Chen, et al., 2013
P7	Embedding NCRB regulated reservoir algorithm into HHYPE (HHYPEREG)	Tefs et al., in preparation (a)
P8	Removal of regulated reservoirs and re-naturalization of flooded reservoirs to pre-development land-cover (HHYPENAT)	Tefs et al., in preparation (b)
P9	Regulation of LGRC inflows at 12 regulation points	*Proprietary Hydro-Québec process
P10	Temporally variant VARS to determine sensitive parameters and ranges for LNRB model ensemble	Pokorny et al., 2020
P11	OLHS to determine optimal distributions of sensitive parameters for LNRB model ensemble	
P12	GLUE to produce probability intervals for flow projections on daily Nelson River discharge (1981-2010)	
P13	Propagation of uncertainty bounds from Nelson River (1981-2010) to all HBDB rivers (1981-2070)	TBD
O1	Ensemble (5 GCM-RCPs) monthly discharge from Arctic rivers using AHYPE	Broesky et al., in preparation
O2	Ensemble (19 GCM-RCPs) daily hydrologic study of HBDB major regions (1981-2070)	MacDonald et al., 2018

O3	Regulated daily discharge of LGRC outlets (1981-2070)	Tefs et al., in preparation (b)
O4	Regulated daily discharge of HBDB outlets (LGRC excluded) (1981-2070)	
O5	Re-naturalized daily discharge for HBDB outlets (1981-2070)	
O6	Nelson River daily discharge uncertainty and probability bounds (1981-2010)	Pokorny et al., 2020
O7	Daily uncertainty and probability bounds for all HBDB rivers (1981-2070)	TBD

9.2 Models and Methods

Modeled Climate Data and Observed Discharge Datasets

Prior to hydrologic modeling, the development of a robust climatic input ensemble was necessary. This began with selecting a set of 14 General Circulation Models (GCMs) varyingly coupled with Representative Concentration Pathways (RCPs) 4.5 and 8.5 for a total of 19 climate simulations. These were selected from the 154 simulations available through the Climate Model Intercomparison Project Phase 5 (CMIP-5; Taylor et al., 2012). The HydroGFD re-analysis climate product (Berg et al., 2018) was chosen as the primary reference dataset product (for bias- correction) and hydroclimatic input (for model calibration) following consultation with Manitoba Hydro and Team 6. This product was chosen because it is: (1) near real-time and would provide overlapping “observed” data during the BaySys fieldwork cruise(s), (2) an ERA-based product, therefore consistent with forcing used in the oceanographic Nucleus for European Modelling of the Ocean (NEMO; Madec et al., 2008) model described in Chapter 6, (3) a corrected reanalysis product used by the Swedish Meteorological and Hydrological Institute (SMHI), and (4) globally available at a resolution consistent with continental-scale modeling (0.5° x 0.5° grid resolution).

Input was prepared for use in hydrologic models using two methods to assign gridded GCM data to sub-basin scale. A set of hydrologic inputs was developed first using Inverse Distance Weighting (IDW; Lu & Wong, 2008) and a second using the Nearest Neighbour (NN) method. IDW was selected and the optimal radius calibrated based on a sensitivity study of the Arctic domain. A large radius produced the smallest global RMSE, but was found to create local errors in specific basins. This was particularly noted in the LGRC during the process of regulating discharge.

For calibration of the hydrological models, observed discharge datasets were compiled. Upstream nodes were calibrated using Water Survey of Canada (WSC) gauges available publicly through their website. These include streamflow records for regulated (Tasks 2.1 and 2.3) and natural (Task 2.1) gauges. To quantify calibration performance at the outlets to the HBC, adjusted and gap-filled records were used, as developed for the 42 largest rivers draining Hudson Bay, James Bay, and Ungava Bay (Déry et al., 2005). Split-sample calibration and validation were performed over the reference period 1981-2010, with the first five years of each decade included in the calibration record and the last five included in the validation record. 101 gauges were selected as described in Section 9.3.

Development of Continental-Scale Hydrologic Models

Task 2.1 comprises the development of continental-scale runoff models of two domains. These models are used together to provide input (in the form of discharge at the river outlets) to the NEMO model. The hydrologic model selected was the Hydrological Predictions for the Environment (HYPE) model (Lindström et al., 2010) developed by the SMHI. It was chosen for its strength in physically-based modeling, particularly in cold regions (i.e., snow accumulation, snowmelt, frozen rivers) and continental-scale hydrologic modeling (Pechlivanidis & Arheimer, 2015). It was also preferred to other models because it is an open-source model onto which new processes have been added according to BaySys needs. Calibration was run using Marko Chain Differential Evolution (MCDE; Vrugt et al., 2009) for a robust calibration with built-in sensitivity analysis.

Hydrologic modeling of the Arctic domain was done using Arctic-HYPE (AHYPE) configuration (Andersson et al., 2015) of HYPE using BaySys climate forcing. The AHYPE model is an application of the HYPE model extending over the complete Arctic drainage basin (excluding Greenland), calibrated to a gap-filled global discharge dataset (Dai & Trenberth, 2002). This gap-filled dataset was also used to drive the NEMO model beyond the Arctic domain; however, regulation rules for extended runoff domain (outside Hudson Bay) were not included in the A- HYPE configuration. The HBC NEMO configuration requires coastal discharge for a domain extending to 20° south. The Arctic Ocean drainage domain model (AHYPE) provides boundary discharge input at a monthly resolution at 3002 outlets for the BaySys NEMO model developed by Team 6. This water reaches the HBC domain through the Hudson Strait (eastern) and the Hecla and Fury Strait (northwestern) as shown in Figure 9.1. Reducing the AHYPE model to only the Hudson Bay domain, the Hudson HYPE (HHYPE) model was created.

Uncertainty Assessment of the LNRB

Task 2.2 comprises a sensitivity study of the Lower Nelson River Basin (LNRB) and uncertainty study of the total discharge of the Nelson River. This is done by examining the sensitivity and associated uncertainty caused by input, model structure, parameter optimization, and output used in the calibration process. In the LNRB itself, multiple historic re-analysis climatic data-products are examined at a 10km grid resolution to establish basin and sub-basin uncertainty (Yue et al., 2002). Beyond the LNRB, the watersheds that drain this region (NCRB) are examined to establish their spatial and temporal correlation to observed data (Asong et al., 2017; Lespinas et al., 2015). For all simulations, the LNRB models were forced by HYPE simulated flows (under the same climate forcing) at the Notigi and JenPeg control points where upstream flows from the greater Nelson-Churchill watershed enter the LNRB.

The hydrologic sensitivity and associated discharge uncertainty of the LNRB in a semi-distributed model, the Variable Infiltration Capacity (VIC; Liang et al., 1994) model is examined. Using the 10km LNRB historic re-analysis datasets, a range of climatic input values were created for the LNRB. This range of input is fed to VIC and three other hydrologic models: Hydrologic Engineer Corps – Hydrologic Modelling System (HEC-HMS; Charley et al., 1995), WATERloo FLOOD forecasting system (WATFLOOD; Kouwen, 1988), and a truncated version of the HHYPE model. A set of sensitive parameters and ranges for each model was developed with the input ensemble using temporally variant Variogram Analysis of Response Surfaces (VARS; Razavi & Gupta, 2016). Following this, a Generalized Likelihood Uncertainty Estimate (GLUE; Beven & Binley, 1992) analysis was run to associate total uncertainty with input and parameter optimization. The parameter sets used in the GLUE analysis were selected using Orthogonal Latin Hypercube Sampling (OLHS; Gan et al., 2014) such that parameters had selection density proportional to their sensitivity.

Regulated Discharge Modelling for the HBDB

The effects of regulation (for hydroelectric power generation) on discharge volume and timing are well-noted in the HBDB (Anctil & Couture, 1994; Déry et al., 2011) as a major effect on freshwater discharge regimes in the last century. The role of reservoir regulation in freshwater dynamics in HYPE is noted as a source of modeling error at the continental scale (Pechlivanidis & Arheimer, 2015). To substantively differentiate the effects of climate change and regulation on freshwater discharge, two versions of the HHYPE model were developed: one with improved regulation in the NCRB and LGRC, one with all forms of regulation removed throughout the entire model, called the re-naturalized model.

The NCRB and LGRC were selected due to their large effects on the outflow timing or volume (due to diversions) to Hudson Bay and James Bay, respectively. Other HBDB heavily fragmented river systems, such as Moose River (Dynesius & Nilsson, 1994), were excluded from this analysis. Although it features many regulation points, the Moose River regulation was not found to affect the timing or volume of water to Hudson Bay significantly. Similarly, although many major river systems in the Arctic contain substantial regulation (i.e., the Ob River), the HBC flow dynamics are insensitive to these effects at the monthly resolution or Arctic Domain input. There were also significant barriers to data-availability regarding observed datasets and regulation practices.

9.3 Operations and Progress to Date

Modeled Climate Data and Observed Discharge Datasets

Details of the study domain, the selected climatic ensemble, and the selection of HYPE as the primary hydrologic modeling system for the region have been compiled in the freshwater section (Chapter 3) of the Integrated Regional Impact Study (IRIS) for Hudson Bay (Stadnyk et al., 2019). The GCM-RCP combinations which make up the climatic input-ensemble (1981- 2070) were bias-corrected by the Ouranos Consortium using quantile mapping (Chen, et al., 2013) referencing HydroGFD over the historic period 1981-2010.

For observed discharge: average annual values, interannual and interdecadal variability, and climate-period trends from major rivers were evaluated as a baseline study to evaluate the hydrologic conditions surrounding Hudson Bay (Déry et al., 2016). A further study expanded on those discharge records to distinguish the historical effects of climate change and regulation using their power spectra and intra-week flow characteristics (Déry et al., 2018). These studies have been used for calibration, validation, and to place modeled discharge in the context of observational proof. To further aid in contextualizing observational studies, a baseline climatic study was conducted to establish average conditions over a historic climate-normal period (1981 to 2010). These averages were used to compute monthly anomalies and rankings for each year of observational field campaigns (summers 2015 to 2019; Lukovich et al., in preparation).

Input assigned to HYPE sub-basins using IDW interpolation was used for the full HBDB domain within the re-naturalized model as well as within the regulated model for the HBDB domain excluding James Bay. James Bay regulated results use NN input to reduce errors in the LGRC regulated system. The use of the full James Bay Drainage Basin (JBDB) rather than the LGRC alone was selected to minimize discontinuity of total flow volumes between regulated and re-naturalized results. The under and over-estimates of specific watersheds are smoothed for IDW results when considering larger regions. Limiting

the NN input to James Bay also preserves input continuity between regulated and re-naturalized results for all sampled field data locations, allowing direct intercomparison in future studies.

Development of Continental-Scale Hydrologic Models

The improved Hudson Bay HYPE (HHYPE) model developed in Task 2.1 has been completed, with results passed to Tasks 2.2 and 2.3. Two new physical processes were added to the existing AHYPE code: prairie non-contributing area (NCA) runoff and routines related to flow into and through frozen soils. A structural process was also added by clustering physiographically similar lakes to bypass individual calibrations (there are 7600 lakes in the HBDB, with three parameters each). Calibration confidence was improved by clustering observation gauges according to groups of flow signatures and selecting a balanced number of gauges from each flow-signature cluster, for a total of 101 regulated and natural gauges. This method was compared against four sets of 101 random gauges which were calibrated using the same calibration methodology. The development of the new HYPE model processes and calibration strategies are detailed in (MacDonald et al., in revision). An application of this model using the BaySys bias-corrected climate ensemble shows the impact of 1.5 and 2.0 °C global warming on elements of the HBDB hydrologic cycle (MacDonald et al., 2018).

Monthly discharge from the arctic outlets (excluding the HBDB) has been generated using 5 members of the 19 BaySys climatic-input ensemble (1981 to 2070) and the AHYPE model. As discussed in Chapter 6, only three of the selected BaySys GCM model simulations include sufficient variables to be used for NEMO modeling. Only these models (and their associated RCPs, for a total of five versions) were modeled in AHYPE for efficiency. Spatial and temporal trends will soon be analysed from this model (Broesky et al., in preparation). The discharge projections developed for this task have been distributed to Team 6 and published as part of a study detailing the calibration and sensitivity of the oceanographic model (Ridenour et al., 2019).

Uncertainty Assessment of the LNRB

The uncertainty study of the LNRB central to Task 2.2 has been completed. Elements of this study include climatic input sensitivity and analysis of uncertainty due to input, single-model uncertainty, multi-model sensitivity, and multi-model uncertainty results. Climatic studies include historical re-analysis dataset comparisons in the industrially-significant and remote (data-sparse) LNRB (Lilhare et al., 2019) and input uncertainty estimates in the larger upstream basin of the NCRB (Pokorny et al., in preparation). The VIC hydrologic model structure has been studied based on parameter optimization, model structure (using multiple combinations of optional model processes), and input (using multiple reanalysis datasets) in the LNRB, assessing sensitivity and associated uncertainty of projected discharges (Lilhare et al., in revision) using VARS. The addition of three other hydrologic models (HHYPE, HEC-HMS, WATFLOOD) and further uncertainty analysis using VARS, OLHS, and GLUE analyses have been used to develop daily probability curves (1981 to 2070) for the Nelson River discharge (Pokorny et al. 2020). These results, along with the discharge ensemble generated by Task 2.3 will be used to develop bay-wide discharge probability curves in Task 2.4, to be undertaken over summer 2019.

Regulated Discharge Modelling for the HBDB

Task 2.3 comprised the creation of regulated discharge records for the NCRB and LGRC basins. This was done by (1) embedding regulation directly into HHYPE in the NCRB (Tefs et al., in preparation (a)) and

(2) coordinating modeling efforts with Hydro-Québec for the LGRC. Together, these results are known as HHYPEREG. The results of the HHYPEREG model (forced using the climatic ensemble) have been distributed for Tasks 2.2 and 2.4 to help generate uncertainty results for the LNRB and HBDB, respectively. A re-naturalized HHYPEREG model (diversions, regulation, and land-cover changes removed: HHYPENAT) has been created. An analysis comparing and contrasting the climatic ensemble results of HHYPENAT and HHYPEREG has been completed (Tefs et al., in preparation (b)). The regulated and re-naturalized outflow ensembles have been distributed to Team 3 for use in nutrient flux estimation (Lee et al., in preparation) and to Team 6 for use in oceanographic modeling (Jafarikhasragh et al, 2019).

It is important to recall that regulated and re-naturalized flows for the NCRB (and HBDB domain excluding the James Bay, which vary insignificantly between regulated and re-naturalized) use the same input interpolation method and can be directly compared to field observations. Conversely, discharge volumes from any given outlet in James Bay are not directly comparable between regulated and re-naturalized due to mixed interpolation methods, with total flow to James Bay being prioritized. Because of this, direct comparison to fieldwork values at the estuary scale is not recommended in James Bay.

9.4 Summary of Results to Date

Modeled Climate Data and Observed Discharge Datasets

The selection of climate models was done using cluster analysis on 10 metrics of climate change (between 1981-2010 and 2041-2070). This method was shown to express over 90% of the total CMIP-5 ensemble variability. Using these climate models as input, overall seasonal discharge trends are shown to have been stable or slowly increasing historically but will increase (with a high degree of trend significance) in all seasons in the future (Stadnyk et al., 2019). Partial results are shown in Figures 9.3 and 9.4.

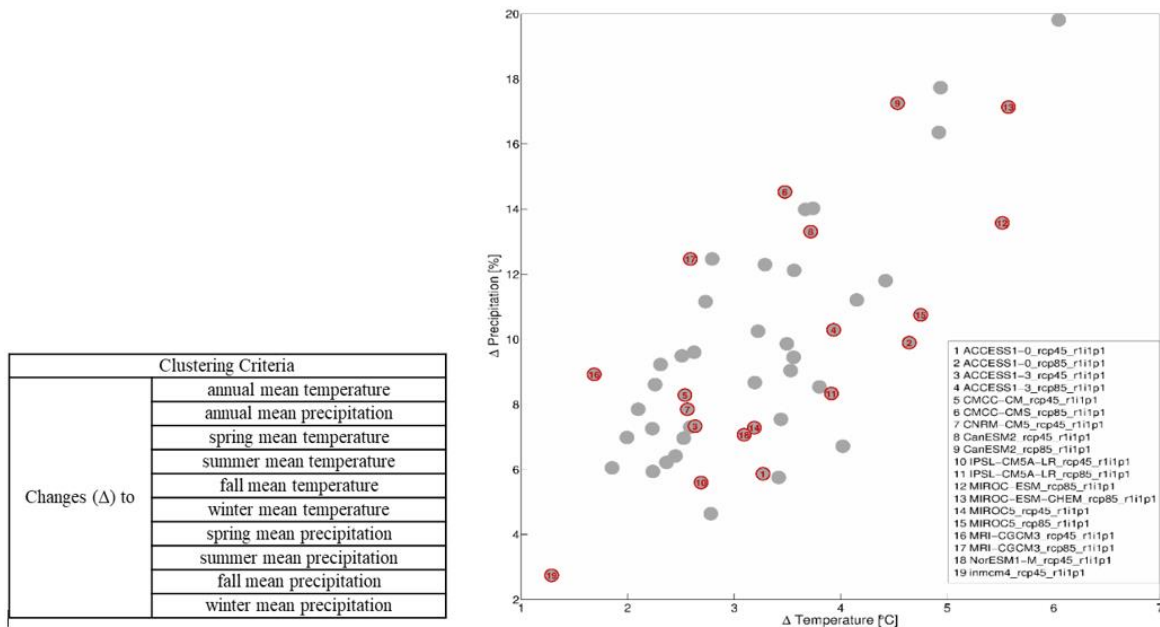


FIGURE 9.3 Climate model clustering criteria and model-ensemble selected for BaySys simulation (shown for two of ten criteria). *Reproduced from: Stadnyk et al., 2019 (Table C-1, Figure C-2).*

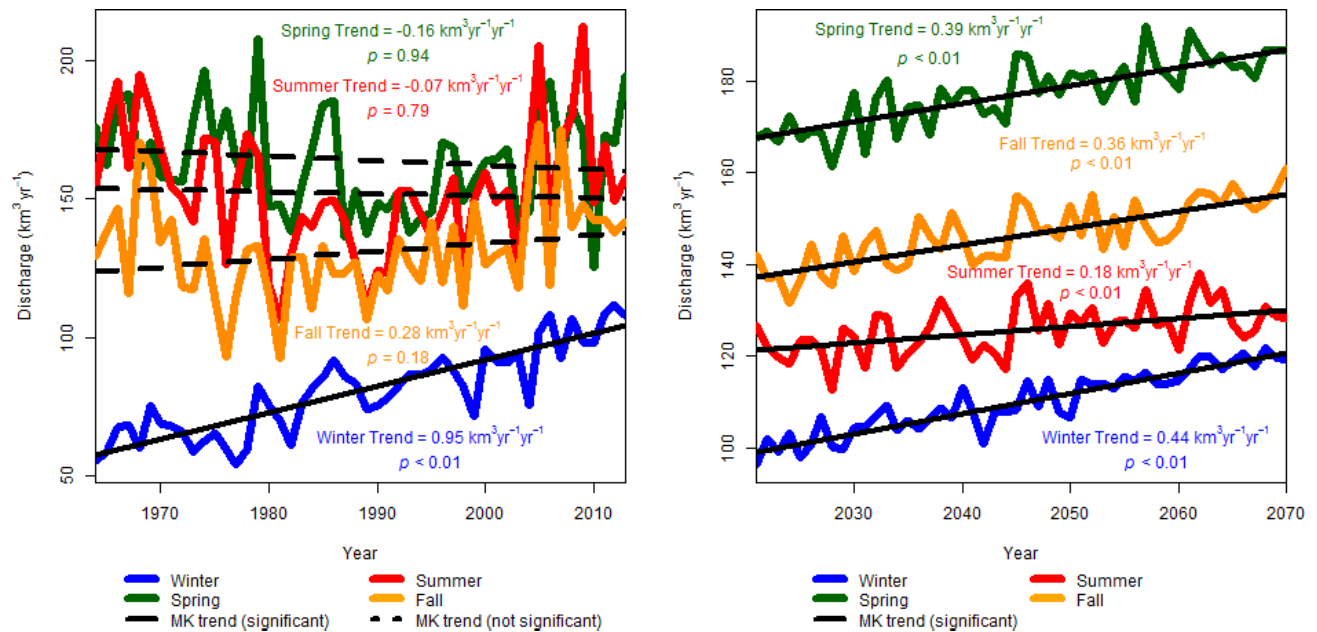


FIGURE 9.4 Seasonal trend analyses and significance of discharge for 21 gauged HBDB rivers for (a) observed, historical (1964-2013) period, and (b) simulated future (2021-2070) period. *Reproduced from: Stadnyk et al., 2019 (Figures 13 and 17).*

Analyzing 21 rivers draining to Hudson Bay with gauged records, distinct trends are seen between regulated and unregulated rivers, such as increasingly divergent inter-annual coefficients of variation. They further show increasingly flattened hydrographs in regulated rivers from 1960 to 2016. This analysis shows the importance of weekly hydropeaking (reduced weekend flows coincident with lower energy demand) in rivers regulated for hydroelectric generation (Déry et al., 2018). Partial results are shown in Figure 9.5, 9.6, and 9.7.

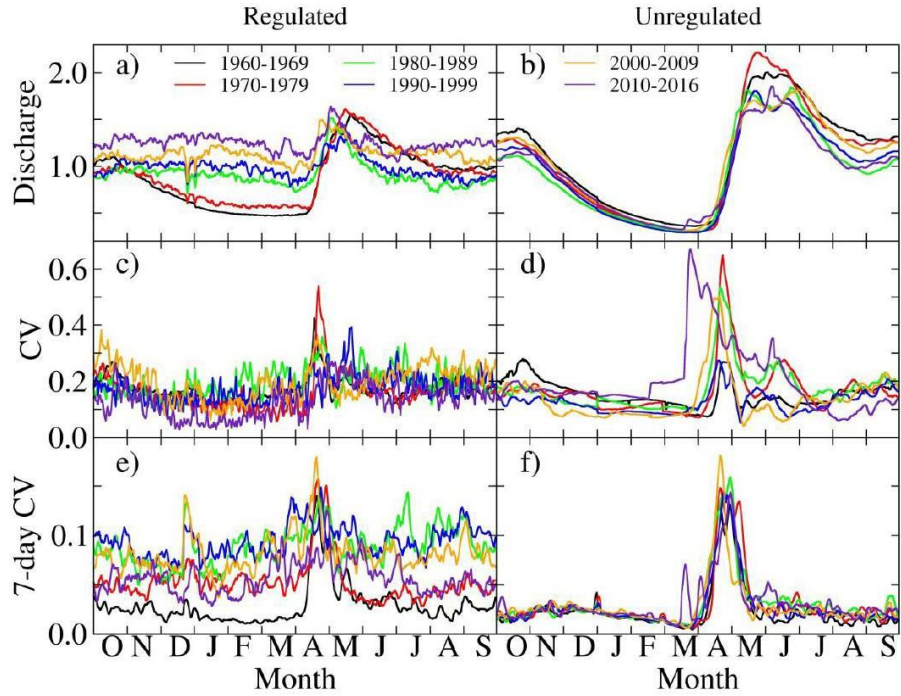


FIGURE 9.5 Decadal water year hydrographs of the (a, b) normalized mean, (c, d) coefficient of variation, and (e, f) coefficient of variation in 7-day moving windows of daily discharge for regulated and unregulated rivers, 1960-2016. *Reproduced from: Déry et al., 2018 (Figure 2).*

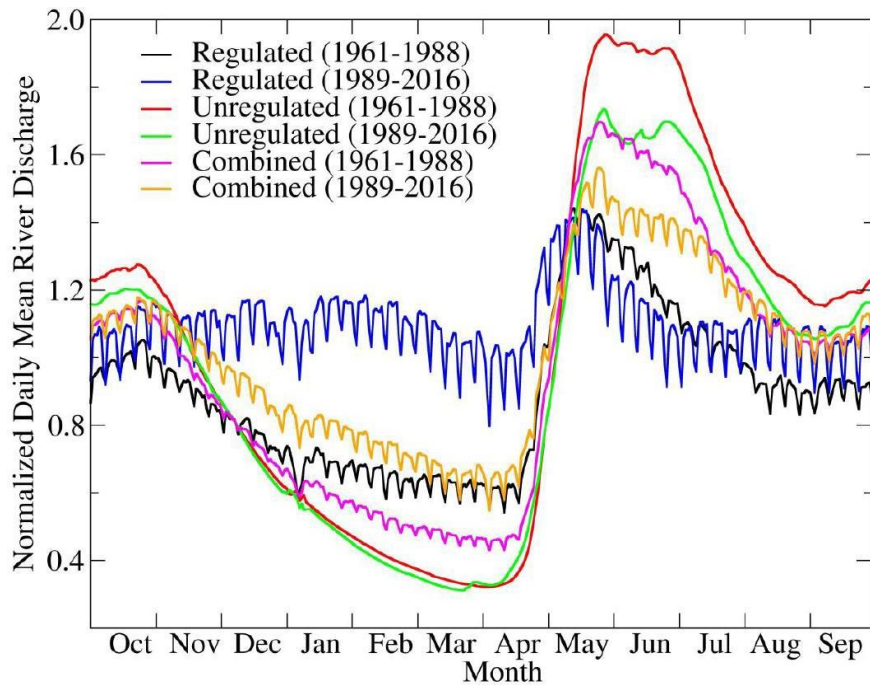


FIGURE 9.6 Water year hydrographs of the normalized mean daily discharge for regulated, unregulated, and combined rivers considering the day of the week during an early (1961-1988) and a late (1989-2016) period. *Reproduced from: Déry et al., 2018 (Figure 3).*

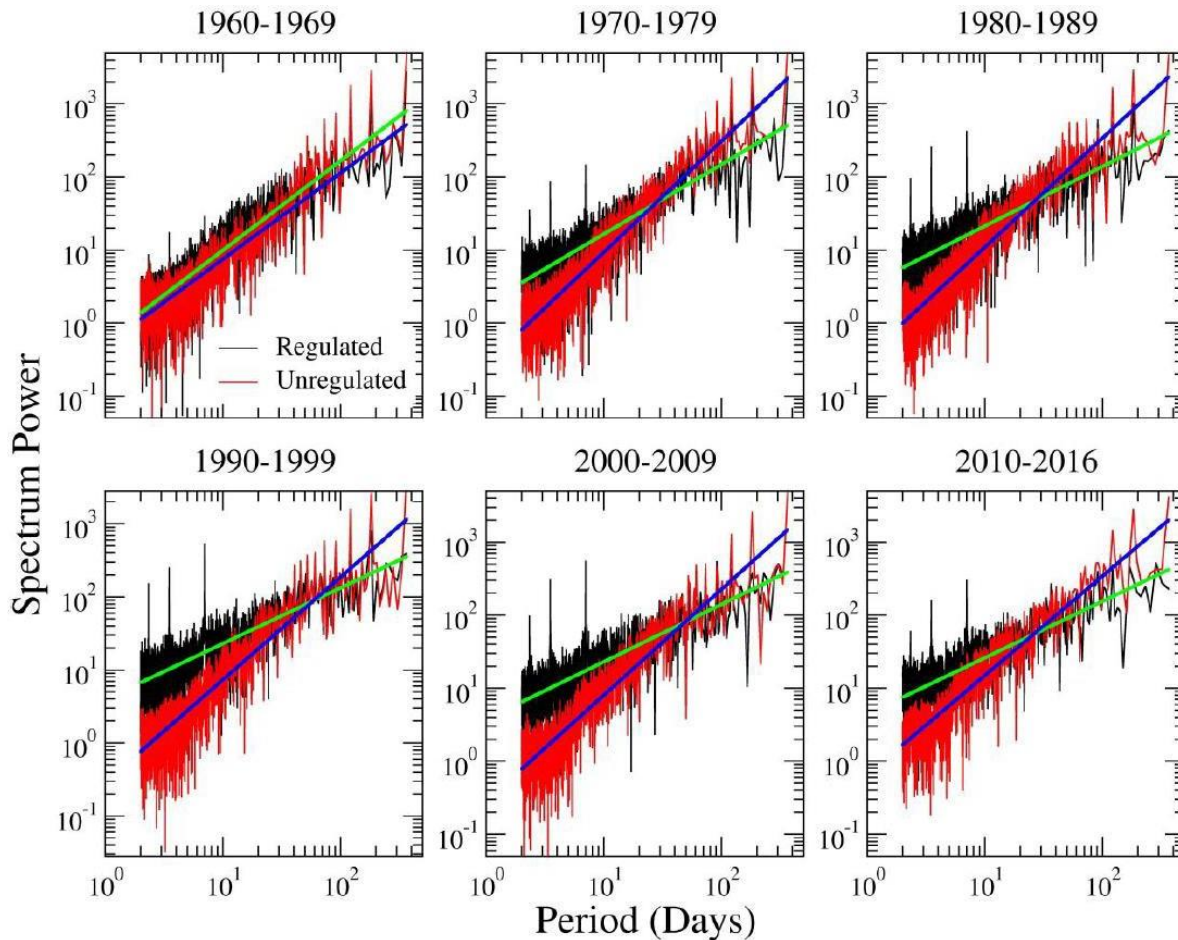


FIGURE 9.7 Decadal spectral analyses of daily discharge for regulated and unregulated rivers, 1960-2016. Thick green and blue lines denote non-linear regressions performed on power spectra covering return periods of 2 to 365 days for the regulated and unregulated rivers, respectively. *Reproduced from: Déry et al., 2018 (Figure 5).*

Monthly distributions of climate-normal (1981-2010) precipitation are much more intense in the eastern HBDB and sparser in the northern and western HBDB. Temperature generally increases inversely to latitude. Discharge is consistently large in the Nelson River and La Grande Rivière (regulated for hydroelectric generation), while the Moose, Koksoak, Albany, and Harricana Rivers (largely unregulated) show the largest seasonal changes due to the spring freshet (Lukovich et al., in preparation). Values for observation years 2016-2018 are not yet generated (pending transfer of up-to-date HydroGFD data from SMHI). Results will be reported when they become available. These will be presented as monthly anomaly charts for precipitation, temperature, and discharge. Partial results are shown in Figures 9.8, 9.9, 9.10, 9.11, 9.12, and 9.13.

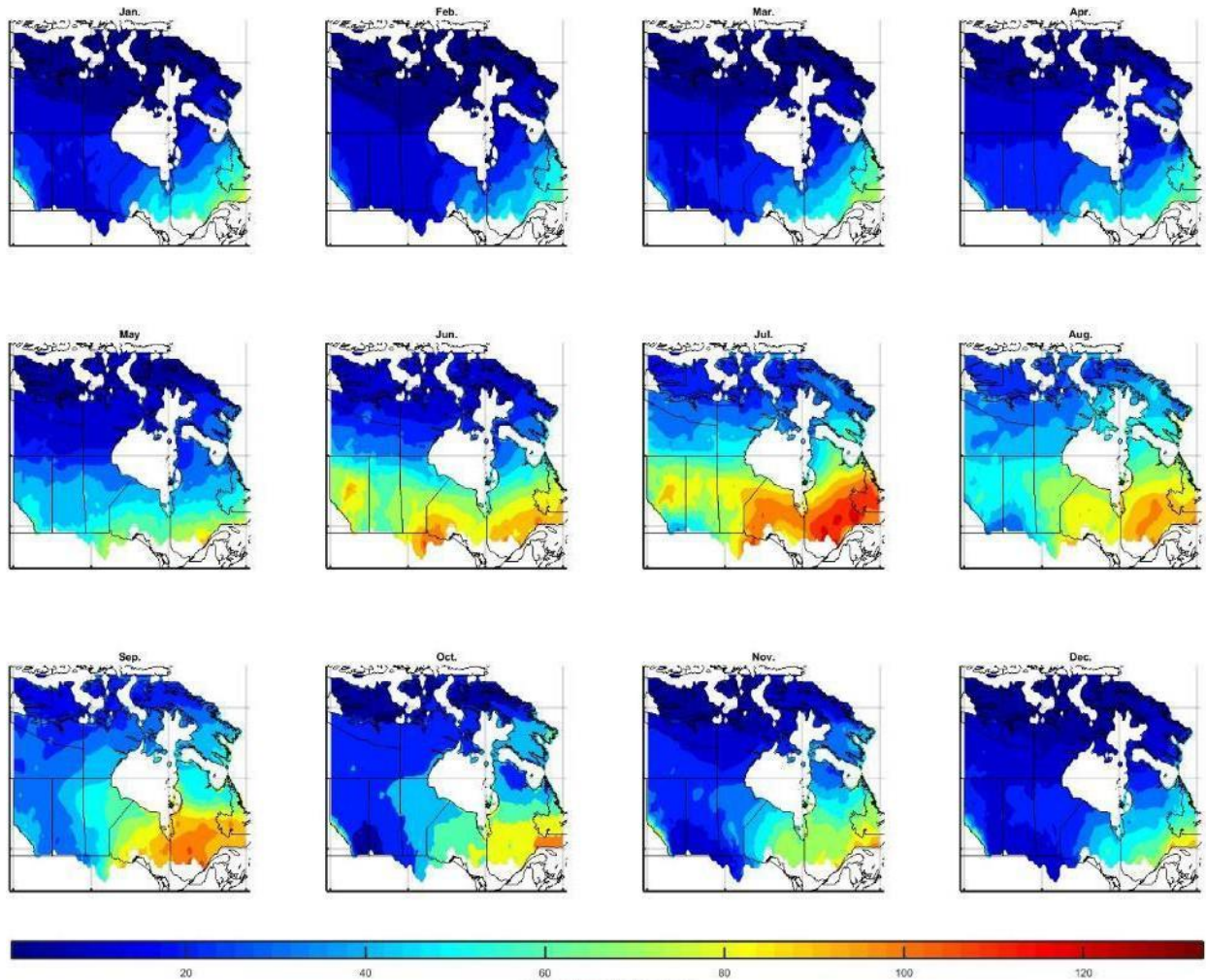


FIGURE 9.8 Average monthly total precipitation [mm] (1981-2010). Contours generated from 0.5° gridded HydroGFD re-analysis data (Berg et al., 2018). *Reproduced from: Lukovich et al., 2018 (Figure TBD) (Confidential pending publication).*

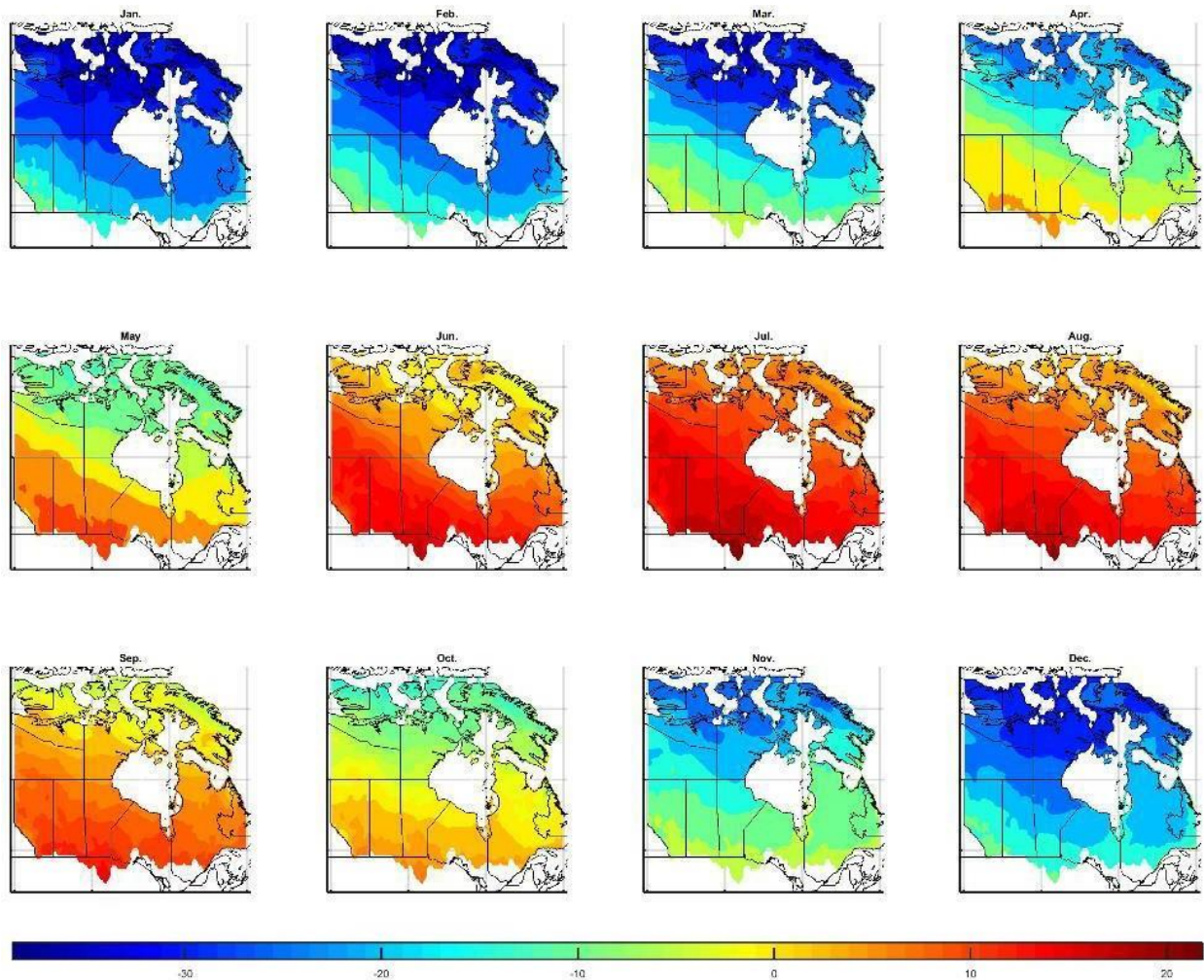


FIGURE 9.9 Average monthly mean air temperature [$^{\circ}\text{C}$] (1981-2010). Contours generated from 0.5° gridded HydroGFD re-analysis data (Berg et al., 2018). *Reproduced from: Lukovich et al., 2018 (Figure TBD) (Confidential pending publication).*

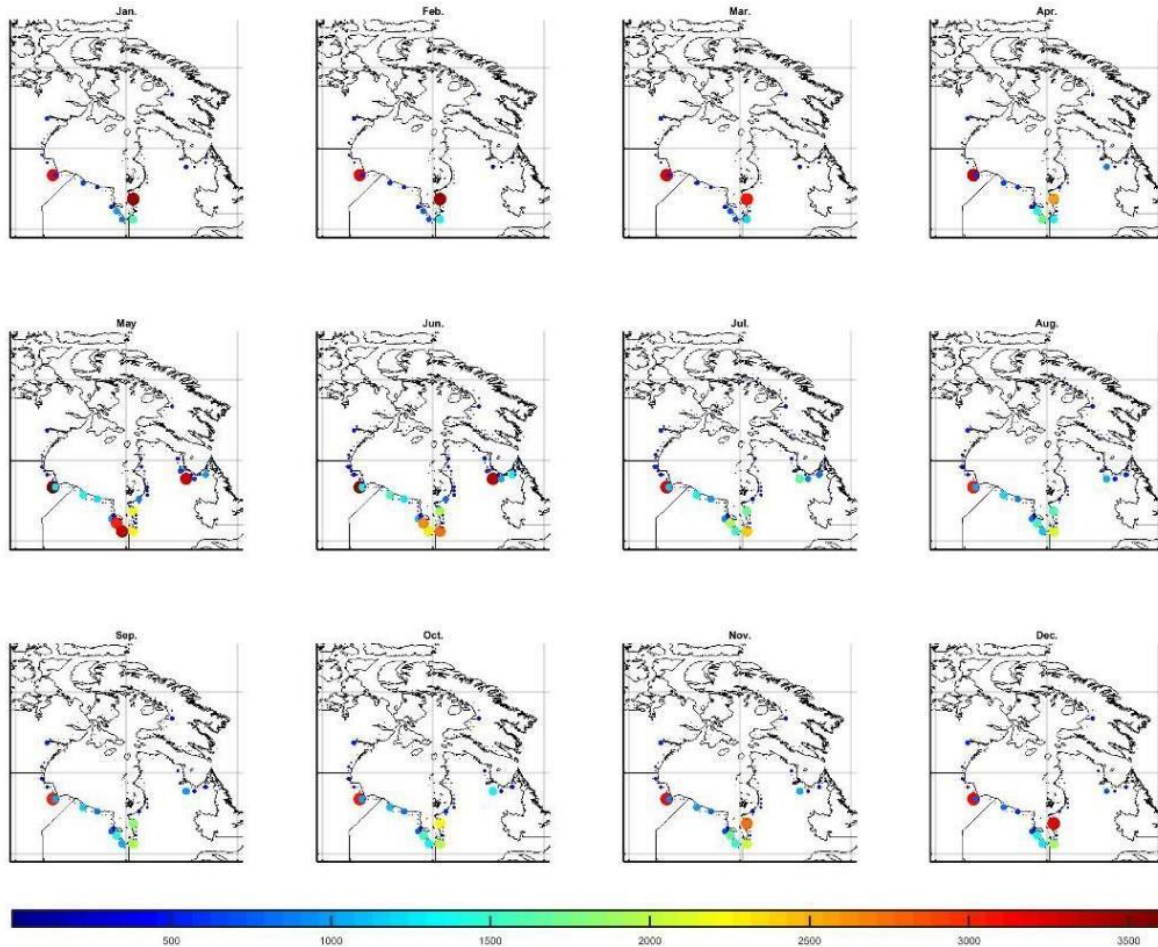


FIGURE 9.10 Average monthly mean discharge [$\text{m}^3 \text{s}^{-1}$] (1981-2010). 398 outlets generated from HYPereg forced by 0.5° gridded HydroGFD re-analysis data (Berg et al., 2018). *Reproduced from: Lukovich et al., 2018 (Figure TBD) (Confidential pending publication).*

FIGURE STILL IN DEVELOPMENT PENDING HYDROGFD DATA 2016 – 2018

FIGURE 9.11 Individual monthly basin-mean total precipitation [mm] (1981-2010). Generated from 0.5° gridded HydroGFD re-analysis data (Berg et al., 2018). Boxes indicate (solid line) reference and (dashed line) observation periods. *Reproduced from: Lukovich et al., 2018 (Figure TBD) (Confidential pending publication).*

FIGURE STILL IN DEVELOPMENT PENDING HYDROGFD DATA 2016 – 2018

FIGURE 9.12 Individual monthly basin-mean mean air temperature [$^\circ\text{C}$] (1981-2010). Generated from 0.5° gridded HydroGFD re-analysis data (Berg et al., 2018). Boxes indicate (solid line) reference and (dashed line) observation periods. *Reproduced from: Lukovich et al., 2018 (Figure TBD) (Confidential pending publication).*

FIGURE STILL IN DEVELOPMENT PENDING HYDROGFD DATA 2016 – 2018

FIGURE 9.13 Individual monthly basin-mean mean discharge [$\text{m}^3 \text{s}^{-1}$] (1981-2010). Sum of 398 outlets generated from HYPereg forced by 0.5° gridded HydroGFD re-analysis data (Berg et al., 2018). Boxes indicate (solid line)

reference and (dashed line) observation periods. *Reproduced from: Lukovich et al., 2018 (Figure TBD) (Confidential pending publication).*

Development of Continental Hydrologic Models

The HHYPE model is improved from the original AHYPE model across numerous model metrics (Nash-Sutcliffe Efficiency: NSE, Kling-Gupta Efficiency: KGE, percent Deviation of mean Volume: %DV) through improved parameterization, calibration and sensitivity analysis, and process addition (MacDonald et al., in revision). Partial results are shown in Figure 9.14, 9.15, and 9.16.

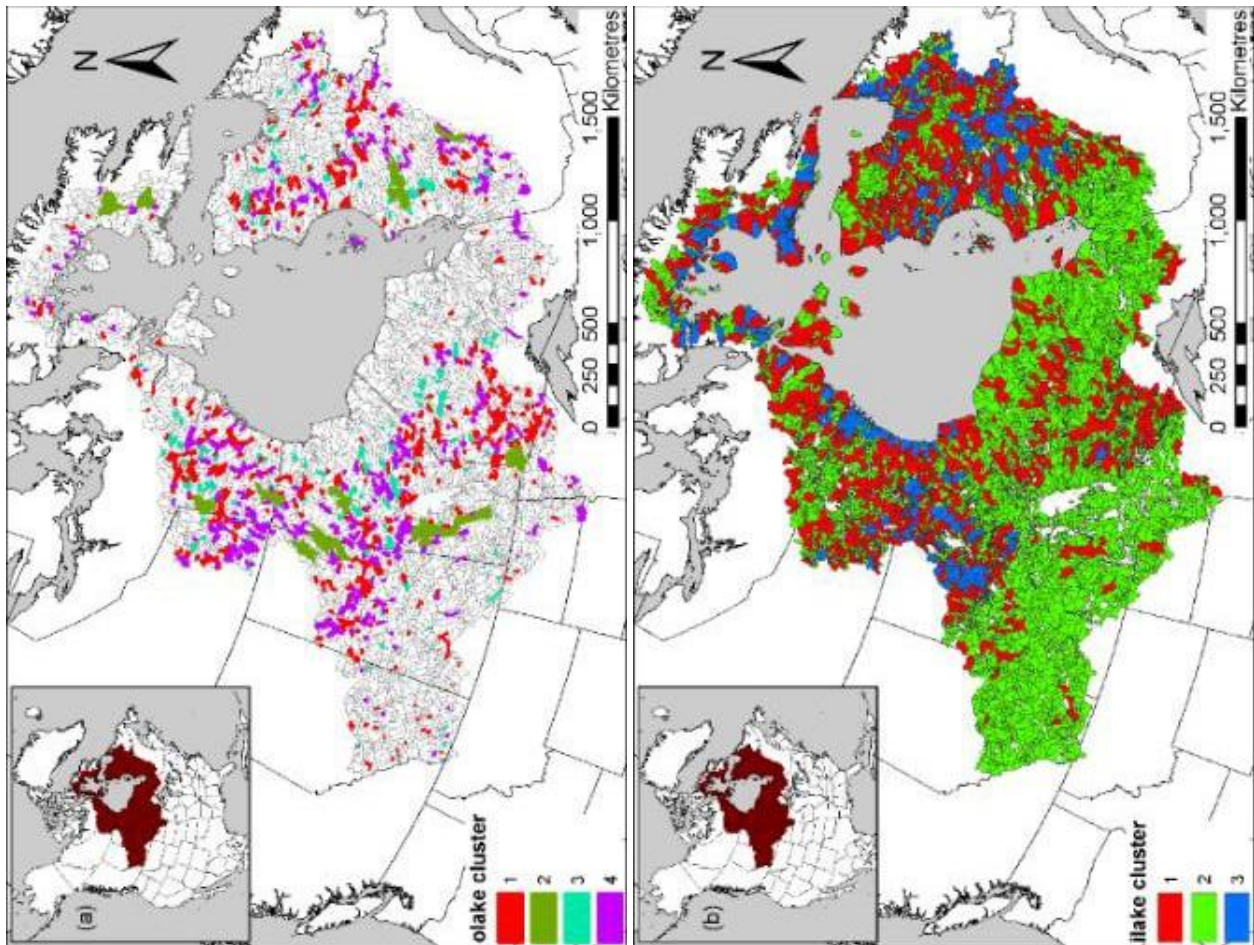


FIGURE 9.14 Maps showing locations of (a) olake clusters, and (b) ilake clusters overlain on A-HYPE subbasins. White subbasins indicate no olakes or ilakes in subbasin. White sub-basins are not included because they are regulated and calibrated separately. *Reproduced from: MacDonald et al., in revision (Figure S1) (Confidential pending publication).*

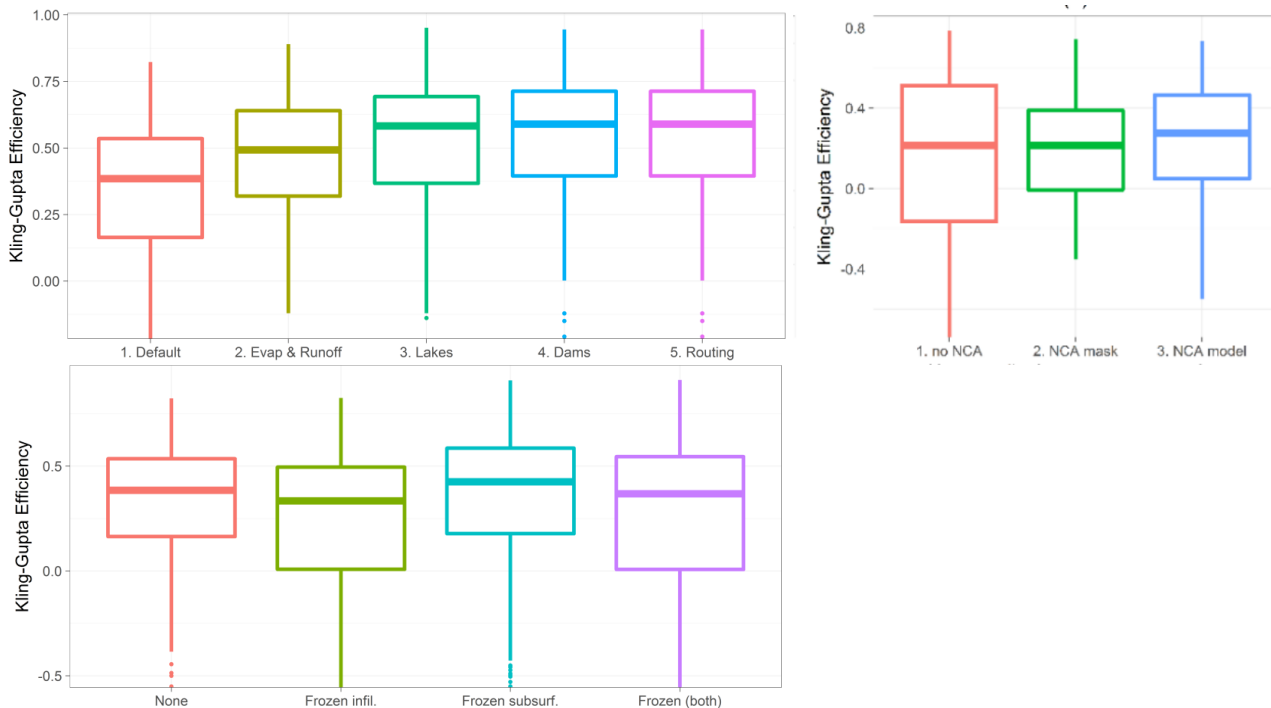


FIGURE 9.15 KGE results (daily discharge, 1971-2013) of model development by process for (a) stepwise calibration over 101 flow signature gauges, (b) NCA parameterizations for 10 gauges, and (c) frozen soil processes over 245 gauges. *Reproduced from: MacDonald et al., in revision (Figures 8, 4b, and 6) (Confidential pending publication).*

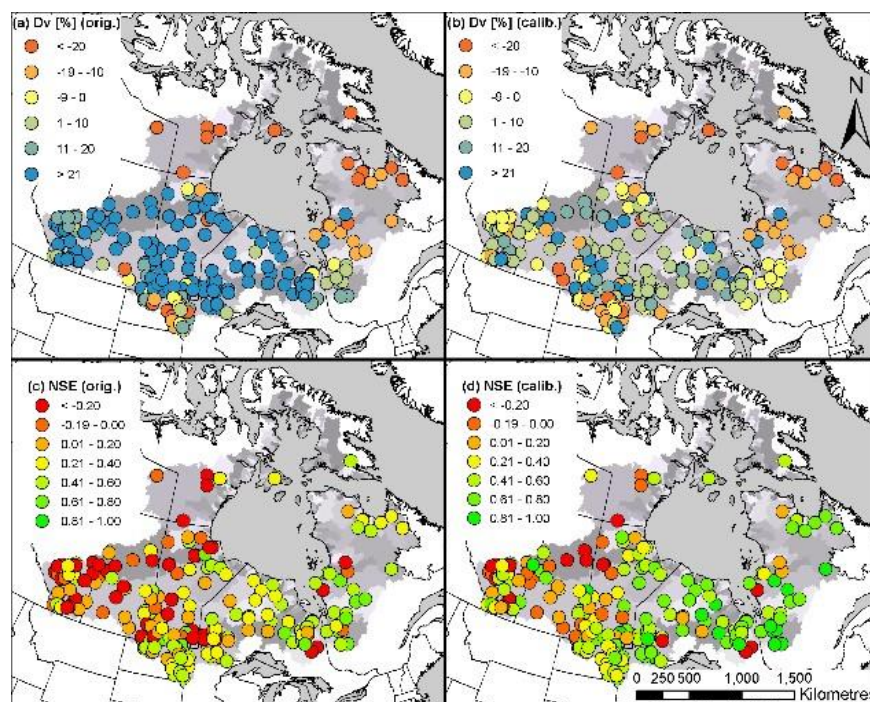


FIGURE 9.16 Spatial plots of model performance statistics: (a) Deviation of runoff volume (original parameters), (b) Deviation of runoff volume (calibrated parameters), (c) Nash-Sutcliffe Efficiency (original parameter), and (d) Nash-Sutcliffe Efficiency (calibrated parameters). *Reproduced from: MacDonald et al., in revision (Figure 9).*

Using this HHYPE model and the BaySys climate ensemble, hydrologic elements were assessed using periods of 1.5 and 2.0 degrees Celsius warming (MacDonald et al., 2018). These show intensifying hydrologic cycles over the entire HBDB. This intensification of the hydrology shows signs of increasing non-linearly between 1.5 and 2.0 degrees warming. This is particularly seen in the northern region (Foxe Basin). Western Hudson Bay shows the smallest increase, but the narrowest confidence intervals. Partial results are shown in Figures 9.17 and 9.18.

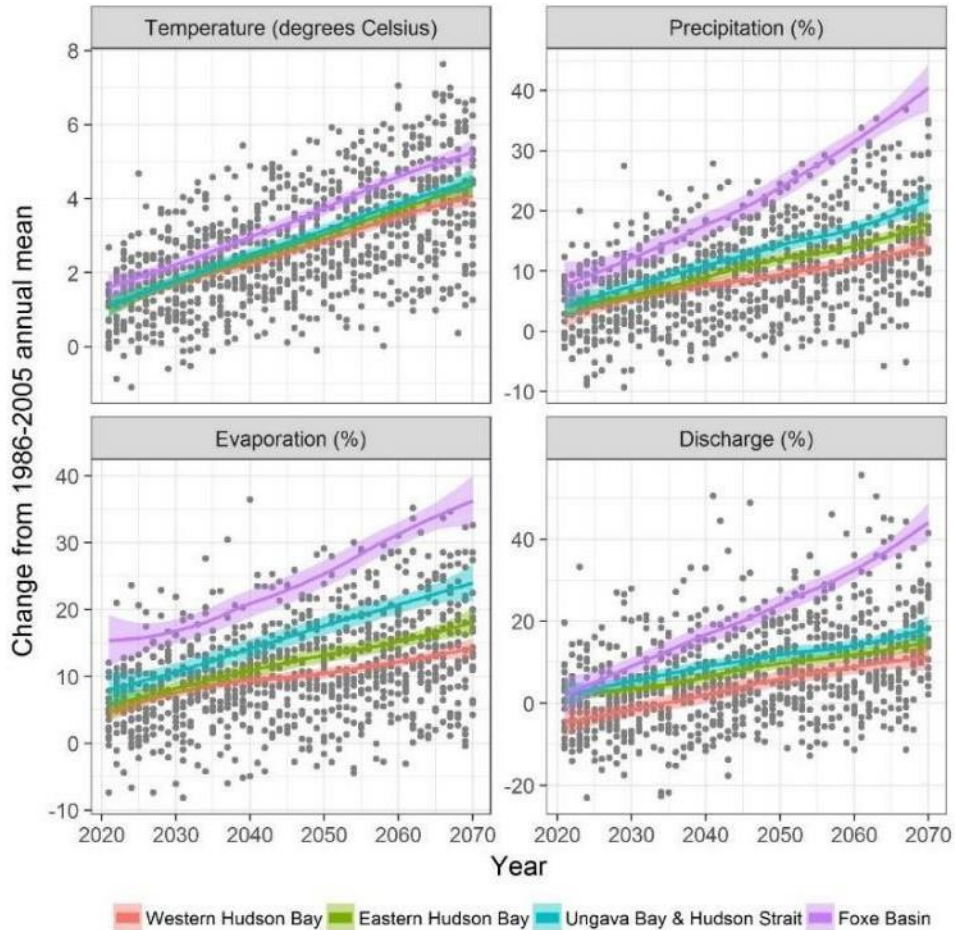


FIGURE 9.17 Projected changes in annual temperature, precipitation, evaporation, and discharge from 1986-2005 annual means using the 19 AHYPE-CMIP5 simulations. Black data points are for the entire HBDB. Coloured locally weighted scatterplot smooth curves are shown for the four regions (grey shading indicates 95% confidence intervals). *Reproduced from: MacDonald et al., 2018 (Figure 2).*

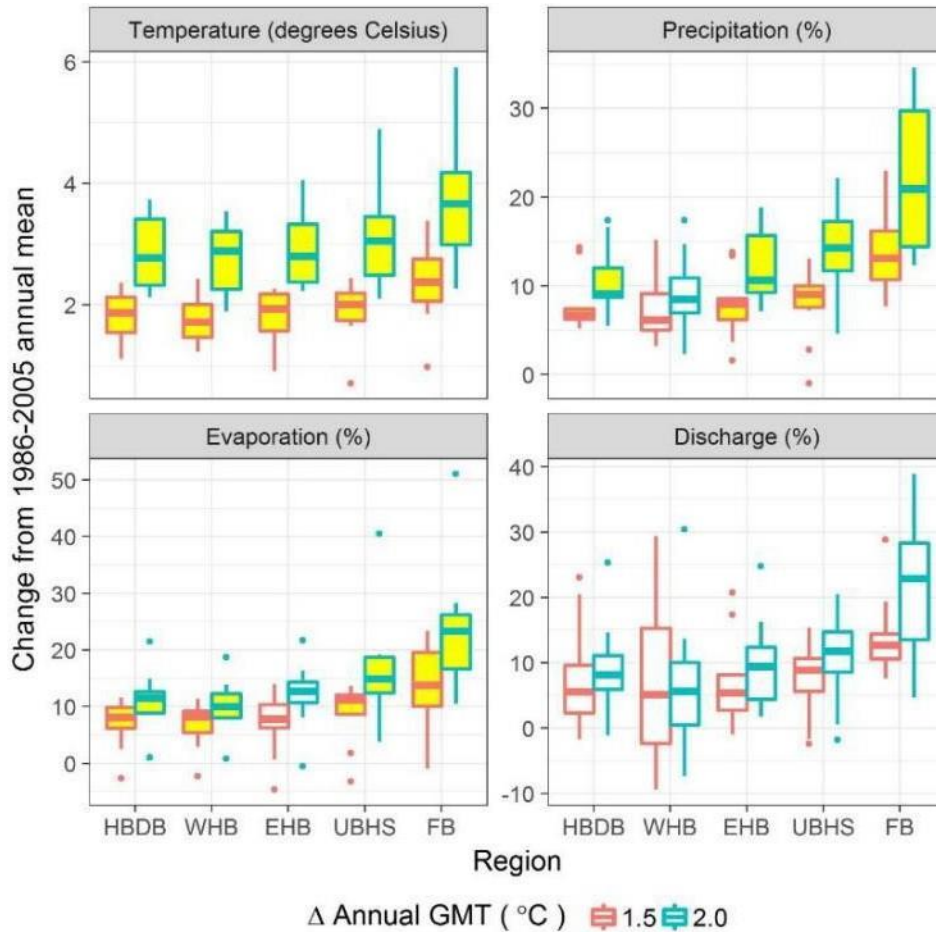


FIGURE 9.18 Projected changes in annual temperature, precipitation, evaporation, and discharge from 1986-2005 for 20-year time slices of GMT increases of 1.5°C and 2.0°C above pre-industrial level. Statistically significant differences resulting from 1.5°C versus 2.0°C GMT warming are highlighted in yellow. Boxplots show the median, 25th, and 75th percentiles at the hinges, and the whiskers extend to show a 95% confidence interval. *Reproduced from: MacDonald et al., 2018 (Figure 3).*

Uncertainty Assessment of the LNRB

An assessment of six historic re-analysis climate products over the LNRB shows the discontinuity of precipitation, even between high-quality re-analysis products and by extension, the value of using an ensemble (whether re-analysis or GCM) rather than any one product (Lilhare et al, 2019). Partial results are shown in Figure 9.19 and 9.20.

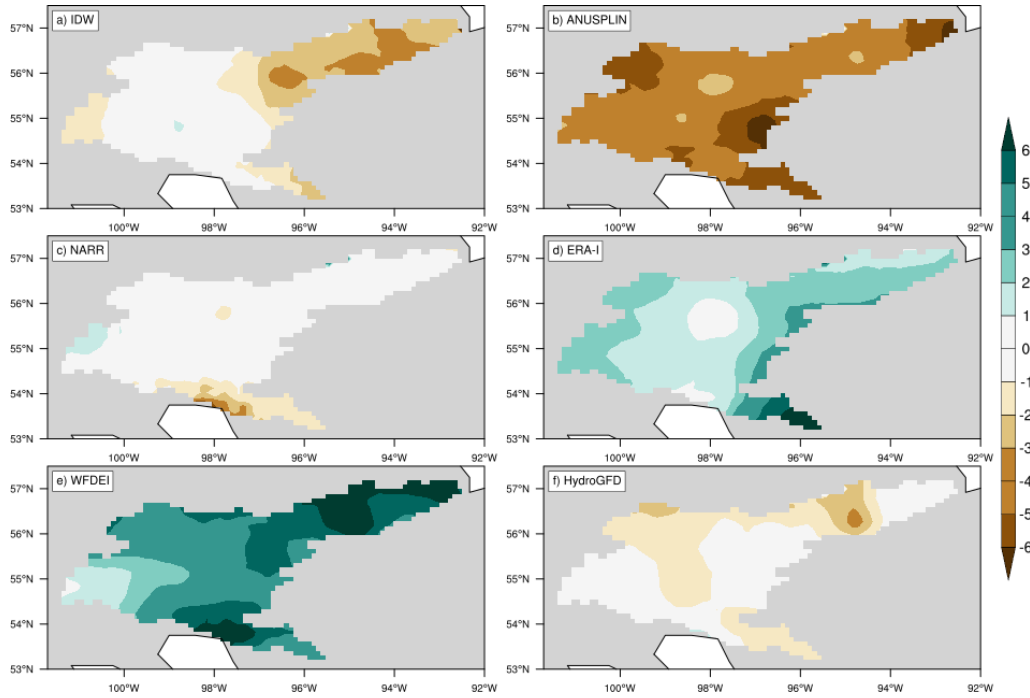


FIGURE 9.19 Bias as measured against the ENSEMBLE total annual precipitation (mm month⁻¹) for the (a) IDW, (b) ANUSPLIN, (c) NARR, (d) ERA-I, (e) WFDEI, and (f) HydroGFD datasets, 1981–2010. *Reproduced from: Lilhare et al., in revision 2019 (Supplementary Figure 3) (Confidential pending publication).*

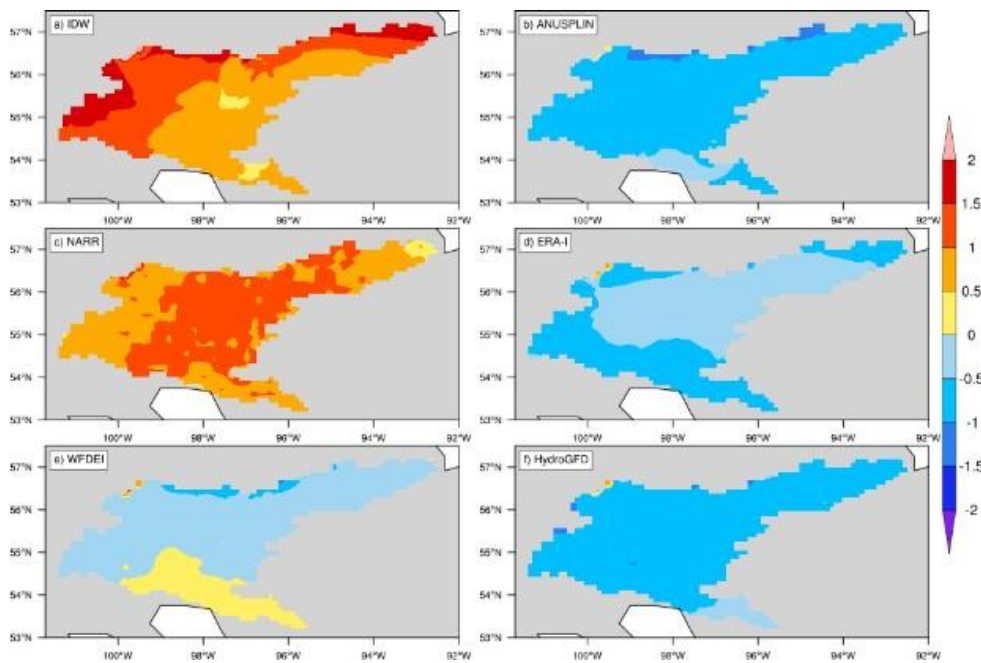


FIGURE 9.20 Bias as measured against the ENSEMBLE mean annual air temperature (°C) for the (a) IDW, (b) ANUSPLIN, (c) NARR, (d) ERA-I, (e) WFDEI, and (f) HydroGFD datasets, 1981–2010. *Reproduced from: Lilhare et al., 2019 (Supplementary Figure 4) (Confidential pending publication).*

A further sensitivity and uncertainty analysis of the LNRB using the VIC hydrological model shows sensitivity of sub-basin discharge to the input products, the calibration metric used, and parameter calibration using VARS and OLHS. These results reinforce the strength of climate-ensembles of input, robust sensitivity analyses, and multi-model ensembles in quantifying uncertainty in discharge projections (Lilhare et al., in revision). Partial results are shown in Figures 9.21, 9.22, and 9.23.

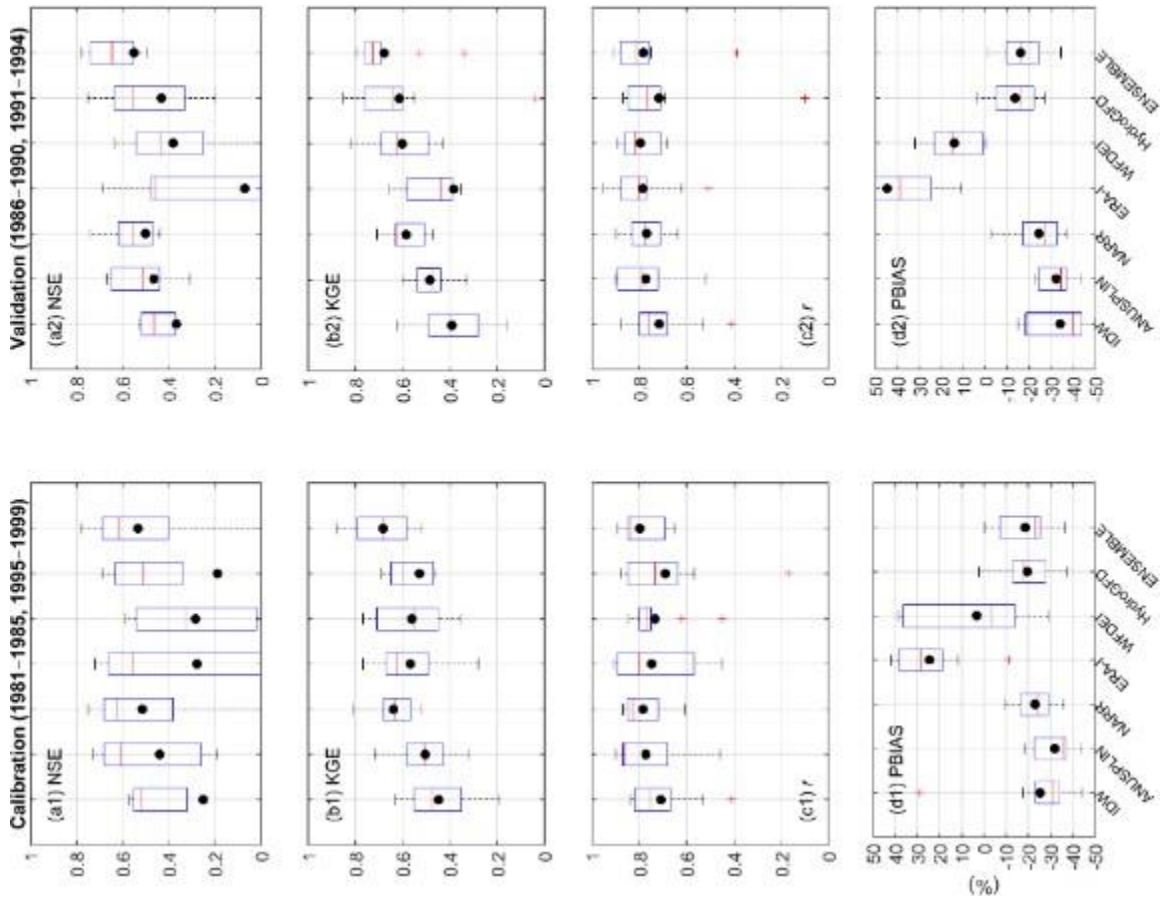


FIGURE 9.21 Boxplots for monthly calibration (a1-d1) and validation (a2-d2) performance metrics, NSE (a1-a2), KGE (b1-b2), r (p -value < 0.05 for all) (c1-c2) and PBIAS (d1-d2), for ten selected sub-watersheds within the LNRB based on IDW-VIC, ANUSPLIN-VIC, NARR-VIC, ERA-I-VIC, WFDEI-VIC, HydroGFD-VIC and ENSEMBLE-VIC simulations. The black dots within each box show the mean, the red lines show the median, the vertical black dotted lines show a range of minimum and maximum values excluding outliers, and the red + signs show the outliers defined as the values greater than 1.5 times the interquartile range of each metrics. *Reproduced from: Lilhare et al., in revision (Figure 3) (Confidential pending publication).*

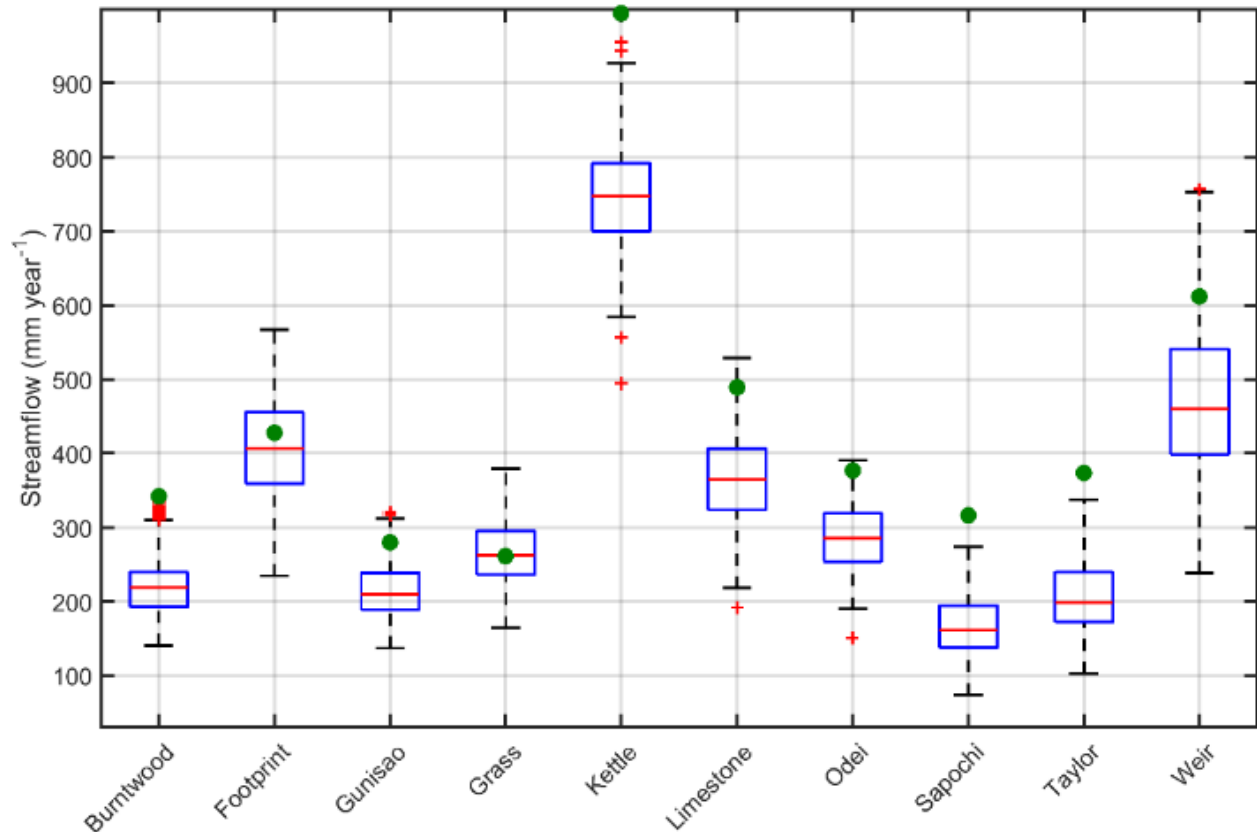


FIGURE 9.22 Annual streamflow sensitivity to parameter uncertainty for all LNRB's sub-watersheds. The green dots show streamflow associated with the control run (calibration), the red lines show the median, the vertical black dotted lines show a range of minimum and maximum values excluding outliers, and the red + signs show the outliers defined as the values greater than 1.5 times the interquartile range of annual streamflow. *Reproduced from: Lihare et al., in revision (Figure 8) (Confidential pending publication).*

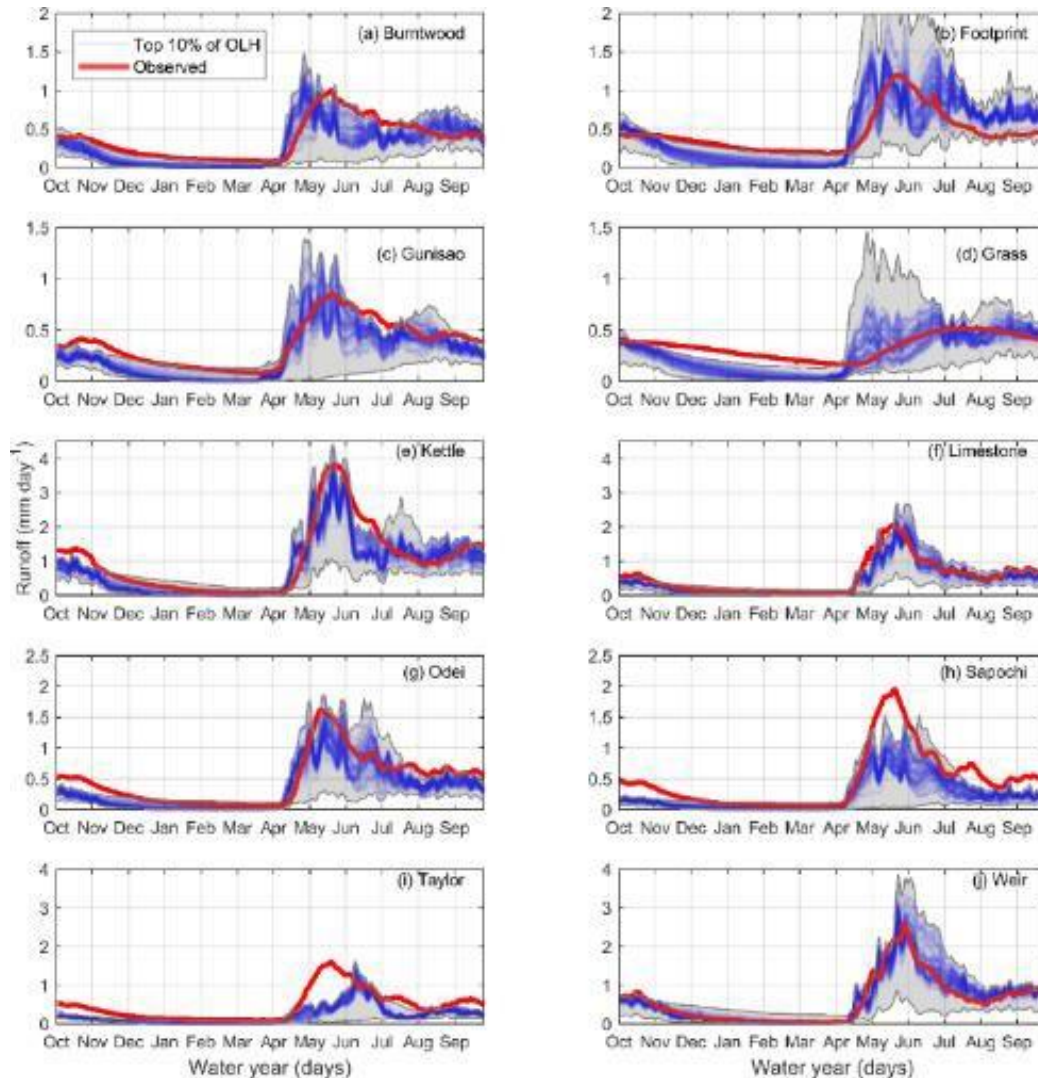


FIGURE 9.23 Streamflow prediction uncertainty associated with estimated parameters from the OLH. Top 10% (shown in blue color) of OLH samples, based on KGE, used for the prediction of observed streamflow for all ten sub-watersheds, water year 1981-2010. Shaded area (grey color) shows the envelope of VIC runs from 600 OLH samples. *Reproduced from: Lilhare et al., in revision (Figure 10) (Confidential pending publication).*

An input study of the NCRB further shows the variability (spatially and temporally) between historic re-analysis climate products, especially in data-sparse regions. By comparing re-analysis products to the Adjusted and Homogenized Climate Change Data (AHCCD), the value is shown of studying not only ensemble-mean but extreme scenarios as well to account for input uncertainty (Pokorny et al., in preparation). Partial results are shown in Figures 9.24, 9.25, and 9.26.

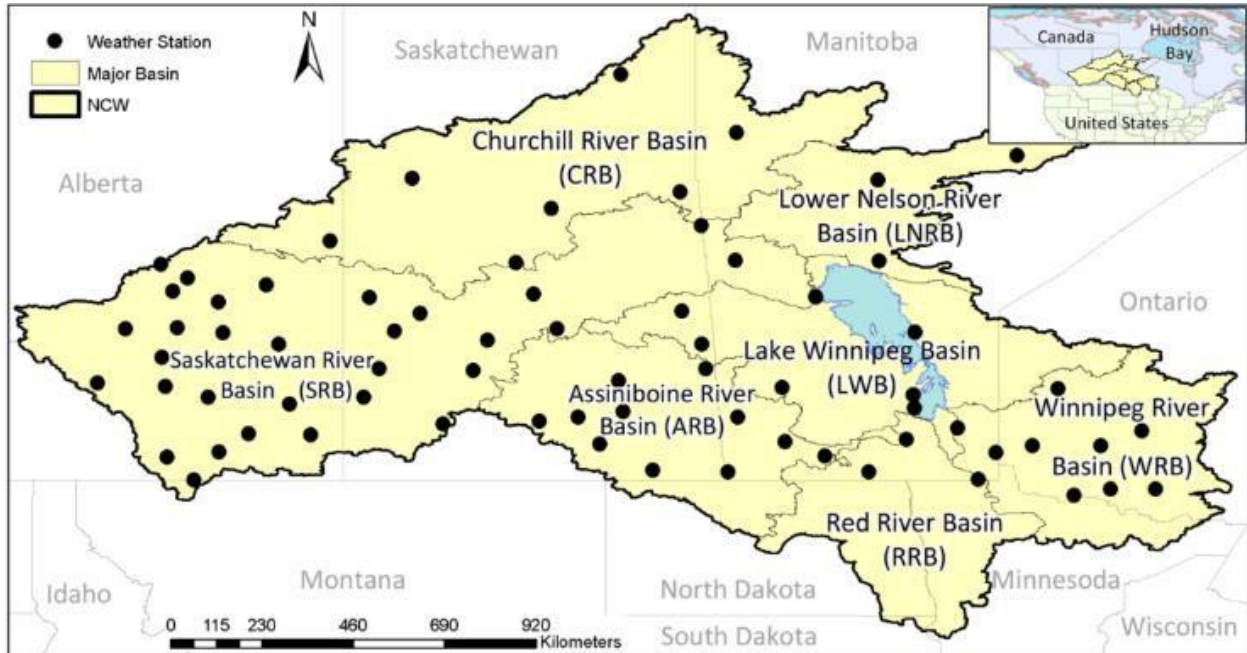


FIGURE 9.24 Map of the Nelson-Churchill Watershed including major basin delineations and 71 selected observed climate station locations. *Reproduced from: Pokorny et al., 2020 (Figure 1) (Confidential pending publication).*

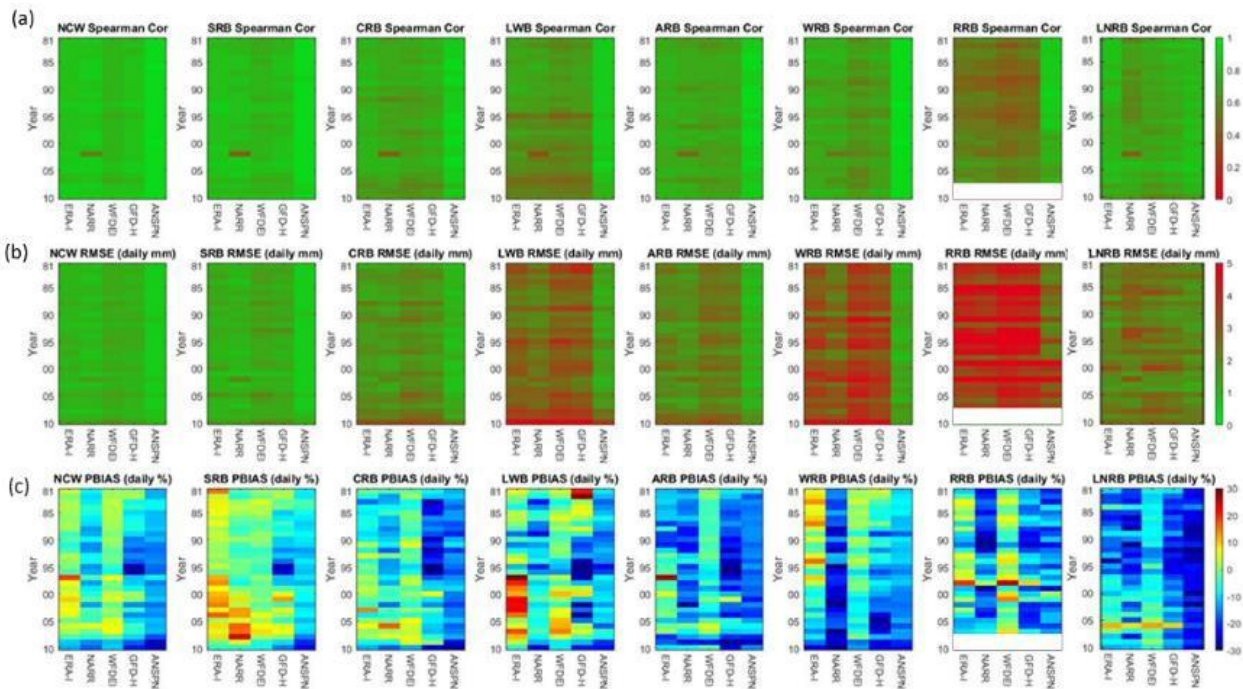


FIGURE 9.25 Daily precipitation spatially aggregated annual continuous statistics with reference to the AHCCD observed data set in each major basin. (a) daily Spearman correlation, (b) daily RMSE, and (c) daily PBIAS. White is used to represent periods with no available data. *Reproduced from: Pokorny et al., 2020 (Figure 3) (Confidential pending publication).*

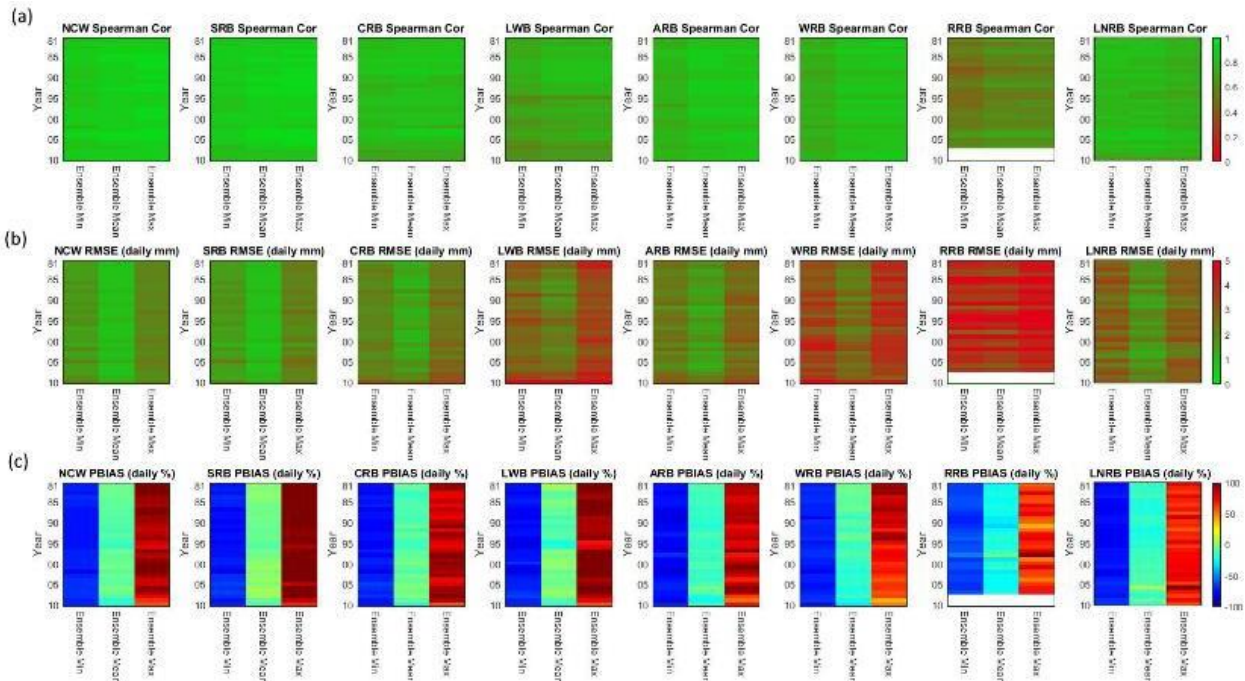


FIGURE 9.26 Basin-averaged daily precipitation continuous yearly statistics with reference to the AHCCD observed data set in each major basin for (a) daily Spearman correlation, (b) daily RMSE, and (c) daily PBIAS for the ensemble minimum, mean, and maximum. *Reproduced from: Pokorny et al., 2020 (Figure 6) (Confidential pending publication).*

By studying multiple historic, re-analysis input products, multiple hydrologic models, and a broad range of model parameters, sources of uncertainty in discharge projections of the Nelson River are evaluated and the associated probability of outflows for stations in the LNRB over the historical period 1981-2010. These results show the greater reliability (using VARS) of parameters calibrated in gridded and semi-distributed models (WATFLOOD and HYPE, respectively) compared to lumped models (HEC-HMS). These results also show the multi-model results for any given input and climate-ensemble for any given model return more robust distributions of discharge values than any single input product or hydrologic model (Pokorny et al., 2020). Partial results are shown in Figures 9.27 and 9.28.

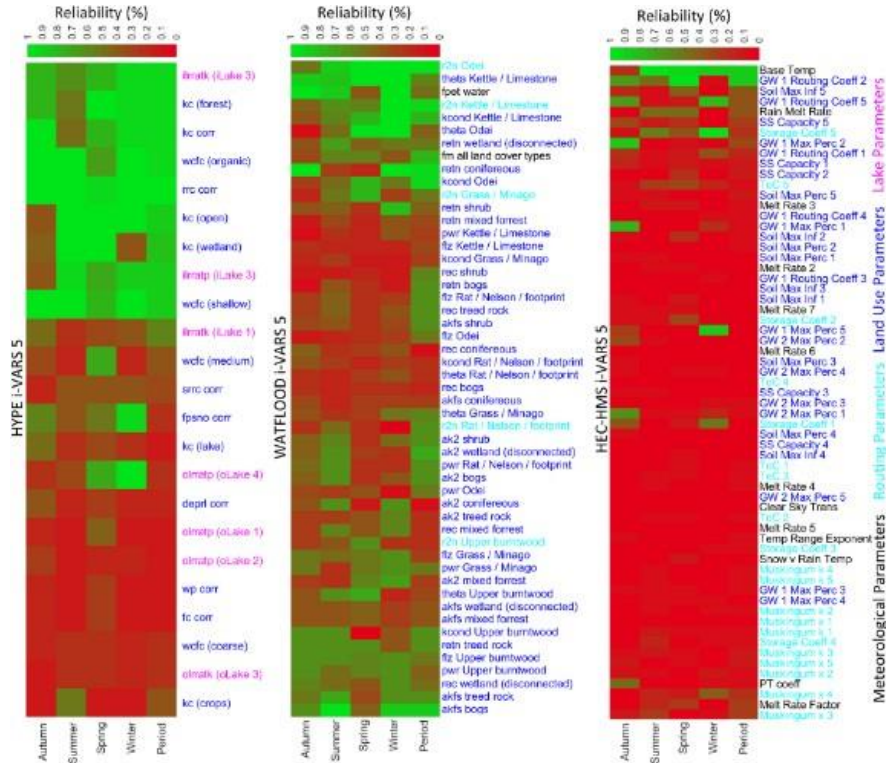


FIGURE 9.27 VARS parameter sensitivity reliabilities were ordered from least (bottom) to most sensitive (top), based on the period sensitivity. Variables are color-coded to reflect their category within the hydrologic model. *Reproduced from: Pokorny et al., 2020 (Figure 2) (Confidential pending publication).*

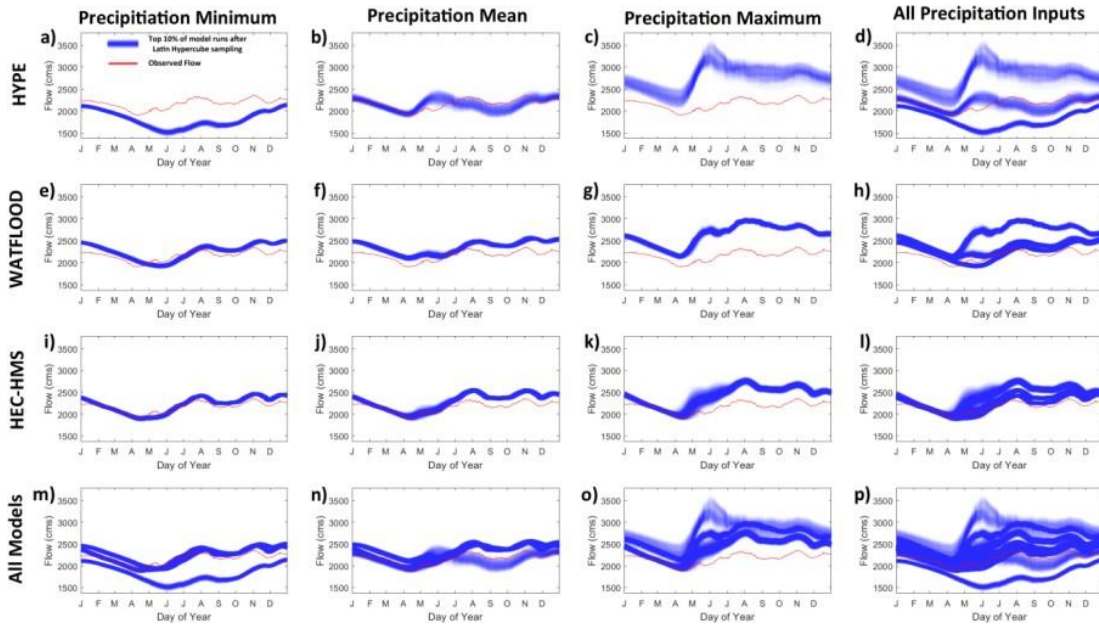


FIGURE 9.28 30-year average hydrographs for the Nelson River at Kelsey, generated by selecting the top 10% of orthogonal Latin Hypercube sampled runs for each hydrologic model and precipitation realization. Simulated hydrographs are darker blue when there was higher density of simulated flows. *Reproduced from: Pokorny et al., 2020 (Supplementary Figure 27).*

Regulated Discharge Modelling for the HBDB

The HHYPE model is further improved by adding a generalized reservoir regulation scheme. This regulation routine emphasizes maintenance of safe Water Surface Levels (WSLs) rather than the current HYPE regulation routine which is primarily calculated based on specified daily outflow (“River and Lakes”, 2019). By increasing sensitivity to daily WSLs and developing an automated calibration procedure, the reservoir discharge results are improved for individual monthly and overall seasonal timeseries (Tefs et al, in preparation (a)). Partial results are shown in Figures 9.29 and 9.30.

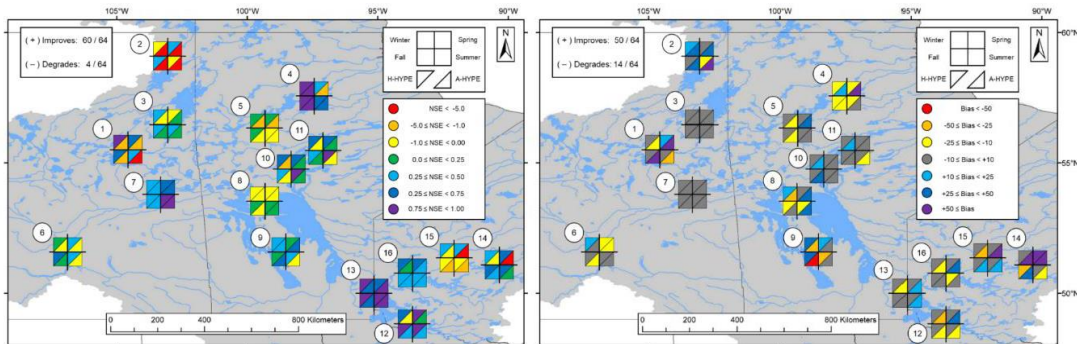


FIGURE 9.29 Seasonal (a) NSE and (b) percent bias of mean over the validation period (1981-2010) using observed reservoir inflows for original regulation (AHYPE) and new regulation routine (HHYPE). *Reproduced from: Tefs et al., in preparation (Figure 7) (Confidential pending publication).*

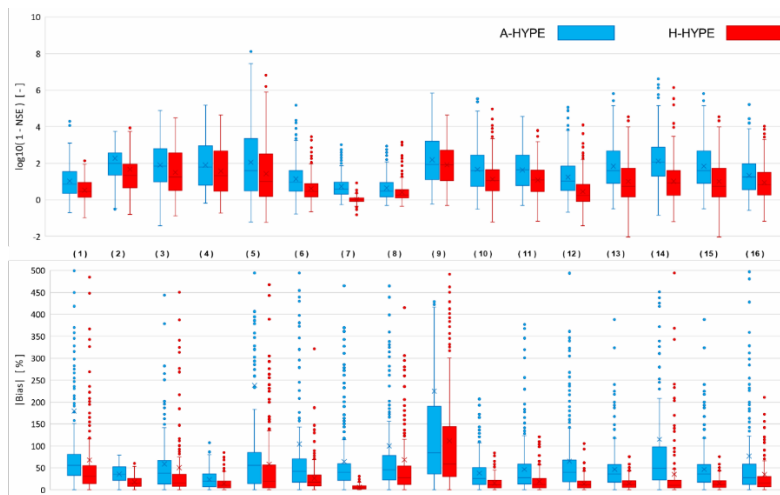


FIGURE 9.30 Distribution of 360 monthly evaluation (1981 to 2010) for (top) NSE error $\log_{10}(1 - NSE)$ and (bottom) absolute mean bias ($|bias|$). Interquartile range (box), 1.5 x inter-quartile range (whiskers,) median (divider), mean (cross) and outliers (dots). Perfect simulation for $\log_{10}(1 - NSE)$ is $-\infty$, for $|Bias|$ is zero percent. *Reproduced from: Tefs et al., in preparation (a) (Figure 9) (Confidential pending publication).*

Using the HHYPREG and HHYPENAT models, differences in discharge trends are identified for the two largest hydroelectric systems in the HBDB (NCRB, LGRC). The effects of regulation and climate change are shown in normalized discharge and discharge coefficient of variation both inter-annually

(within 30-year climatic periods) and inter-scenario (between climate ensemble members). Climate change dictates the majority of changes to the volume of flow between three climate-normal periods (1981-2010, 2021-2050, and 2041-2070), where regulation is responsible for decreased variation between individual years and across larger climatic periods (Tefs et al., in preparation (b)). Partial results are shown in Figures 9.31 and 9.32.

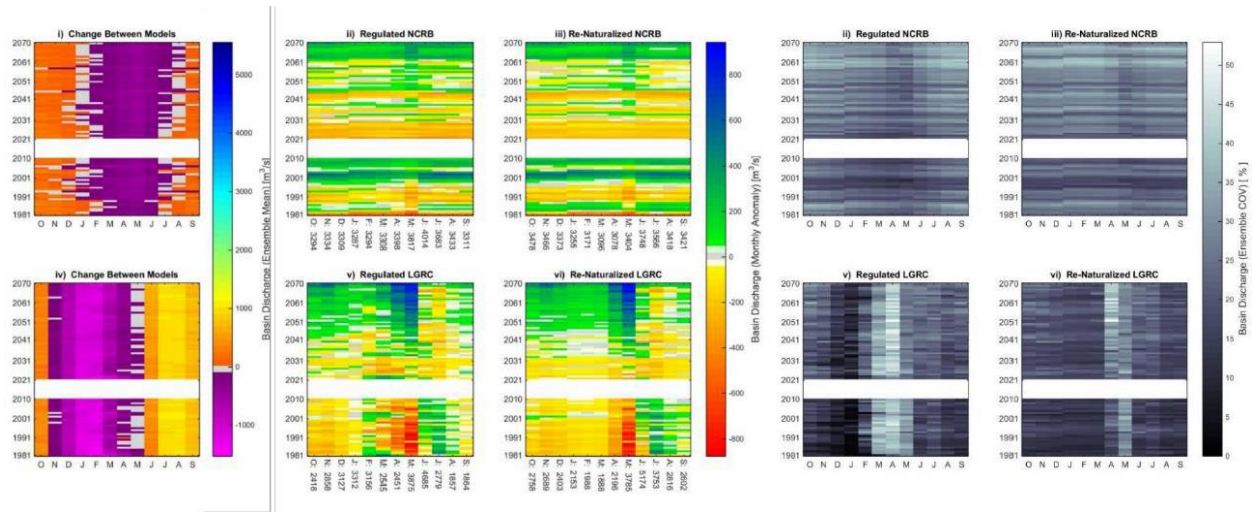


FIGURE 9.31 (a) Anomaly maps by year and month for (i, ii, iii) NCRB and (iv, v, vi) LGRC, (ii, iv) regulated model and (iii, vi) re- naturalized model and (i, iv) the difference ($\Delta = \text{Nat.} - \text{Reg.}$). Anomaly is relative to monthly average (1981-2070), listed below each map and (b) inter-scenario COV maps by year and month for (ii, iii) NCRB and (v, vi) LGRC, (ii, iv) regulated model, and (iii, vi) re- naturalized model. *Reproduced from: Tefs et al., in preparation (b) (Figures 5 and 6) (Confidential pending publication).*

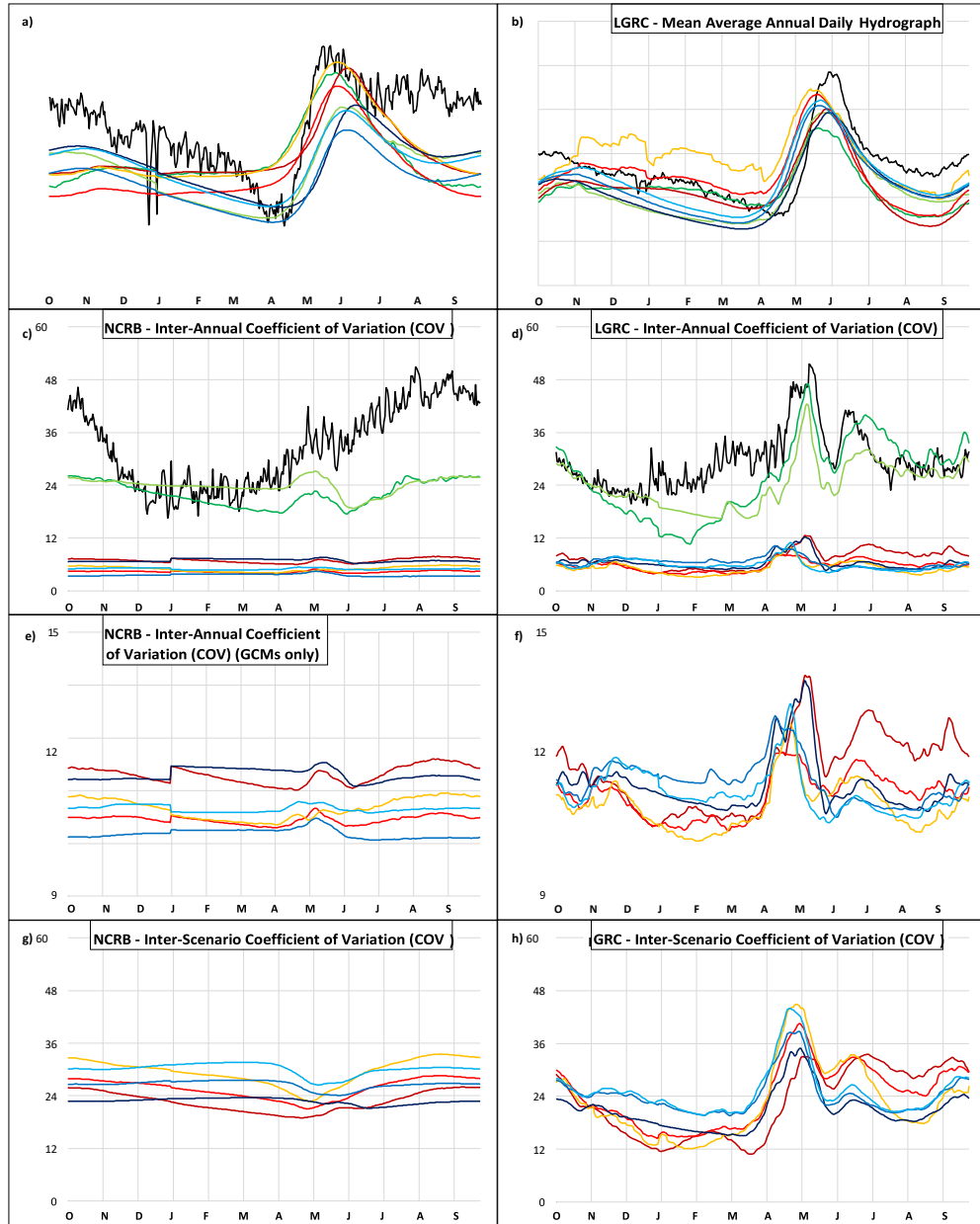


Figure 9.32 (a, b) Average annual daily discharge, (c, d, e, f) inter-annual COV and (g, h) inter-scenario COV. Charts shown for the combined (b, d, f, h) LGRC and (a, c, e, g) NCRB outlets. Regulated models (reds), re-naturalized models (blues), shown for different time-periods (darkest: 1981-2010, lightest: 2041-2070, mid-time: 2021-2050). Re-analysis products (regulated: light green, re-naturalized: light green) and observed data (black). *Reproduced from: Tefs et al., in preparation (b) (Figure 8) (Confidential pending publication).*

Non-BaySys Publications Referenced

- Ajami, N.K.; Duan, Q.; Sorooshian, S. (2007). An integrated hydrologic Bayesian multimodel combination framework: Confronting input, parameter, and model structure uncertainty in hydrologic prediction. *Water Resources Research*, 43(1).
- Ancil, F.; Couture, R. (1994). Cumulative impacts of hydroelectric development on fresh-water levels of Hudson Bay. *Canadian Journal of Civil Engineering*, 21(2), 297-306.
- Andersson, J.; Pechlivanidis, I.; Gustafsson, D.; Donnelly, C.; Arheimer, B. (2015). Key factors for improving large-scale hydrological model performance. *European Water*, 49, 77-88.
- Arheimer, B.; Donnelly, C.; Lindström, G. (2017). Regulation of snow-fed rivers affects flow regimes more than climate change. *Nature Communications*, 8(62).
- Asong, Z.E.; Razavi, S.; Whaeter, H.S.; Wong, J.S. (2017). Evaluation of integrated multi-satellite retrievals for GPM (IMERG) over southern Canada against ground precipitation observations: A preliminary assessment. *Journal of Hydrometeorology*, 18(4), 1033-1050.
- Berg, P.; Donnelly, C.; Gustafsson, D. (2018). Near-real-time adjusted re-analysis forcing data for hydrology. *Hydrology and Earth System Sciences*, 22(2), 989-1000.
- Beven, K. (2007). Towards integrated environmental models of everywhere: Uncertainty, data, and modelling as a learning process. *Hydrology and Earth System Sciences*, 11(1), 460-467.
- Beven, K.; Binley, A. (1992). The future of distributed models - Model calibration and uncertainty prediction. *Hydrological Processes*, 6(3), 279-298.
- Bring, A.; Shiklomanov, A.; Lammers, R.B. (2017). Pan-Arctic river discharge: Prioritizing monitoring of future climate change hot spots. *Earth's Future*, 5, 72-92.
- Charley, W.; Pabst, A.; Peters, J. (1995). The Hydrologic Modeling System (HEC-HMS): Design and development issues. *Computing in Civil Engineering*, 1-2, 131-138.
- Chen, J.; Brissette, F.P.; Chaumont, D.; Braun, M. (2013). Finding appropriate bias correction methods in downscaling precipitation for hydrologic impact studies over North America. *Water Resources Research*, 49(7), 4187-4205.
- Chen, J.; Brissette, F.P.; Poulin, A.; Leconte, R. (2011). Overall uncertainty of the hydrological impacts of climate change for a Canadian watershed. *Water Resources Research*, 47, W12509.
- Dai, A.; Trenberth, K.E. (2002). Estimates of freshwater discharge from continents: Latitudinal and seasonal variations. *Journal of Hydrometeorology*, 3(6), 660-687.
- DeBeer, C.M.; Wheeler, H.S.; Carey, S.K.; Chun, K.P. (2016). Recent climatic, cryospheric, and hydrological changes over the interior of western Canada: A review and synthesis. *Hydrology and Earth Systems Sciences*, 20, 1573-1598.
- Déry, S.J.; Stieglitz, M.; McKenna, E.C.; Wood, E.F. (2005). Characteristics and trends of river discharge into Hudson, James, and Ungava Bays, 1964-2000. *Journal of Climate*, 18, 2540- 2557.
- Déry, S.J.; Mlynowski, T.J.; Hernandez-Henriquez, M.A.; Straneo, F. (2011). Interannual variability and interdecadal trends in Hudson Bay streamflow. *Journal of Marine Systems*, 88(3) Special Issue, 341-351.

- Dynesius, M.; Nilsson, C. (1994). Fragmentation and flow regulation of river systems in the northern third of the world. *Science, New Series*, 266(5186), 753-762.
- Gan, Y.J.; Daun, Q.Y.; Gong, W.; Tong, C.; Sun, Y.W.; Chu, W.; Ye, A.Z.; Miao, C.Y.; Di, Z.H. (2014). A comprehensive evaluation of various sensitivity analysis methods: A case study with a hydrological model. *Environmental Modelling & Software*, 51, 269-285.
- Gelfan, A.; Gustafsson, D.; Motovilov, Y.; Arheimer, B.; Kalugin, A.; Krylenko, I.; Lavrenov, A. (2017). Climate change impacts on the water regimes of two great Arctic rivers: Modelling and uncertainty issues. *Climatic Change*, 141, 499-515.
- Granskog, M.A.; Kuzyk, Z.A.; Azetsu-Scott, K.; Macdonald, R.W. (2011). Distributions of runoff, sea-ice melt, and brine using $\delta^{18}\text{O}$ and salinity data: A new view on freshwater cycling in Hudson Bay. *Journal of Marine Systems*, 88(3), 362-374.
- Kouwen, N. (1988). WATFLOOD: a micro-computer based flood forecasting system based on real-time weather radar. *Canadian Water Resources Journal*, 13(1), 62-77.
- Lespinas, F.; Fortin, V.; Roy, G.; Rasmussen, P.; Stadnyk, T.A. (2015). Performance evaluation of the Canadian precipitation analysis (CaPA). *Journal of Hydrometeorology*, 16(5), 2045-2064.
- Liang, X.; Lettenmaier, D.P.; Wood, E.F.; Burges, S.J. (1994). A simple hydrologically based model of land-surface water and energy fluxes for general-circulation models. *Journal of Geophysical Research-Atmospheres*, 99(D7), 14415-14428.
- Lindström, G.; Pers, C.; Rosberg, R.; Strömqvist, J.; Arheimer, B. (2010). Development and test of the HYPE (Hydrological Predictions for the Environment) model – A water quality model for different spatial scales. *Hydrological Research*, 41(3-4), 295-319.
- Lu, G.Y.; Wong, D.W. (2008). An adaptive inverse-distance weighting spatial interpolation technique. *Computational Geoscience*, 34(9), 1044–1055.
- Pechlivanidis, I.; Arheimer, B. (2015). Large-scale hydrological modelling by using modified PUB recommendations: the India-HYPE case. *Hydrology and Earth System Sciences*, 19(11), 4559-4579.
- Razavi, S.; Gupta, H.V. (2016). A new framework for comprehensive, robust, and efficient global sensitivity analysis: Theory. *Water Resources Research*, 52(1), 423-439.
- River and Lakes [HYPE Model Documentation]. (2019) Retrieved from: http://www.smhi.net/hype/wiki/doku.php?id=start:hype_model_description:hype_routing.
- Taylor, K.E.; Stouffer, R.J.; Meehl, G.A. (2012). An overview of CMIP5 and the experiment design. *Bulletin of the American Meteorological Society*, 93(4), 485-498.
- Tebaldi, C.; Knutti, R. (2007). The use of multi-model ensemble in probabilistic climate projections. *Philosophical Transactions of the Royal Society – Mathematical, Physical, and Engineering Sciences*, 365(1857), 2053-2075.
- Vancoppenolle, M.; Fichefet, T.; Goosse, H.; Bouillon, S.; Madec, G.; Maqueda, M.A.M. (2008) Simulating the mass balance and salinity of arctic and Antarctic seas ice: Model description and validation. *Ocean Modelling*, 27(1-2), 33-53.

- Vrugt, J.A.; ter Braak, C.J.F.; Diks, C.G.H.; Robinson, B.A.; Hyman, J.M.; Hidgon, D. (2009). Accelerating Markov Chain Monte Carlo simulation by differential evolution with self-adaptive randomized subspace sampling. *International Journal of Nonlinear Sciences and Numerical Simulation*, 10(3), 273-290.
- Wada, Y.; Bierkens, M.F.P.; de Roo, A.; Diermeyer, P.A.; Famiglietti, J.S.; Hanasaki, N.; Konar, M.; Liu, J.; Schmied, H.M.; Oki, T.; Pokhrel, Y.; Sivapalan, M.; Troy, T.J.; van Dijk, A.I.J.M.; van Emmerik, T.; van Huijgevoort, M.H.J.; van Lanen, H.A.J.; Vorosmarty, C.J.; Wanders, N.; Wheatler, H. (2017). Human-water interface in hydrological modelling: current status and future directions. *Hydrology and Earth System Sciences*, 21, 4169-4193.
- Wagener, T.; McIntyre, N.; Lees, M.J.; Wheatler, H.S.; Gupta, H.V. (2003). Towards reduced uncertainty in conceptual rainfall-runoff modelling: Dynamic identifiability analysis. *Hydrological Processes*, 17(2) 455-476.
- Yue, S.; Pilon, P.; Phinney, B.; Cavadias, G. (2002). The influence of autocorrelation on the ability to detect trend in hydrological series. *Hydrological Processes*, 16(9), 1807-1829.

BaySys Publications Referenced

- Barber, D.G. (2014). BaySys – Contributions of climate change and hydroelectric regulation to the variability and change of freshwater-marine coupling in the Hudson Bay system. Retrieved from: http://umanitoba.ca/faculties/environment/department/ceos/mdeia/BaySys_PROJECT_DESCRIPTION.pdf
- Broesky, M.; Solonga, R.; Stadnyk, T.A.; Shiklomanov, A.; Déry, S.J.; Tefs, A.A.G. (in preparation). Trends in Hudson Bay far-field runoff. To be submitted to *Environmental Research*.
- Déry, S.J.; Stadnyk, T.A.; MacDonald, M.K.; Gaudi-Sharma, B. (2016). Recent trends and variability in river discharge across northern Canada. *Hydrology and Earth System Sciences*, 20(12), 4801-4818.
- Déry, S.J.; Stadnyk, T.A.; MacDonald, M.K.; Koenig, K.A. (2018). Flow alteration impacts on Hudson Bay river discharge. *Hydrological Processes*, 32(24), 3576-3587.
- JafariKhasragh, S., Lukovich, J., Hu, X., Myers, P., Sydor, K., & Barber, D. (2019). Modelling Sea Surface Temperature (SST) in the Hudson Bay Complex Using Bulk Heat Flux Parameterization: Sensitivity to Atmospheric Forcing, and Model Resolution. *Atmosphere-Ocean*, 57(2), 120–133. <https://doi.org/10.1080/07055900.2019.1605974>
- Lee, J.; Tremblay, J.E.; other contributing authors TBD (in preparation). A contemporary nutrient budget for Hudson Bay. To be submitted to *Elementa: Science of the Anthropocene*.
- Lilhare, R., Déry, S., Pokorny, S., Stadnyk, T.A., & Koenig, K.A. (2019) Intercomparison of Multiple Hydroclimatic Datasets across the Lower Nelson River Basin, Manitoba, Canada, *Atmosphere-Ocean* 57:4, 262-278, <https://doi.org/10.1080/07055900.2019.1638226>
- Lilhare, R.; Pokorny, S.; Déry, S.J.; Stadnyk, T.A.; Koenig, K.A. (in revision). Evaluating uncertainties in hydrological modelling over the Lower Nelson River Basin, Manitoba, Canada.

Submitted to *Water Resources Research*.

- Lukovich, J.V.; Myers, P.G.; Ridenour, N.; Jafarikhasragh, S.; Wong, K.; Sydor, K.; Tefs, A.A.G., Stadnyk, T.A.; Deschepper, I.; Kirillov, S.; Munson, K.; Babb, D.; Ehn, J. (in review). Simulated relative climate change and regulation impacts on sea ice and oceanographic conditions in the Hudson Bay Complex. Submitted to *Elementa: The Science of the Anthropocene* special issue.
- MacDonald, M.K.; Stadnyk, T.A.; Déry, S.J.; Braun, M.; Gustafsson, D.; Isberg, K.; Arheimer, B. (2018). Impacts of 1.5 and 2.0 degrees C warming on pan-Arctic River discharge into the Hudson Bay complex through 2070. *Geophysical Research Letters*, 45(15), 7561-7570.
- MacDonald, M.K.; Stadnyk, T.A.; Déry, S.J.; Gustafsson, D.; Isberg, K.; Arheimer, B.; Tefs, A.A.G. (in revision). Improved high-latitude water storage for hydrological modelling of the Hudson Bay Drainage Basin. Submitted to *Hydrological Processes*.
- Pokorny, S.; Stadnyk, T.A.; Ali, G.; Lilhare, R.; Déry, S.J.; Koenig, K.A. (in preparation). Assessment of ensemble-based gridded climate data and evaluation of uncertainty in hydrologic modelling, arising from input selection. To be submitted to journal TBD.
- Pokorny, S., Stadnyk, T.A., Ali, G., Déry, S.J., Lilhare, R., Koenig, K. (2020). Cumulative effects of uncertainty on simulated streamflow in a hydrologic modelling environment. *Elementa: Science of the Anthropocene* 9(1): 431. <https://doi.org/10.1525/elementa.431>
- Ridenour, N. A., Hu, X., Jafarikhasragh, S., Landy, J. C., Lukovich, J. V., Stadnyk, T. A., Sydor, K., Myers, P. G., & Barber, D. G. (2019). Sensitivity of freshwater dynamics to ocean model resolution and river discharge forcing in the Hudson Bay Complex. *Journal of Marine Systems* 196, 48-64. <https://doi.org/10.1016/j.jmarsys.2019.04.002>
- Stadnyk, T.A.; Déry, S.J.; MacDonald, M.K.; Koenig, K.A. (2019). Freshwater System. In Barber, D.; Kuzyk, Z.; Candlish, L. *An Integrated Regional Impact Assessment of Hudson Bay: Implications of a Changing Environment*. Québec City, QC, Canada.
- Tefs, A.A.G.; MacDonald, M.K.; Stadnyk, T.A.; Koenig, K.A.; Hamilton, M; Slota, P.; Crawford, J. (in preparation (a)). Simulating effects of Nelson-Churchill River regulation controls on reservoir performance in HYPE. To be submitted to *Hydrological Sciences*.
- Tefs, A.A.G.; MacDonald, M.K.; Stadnyk, T.A.; Koenig, K.A.; Déry, S.J.; Slota, P.; Guay, C.; Hamilton, M.; Thiemonge, N.; Vieira, M.; Pokorny, S. (in preparation (b)). Modelling the relative effects of climate change and hydroelectric development on the changing freshwater exports to Hudson Bay. To be submitted to *Journal of the Canadian Water Resources Association*

CHAPTER 10 NEMO MODELING

PROJECT CONTRIBUTORS Jennifer Lukovich¹; Paul G. Myers²; Natasha Ridenour²; Shabnam Jafarikhasragh¹ Xianmin Hu², Nathan Grivault², Yiran Xu², Inge Deschwepper³, Liam Buchart², Laura Castro de la Guardia², Yarisbel Garcia-Quintana²

¹Centre for Earth Observation Science, University of Manitoba, 535 Wallace Building, Winnipeg, MB

²Earth and Atmospheric Sciences, University of Alberta, 116 St. and 85 Ave., Edmonton, AB

³Département de Biologie, Université Laval, Pavillon Alexandre-Vachon 1045, av. de la Médecine, local 2064, Québec, QC

CITE CHAPTER AS Lukovich, J., Myers, P.G., Ridenour, N., Jafarikhasragh, S. 2019. NEMO Modeling. Chapter 10 in, *Hudson Bay Systems Study (BaySys) Phase 1 Report: Campaign Reports and Data Collection*. (Eds.) Landry, DL & Candlish, LM. pp. 260-271.

10.1 Objectives and Background

The objective of Team 6 is to support the other BaySys teams in investigating the relative impacts of climate change and regulation on freshwater-marine coupling within the Hudson Bay Complex (Foxye Basin, Hudson Bay, James Bay, and Hudson Strait). In support of Team 1 hypotheses, a sea ice and oceanographic model will be used to further study the effects of freshwater loading and ice cover on the circulation of Hudson Bay. This modeling perspective will be based on the Nucleus for European Modeling of the Ocean (NEMO) ocean general circulation model coupled to the LIM2 sea-ice model. Central also to Team 6 goals is the development of an integrated observational-modeling framework that will provide insight on, and improved representation of, physical, biological, and biogeochemical processes in the Hudson Bay system. The modeling will provide a framework and tool with which to simulate projected changes in marine state and dynamic variables, while also enabling the integration of observations and numerical analyses.

Hudson Bay acts as a conduit between the Arctic and North Atlantic Oceans (Ingram and Prinsenberg, 1998). A dominant source of freshwater to Hudson Bay is through river discharge (Déry et al., 2011). Anthropogenic influences on this discharge include diversions, dams, and reservoirs. Whereas near-shore effects of regulation include changes in density and salinity, off-shore effects are unknown. Previous studies have demonstrated that higher streamflow in winter favors sea ice formation due to the freshening of surface waters (Ingram and Prinsenberg, 1998, Saucier et al., 2004), in addition to an extension of under-ice plumes (Whittaker, 2006). Approximately thirty percent of Hudson Bay is unregulated, with natural flow confined to Chesterfield Inlet. Precipitation and ice melt in summer are additional sources of freshwater to Hudson Bay. By contrast, freshwater is removed through ice growth and evaporation. The Hudson Bay Complex is further characterized by two distinct marine locations: the Hudson Bay and James Bay marine regions (Stewart and Lockhart, 2005). The Hudson Bay marine region is distinguished by Arctic water due to exchanges with Foxye Basin and Hudson Strait, enhanced mixing and biological productivity in nearshore/coastal relative to offshore locations, and steep density gradients and stratification in summer associated with an upper layer of fresh water due sea ice melt and runoff. By contrast, James Bay is distinguished predominantly by freshwater due to runoff from land and is a shallower, more dilute region whose oceanographic features are shared by the southeastern segment of Hudson Bay (due to freshwater released in summer from melting ridged ice). In addition to this north-south characterization, recent studies have further highlighted the existence of a northwest/southeast gradient in sea ice conditions, particularly during spring, while also demonstrating the impact of hemispheric-scale and regional atmospheric patterns on sea ice state (Hochheim and Barber, 2010; Hochheim et al., 2011).

Previous modeling studies of the Hudson Bay system have captured seasonal variability in contributions to volume transport in Hudson Bay (Saucier et al., 2004; St. Laurent et al., 2011). In this project, we use an Arctic NEMO configuration (Figure 10.1) to provide a local (20-100 km; estuary and coastal) and a regional (~100 – 1000 km; bay-wide) perspective and understanding of changes in freshwater-marine coupling in response to a changing climate and regulated and naturalized regimes. The Arctic configuration further enables a link between Arctic and sub-Arctic domains and ocean, sea-ice, and atmospheric phenomena, to consider the tightly integrated nature of the high latitude climate system in examining impacts on the Hudson Bay Complex.

Team 6 is thus focused on the application of a modeling framework for the BaySys project that will provide insight into the relative effects of climate change and hydroelectric regulation on physical and biogeochemical conditions in the Hudson Bay system. Thus the BaySys NEMO analysis will be exclusively focused on the HB complex. Central to this framework is an assessment, for each of the naturalized, regulated, and climate change regimes, of the freshwater budget that monitors relative

contributions from river discharge, precipitation, and evaporation, and sea ice melt. Significant also is an assessment of changes in the stability of the water column monitored through T/S profiles throughout the basin and ocean-sea ice atmosphere interactions based on an investigation of heat, salt, and momentum fluxes. Central to this framework is in addition an understanding of freshwater-marine coupling in the context of dynamics. In particular, changes in dynamical phenomena including upwelling, mixing, and polynya formation will be evaluated through the investigation of freshwater circulation, ocean currents, and sea ice dynamics. Diagnostics designed to quantify thermodynamic and dynamical processes will be developed as a contribution to the integrated observational-modeling framework and collaboration with other BaySys teams.

Team 6 specific goals are thus as follows:

1. To use HYPE discharge and bias-corrected CMIP5 data from Team 2 to drive NEMO model simulations to provide output in the Hudson Bay Complex, in the form of ice and oceanographic variables relevant for BaySys teams 1, and 3 – 5.

2. To investigate the relative impacts of climate change and regulation on freshwater-marine coupling within the HBC from a modeling perspective using the NEMO model

3. To provide an integrated observational-modeling freshwater/marine framework for model-data comparison on local (~ 20 - 100 km; estuary and coastal) and regional (~100 - 1000 km; bay-wide) scales

4. To improve our understanding of physical mechanisms responsible for observed phenomena based on observations and historical simulations, and to improve the representation of these processes for future simulations

5. To investigate and improve our understanding of freshwater dynamics, as well as momentum, mass, and heat flux in HBC in response to climate change and regulation. In addition, we seek to address the following hypothesis:

H6.1 Freshwater-marine coupling is expected to be influenced on local scales by regulation through changes in seasonality and timing of FW discharge that will influence upwelling, coastal/offshore interactions, mixing, the formation of the seasonal ice zone, polynya formation, and timing and magnitude of density-driven currents, and on regional scales by climate change through bay-wide changes in sea ice state and dynamics, FW circulation, OSA interactions due to local and non-local oceanographic and atmospheric forcing.

10.2 Models

The first paragraph of Task 1.5 of the original BaySys proposal states “In support of Team 1 hypotheses, sea ice and oceanographic models will be used to further study the effects of freshwater loading and ice cover on the circulation of Hudson Bay. The Nucleus for European Modeling of the Ocean (NEMO) model [Vancoppenolle et al., 2009a, 2009b] will be used. The implementation of the NEMO ice-ocean model at the University of Manitoba (U. Manitoba) is based on a configuration used and provided by the Bedford Institute of Oceanography (BIO) to obtain projections of sea ice state and dynamical variables in the Beaufort Sea, Hudson Bay, and Baffin Bay regions. It will provide a framework and tool with which

to simulate projected changes in marine state and dynamic variables, while also enabling the integration of observations and numerical analyses.

The configuration of the NEMO model specified here is that provided to CEOS by the Bedford Institute of Oceanography (DFO). This configuration was provided to CEOS, based upon version 3.1 of NEMO, by Youyu Lu. This configuration is otherwise known as CREG - Canadian Regional (Youyu Lu; Frédéric Dupont, personal communication). The configuration resolution was set to a resolution of 0.25 degrees as stated in the original proposal (“In our study, the model will be run with ¼-degree grid spacing - for a horizontal resolution of ~ 10 km–15 km within Hudson Bay”). I attach a copy of the model output showing the domain of the Bedford/CREG NEMO model configuration, provided to me by Frédéric Dupont (ECCC), as Figure 1.

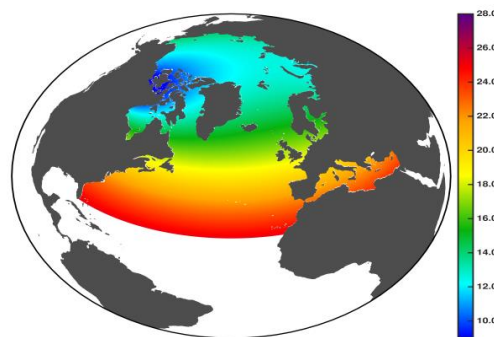


FIGURE 10.1 CREG025/BIO NEMO Model Configuration showing the domain and the model grid size resolution in km

As Figure 10.1 shows, with the NEMO configuration from the original BaySys proposal, it is specified that the NEMO modeling was to be carried out using a configuration that included within its domain the Arctic and *Atlantic* Oceans. And that this modeling was to be carried out at a resolution of ¼ degrees to allow for the significant number of long integrations planned for the BaySys project.

The switch to ANHA configuration in winter 2015, was based on comments from the original proposal review. In addition, Dr. Paul Myers from the University of Alberta was approached to join BaySys to add an ocean modeler to the team. The group at the University of Alberta has been running the NEMO model for several years and has since 2012 been using the Arctic Northern Hemisphere Atlantic (ANHA) configuration for all their simulations. This configuration was developed through previous NSERC funded projects, in close collaboration with DFO and ECCC (through the CONCEPTS initiative). It is functionally equivalent to the government CREG configuration other than the southern boundary being moved south (to 20S). This was done to avoid issues with cutting the Atlantic Meridional Overturning Circulation (important for climate-related questions), and to push potential issues with the open boundary conditions south of the Equator, well away from the study region(s). Given that the CREG configuration was developed with a focus more on operational and forecasting questions, the location of the southern boundary was deemed sufficient for those applications. I note that since this time, for climate-based applications, newer NEMO configurations have been developed by DFO, pushing the southern Atlantic boundary down to near the Equator (for the same reasons this was done with ANHA – Youyu Lu,

personnel communication). The ANHA configuration is shown in Figure 10.2. We also note that given the continual development occurring with the ANHA configuration, it is now running at the newest version of NEMO, v3.6, including all the associated model improvements and code optimizations.

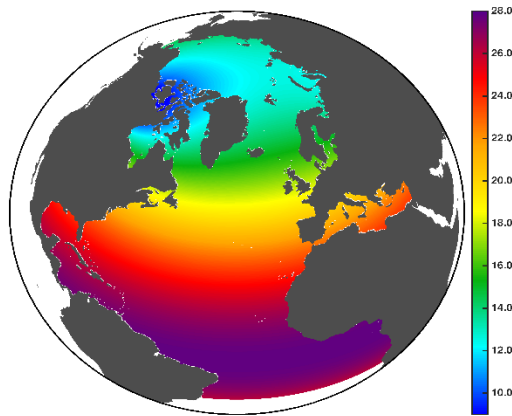


FIGURE 10.2 ANHA4 model configuration showing the domain and the model grid cell resolution in km

Although figures 10.1 and 10.2 might make it seem that the CREG/BIO and ANHA configurations are quite different, this is not the case and is more a function of map projection used. Model resolution and domain are the same from the southern boundary of CREG (20N), including the North Atlantic Ocean, Hudson Bay, the Canadian Arctic, and the Arctic Ocean. The only difference is that the ANHA configuration includes additional grid cells farther south, for the reasons specified in the previous paragraph (climate applications).

Evaluation of trade-offs: Repeating from the original question above, Evaluate trade-offs in terms of benefits to the project vs additional uncertainty and time/resources for the additional modeling area.

1 - Time/Resources

NEMO uses a tri-polar grid to deal with issues like the pole-singularity. This makes the model resolution highest (and thus needing the most model grid cells) near to the model poles. Thus, as can be seen in Figure 10.2, model resolution is finest in the Canadian Arctic, and in general at high latitudes and in and around the Arctic Ocean. The model resolution is coarsest near the Equator (Figure 10.2), and thus, although one can see a large region of ‘purple’ in Figure 10.2, it does not encompass a large number of grid cells. And the model CPU cost is a function of the number of grid nodes it needs to solve each equation for. Thus, the part of the ANHA configuration within the South Atlantic absorbs only ~5% of the model CPU cost and thus is not a significant cost in time or computational resources. Additionally, the

ANHA configuration uses NEMO v3.6, while the CEOS configuration in the original BaySys proposal was based on NEMO v3.1, with v3.6 at least 30-40% faster than v3.1.

Thus, in conclusion, the ANHA NEMO configuration runs significantly faster than the originally proposed CEOS NEMO configuration, even with its small number of additional grid cells in the Atlantic. Thus, there is no trade-off, and using the ANHA configuration will save the project time and computational resources.

II – Additional Uncertainty

As can be seen in figure 10.1, the original CEOS configuration specified in the original proposal included significant far-field domains, including the Arctic Ocean and much of the Atlantic Ocean. This may not have been the focus of initial discussions and planning, but the proposed NEMO domain always required inputs for atmospheric forcing and runoff over a domain much wider than the Hudson Bay Complex. So even if not explicitly laid out in the proposal, there was always an expectation that different runoff and forcing products would have been needed (even if that potentially enhanced the project uncertainty). Additionally, given that the CEOS/BIO configuration is regional (like ANHA), and not global, this always meant that open boundary conditions for the climate scenarios needed to be provided (at Bering Strait and in the Atlantic).

Team 2's exceptional additional effort has now provided HYPE based runoff products for the Arctic Ocean and its watershed. But that still leaves additional products needed for the NEMO model (Greenland runoff, and river runoff around the Atlantic Ocean), *regardless* of whether the CEOS/BIO or ANHA configuration is used. Given that the additional regions needing another runoff product in ANHA are far from the Hudson Bay Complex, the uncertainty should be no larger than for the originally proposed CEOS/BIO configuration, which still would have needed the same additional runoff products in its Atlantic domain.

Given the multiple climate scenarios, as well as HYPE based naturalized and regulated runoff scenarios for the Hudson Bay Complex, the NEMO modeling will still produce identical experiments where only one parameter is changed (within the HBC), allowing for the study of the role of climate change and regulation, as originally proposed. The need for far-field runoff fields, as well as open boundary conditions, may bring in uncertainty, but that was always the case, even with the CEOS/BIO version of NEMO originally proposed.

Thus, in conclusion, if using multiple runoff products is unavoidable (which is the case since Team 2 is not modeling Greenland runoff), the use of the ANHA configuration of NEMO is not increasing project uncertainty since the closest 'missing' sources, Greenland and runoff around the North Atlantic would have to have been treated the same way in the originally proposed NEMO experiments. This is a question that needs to be explored with sensitivity experiments, regardless of the configuration used.

III - Summary, Recommendations, and Next Steps

In summary, the ANHA configuration is comparable to the BIO configuration described in the initial BaySys proposal, with the exception of a more southerly Atlantic boundary that has a limited impact on computational cost or time required to complete experiments. The ANHA configuration provides a

comprehensive tool with which to assess the relative impacts of climate change and regulation on freshwater-marine coupling in the HBC.

In regards to recommendations and next steps, it is suggested that Team 6 proceed with historical and future simulations using the ANHA configuration of NEMO, discharge data from Team 2 for the HBC and Arctic domains, and bias-corrected atmospheric forcing data from Ouranos for the ANHA domain as outlined in the more recent proposal for Team 6. Discharge data for Greenland and beyond the Arctic domain will be provided by RACMO and CanESM2, respectively. The historical and future simulations will be complemented by additional experiments to examine both parameters as well as input data sensitivity analysis. These experiments will address questions related to the runoff products used, the bias correction of the atmospheric forcing, as well as the model open boundary conditions. Additional model evaluation in the HBC will be carried out in collaboration with Environment and Climate Change Canada (ECCC), using their RIOPS forecast system.

10.3 Methods

In support of Team 6 goals and its hypothesis, sea ice and oceanographic models will be used to further study the effects of freshwater loading and ice cover on the circulation of Hudson Bay. The Nucleus for European Modeling of the Ocean (NEMO) model coupled to the LIM2 sea-ice model [Vancoppenolle et al., 2009; Rousset et al., 2015] will be used in an Arctic configuration developed by Paul Myers and his team at the University of Alberta, which encompasses the Hudson Bay Complex as part of its ocean domain (e.g. Hu and Myers, 2018). This configuration will provide a framework and tool with which to simulate projected changes in marine state and dynamic variables, while also enabling the integration of observations and numerical analyses within the HBC. The analysis domain used by Team 6 is depicted in Figure 10.1.

In terms of the sea ice model, the LIM2 ice model uses Elastic-Viscous-Plastic rheology (EVP) (Hunke and Dukowicz, 1997), implemented on a C-grid (Bouillon et al., 2009), and with thermodynamics based on two layers of ice and one layer of snow (Fichefet and Maqueda, 1997). It is coupled to the ocean model at every ocean time step, with a non-linear quadratic drag of the shear between the ice and ocean. The model has been found to accurately simulate sea-ice in the Arctic Ocean (Johnson et al., 2012) and the Canadian Arctic Archipelago (Hu and Myers, 2018). Thus, in general, NEMO with LIM2 reproduces real ice conditions well. This includes the current downward trend in summer sea-ice extent including the minima in 2007 and 2012. In terms of the monthly cycle of ice growth and decline, NEMO is consistently within one standard deviation of the reanalysis data. NEMO's seasonal cycle is also in good agreement with the NSIDC reanalysis data.

In our study, the model will be run with 1/4-degree grid spacing (for a horizontal resolution of ~ 10km–15 km within Hudson Bay) and will include up to 50 unequally-spaced vertical levels. Enhanced vertical resolution in the upper layers will allow for detailed examination of changes in freshwater and stratification in our analysis domain of the HBC (Figure 10.1), where all relevant mixing processes, including tides, will be considered, as needed when the historical model simulations are evaluated against the field observations.

Projections will be computed relative to a 1979–2009 climatology from NEMO hindcast simulations. The model will then be forced with CMIP-5 historical and climate scenarios and freshwater forcing to predict

future sea ice and oceanographic conditions in Hudson Bay. Details of the model forcing will be further discussed in the following section. Variables modeled will be selected based on the integrated science plan, and will include, at a minimum, projections of ice concentration, thickness and drift velocity, as well as salinity, temperature, and ocean current profiles throughout the Bay.

Specifically, the Arctic configuration of the NEMO model will be used to estimate relative contributions of hydroelectric regulation and climate change to changes in ocean, sea ice, and biological processes in the HBC. Numerical experiments will be conducted in two phases. In Phase I, we will force simulations with historical climate data, and available discharge data from 1979–2009. In Phase II, we will use climate and runoff output to force simulations from 2010 to 2070 (although analysis will mainly focus on the decades of 2030s and 2050s for ocean and sea ice processes). The same simulated climate and river discharge forcing will inform Team 3 studies on the ecosystem and biogeochemical process changes. Changes in freshwater-marine coupling due to regulation and climate change impacts will be studied by between-model comparison of parameters and derived entities including temperature and salinity profiles at strategic locations throughout the Bay, sea ice concentration, and thickness, and circulation and mixed-layer depth, amongst others. Model related mixing processes will be compared with in situ BaySys observations of these processes to better understand the relative contributions of regulation relative to that of climate change across the HBC.

It should be noted that the pan-Arctic domain is essential in ensuring that the climate change signal (a hemispheric-scale phenomenon) within the HBC is adequately simulated. Previous studies (Ingram and Prinsenber, 1998; Jones et al., 2003) have demonstrated that waters from the Canadian Arctic, Siberian Rivers, and Pacific Water (Bering Strait) all enter the HBC over timescale is 2 to 10 years. Given that Hudson Bay is filled with Arctic Waters, and Climate Change is expected to have the largest impacts at high latitude, understanding the response of HBC to a changing climate requires inputs that represent how the Arctic is responding to the climate forcing, potentially modifying the inputs to the HBC. It is also important to note that given the timescale of the response, it is the overall changes to forcing and runoff from the Arctic that will be important, not short-term changes in regulation in that region, as those effects will be integrated out over the transit times of the given waters to the HBC.

10.4 Inputs

Inputs to the NEMO model include initial conditions, open boundary conditions, river discharge, and atmospheric forcing. Team 2 provides naturalized and regulated HYPE river discharge for Hudson Bay, in addition to naturalized HYPE river discharge for the Arctic. Team 2 is also providing a river discharge envelope including maximum, minimum, and mean discharge values for naturalized and regulated flow regimes for Hudson Bay that will be used in NEMO runoff/discharge sensitivity analyses (see Section 9.3). RACMO2 supplies Greenland discharge, while ECCO CanESM2 provides discharge for the remainder of the domain. NEMO is initialized using the publicly available Global Ocean Reanalysis and Simulations (GLORYS) 3D temperature and salinity, and 2D sea surface height and sea ice. Open boundary conditions will be provided from the appropriate CMIP5 scenarios.

Atmospheric forcing, including temperature, precipitation (including snow), surface air pressure, specific humidity, near-surface zonal and meridional wind components, downwelling shortwave and longwave radiation is supplied by Ouranos from CMIP5 scenarios. Five CMIP5 scenarios will be evaluated: GFDL rcp4.5, MIROC5 rcp4.5, and rcp8.5, MRI-CGCM3 rcp4.5, and rcp8.5. These were selected as a subset of

the 19 scenarios used by Team 2 for maximum coverage of the ΔT , ΔP phase space. Four of the eight variables including temperature, precipitation, zonal and meridional winds are bias-corrected by Ouranos using a translation bias correction approach and ECMWF ERA-Interim reanalysis data, to ensure consistency with the WFDEI atmospheric forcing product (which incorporates ERA data) used by Team 2. Data is provided for the 1970 – 2070 timeframe.

Please refer to the product descriptions provided by T. Stadnyk for Team 2, and Marco Braun from Ouranos for additional information on discharge and atmospheric data respectively provided as inputs to Team 6, in addition to a meteorological and hydrological forcing data study justifying the selection of ERA-Interim reanalysis for bias-correction to ensure consistency in Teams 2 and 6 forcing.

10.5 Operations and Progress to Date

Operations and progress to date include the completion of simulations for sensitivity studies, training of HQP, dissemination of NEMO output, and continued research and analysis. Specific accomplishments are as follows:

Simulations

ANHA configuration of the NEMO model upgraded to v3.6, leading to a significant increase in its computational speed.

Bias-corrected CMIP5 data and HYPE discharge data were provided by Ouranos and Team 2 in September 2018; historical simulations subsequently launched.

Experiments launched with ERA atmospheric forcing and finalized HYPE and Arctic-HYPE river discharge data produced by Team 2 are running and include:

- a) ERA-Interim (ERA-Interim forcing, calibrated HYPE and Arctic-HYPE)
- b) MIROC (MIROC forcing, calibrated HYPE and Arctic-HYPE)
- c) SAL tide correction for tidal sensitivity analysis (CGRF, monthly runoff, Greenland melt)
- d) AGRIF CAA12 (ERA-Interim forcing, calibrated HYPE, HBC runoff, and HBC inflow tracers) – not run for BaySys but the output will potentially be useful for BaySys

NEMO experiments with explicit tidal forcing run, and are presently being evaluated.

Inge Deschepper (from Team 3) visited the University of Alberta to integrate her coupled pelagic and sympagic ecosystems model into the ANHA configuration of NEMO. We are awaiting the finalized version of this module for inclusion in the future simulations.

NEMO model output made available to BaySys researchers (and their HQP) to assist with their analysis (including Sergei Kirillov, Zou Zou Kuzyk, Igor Dmitrenko, Simon Belanger, and Jean-Eric Tremblay).

Atmospheric Forcing from ECCO was obtained through to summer 2018, with model simulations extended through this period, to support comparison with ECCO's RIOPS system, once provided by ECCO.

Analysis and Evaluation

- a) Initial model evaluation for years prior to BaySys completed in a study led by HQP Natasha Ridenour, in review
- b) Evaluation of freshwater circulation and anomalous features completed by HQP Natasha Ridenour
- c) SST analysis and sensitivity to atmospheric forcing and resolution completed by HQP Shabnam JafariKhasragh and in review
- d) Sensitivity of modeled sea ice volume budget to atmospheric forcing led by Shabnam JafariKhasragh in preparation
- e) Baseline evaluation outlining atmospheric and discharge conditions for 2016-2018 BaySys timeframe in preparation

Planning

- a) Simulations launched (ERA-Interim, MIROC5), historical and future simulations for naturalized flow available in April
- b) BaySys subgroup established to conduct
 - i) Baseline evaluation and model-data comparison, and
 - ii) Relative climate change and regulation impacts assessment for relevant team variables

Initial baseline evaluation results to be made available in February.

10.6 Preliminary Results

Preliminary results include an evaluation of the NEMO and analysis of NEMO model output. Specific results and contributions include studies pertaining to:

Modeled sea surface temperature (SST) and sensitivity to atmospheric forcing and model resolution showing model sensitivity to surface atmospheric forcing, led by Shabnam JafariKhasragh and Team 6 colleagues. This paper is in review following an initial review requesting minor revisions.

Freshwater dynamics and sensitivity to river discharge forcing and model resolution for the 2004 – 2016 timeframe, led by Natasha Ridenour in collaboration with Teams 1, 2, and 6 colleagues. This paper is in review following an initial review requesting minor revisions.

Summer freshwater circulation using the high-resolution model output and AVISO data showing a previously overlooked anticyclonic circulation feature in southeast Hudson Bay was discovered by Natasha Ridenour, led by Natasha Ridenour and Team 1 and 6 colleagues.

Each noted paper serves as a foundation for subsequent studies investigating relative climate change and regulation impacts on freshwater dynamics and heat flux using NEMO output from future simulations with naturalized and regulated discharge data. Each study also contributes to the development of an integrated observational-modeling framework as well as improved understanding of model parameterization and the physical mechanisms responsible for observed phenomena (i.e. anticyclonic circulation in southeast HB in summer, and model sensitivity to atmospheric forcing). Evaluation of sea ice drift and deformation for ice beacons deployed in winter, 2017 has been completed for comparison with modeled ice drift, and tools developed to facilitate comparison of modeled and observed dynamical phenomena.

References Cited

- Bouillon, S., Maqueda, M. A. M., Legat, V., & Fichefet, T. (2009). An elastic–viscous–plastic sea ice model formulated on Arakawa B and C grids. *Ocean Modelling*, 27(3-4), 174-184.
- Déry, S. J., Mlynowski, T. J., Hernández-Henríquez, M. A., & Straneo, F. (2011). Interannual variability and interdecadal trends in Hudson Bay streamflow. *Journal of Marine Systems*, 88(3), 341-351.
- Fichefet, T., & Maqueda, M. M. (1997). Sensitivity of a global sea ice model to the treatment of ice thermodynamics and dynamics. *Journal of Geophysical Research: Oceans*, 102(C6), 12609-12646.
- Hochheim, K. P., Lukovich, J. V., & Barber, D. G. (2011). Atmospheric forcing of sea ice in Hudson Bay during the spring period, 1980–2005. *Journal of Marine Systems*, 88(3), 476-487.
- Hochheim, K. P., & Barber, D. G. (2010). Atmospheric forcing of sea ice in Hudson Bay during the fall period, 1980–2005. *Journal of Geophysical Research: Oceans*, 115(C5).
- Hunke, E. C., & Dukowicz, J. K. (1997). An elastic–viscous–plastic model for sea ice dynamics. *Journal of Physical Oceanography*, 27(9), 1849-1867.
- Ingram, R. G., & Prinsenber, S. (1998). Coastal oceanography of Hudson Bay and surrounding eastern Canadian Arctic waters. *The sea*, 11(29), 835-859.
- Jones, E. P., Swift, J. H., Anderson, L. G., Lipizer, M., Civitarese, G., Falkner, K. K., ... & McLaughlin, F. (2003). Tracing Pacific water in the North Atlantic ocean. *Journal of Geophysical Research: Oceans*, 108(C4).
- Johnson, M., Proshutinsky, A., Aksenov, Y., Nguyen, A. T., Lindsay, R., Haas, C., ... & De Cuevas, B. (2012). Evaluation of Arctic sea ice thickness simulated by Arctic Ocean Model Intercomparison Project models. *Journal of Geophysical Research: Oceans*, 117(C8).
- Rousset, C., Vancoppenolle, M., Madec, G., Fichefet, T., Flavoni, S., Barthélemy, A., ... & Vivier, F. (2015). The Louvain-La-Neuve sea ice model LIM3. 6: global and regional capabilities. *Geoscientific Model Development*, 8(10), 2991-3005.

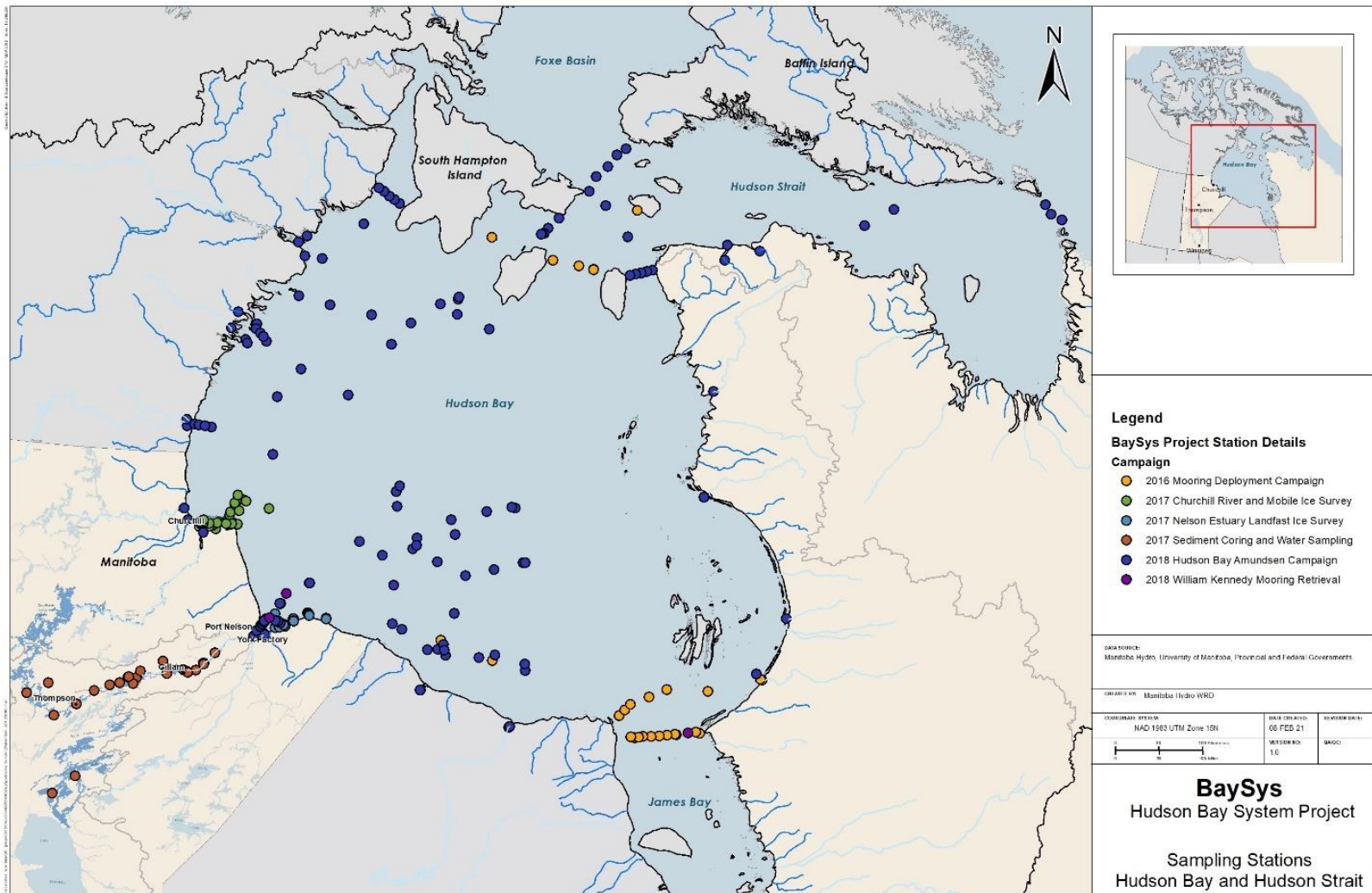
Saucier, F. J., Senneville, S., Prinsenber, S., Roy, F., Smith, G., Gachon, P., ... & Laprise, R. (2004). Modelling the sea ice-ocean seasonal cycle in Hudson Bay, Foxe Basin and Hudson Strait, Canada. *Climate Dynamics*, 23(3-4), 303-326.

St-Laurent, P., Straneo, F., Dumais, J. F., & Barber, D. G. (2011). What is the fate of the river waters of Hudson Bay?. *Journal of Marine Systems*, 88(3), 352-361.

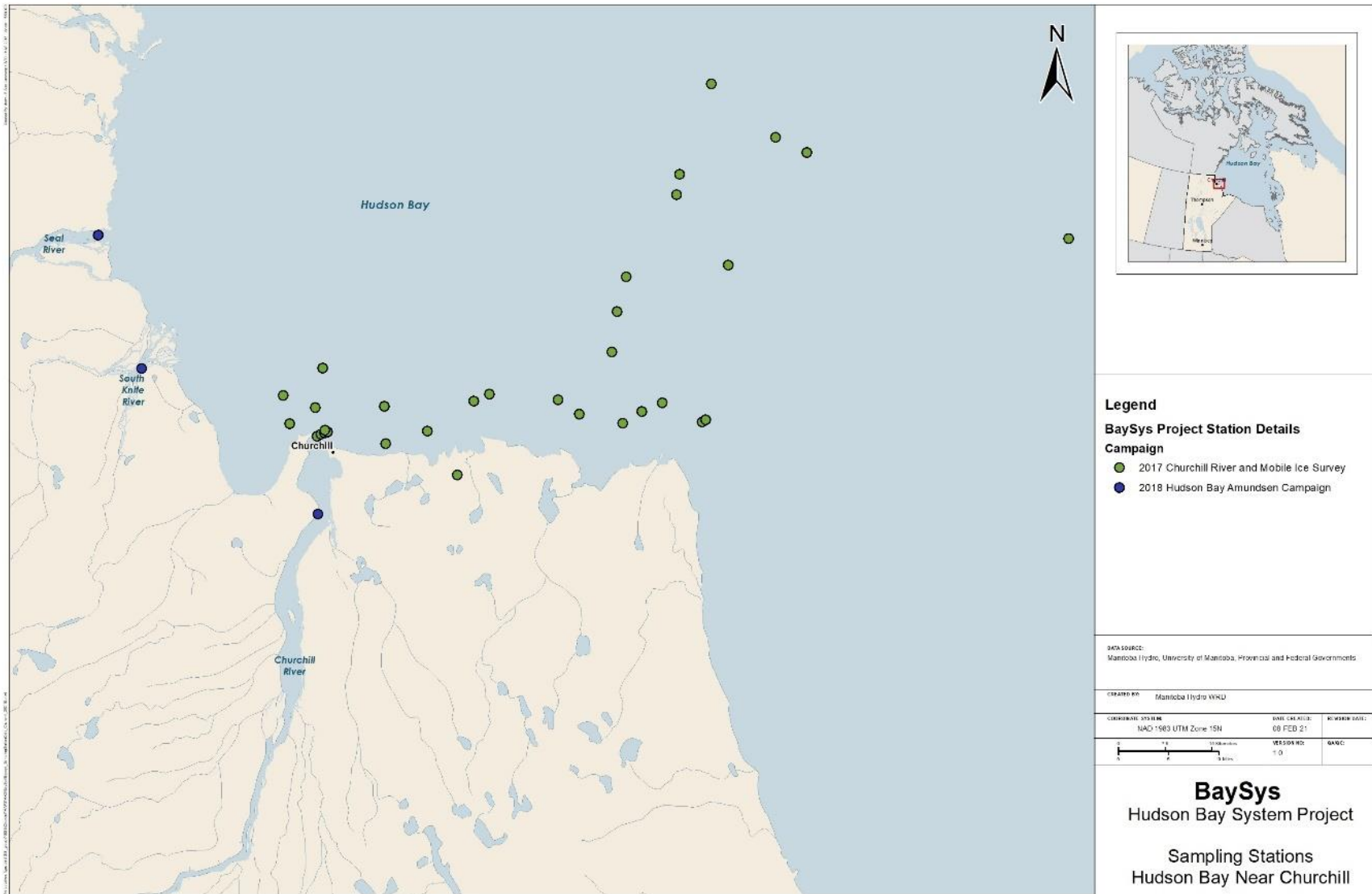
Stewart, D. B., & Lockhart, W. L. (2005). *An overview of the Hudson Bay marine ecosystem*. Department of Fisheries and Oceans, Central and Arctic Region.

Vancoppenolle, M., Fichefet, T., Goosse, H., Bouillon, S., Madec, G., & Maqueda, M. A. M. (2009). Simulating the mass balance and salinity of Arctic and Antarctic sea ice. 1. Model description and validation. *Ocean Modelling*, 27(1-2), 33-53.

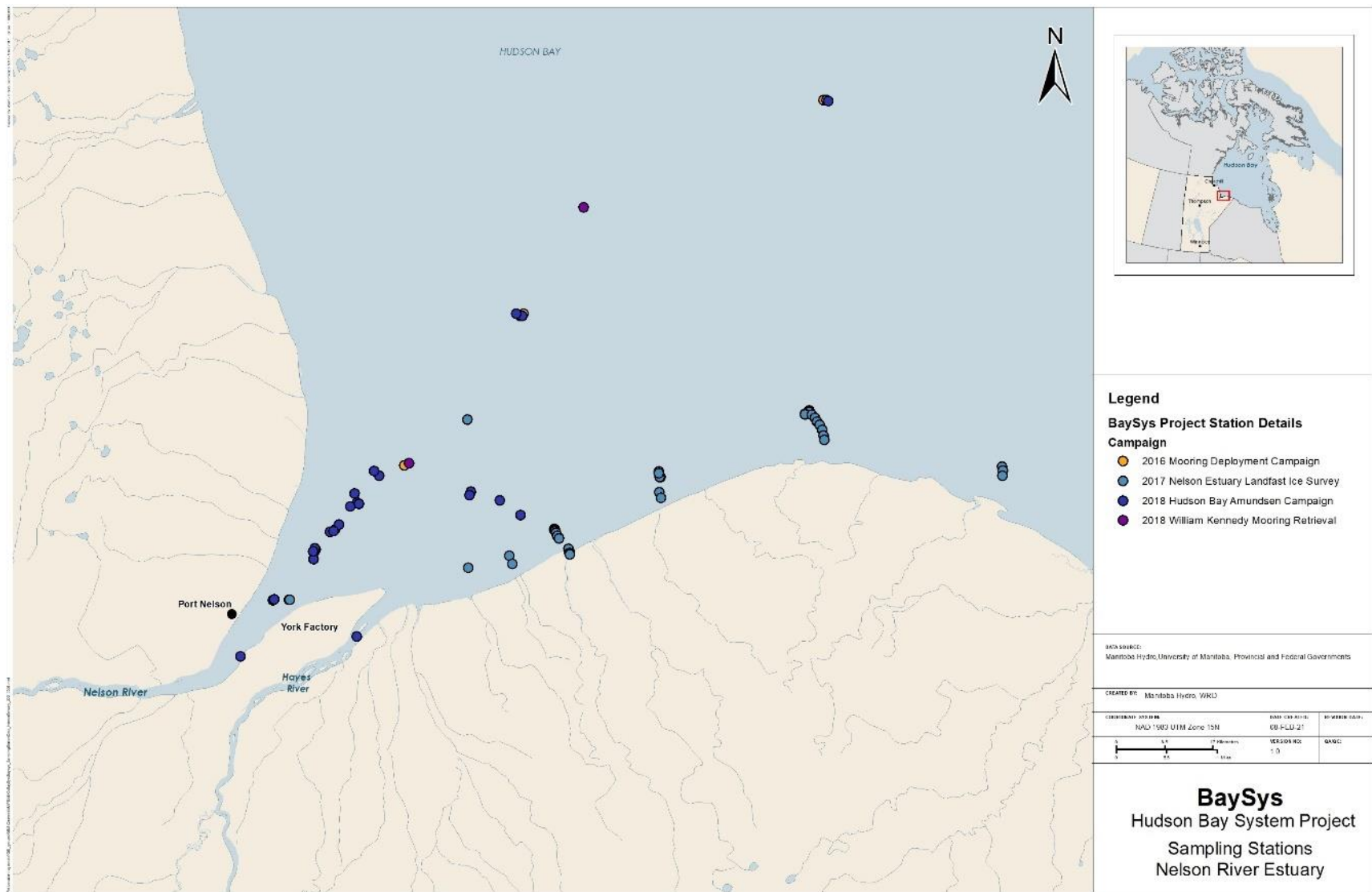
BAYSYS CAMPAIGN STATIONS 2016-2018



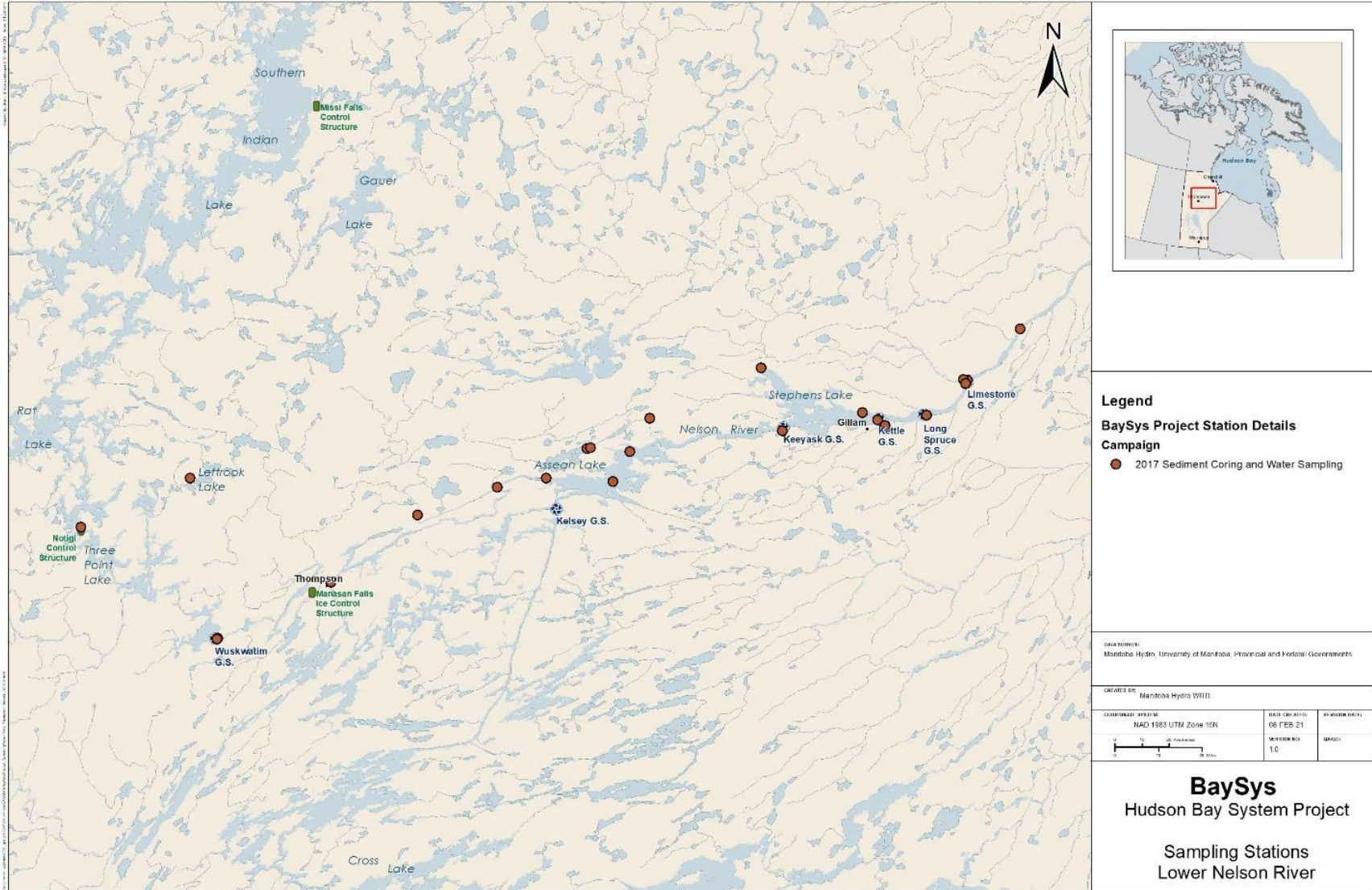
Map of Hudson Bay Complex indicating all BaySys project station locations, including ocean, sea ice, river, and estuary stations.



Map of Churchill river and estuary region indicating all BaySys project station locations, including ocean, sea ice, river, and estuary stations.



Map of Nelson estuary region indicating all BaySys project station locations, including ocean, sea ice, river, and estuary stations.



Map of Nelson River and surrounding lakes region indicating all BaySys project station locations.

BaySys station details from all 2016 campaigns

Station ID	Collection Date	Station Type	Campaign	Description	Lat.	Long.	Bottom Depth (m)
BS04	2016-09-27	Estuary	2016 Mooring Deployment	Nelson River Estuary	57.5032	-91.7917	
BS06	2016-09-28	Estuary	2016 Mooring Deployment	Nelson River Estuary	57.8294	-90.8907	
BS07	2016-09-29	Estuary	2016 Mooring Deployment	Nelson River Estuary	57.2658	-92.1484	
BS08	2016-09-30	Estuary	2016 Mooring Deployment	Nelson River Estuary	56.7584	-86.9723	
BS09	2016-09-30	Estuary	2016 Mooring Deployment	Nelson River Estuary	56.3338	-85.4996	
CI01	2016-10-06	Ocean	2016 Mooring Deployment	Coats Island	62.463	-80.3352	194
CI02	2016-10-08	Ocean	2016 Mooring Deployment	Coats Island	62.7323	-81.703	208
CI03	2016-10-07	Ocean	2016 Mooring Deployment	Coats Island	63.2689	-83.759	106
JB00	2016-10-01	Ocean	2016 Mooring Deployment	James Bay	54.6408	-79.8615	46
JB01	2016-10-01	Ocean	2016 Mooring Deployment	James Bay	54.678	-79.9582	50
JB02	2016-10-01	Ocean	2016 Mooring Deployment	James Bay	54.6829	-80.1871	101
JB03	2016-10-02	Ocean	2016 Mooring Deployment	James Bay	54.6936	-80.511	111
JB04	2016-10-02	Ocean	2016 Mooring Deployment	James Bay	54.7029	-80.5487	107
JB05	2016-10-02	Ocean	2016 Mooring Deployment	James Bay	54.7102	-80.7771	97
JB06	2016-10-02	Ocean	2016 Mooring Deployment	James Bay	54.7219	-80.9997	77
JB07	2016-10-02	Ocean	2016 Mooring Deployment	James Bay	54.7347	-81.2292	63
JB08	2016-10-02	Ocean	2016 Mooring Deployment	James Bay	54.7565	-81.4555	45
JB09	2016-10-02	Ocean	2016 Mooring Deployment	James Bay	54.7607	-81.6972	33
JB10	2016-10-03	Ocean	2016 Mooring Deployment	James Bay	55.1557	-82.0405	24
JB11	2016-10-03	Ocean	2016 Mooring Deployment	James Bay	55.2313	-81.8452	47
JB12	2016-10-03	Ocean	2016 Mooring Deployment	James Bay	55.313	-81.6631	64
JB13	2016-10-03	Ocean	2016 Mooring Deployment	James Bay	55.3833	-81.099	95
JB14	2016-10-03	Ocean	2016 Mooring Deployment	James Bay	55.4501	-80.5538	105
JB15	2016-10-03	Ocean	2016 Mooring Deployment	James Bay	55.2914	-79.4019	170
JB85	2016-10-02	Ocean	2016 Mooring Deployment	James Bay	54.7541	-81.5831	
JB95	2016-10-02	Ocean	2016 Mooring Deployment	James Bay	54.7832	-81.7969	
KU01	2016-10-04	Ocean	2016 Mooring Deployment	Kujjaurapik	55.2875	-77.8054	43

KU02	2016-10-04	Ocean	2016 Mooring Deployment	Kujjaurapik	55.3092	-77.8545	97
MI01	2016-10-08	Ocean	2016 Mooring Deployment	Mansel Island	62.2363	-78.7249	68
MI02	2016-10-08	Ocean	2016 Mooring Deployment	Mansel Island	62.5662	-80.8303	125
M06	2016-09-29	Estuary	2016 Mooring Deployment	Nelson River Estuary	57.1339	-92.4091	
AN01	2016-09-26	Estuary	2016 Mooring Deployment	Churchill Estuary	59.9693	-91.9524	109
NE01	2016-09-29	Estuary	2016 Mooring Deployment	Nelson River Estuary	57.1321	-92.4117	29.7
NE02	2016-09-27	Estuary	2016 Mooring Deployment	Nelson River Estuary	57.5001	-91.8016	46
NE03	2016-09-28	Estuary	2016 Mooring Deployment	Nelson River Estuary	57.8294	-90.8815	54
NI01	2016-10-09	Ocean	2016 Mooring Deployment	Nottingham Island	63.2601	-78.354	
S01	2016-09-30	River	2016 Mooring Deployment	Nelson River	55.9608	-87.7073	
W01	2016-09-30	River	2016 Mooring Deployment	Winisk River	55.2148	-85.241	
WI01	2016-10-06	Ocean	2016 Mooring Deployment	Near Mansel Island	62.4585	-80.338	

BaySys station details from all 2017 campaigns.

Station ID	Collection Date	Station Type	Campaign	Description	Lat	Long	Bottom Depth (m)
TL-17-01	2017-03-02	Lake	2017 Sediment Coring and Water Sampling	Threepoint Lake	55.6715	-98.871263	6.7
TL-17-02	2017-03-02	Lake	2017 Sediment Coring and Water Sampling	Threepoint Lake	55.6830	-98.876601	1.7
LL-17-01	2017-03-03	Lake	2017 Sediment Coring and Water Sampling	Leftrook Lake	56.0623	-98.7176	10
LL-17-02	2017-03-03	Lake	2017 Sediment Coring and Water Sampling	Leftrook Lake	56.0667	-98.731932	1
AL-17-01	2017-03-04	Lake	2017 Sediment Coring and Water Sampling	Assean Lake	56.2459	-96.3746	8.3

AL-17-02	2017-03-05	Lake	2017 Sediment Coring and Water Sampling	Assean Lake	56.2429	-96.369439	1
SpL-17-01-A	2017-04-03	Lake	2017 Sediment Coring and Water Sampling	Split Lake	56.2427	-96.1196	5.7
SpL-17-01-B	2017-04-03	Lake	2017 Sediment Coring and Water Sampling	Split Lake	56.2427	-96.1196	5.7
SpL-17-01-C	2017-04-04	Lake	2017 Sediment Coring and Water Sampling	Split Lake	56.1413	-96.2109	9
StL-17-02	2017-04-04	Lake	2017 Sediment Coring and Water Sampling	Stephens Lake	56.3993	-94.7375	1.8
NR1	2017-07-29	River	Sediment Coring and Water Sampling	Nelson River at Conwapa	56.687	-93.7983	
NR2	2017-07-28	River	Sediment Coring and Water Sampling	Nelson River downstream of Limestone GS	56.5152	-94.1139	
NR3	2017-07-29	River	Sediment Coring and Water Sampling	Nelson River downstream of Longspruce GS	56.3957	-94.3521	
NR4	2017-07-29	Lake	Sediment Coring and Water Sampling	Stephens Lake upstream of Kettle GS	56.3772	-94.6448	
NR5	2017-07-30	Lake	Sediment Coring and Water Sampling	Stephen Lake northwest arm	56.5373	-95.3535	
NR6	2017-07-29	River	Sediment Coring and Water Sampling	Nelson River at Keeyask GS South	56.3319	-95.2131	
NR7	2017-07-27	River	Sediment Coring and Water Sampling	Nelson River at Kichi Sipi Bridge	54.5618	-97.7444	
NR8	2017-07-28	River	Sediment Coring and Water Sampling	Nelson River at Norway House ferry	54.2503	-98.3557	
LR1	2017-07-29	River	Sediment Coring and Water Sampling	Limestone River	56.5167	-94.1353	

KR1	2017-07-29	River	Sediment Coring and Water Sampling	Kettle River	56.3583	-94.5999	
AR1	2017-07-30	River	Sediment Coring and Water Sampling	Assean River	56.3566	-96.0092	
OR1	2017-07-31	River	Sediment Coring and Water Sampling	Odei River	55.9948	-97.3574	
BR1	2017-07-30	River	Sediment Coring and Water Sampling	Burntwood River upstream of Split Lake	56.1423	-96.6075	
BR2	2017-07-30	River	Sediment Coring and Water Sampling	Burntwood River downstream Odei River	56.1028	-96.8962	
BR3	2017-07-31	River	Sediment Coring and Water Sampling	Burntwood River at Thompson	55.7538	-97.8413	
BR4	2017-07-31	River	Sediment Coring and Water Sampling	Burntwood river downstream of Wuskwatim GS	55.5405	-98.4787	
BR5	2017-07-31	River	Sediment Coring and Water Sampling	Burntwood River downstream of Wuskwatim GS	55.5385	-98.4834	
BR6	2017-07-31	River	Sediment Coring and Water Sampling	Notigi Lake upstream of control structure	55.8685	-99.3362	
Limestone GS	2017	River	Sediment Coring and Water Sampling	Upstream of Limestone Generating Station	56.5029	-94.1221	
AL	2017	River	Sediment Coring and Water Sampling	Assean River	56.2493	-96.3536	
Survey 1	2017-03-18	Landfast Ice	Nelson Estuary Landfast Ice Survey	Near the shore of Hudson Bay between the mouth of the Nelson River and Cape Tatnam (Drone)	57.1245	-91.6696	
Survey 2	2017-03-18	Landfast Ice	Nelson Estuary Landfast Ice Survey	Near the shore of Hudson Bay between the mouth of the Nelson River and	57.1298	-91.6732	

				Cape Tatnam (Drone)			
Survey 3	2017-03-19	Landfast Ice	Nelson Estuary Landfast Ice Survey	Near the shore of Hudson Bay between the mouth of the Nelson River and Cape Tatnam (Drone)	57.1229	-91.6702	
Survey 4	2017-03-22	Landfast Ice	Nelson Estuary Landfast Ice Survey	Near the shore of Hudson Bay between the mouth of the Nelson River and Cape Tatnam (Drone)	57.0551	-92.4886	
Survey 5	2017-03-22	Landfast Ice	Nelson Estuary Landfast Ice Survey	Near the shore of Hudson Bay between the mouth of the Nelson River and Cape Tatnam (Drone)	57.0549	-92.4866	
Survey 6	2017-03-24	Landfast Ice	Nelson Estuary Landfast Ice Survey	Near the shore of Hudson Bay between the mouth of the Nelson River and Cape Tatnam (Drone)	57.1607	-91.7124	
Survey 7	2017-03-25	Landfast Ice	Nelson Estuary Landfast Ice Survey	Near the shore of Hudson Bay between the mouth of the Nelson River and Cape Tatnam (Drone)	57.1602	-91.7126	
Survey 8	2017-03-24	Landfast Ice	Nelson Estuary Landfast Ice Survey	Near the shore of Hudson Bay between the mouth of the Nelson River and Cape Tatnam (Drone)	57.1601	-91.7126	
Survey 9	2017-03-25	Landfast Ice	Nelson Estuary Landfast Ice Survey	Near the shore of Hudson Bay between the mouth of the Nelson River and Cape Tatnam (Drone)	57.24	-91.4007	

Survey 10	2017-03-25	Landfast Ice	Nelson Estuary Landfast Ice Survey	Near the shore of Hudson Bay between the mouth of the Nelson River and Cape Tatnam (Drone)	57.2404	-91.4021	
Survey 11	2017-03-25	Landfast Ice	Nelson Estuary Landfast Ice Survey	Near the shore of Hudson Bay between the mouth of the Nelson River and Cape Tatnam (Drone)	57.249	-91.4052	
Survey 12	2017-03-25	Landfast Ice	Nelson Estuary Landfast Ice Survey	Near the shore of Hudson Bay between the mouth of the Nelson River and Cape Tatnam (Drone)	57.2466	-91.4048	
Survey 13	2017-03-28	Landfast Ice	Nelson Estuary Landfast Ice Survey	Near the shore of Hudson Bay between the mouth of the Nelson River and Cape Tatnam (Drone)	57.3381	-90.9623	
Survey 14	2017-03-28	Landfast Ice	Nelson Estuary Landfast Ice Survey	Near the shore of Hudson Bay between the mouth of the Nelson River and Cape Tatnam (Drone)	57.3389	-90.9598	
Survey 15	2017-03-28	Landfast Ice	Nelson Estuary Landfast Ice Survey	Near the shore of Hudson Bay between the mouth of the Nelson River and Cape Tatnam (Drone)	57.3375	-90.9602	
Survey 16	2017-03-28	Landfast Ice	Nelson Estuary Landfast Ice Survey	Near the shore of Hudson Bay between the mouth of the Nelson River and Cape Tatnam (Drone)	57.3339	-90.9729	

Survey 17	2017-03-28	Landfast Ice	Nelson Estuary Landfast Ice Survey	Near the shore of Hudson Bay between the mouth of the Nelson River and Cape Tatnam (Drone)	57.3335	-90.9736	
Survey 18	2017-03-28	Landfast Ice	Nelson Estuary Landfast Ice Survey	Near the shore of Hudson Bay between the mouth of the Nelson River and Cape Tatnam (Drone)	57.3334	-90.9732	
Survey 19	2017-03-28	Landfast Ice	Nelson Estuary Landfast Ice Survey	Near the shore of Hudson Bay between the mouth of the Nelson River and Cape Tatnam (Drone)	57.1208	-91.6702	
Survey 20	2017-04-07	Landfast Ice	Nelson Estuary Landfast Ice Survey	Near the shore of Hudson Bay between the mouth of the Nelson River and Cape Tatnam (Drone)	57.1026	-91.9661	
Survey 21	2017-04-07	Landfast Ice	Nelson Estuary Landfast Ice Survey	Near the shore of Hudson Bay between the mouth of the Nelson River and Cape Tatnam (Drone)	57.1026	-91.9658	
Survey 22	2017-04-07	Landfast Ice	Nelson Estuary Landfast Ice Survey	Near the shore of Hudson Bay between the mouth of the Nelson River and Cape Tatnam (Drone)	57.1205	-91.8459	
Survey 23	2017-04-07	Landfast Ice	Nelson Estuary Landfast Ice Survey	Near the shore of Hudson Bay between the mouth of the Nelson River and Cape Tatnam (Drone)	57.1076	-91.8379	

Survey 24	2017-04-13	Landfast Ice	Nelson Estuary Landfast Ice Survey	Near the shore of Hudson Bay between the mouth of the Nelson River and Cape Tatnam (Drone)	57.1604	-91.7129	
Survey 25	2017-04-13	Landfast Ice	Nelson Estuary Landfast Ice Survey	Near the shore of Hudson Bay between the mouth of the Nelson River and Cape Tatnam (Drone)	57.1604	-91.7122	
Survey 26	2017-04-13	Landfast Ice	Nelson Estuary Landfast Ice Survey	Near the shore of Hudson Bay between the mouth of the Nelson River and Cape Tatnam (Drone)	57.1471	-91.702	
Survey 27	2017-04-13	Landfast Ice	Nelson Estuary Landfast Ice Survey	Near the shore of Hudson Bay between the mouth of the Nelson River and Cape Tatnam (Drone)	57.1471	-91.7007	
1_2017	2017-02-23	Landfast Ice	Nelson Estuary Landfast Ice Survey	Nelson Estuary	57.1615	-91.7139	4.05
2_2017	2017-02-23	Landfast Ice	Nelson Estuary Landfast Ice Survey	Nelson Estuary	57.1601	-91.7129	3.72
3_2017	2017-02-23	Landfast Ice	Nelson Estuary Landfast Ice Survey	Nelson Estuary	57.1579	-91.7106	3.48
4_2017	2017-02-23	Landfast Ice	Nelson Estuary Landfast Ice Survey	Nelson Estuary	57.1556	-91.7088	2.95
5_2017	2017-02-23	Landfast Ice	Nelson Estuary Landfast Ice Survey	Nelson Estuary	57.1506	-91.7049	2.31
6_2017	2017-02-23	Landfast Ice	Nelson Estuary Landfast Ice Survey	Nelson Estuary	57.1467	-91.7007	1.62

7_2017	2017-02-25	Landfast Ice	Nelson Estuary Landfast Ice Survey	Nelson Estuary	57.3369	-91.9617	7.94
8_2017	2017-02-25	Landfast Ice	Nelson Estuary Landfast Ice Survey	Nelson Estuary	57.3320	-90.953	7.00
9_2017	2017-02-25	Landfast Ice	Nelson Estuary Landfast Ice Survey	Nelson Estuary	57.3275	-90.9448	6.35
10_2017	2017-02-25	Landfast Ice	Nelson Estuary Landfast Ice Survey	Nelson Estuary	57.3213	-90.9391	6.30
11_2017	2017-02-25	Landfast Ice	Nelson Estuary Landfast Ice Survey	Nelson Estuary	57.3163	-90.9312	4.73
12_2017	2017-02-25	Landfast Ice	Nelson Estuary Landfast Ice Survey	Nelson Estuary	57.3076	-90.9241	3.72
13_2017	2017-02-25	Landfast Ice	Nelson Estuary Landfast Ice Survey	Nelson Estuary	57.2986	-90.9214	1.70
14_2017	2017-02-25	Landfast Ice	Nelson Estuary Landfast Ice Survey	Nelson Estuary	57.2919	-90.919	1.56
15_2017	2017-02-27	Landfast Ice	Nelson Estuary Landfast Ice Survey	Nelson Estuary	57.2402	-90.4022	6.53
16_2017	2017-02-27	Landfast Ice	Nelson Estuary Landfast Ice Survey	Nelson Estuary	57.2336	-90.401	5.79
17_2017	2017-02-27	Landfast Ice	Nelson Estuary Landfast Ice Survey	Nelson Estuary	57.2256	-90.4017	4.73
18_2017	2017-02-27	Landfast Ice	Nelson Estuary Landfast Ice Survey	Nelson Estuary	57.2163	-91.4053	3.24
19_2017	2017-02-27	Landfast Ice	Nelson Estuary Landfast Ice Survey	Nelson Estuary	57.2072	-91.3998	1.67
Simba 01	2017-02-09	Ice flow	Churchill River and Mobile Ice Survey	Churchill River	59.1451	-93.2108	74

Simba 02	2017-02-12	Ice flow	Churchill River and Mobile Ice Survey	Churchill River	59.0436	-93.0662	68
Simba 03	2017-02-10	Ice flow	Churchill River and Mobile Ice Survey	Churchill River	59.2276	-92.933	61
Button Bay	2017-02-04	Ice flow	Churchill River and Mobile Ice Survey	Churchill River	58.8083	-94.2867	
Est-1	2017-02-04	Ice flow	Churchill River and Mobile Ice Survey	Churchill River	58.7907	-94.2104	
Est-2	2017-02-04	Ice flow	Churchill River and Mobile Ice Survey	Churchill River	58.7935	-94.1996	
Est-3	2017-02-05	Ice flow	Churchill River and Mobile Ice Survey	Churchill River	58.796	-94.1891	
Est-4	2017-02-05	Ice flow	Churchill River and Mobile Ice Survey	Churchill River	58.7969	-94.1807	
Pan 1, Marine 1	2017-02-07	Ice flow	Churchill River and Mobile Ice Survey	Churchill River	59.0784	-92.1108	
Pan 2	2017-02-08	Ice flow	Churchill River and Mobile Ice Survey	Churchill River	58.738	-93.8182	
Pan 3	2017-02-08	Ice flow	Churchill River and Mobile Ice Survey	Churchill River	58.9173	-93.3902	
Pan 4	2017-02-08	Ice flow	Churchill River and Mobile Ice Survey	Churchill River	58.976	-93.3767	
Pan 5	2017-02-08	Ice flow	Churchill River and Mobile Ice Survey	Churchill River	59.0259	-93.3512	
Pan 6	2017-02-09	Ice flow	Churchill River and Mobile Ice Survey	Churchill River	59.1451	-93.2108	
Pan 7	2017-02-09	Ice flow	Churchill River and Mobile Ice Survey	Churchill River	N/A	N/A	

Pan 8	2017-02-09	Ice flow	Churchill River and Mobile Ice Survey	Churchill River	N/A	N/A	
Pan 9	2017-02-09	Ice flow	Churchill River and Mobile Ice Survey	Churchill River	N/A	N/A	
Pan 10	2017-02-10	Ice flow	Churchill River and Mobile Ice Survey	Churchill River	59.0436	-93.0662	
Pan 11, Marine 2	2017-02-10	Ice flow	Churchill River and Mobile Ice Survey	Churchill River	59.2276	-92.933	
Pan 12	2017-02-10	Ice flow	Churchill River and Mobile Ice Survey	Churchill River	N/A	N/A	
Pan 13	2017-02-10	Ice flow	Churchill River and Mobile Ice Survey	Churchill River	N/A	N/A	
Pan 14	2017-02-10	Ice flow	Churchill River and Mobile Ice Survey	Churchill River	N/A	N/A	
Pan 15	2017-02-10	Ice flow	Churchill River and Mobile Ice Survey	Churchill River	59.2055	-92.8448	
Pan 16	2017-02-11	Ice flow	Churchill River and Mobile Ice Survey	Churchill River	58.8441	-93.2497	
Pan 17	2017	Ice flow	Churchill River and Mobile Ice Survey	Churchill River	58.8169	-93.1385	
Pan 18	2017	Ice flow	Churchill River and Mobile Ice Survey	Churchill River	58.8145	-93.3593	
Pan 19	2017	Ice flow	Churchill River and Mobile Ice Survey	Churchill River	58.8481	-93.5398	
Pan 20	2017	Ice flow	Churchill River and Mobile Ice Survey	Churchill River	58.8548	-93.7312	
Pan 21	2017	Ice flow	Churchill River and Mobile Ice Survey	Churchill River	58.8003	-93.9032	

Pan 22	2017	Ice flow	Churchill River and Mobile Ice Survey	Churchill River	59.1745	-93.2032	
Pan 23, Marine 3	2017	Ice flow	Churchill River and Mobile Ice Survey	Churchill River	59.3047	-93.1147	
Pan 24	2017	Ice flow	Churchill River and Mobile Ice Survey	Churchill River	58.8197	-93.1287	
Pan 25	2017	Ice flow	Churchill River and Mobile Ice Survey	Churchill River	58.8316	-93.3063	
Pan 26	2017	Ice flow	Churchill River and Mobile Ice Survey	Churchill River	58.8275	-93.4807	
Pan 27	2017	Ice flow	Churchill River and Mobile Ice Survey	Churchill River	58.7993	-94.1882	
Pan 28	2017	Ice flow	Churchill River and Mobile Ice Survey	Churchill River	58.7817	-94.0189	
Pan 29	2017	Ice flow	Churchill River and Mobile Ice Survey	Churchill River	58.8446	-93.7747	
Pan 30, Marine 4	2017	Ice flow	Churchill River and Mobile Ice Survey	Churchill River	58.8353	-94.0233	
Pan 31	2017	Ice flow	Churchill River and Mobile Ice Survey	Churchill River	58.832	-94.2163	
Pan 32	2017	Ice flow	Churchill River and Mobile Ice Survey	Churchill River	58.8485	-94.3061	
Pan 33	2017	Ice flow	Churchill River and Mobile Ice Survey	Churchill River	58.8889	-94.1978	

BaySys station details from all 2018 campaigns.

Station ID	Collection Date	Alt. ID	Alt. ID Year	Station Type	Campaign Name	Station Description	Lat	Long	Bottom Depth (m)
1	2018-05-31	356		Ocean	Amundsen Leg 1	Nutrient	60.8133	-64.5334	328.75
2	2018-05-31	354		Ocean	Amundsen Leg 1	Nutrient	60.9735	-64.7734	571.13
3	2018-06-01	352		Ocean	Amundsen Leg 1	Nutrient	61.1502	-64.8087	430.12
4	2018-06-01	HN01		Ocean	Amundsen Leg 1	Nutrient	62.0405	-69.6133	285
5	2018-06-02	FB01(A)		Ocean	Amundsen Leg 1	Nutrient	64.2865	-78.2308	233.03
6	2018-06-03	FB01(B)		Ocean	Amundsen Leg 1	Nutrient	64.2236	-78.6244	276.08
7	2018-06-03	FB02		Ocean	Amundsen Leg 1	Nutrient	64.0653	-79.0624	270
8	2018-06-03	M19		Ocean	Amundsen Leg 1	Nutrient	63.9494	-79.5646	320.34
9	2018-06-03	FB03		Ocean	Amundsen Leg 1	Basic	63.7302	-79.9264	103
10	2018-06-04			Ocean	Amundsen Leg 1	Nutrient	63.4474	-79.4428	201.58
11	2018-06-04			Ocean/Combination	Amundsen Leg 1	Full/Ice	62.8651	-78.8984	320.87
12	2018-06-05			Ocean	Amundsen Leg 1	Nutrient	63.3958	-81.2244	85.78
13	2018-06-05			Ocean	Amundsen Leg 1	Nutrient	63.2646	-81.6708	148.03
14	2018-06-05			Ocean	Amundsen Leg 1	Nutrient	63.1967	-81.8557	
15	2018-06-05	CMO-C		Ocean	Amundsen Leg 1	Basic	63.1934	-81.9231	187.93
16	2018-06-06			Ocean/Combination	Amundsen Leg 1	Full/Ice	62.2794	-85.9089	136.81
17	2018-06-07			Ocean	Amundsen Leg 1	Basic	63.1846	-90.0357	88.43
18	2018-06-08	CMO-D		Ocean/Combination	Amundsen Leg 1	Full/Ice	63.7137	-88.4168	115.61
19	2018-06-09			Ocean/Combination	Amundsen Leg 1	Full/Water	61.8468	-92.1129	74.89
20	2018-06-10			Ocean	Amundsen Leg 1	Nutrient	61.3743	-90.942	112.15
21	2018-06-10			Ocean/Combination	Amundsen Leg 1	Full/Ice	60.9102	-89.3595	149.58
22	2018-06-10			Ocean/Combination	Amundsen Leg 1	Full/Water	60.4231	-94.0023	239.9
23	2018-06-12	M6		Ocean	Amundsen Leg 1	Nutrient	60.9221	-91.7809	110.52
24	2018-06-12			Ocean/Combination	Amundsen Leg 1	Full/Ice	61.696	-87.7618	189.39

25	2018-06-13			Ocean/Combination	Amundsen Leg 1	Full/Ice	62.0218	-87.0086	148.19
26	2018-06-14			Ocean	Amundsen Leg 1	Nutrient	62.2042	-88.3775	131.46
27	2018-06-14			Ocean	Amundsen Leg 1	Nutrient	62.5836	-90.9228	61.02
28	2018-06-15			Ocean	Amundsen Leg 1	Basic	62.4155	-89.8339	163.63
29	2018-06-16	CMO-B		Ocean/Combination	Amundsen Leg 1	Full	61.7698	-84.3091	176.99
31	2018-06-18	NE02		Ocean	Amundsen Leg 1	Nutrient	57.5001	-91.7953	47.4
32	2018-06-19			Ocean/Combination	Amundsen Leg 1	Full/Ice	56.984	-88.1158	32.97
33	2018-06-20			Ocean/Combination	Amundsen Leg 1	Ice Sampling	56.6114	-87.0904	47.49
34	2018-06-21			Ocean/Combination	Amundsen Leg 1	Full/Ice	56.4998	-86.8688	43.78
35	2018-06-22			Ocean/Combination	Amundsen Leg 1	Nutrient	57.1798	-86.4995	61.46
36	2018-06-22			Ocean/Combination	Amundsen Leg 1	Full/Ice	57.7741	-86.0313	128.34
37	2018-06-23			Ocean	Amundsen Leg 1	Nutrient	58.4689	-86.2255	169.68
38	2018-06-23			Ocean/Combination	Amundsen Leg 1	Full/Ice	58.7224	-86.305	181.31
39	2018-06-24			Ocean	Amundsen Leg 1	Nutrient	58.4748	-87.4385	182.66
40	2018-06-24			Ocean	Amundsen Leg 1	Basic	58.2326	-88.5635	90.62
41	2018-06-25			Ocean	Amundsen Leg 1	Nutrient	58.0189	-9999	71.08
42	2018-06-25	NE03		Ocean	Amundsen Leg 1	Mooring Recovery	57.8278	-90.8759	53.82
43	2018-06-27	15		Ocean	Amundsen Leg 1	Basic	63.1917	-81.9668	192.62
44	2018-06-28	CMO-A, AN01		Ocean	Amundsen Leg 1	59.9747	-91.9506	Decimal Degrees	m
45	2018-06-30			Ocean	Amundsen Leg 1	Basic	57.223	-91.9554	16.66
46	2018-07-01			Ocean	Amundsen Leg 1	Basic	57.5032	-91.8129	41.2
FB05-H	2018-06-02			Ice flow	Amundsen Leg 1	Hudson Strait Heli	-9999	-9999	
M.I. H1	2018-06-04			Ice flow	Amundsen Leg 1	Mansel Island Heli	62.2439	-78.3126	
M.I. H2	2018-06-04			Ice flow	Amundsen Leg 1	Mansel Island Heli	62.2429	-78.5166	
M.I. H3	2018-06-04			Ice flow	Amundsen Leg 1	Mansel Island Heli	62.2419	-78.7206	
M.I. H4	2018-06-04			Ice flow	Amundsen Leg 1	Mansel Island Heli	62.2408	-78.9246	
M.I. H5	2018-06-04			Ice flow	Amundsen Leg 1	Mansel Island Heli	62.2398	-79.1286	

Northwest HB RIS 1	2018-06-06			Ice flow	Amundsen Leg 1	Northwest HB Remote Ice Station Heli	62.0798	-85.36	
Northwest HB RIS 2	2018-06-06			Ice flow	Amundsen Leg 1	Northwest HB Remote Ice Station Heli	62.3279	-85.2619	
Northwest HB RIS 3	2018-06-06			Ice flow	Amundsen Leg 1	Northwest HB Remote Ice Station Heli	62.3604	-85.2203	
R.W.S H1	2018-06-08			Ice flow	Amundsen Leg 1	Roes Welcome Sound Heli	64.0049	-87.0154	
R.W.S H2	2018-06-08			Ice flow	Amundsen Leg 1	Roes Welcome Sound Heli	64.0739	-87.1999	
R.W.S H3	2018-06-08			Ice flow	Amundsen Leg 1	Roes Welcome Sound Heli	64.1391	-87.3856	
R.W.S H4	2018-06-08			Ice flow	Amundsen Leg 1	Roes Welcome Sound Heli	64.2236	-87.5592	
R.W.S H5	2018-06-08			Ice flow	Amundsen Leg 1	Roes Welcome Sound Heli	64.292	-87.7409	
C.I. H1	2018-06-08			River	Amundsen Leg 1	Chesterfield Inlet Heli	63.4752	-90.8744	
C.I. H2	2018-06-08			River	Amundsen Leg 1	Chesterfield Inlet Heli	63.5688	-90.5472	
C.I. H3	2018-06-08			River	Amundsen Leg 1	Chesterfield Inlet Heli	63.2368	-90.6563	
F.R. River Station	2018-06-09			River	Amundsen Leg 1	Ferguson River Heli	62.0723	-93.351	
F.R. Landfast 1	2018-06-09	Ferguson Estuary		River	Amundsen Leg 1	61.8796	-92.8451	Decimal Degrees	
F.R. Landfast 2	2018-06-09			River	Amundsen Leg 1	Ferguson River Heli	61.8173	-92.7918	
Wil.R. River Station	2018-06-09			River	Amundsen Leg 1	Wilson River Heli	62.338	-93.1129	
Wil.R. Landfast 1	2018-06-09	Wilson Estuary		River	Amundsen Leg 1	62.126	-92.4869	Decimal Degrees	
Wil.R. Landfast 2	2018-06-09			River	Amundsen Leg 1	Wilson River Heli	62.1333	-92.4522	
Wil.R. Z1	2018-06-09			Ocean	Amundsen Leg 1	Wilson River Zodiac	62.0574	-92.473	
Wil.R. Z2	2018-06-09			Ocean	Amundsen Leg 1	Wilson River Zodiac	61.9853	-92.3349	
Wil.R. Z3	2018-06-09			Ocean	Amundsen Leg 1	Wilson River Zodiac	61.9211	-92.2151	
T.R. River Station	2018-06-11			River	Amundsen Leg 1	Thlewiaza River Heli	60.4351	-94.8167	

T-A.R. River Station	2018-06-11			River	Amundsen Leg 1	Tha-anne River Heli	60.5461	-94.8292	
T-A.R. Z1	2018-06-11			Ocean	Amundsen Leg 1	Tha-anne River Zodiac	60.4712	-94.5673	
T-A.R. Z2	2018-06-11			Ocean	Amundsen Leg 1	Tha-anne River Zodiac	60.4592	-94.4157	
T-A.R. Z3	2018-06-11			Ocean	Amundsen Leg 1	Tha-anne River Zodiac	60.4434	-94.2228	
Seal.R. River Station	2018-06-28			River	Amundsen Leg 1	Seal River Heli	59.0739	-94.8344	
K.R. River Station	2018-06-28			River	Amundsen Leg 1	Knife River Heli	58.8831	-94.7031	
C.R. River Station	2018-06-28			River	Amundsen Leg 1	Churchill River Heli	58.6781	-94.2033	
N.R. River Station	2018-06-18			River	Amundsen Leg 1	Nelson River Heli	56.9659	-92.6305	
H.R. Station	2018-06-18			River	Amundsen Leg 1	Hayes River Heli	56.9955	-92.2924	
Sev.R. River Station	2018-06-19			River	Amundsen Leg 1	Severn River Heli	55.9603	-87.7081	
Win.R. River Station	2018-06-21			River	Amundsen Leg 1	Winisk River Heli	55.2218	-85.2068	
34_HeliA	2018-06-20			Ice flow	Amundsen Leg 1	Helicopter Sampling	56.6833	-86.9083	
34_HeliB	2018-06-20			Ice flow	Amundsen Leg 1	Helicopter Sampling	56.5867	-86.8968	
34_HeliC	2018-06-21			Ice flow	Amundsen Leg 1	Helicopter Sampling	56.1072	-84.5633	
34_HeliD	2018-06-21			Ice flow	Amundsen Leg 1	Helicopter Sampling	56.4099	-85.8918	
36_HeliA	2018-06-22			Ice flow	Amundsen Leg 1	Helicopter Sampling	57.8781	-84.22	
36_HeliB	2018-06-22			Ice flow	Amundsen Leg 1	Helicopter Sampling	57.8291	-85.1337	
36_HeliC	2018-06-22			Ice flow	Amundsen Leg 1	Helicopter Sampling	58.2978	-87.6057	
36_HeliD	2018-06-22			Ice flow	Amundsen Leg 1	Helicopter Sampling	58.0513	-86.8623	
38_HeliA	2018-06-23			Ice flow	Amundsen Leg 1	Helicopter Sampling	58.7909	-84.2376	
38_HeliB	2018-06-23			Ice flow	Amundsen Leg 1	Helicopter Sampling	58.7916	-85.1604	
38_HeliC	2018-06-23			Ice flow	Amundsen Leg 1	Helicopter Sampling	59.2654	-87.9881	
38_HeliD	2018-06-23			Ice flow	Amundsen Leg 1	Helicopter Sampling	59.0165	-87.9881	
N.E. South Tran 1	2018-06-29			Estuary	Amundsen Leg 1	Nelson Estuary	57.1842	-91.8111	
N.E. South Tran 2	2018-06-29			Estuary	Amundsen Leg 1	Nelson Estuary	57.2081	-91.8711	

N.E. South Tran 3	2018-06-29			Estuary	Amundsen Leg 1	Nelson Estuary	57.2176	-91.9585	
N1a	2018-06-29			Estuary	Amundsen Leg 1	Nelson River Transect	57.0543	-92.5351	
N1b	2018-06-29			Estuary	Amundsen Leg 1	Nelson River Transect	57.0558	-92.5313	
N2	2018-06-29			Estuary	Amundsen Leg 1	Nelson River Transect	57.1191	-92.4165	
BN3a	2018-06-29			Estuary	Amundsen Leg 1	Nelson River Transect	57.1358	-92.4118	
BN3b	2018-06-30			Estuary	Amundsen Leg 1	Nelson River Transect	57.1311	-92.4174	
BN4a	2018-06-30			Estuary	Amundsen Leg 1	Nelson River Transect	57.166	-92.3519	
BN4b	2018-06-30			Estuary	Amundsen Leg 1	Nelson River Transect	57.1615	-92.3673	
BN5a	2018-06-30			Estuary	Amundsen Leg 1	Nelson River Transect	57.1731	-92.3411	
BN5b	2018-06-30			Estuary	Amundsen Leg 1	Nelson River Transect	57.1628	-92.3574	
BN6a	2018-06-30			Estuary	Amundsen Leg 1	Nelson River Transect	57.2078	-92.2868	
BN6b	2018-06-30			Estuary	Amundsen Leg 1	Nelson River Transect	57.2019	-92.308	
BN7a	2018-06-30			Estuary	Amundsen Leg 1	Nelson River Transect	57.25	-92.2217	
BN7b	2018-06-30			Estuary	Amundsen Leg 1	Nelson River Transect	57.2579	-92.237	
N3	2018-06-30			Estuary	Amundsen Leg 1	Nelson River Transect	57.2059	-92.2825	
N4	2018-06-30			Estuary	Amundsen Leg 1	Nelson River Transect	57.2222	-92.294	
IB13	2018-06-19			Ice flow	Amundsen Leg 1	Ice Beacon Deployment Via Heli	56.6173	-87.4002	
IB17	2018-06-18			Ice flow	Amundsen Leg 1	Ice Beacon Deployment Via Heli	58.4802	-89.2547	
IB18	2018-06-22			Ice flow	Amundsen Leg 1	Ice Beacon Deployment Via Heli	58.3499	-87.4718	
IB19	2018-06-19			Ice flow	Amundsen Leg 1	Ice Beacon Deployment Via Heli	57.7233	-88.2825	
IB20	2018-06-23			Ice flow	Amundsen Leg 1	Ice Beacon Deployment Via Heli	59.3507	-87.8543	

IB21	2018-06-21			Ice flow	Amundsen Leg 1	Ice Beacon Deployment Via Heli	56.422	-85.4002	
IB22	2018-06-23			Ice flow	Amundsen Leg 1	Ice Beacon Deployment Via Heli	58.8122	-84.3463	
IB23	2018-06-19			Ice flow	Amundsen Leg 1	Ice Beacon Deployment Via Heli	57.0884	-88.4002	
IB25	2018-06-22			Ice flow	Amundsen Leg 1	Ice Beacon Deployment Via Heli	57.8789	-84.1463	
IB26	2018-06-21			Ice flow	Amundsen Leg 1	Ice Beacon Deployment Via Heli	56.2193	-84.5491	
731	2018-07-08			Ocean	Amundsen Leg 2	Basic	55.408	-77.928	124
730	2018-07-08			Ocean	Amundsen Leg 2	Basic	56.184	-76.723	138
736Z	2018-07-09			Ocean	Amundsen Leg 2	Basic	58.423	-78.312	99
689	2018-07-11			Ocean	Amundsen Leg 2	Basic	62.342	-75.535	120
341	2018-07-12			Ocean	Amundsen Leg 2	Basic	61.958	-70.755	307
736	2018-07-09			Ocean	Amundsen Leg 2	Zodiac	58.4408	-78.1081	15
Riviere Puvimituq	2018-07-10			River	Amundsen Leg 2	Riviere Puvimituq	60.0725	-77.2469	
689Z	2018-07-11			Ocean	Amundsen Leg 2	Zodiac	62.2852	-75.5220	20
Riviere Foucault	2018-07-11			River	Amundsen Leg 2	Riviere Foucault	62.1081	-75.7583	
Riviere Deception	2018-07-11			River	Amundsen Leg 2	Riviere Deception	62.0975	-74.4956	
SH_1	2018-09-02			Estuary	William Kennedy Mooring Retrieval	Nelson Estuary	57.26895	-92.1346	24
SH_2	2018-09-02			Estuary	William Kennedy Mooring Retrieval	Nelson Estuary	57.66983	-91.6084	24
James Bay Mooring	2018-09-14			Ocean	William Kennedy Mooring Retrieval	James Bay	54.68313	-80.1871	100